

**SYNTHESIS AND COMPATIBILIZING EFFECT OF
WELL DEFINED LINEAR AND BRANCHED COPOLYMERS
IN HETEROGENEOUS POLYSTYRENE-RUBBER BLENDS**

A thesis submitted to the

UNIVERSITY OF PUNE

for the degree of

DOCTOR OF PHILOSOPHY

in

CHEMISTRY

by

SRUTI CHATTOPADHYAY

Polymer Chemistry Division

National Chemical Laboratory

Pune - 411 008

INDIA

June 1999

DEDICATED

**To my parents,
Husband,
Brother,
Sister**

ACKNOWLEDGEMENT

I got the opportunity to associate myself with Dr. S. Sivaram, Deputy Director and Head, Polymer Chemistry Division, NCL, Pune, as my research supervisor. Being an outstanding scientist with a kind and understanding nature, he made the training comfortable, inspiring and enlightening. I wish to place on record my deep sense of gratitude to him who helped me immensely at this critical stage of my career. He taught, criticized, encouraged and advised me during all stages of my work. I will always be indebted to this patient and outstanding gentleman.

I am indebted to Dr. Sarwade, Dr. S. Chakrapani, Dr. S. Thomas, Dr. D. Baskaran, Dr. R.A. Kulkarni, Dr. Wadgaonkar and Dr. T.P. Mohandas for their valuable suggestions and useful discussion during the course of the thesis work.

I owe deeply to ever-trustful Prodeep, Radhakrishnan, Rajesh, Sahida, Mahua, Subarna, Saptarshi for always being with me.

I am grateful to Mr. Menon, Mrs. Dhoble, Ms. Smita, Dr. Ramesh, Dr. Jog and Dr. Lele for the help and suggestions for the instrumental analysis.

I am also thankful to Dr. Khisti, Tushar, Binod, Nikhil, Arnab, Sanigrahi, Hait, Soumen, Nabin, Sanjay and Sourav.

I am thankful to my friends Ananya, Sowmya, Krishanu, Debu, Sundar, Dibu, Dinu, Sunil, Bikhas, Anjan, Tanya, Sipra, Nihar, Koushik, Arijit, Subha, Annit, Rajaram, Subhas, Nabi, Nagesh, Laha, Raghu for all that they have done for me.

I wish to offer my sincere thanks to the members of Polymer Chemistry Division, colleagues and friends for their wholehearted cooperation during the course of this work.

I wish to thank Suryavanshi, Gracy and Shaikh for the help in official matters and Shelar for laboratory matter.

I am thankful to glass blowing section, Mr. H. P. Chakrabarty and his colleagues for fabrication of specially designed glass apparatus.

The constant love, support and encouragement by my beloved parents and dearly loved family members have been the main driving force for me over the whole period. I would like to convey my appreciation to my husband Apurba for his moral support and encouragement all the time.

Finally, I would like to thank the Director, National Chemical Laboratory, for allowing me to present the work in the form of a thesis and Council of Scientific and Industrial Research, New Delhi for the award of research fellowship for the last five years.

(Sruti Chattopadhyay)



राष्ट्रीय रासायनिक प्रयोगशाला (वैज्ञानिक तथा औद्योगिक अनुसंधान परिषद) पुणे - 411 008.

NATIONAL CHEMICAL LABORATORY (COUNCIL OF SCIENTIFIC & INDUSTRIAL RESEARCH) PUNE 411 008. (INDIA)

Dr. S. Sivaram
Polymer Chemistry Division
Tel & Fax : 0091-020-5893234
E-mail: sivaram@ems.ncl.res.in

DECLARATION

Certified that the work incorporated in the thesis "*Synthesis and compatibilizing effect of well defined linear and branched copolymers in heterogeneous polystyrene-rubber blends*" submitted by Mrs. Sruti Chattopadhyay was carried out by the candidate under my supervision. Such material as has been obtained from other sources has been duly acknowledged in the thesis.

(S.Sivaram)

Research Guide

CONTENTS

* Abstract	i
* Glossary	iii
* List of Tables	iv
* List of Figures	vi

Chapter I. Concept and Mechanism of Compatibilization

1.1	Historical developments	1
1.2	Polymer blends and alloys	1
1.2.1	Methods of blending	2
1.2.2	Types of blends: Terminology	2
1.3	Background	3
1.3.1	Introduction	3
1.3.2	Polymer blend compatibility	4
1.3.2.1	Definition	4
1.3.2.2	Polymer blend phase behavior	6
1.3.2.3	Flory-Huggins –Staverman theory	8
1.3.2.4	Kinetics of phase separation	11
1.3.2.5	Measuring miscibility and compatibility	15
1.3.2.6	Properties of multiphase polymer blend	16
1.3.3	Polymer blend interfaces	17
1.3.3.1	Theory of the interface	17
1.3.3.2	Measurement of interfacial tension	20

1.3.3.3	1.3.3.3 Measurement of interfacial structure	23
1.3.3.4	Measurement of interfacial strength and phase adhesion	25
1.3.4	Block and graft copolymers	26
1.3.4.1	Synthesis	26
1.3.4.2	Structure and thermodynamics	28
1.4	Theory of compatibilization	31
1.4.1	Methods of compatibilization	31
1.4.1.1	Thermodynamic miscibility	31
1.4.1.2	Addition of block copolymers	31
1.4.1.2.1	Effect of diblocks on blend phase behavior	31
1.4.1.2.2	Effect of diblocks on interfacial tension and structure	32
1.4.1.3	Graft copolymers	35
1.4.1.4	Alternating or multiblock copolymer	36
1.4.1.5	Addition of functional polymers	36
1.4.1.6	Reactive compatibilization	36
1.4.2	Effect of molecular architecture of compatibilizer	37
1.4.3	Determination of compatibilization	39
1.4.3.1	Effect on morphology	39
1.4.3.1.1	Presence at interface	39
1.4.3.1.2	Domain size	40
1.4.3.1.3	Microscopy	41
1.4.3.2	Mechanical properties	42
1.5	Summary	42

Chapter II. Objectives of the Present Investigation

2.1	Introduction	52
2.2	Objective of the present work	53
2.3	Approaches	54
2.4	References	56

**Chapter III. Synthesis and Characterization of Linear and
Branched Polymers via Living Anionic Polymerization
Technique**

3.1	Introduction	57
3.2	Materials	64
3.3	Purification of solvents and other reagents	64
3.3.1	Purification of nitrogen gas	64
3.1.2	Solvents	64
3.1.3	Monomers	65
3.4	Synthesis of alkyl lithium initiator	66
3.4.1	Estimation of initiator concentration	66
3.5	Methods of polymerization and copolymerization	67
3.5.1	Synthesis of linear diblock copolymer of styrene and isoprene (PS-b-PI)	67
3.5.1.1	Extraction of dead homopolymer from diblock copolymer by selective solvent treatment	69

3.5.2	Synthesis of star-branched copolymer	69
3.6	Characterization of polymers	70
3.6.1	Determination of molecular weight using SEC-RI	70
3.6.2	Determination of absolute molecular weight using SEC-MALLS	70
3.7	Results and discussion	71
3.7.1	Determination of dn/dc values	71
3.7.2	Characterization of linear PS-b-PI	72
3.7.3	Characterization of star-branched copolymers	74
3.7.4	Determination of copolymer compositions by ^1H NMR	74
3.7.5	Confirmation of structure of copolymer by FT-IR	75
3.8	Conclusions	76
3.9	References	77

Chapter IV. Compatibilizing Effect of Poly (Styrene)-b-Poly (Isoprene) Copolymers in Heterogeneous Polystyrene / Natural Rubber Blends

4.1	Introduction	79
4.2	Experimental	80
4.2.1	Materials	80
4.2.2	Synthesis of PS-b-PI	81
4.2.3	Characterization of PS-b-PI	81
4.2.4	Preparation of blends	81
4.2.5	Analysis	82

4.2.5.1	Morphological observations	82
4.2.5.2	DSC study	82
4.2.5.3	Measurement of mechanical properties	82
4.3	Results and discussion	83
4.3.1	Effect of block copolymer concentration on morphology	83
4.3.2	Effect of molecular weight of NR on morphology	90
4.3.3	Effect of block copolymer concentration on particle size distribution	91
4.3.4	Effect of block copolymer molecular weight on particle size distribution	92
4.3.5	Effect of block copolymer composition on morphology	95
4.3.6	Effect of mode of addition of block copolymer	96
4.3.7	Effect of copolymer concentration on blend miscibility	97
4.3.8	Effect of block copolymer on mechanical properties	99
4.3.9	Interfacial area occupied per molecule and physical model of conformation of the block copolymer at the blend interface	101
4.4	Conclusions	107
4.5	References	109

Chapter V. Heteroarm Star Polymers as Emulsifying Agents and Influence of Molecular Architecture of Compatibilizer in Polymer Blends

5.1	Introduction	112
5.2	Experimental	114
5.2.1	Materials	114

5.2.2	Synthesis of copolymers	114
5.2.3	Characterization of star branched polymers	114
5.2.4	Preparation of blends	114
5.2.5	Analysis	115
5.2.5.1	Morphological observation	115
5.2.5.2	DSC study	115
5.2.5.3	Measurement of mechanical properties	115
5.3	Results and discussion	116
5.3.1	Effect of heteroarm star polymer (HS ₁) concentration on morphology	116
5.3.2	Effect of heteroarm star polymer (HS ₁) concentration on particle size distribution	119
5.3.3	Effect of heteroarm star polymer (HS ₁) concentration on blend miscibility	120
5.3.4	Effect of heteroarm star polymer (HS ₁) on mechanical properties	121
5.3.5	Effect of number of arms of heteroarm star polymer on morphology	122
5.3.6	Effect of number of arms of heteroarm star polymer on mechanical property	129
5.4	Comparative study of compatibilizing efficiency of linear diblock, heteroarm star and starblock copolymer having similar arm molecular weight and chemical composition	130
5.4.1	Effect of molecular architecture on morphology	130
5.4.2	Effect of molecular architecture on CMC	135
5.4.3	Effect of molecular architecture on mechanical properties	136
5.5	Conclusions	137
5.6	References	138

Chapter VI. Compatibility Studies on Solution of Polymer Blends (Polystyrene/Natural Rubber) by Viscometric and Phase Separation Technique

6.1	Introduction	140
6.1.1	Theory	140
6.2	Experimental	144
6.2.1	Materials	144
6.2.2	Synthesis of PS-b-PI	144
6.2.3	Characterization of the materials used	144
6.2.4	Analysis	145
6.2.4.1	Dilute solution viscometry (DSV) measurements	145
6.3	Results and discussion	146
6.3.1	Chee's method	146
6.3.2	Intrinsic viscosity of transfer	147
6.3.3	Heat of mixing and compatibility	149
6.3.4	Density and compatibility	150
6.3.5	Polymer blend-solvent interaction	151
6.3.6	Phase separation behavior	153
6.3.6.1	Effect of block copolymer concentration	153
6.3.6.2	Effect of nature of solvent on phase separation	155
6.3.6.3	Effect of mode of addition on phase separation	156
6.3.6.4	Effect of block copolymer/homopolymer molecular weight on phase separation	157

6.4	Conclusions	158
6.5	References	160

Chapter VII. Compatibilizing Effect of PS-b-PI in Heterogeneous SAN/NR Blends

7.1	Introduction	162
7.2	Experimental	164
7.2.1	Materials	164
7.2.2	Synthesis of PS-b-PI	164
7.2.3	Characterization of PS-b-PI	164
7.2.4	Preparation of blends	165
7.2.5	Analysis	165
	7.2.5.1 Morphological observations	165
	7.2.5.2 Measurement of mechanical property	165
7.3	Results and discussion	165
7.3.1	Compatibilization study of PS-b-PI in SAN/NR blends	165
	7.3.1.1 Effect of block copolymer concentration on morphology	165
	7.3.1.2 Effect of block copolymer concentration on particle size distribution of SAN/NR blends	169
7.3.2	Comparative study of properties of commercial ABS and compatibilized blend of SAN/NR/PS-b-PI	170
	7.3.2.1 Morphological observations	171
	7.3.2.2 Determination of impact strength	174

7.3.3	Comparative study of properties of commercial HIPS and compatibilized blend of PS/NR/PS-b-PI having similar chemical composition of HIPS	175
7.3.3.1	Morphological observation	175
7.3.3.2	Determination of impact strength	178
7.4	Conclusions	179
7.5	References	180
<hr/>		
Chapter VIII. Summary and Conclusions		181
<hr/>		

*** Synopsis**

ABSTRACT

This thesis presents results on the synthesis and characterization of linear diblock and star-branched copolymers of styrene and isoprene by anionic polymerization and their application as compatibilizers in heterogeneous poly(styrene)/rubber blends.

Linear diblock copolymers of styrene and isoprene with \overline{M}_n in the range of 50,000 to 2.6×10^5 and with narrow polydispersities (<1.10) were synthesized over a wide range of composition. Star-branched copolymers of styrene and isoprene having different molecular architectures were also synthesized successfully. The chemical composition was established by ^1H NMR. The structure of copolymers was confirmed by FT-IR.

The consequence of adding a diblock copolymer poly(styrene)-b-poly(isoprene) (PS-b-PI) to an immiscible blend of poly(styrene) (PS)/natural rubber (NR) on properties, such as, morphology, particle size distribution, critical micelle concentration (CMC), thermal transition and mechanical properties of the blends were investigated. Scanning electron microscopy (SEM) showed that the block copolymer reduced the domain size of the dispersed phase in the blends. The compatibilizing effect was also investigated as a function of block copolymer molecular weight, composition and concentration. The effect of homopolymer molecular weight, processing conditions and mode of addition on the morphology of the dispersed phase were also investigated by optical microscopy and SEM. The compatibilizing effect of the diblock copolymer arises due to its presence at the interface of PS and NR phases. The respective block segments penetrate into the corresponding phases.

Compatibilizing ability of heteroarm star polymer composed of PS and PI diverged from DVB core was investigated. By using this copolymer as a compatibilizer of an immiscible PS/NR blend, a sharp reduction in particle size was observed. Mechanical properties of the compatibilized blends also improved indicating that the effective penetration of each arm of the heteroarm star into the blend component was operative. The influence of number of arms of star was also studied. In spite of

complex molecular architecture of heteroarm star, it appears to easily migrate to the blend interface.

Molecular architectural effect of compatibilizer was studied using star-block, heteroarm star and linear diblock of PS and PI copolymers as compatibilizer. It was found that heteroarm star polymer having higher number of PS and PI arms were the most efficient.

Dilute solution viscosity (DSV) measurement was used to study the miscibility of polymer blends. Using this approach, blends of PS with NR have been found to be immiscible. Chee's method was applied to determine ΔB and μ of polymer blend solution, where ΔB and $\mu \geq 0$ signifies miscibility and < 0 indicates phase separation. The influence of the nature of the solvent on the miscibility of polymer blend was also studied.

The compatibilizing effect of PS-*b*-PI in heterogeneous SAN (styrene-co-acrylonitrile) /NR blend was studied. It was found that with increasing amount of the block copolymer, the particle domain size decreased and leveled off at critical micelle concentration (CMC). The influence of block copolymer concentration on impact strength of the blends was also studied. In this approach using an A-*b*-C diblock copolymer to bridge the incompatibility gap between two polymers B and C have also proven to be valid when A and B is compatible.

A comparative evaluation of properties, such as particle size of the dispersed phase and impact strength of commercial ABS and HIPS with compatibilized SAN/NR and PS/NR blends, prepared in the laboratory were made

GLOSSARY

B	Linear block copolymer
n-BuLi	Butyllithium
s-BuLi	Secondary butyllithium
CMC	Critical micelle concentration
DVB	Divinyl benzene
DSC	Differential Scanning Calorimetry
$[\eta]$	Intrinsic viscosity
GPC	Gel Permeation Chromatography
g	Gram
h	Hours
HS	Hetero arm star
HIPS	High impact polystyrene
ΔH_m	Heat of mixing
IR	Infra Red
\overline{M}_n	Number average molecular weight
MWD	Molecular weight distribution
MALLS	Multi angle lesser light scattering
min	Minutes
mL	Milliliter
NMR	Nuclear Magnetic Resonance
NR	Natural rubber
PS	Poly(styrene)
PS-b-PI	Poly(styrene)-block-poly(isoprene)
SEM	Scanning electron microscope
SEC	Size exclusion chromatography
SB	Star block
SAN	Styrene/acrylonitrile copolymer
THF	Tetrahydrofuran
T_g	Glass transition temperature
wt %	Weight percentage

LIST OF TABLES

3.1	dn/dc values of linear-diblock and star-branched copolymers	72
3.2	Characteristics of block copolymers synthesized	73
3.3	Characteristics of the copolymers synthesized	74
4.1	Characteristics of materials used	81
4.2	Effect of block copolymer molecular weight on particle size distribution	93
4.3	Effect of block copolymer composition on morphology	95
4.4	DSC study of 50/50 PS/NR blend	98
4.5	Mechanical Properties of 50/50 PS/NR blend	101
4.6	Dispersed phase radius (r) at CMC and ' Σ ' values of the system	105
5.1	Characteristics of materials used	116
5.2	DSC study of 50/50 PS/NR blend	121
5.3	Mechanical Property measurement of 30/70 PS/NR blend using heteroarm star polymer (HS ₁) as compatibilizer	122
5.4	DSC study of copolymers	123
5.5a	Comparison of mechanical properties of PS/NR blend using different heteroarm star polymers as a compatibilizer	129
5.5b	Comparison of tensile impact properties of PS/NR blends using different heteroarm star polymers as a compatibilizer	129
5.6	Comparison of CMC values	135
5.7a	Comparison of tensile impact strength	136
5.7b	Comparison of mechanical properties	137
6.1a	Characteristics of the materials used	144
6.1b	Characteristics of the block copolymers synthesized	144
6.2	Intrinsic viscosity of transfer for different blend systems	149

6.3	Observed and calculated densities of solution of PS/NR blend in toluene at 25 °C	151
6.4	Interaction parameter for the polymer-polymer system	152
6.5	Interaction parameter for polymer blend-solvent system	152
6.6	Phase separation times for various PS/NR blends (time in hours)	154
6.7	Volume fraction of the phase separated NR layer	155
7.1	Characteristics of materials used	164
7.2	Characteristics of block copolymers synthesized	165

LIST OF FIGURES

1.1	Polymer phase diagram types: a) hourglass, b) UCST, c) LCST	6
1.1	Polymer phase diagram type d) UCST/LCST, e) loop	7
1.2	Ternary phase diagram for a polymer-polymer-solvent system	11
1.3	Phase diagram showing the regions with various types of phase separation mechanisms: N = nucleation and growth, SD = spinodal decomposition	12
1.4	Schematic representation of the process occurring during the melt blending of two polymers	14
1.5	Block copolymer morphologies in the strong segregation limit, shown for PS-b-PI as function of styrene volume fraction	30
1.6	Variation on interfacial tension vs. concentration of added block copolymer for a variety of block molecular weight	33
3.1	Localized-delocalized equilibrium of chain ends	59
3.2 i	Distillation apparatus, (S) rubber septum, (T) three-way stop-cock, vacuum or nitrogen line is connected through is way	66
3.2 ii	Reactor for synthesizing block copolymer in bulk	68
3.2 iii	Reactor for synthesizing branched copolymer	70
3.3	Schematic representation of star-branched copolymers	71
3.4	GPC chromatogram of linear diblock copolymer (B_3)	73
3.5	^1H NMR spectrum of PS-b-PI	75
3.6	IR spectrum of PS-b-PI	76
4.1	Effect of block copolymer concentration on the domain size of the dispersed phase of different PS/NR blends	83
4.2	Effect of block copolymer concentration on inter particle distance of the dispersed phase in 30/70 PS/NR blends	84

4.3	SEM photographs of 50/50 PS/NR blends with block copolymer loading (a) 0%, (b) 1.5 %, (c) 3.5 %, (d) 5 % and (e) 6 %	86
4.4	SEM photographs of (a) 40/60/0 (b) 40/60/0, 2 days acetone etching, (c) 40/60/1, 2 days acetone etching (d) 40/60/ 1, 7 days acetone etching (e) 40/60/1.5, 7days acetone etching	89
4.5	Influence of molecular weight of NR on morphology	90
4.6	Effect of molecular weight of NR on CMC	91
4.7	Effect of PS-b-PI concentration on domain size distribution of 30/70 PS/NR blends	92
4.8	Effect of the molecular weight of the interfacial agent on the emulsification	94
4.9	Effect of mode of addition of block copolymer on blend morphology	97
4.10	DSC of 50/50 PS/NR blend	98
4.11	Tensile Impact strength of PS/NR blends with different blend composition	100
4.12	Effect of block copolymer volume fraction on particle size distribution	103
4.13	Effect of homopolymer molecular weight on the calculated area occupied by the copolymer molecule at the blend interface, Σ	106
4.14	Physical models illustrating the conformation of the copolymer at the interface	107
5.1	Effect of heteroarm star polymer (HS_1) concentration on the domain size of the dispersed phase of different PS/NR blends	118
5.2	Effect of heteroarm star polymer (HS_1) concentration on interparticle distance of the dispersed phase in 30/70 PS/NR blends	118
5.3	Particles distribution of dispersed NR in PS/NR blends (30/70 w/w) compatibilized by different amounts of HS_1 . (5.3a) Blends containing 0 wt % copolymer; (5.3b) blends containing 0.5 wt % copolymer and (5.3c) blends containing 1.0 wt % copolymer	120
5.4	Tensile impact strength of PS/NR blends using heteroarm star polymer (HS_1) as compatibilizer	122

5.5	SEM photographs of PS/NR blends (a) 30/70/1, HS ₁ as compatibilizer, (b) 30/70/1, HS ₁ as compatibilizer-7days acetone etching, (c) 30/70/1, HS ₂ as compatibilizer, (d) 30/70/1, HS ₂ as compatibilizer-7days acetone etching, (e) 50/50/1, HS ₁ as compatibilizer, (f) 50/50/1, HS ₁ as compatibilizer-7 days acetone etching, (g) 50/50/1, HS ₂ as compatibilizer and (h) 50/50/1, HS ₂ as compatibilizer-7 days acetone etching	128
5.6	SEM photographs of 40/60/1 PS/NR blend (a) B ₅ as compatibilizer, (b) B ₅ as compatibilizer-etched for 2 days, (c) B ₅ as compatibilizer-etched for 7 days, (d) HS ₁ as compatibilizer, (e) HS ₁ as compatibilizer- etched for 2 days, (f) HS ₁ as compatibilizer- etched for 7 days, (g) SB as compatibilizer, (h) SB as compatibilizer- etched for 2 days and (i) SB as compatibilizer- etched for 7 days	134
5.7	Schematic representation of HS polymer at blend interface	135
6.1	Plot of Chee's factor ΔB vs. wt. fraction of polymer B (NR) for PS/NR (polymer A /polymer B) blends in toluene at 25 °C	146
6.2	Plot of Chee's factor μ vs. wt. fraction of polymer NR (polymer B) for PS/NR (polymer A /polymer B) blends in toluene at 25 °C	147
6.3	η_{sp}/C vs C for PS/NR blend solution of different composition in toluene at 25 °C	148
6.4	Plots of η_{sp}/C vs C of PS for PS/NR blends in pure and 'mixed' solvents at 25 °C	148
6.5	Plots of η_{sp}/C vs C of NR for PS/NR blends in pure and 'mixed' solvents at 25 °C	149
6.6	Heat of mixing (ΔH) vs. wt % of PS (polymer A) in PS/NR blends	150
6.7	The influence of block copolymer on phase separation of 50/50 PS/NR blends	153
7.1	Optical photographs of SAN/NR (40/60) blends with block copolymer loading (a) 0 %, (b) 2%, (c) 3.5%, (d) 6 % and (e) 7.5 % Scale used : 1 mm = 2 μ m	168
7.2	Effect of PS-b-PI concentration on particle size of SAN/NR blends	169

7.3	Effect of PS-b-PI concentration on domain size distribution of 40/60 SAN/NR blends	170
7.4	Tensile impact strength of SAN/NR (40/60 wt/wt) using PS-b-PI as compatibilizer	171
7.5	Optical photographs of (a) ABS. SAN/NR (95/5) blends with block copolymer loading (b) 0 %, (c) 2%, (d) 3.5%, (e) 5 % and (f) 6 % Scale used : 1 mm = 2 μ m	173
7.7	Impact strength of compatibilized SAN/NR (95/5 wt/wt) blend compared with commercial ABS	174
7.8	Optical photographs of (a) HIPS. PS/NR (94/6) blends with block copolymer loading (b) 0 %, (c) 2%, (d) 5%, (e) 7.5 % and (f) 9 %. Scale used : 1 mm = 2 μ m	177
7.9	Impact strength of compatibilized PS/NR (94/6 wt/wt) blend compared with commercial HIPS	178

CHAPTER I

CONCEPT AND MECHANISM OF COMPATIBILIZATION

1.1 Historical developments

Mixing has been a natural preoccupation of the humans from the dawn of civilization and has been practiced with conventional materials like metals, natural fibers etc. Blending is a natural way to widen the range of properties of available materials. This has been well illustrated by the history of polymer blends. In 1846 only natural rubber (NR) and gutta percha (GP) were available and these were blended. Once nitrocellulose (NC) was invented, its blend with NR was patented in 1985 – three years before commercialization of NC. Cellulose acetate (CA) was invented and was combined with NC. Comparing the dates of commercialization and blending of new polymers, one is amazed by the closeness of these dates. For example, PVC and NBR were commercialized in 1932, while their blends were announced in 1936.

1.2 Polymer blends and alloys

Polymer blends provides a powerful route to engineering new properties in materials using available polymers. The rapid increase in the use of blends is one of the most prominent features of the polymer industry over the last several years. A parallel effort in understanding the science of blends characterizes much of current polymer technology. The driving force for the increasing utility of blends are related to the high cost of producing entirely new polymer molecules relative to that for blends of existing materials and to the ability of blends to produce materials with combinations of properties superior to those of single polymers. The subject is vast and has received much attention in recent years both from experimental and theoretical points of view. More recently, considerable research effort in polymer blends and alloys, in both academia and industry, has led to a mushrooming growth of the patent and scientific literature. A number of books, reviews and congress proceedings covering all aspects of the preparation, phase behavior, and applications of the different types of blends have been published¹⁻¹⁴. The primary advantages in employing polymer blends or alloys are as follows: (a) higher performance at a reasonable price, (b)

modification of performance to keep pace with developing market, (c) extending the performance of expensive resins, (d) reuse of plastic scrap, and (e) generation of unique materials with respect to optimum balance of processability and/or performance. So, the recent industrial efforts have been directed towards development of : (i) blends with high performance polymers, (ii) multiphase blends, with several polymers, and/or reinforcements, (iii) reactive processing, (iv) blends with controlled morphology and (v) blends from recycled materials.

1.2.1 Methods of blending

The manner by which two polymers are mixed together is of vital importance in controlling the properties of blends^{4, 5}. Methods of preparation of blends can be classified as : (i) melt mixing, (ii) solvent casting, (iii) co-precipitation, (iv) latex-blending, and (v) interpenetrating polymer networks (IPN).

(i) melt mixing involves mixing of two polymers in the molten state under shear and is usually achieved with the help of either a Brabender Plasticoder type batch mixer or an extruder (single or double screw). For economic reasons mechanical blending predominates commercial applications.

(ii) solvent casting involves dissolving the polymers in a common solvent and casting a film from solution.

(iii) co-precipitation involves dissolving the polymers in a common solvent and the subsequent removal of solvent by precipitation using a nonsolvent.

(iv) latex-blending involves mixing the lattices of two polymers and spraying the mixture followed by drying.

(v) interpenetrating polymer networks (IPN) technology involves the polymerization of one monomer usually dissolved in a solvent containing a polymer.

1.2.2 Types of blends: Terminology

Polymer blend: A mixture of at least two polymers or copolymers.

Homogeneous blend: A mixture of two homologous polymers, usually narrow molecular weight distribution fractions of the same polymer. In this blend, both blend components lose part of their identity and the final properties usually are the arithmetical average of both blend components.

Heterogeneous blend: The properties of all blend components are present. Weakness of one polymer can to a certain extent be camouflaged by strengths of the other.

Miscible polymer blend: Polymer blend which are homogeneous down to the molecular level, associated with the negative value of free energy of mixing: $\Delta G \cong \Delta H \leq 0$.

Immiscible polymer blend: Any polymer blends whose $\Delta G \cong \Delta H \geq 0$.

Compatible polymer blend: A term indicating a commercially attractive polymer mixture with enhanced physical properties over the constituent polymers.

Polymer alloy: An immiscible polymer blend having a modified interface and/or morphology.

1.3 Background

The development of a scientific understanding of compatibilization at a molecular level probably trails its application by a few years. This is the result of both theoretical and experimental advances. There has been an increasing interest in understanding the nature of polymer and polymer chains near interfaces and surfaces and the science of compatibilization has benefited from this. Particularly important in this area is the increasing ability to probe the details of the structure of the chains at an interface and ways to calculate the configurations of such chains. While many questions about the utilization of compatibilizers still remain to be answered, great progress has been made in knowing how these molecules migrate to the interface in a blend and the effects the morphology and physical properties of the blend.

1.3.1 Introduction

Some of the important question in polymer blends are (a) how to design a compatibilizer for a given polymer blend (b) what kind of polymeric compatibilizer will work best in a given blend and (c) how best to make that compatibilizer. It is important to have a background in several areas of polymer science that are crucial to understanding the process of compatibilization. These areas are:

Polymer blend compatibility: How polymer blends differ from mixtures of other kind molecules? This is due mainly to the rarity of finding true solubility in mixtures of two polymers and the slowness by which immiscible blends separate into two phases. It is also important to have a measure of blend compatibility and, thus, know when compatibilizers are effective.

Interfaces: Since compatibilization is directly related to blend morphology and phase dimensions, it is critical to know the characteristics of the interface between the components. The key concepts which control the behavior of polymers at interfaces are interfacial tension, the size or thickness of the interface as well as the adhesion and mechanical connection between the phases.

Synthesis of block and graft copolymers: Compatibilizers are polymeric analogs of surfactants in that they are interfacially active materials that have an amphiphilic character. Thus it is necessary to make a molecule that has sections which are miscible with each of the components. Since in most cases of interest the blend components are quite incompatible, it will be very difficult to find a homopolymer miscible with both of them, so the compatibilizer will need to have chemically different sections or blocks.

1.3.2 Polymer blend compatibility

In order to understand how compatibilizers work to improve polymer blends and why one type is to be preferred over another, it is necessary to have some background in the thermodynamics and kinetics of polymer mixtures. For a complete treatment of the thermodynamics of polymer blends several text books^{15, 16, 17} are referred.

The two main facts of blend thermodynamics which are important for the development of the compatibilizers are an understanding of the general incompatibility between the components as well as the factors that promote miscibility since the arms or blocks of the compatibilizer will need to be miscible with one component or the other.

1.3.2.1 Definition

Miscibility: Two polymers are miscible with each other if the free energy of mixing is negative. As such, this is a function of chemical structure of the polymer (e.g molecular weight, its distribution, copolymer composition) and thermodynamic variables such as temperature, pressure and blend composition. True miscibility is uncommon for polymer mixtures.

Compatibility: While miscibility has a strict thermodynamic meaning ($\Delta G \cong \Delta H \leq 0$), compatibility is defined in operational terms. It is also relative. A blend may be more or less compatible if it is closer or further from miscibility. A completely compatible system is thus a miscible one. The compatibility of a particular blend might be related

to how 'good' a particular property of it is, e.g. a direct and meaningful measure is morphological: the scale on which polymers are mixed, that is, the size of the phase separated domains. Domain size and growth are system responses, which reflects the thermodynamic driving forces for phase separation. It is important to realize that the highest degree of compatibility (that is miscibility) does not always mean the best engineering properties. This goal is to achieve a 'controlled' level of phase separation. However, in most cases, due to the preponderance of immiscibility in polymer blends, the need is to increase the compatibility of a particular blend.

Compatibilization: Any modification of a blend, which increases its compatibility can be termed as compatibilization. By far the most successful method of compatibilization has been the introduction of block or graft copolymers as compatibilizers.

Compatibilizer: A polymer which when added to a blend, increases the degree of compatibility. Compatibilizers decrease the scale of phase separation in the blend. It is preforce to be found at the interface between the phases (polymeric surfactant). In order to be effective, a compatibilizer should be polymeric and generally has chemically distinct segments. In some cases, even a homopolymer can serve as a compatibilizer.

Characteristics of compatibilizers:

(i) A compatibilizer is not simply an additive, which improves some property of a blend. An additive can improve properties (e.g. by changing the properties of one component) without changing the thermodynamics or morphology of the blend. Such additives may indeed be quite useful. However, only if they affect compatibility they should be called compatibilizers.

(ii) A compatibilizer is also not a process. Curing or crosslinking can fix a blend at a certain degree and size of phase separation, as can crystallization, but this should only be viewed as preserving a certain degree of compatibility^{18, 19}. Similarly, shearing can change the critical temperature of a blend, but this does not affect its compatibility²⁰. All of these processes can be used to improve the performance of a blend, but are not compatibilizers.

(iii) A compatibilizer is also not a molecule, which changes the region of miscibility in the phase diagram of the blend. A number of polymers may do this (e.g. low

molecular weight versions of one of the components, or random copolymers²¹⁾ without changing the compatibility of the blend. The polymers that affect the miscibility generally do not act as interfacial agents, but rather operate by modifying the phase properties.

1.3.2.2 Polymer blend phase behavior

All types of phase behavior displayed by polymer blends are also found in mixtures of small molecules, since both systems must obey the same thermodynamics. However, the probability of encountering one kind of phase behavior or the other in a particular mixture is quite different for a pair of polymers than it is for two small molecules (or for a polymer solution). In this discussion the main emphasis is given to binary polymer blends at ambient pressure.

Infact, every blend will be miscible under some conditions of temperature and composition. For most pairs of polymers, this region is limited to very low amounts of one polymer in the other. This leads to an hour glass type of phase diagram as shown in the **Figure 1.1a**, so called because of shape

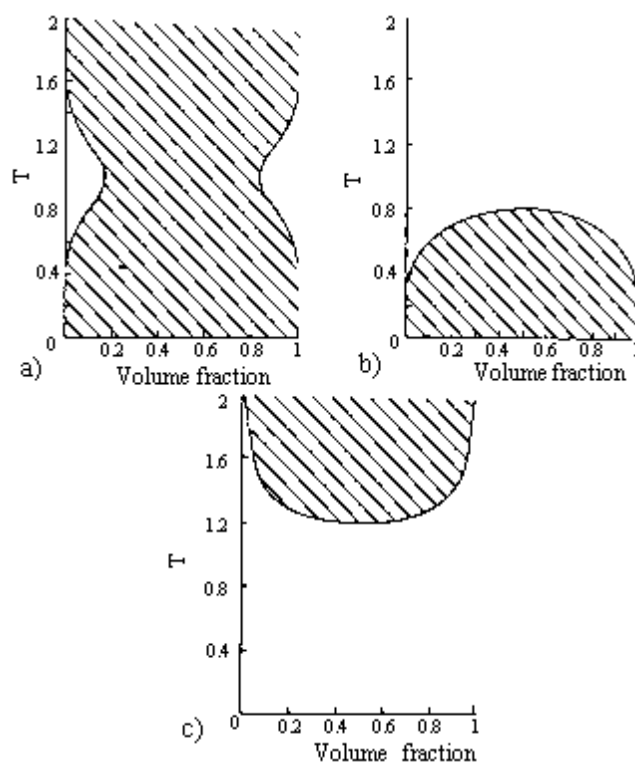


Figure 1.1. Polymer phase diagram types: a) hourglass, b) UCST, c) LCST

At nearly every composition, the blend is not miscible at any temperature. In most cases of high polymers, the miscible region is so narrow that it has not been measured. Blends showing this kind of phase behavior are often simply termed immiscible. The kind of phase diagram most familiar to those who study mixtures of small molecules such as metal alloys is one in which the components are soluble at high temperature and phase separate only below a certain temperature, the magnitude of which depends on composition. The two phase region is often called a 'miscibility gap'. The critical temperature for such a situation is called an 'upper critical solution temperature' or UCST, because it is the highest temperature at which there is some range of composition where the blend is immiscible. Above the UCST the blend is miscible at all compositions. A phase diagram with such a UCST is thus called a UCST phase diagram. This is shown in **Figure 1.1b**. The opposite case where the mixture is miscible at low temperature but begins to phase separate as it is heated. Here the critical temperature is called a 'lower critical solution temperature' or LCST. Such behavior is quite rare for small molecule, but is often found for polymer blend solutions and blends. An LCST type of phase diagram is given in **Figure 1.1c**. It is also possible for a blend to display both an LCST and a UCST (**Figure 1.1d**), but this has been reported only rarely²². It is of course not only possible for the LCST to be higher than the UCST (**Figure 1.1d**) but the reverse can be true. This then leads to a region of immiscibility in the middle of the phase diagram, with one-phase region above and below it (**Figure 1.1e**). Such a diagram has never been shown for a polymer blend and is also quite rare for mixtures of small molecules.

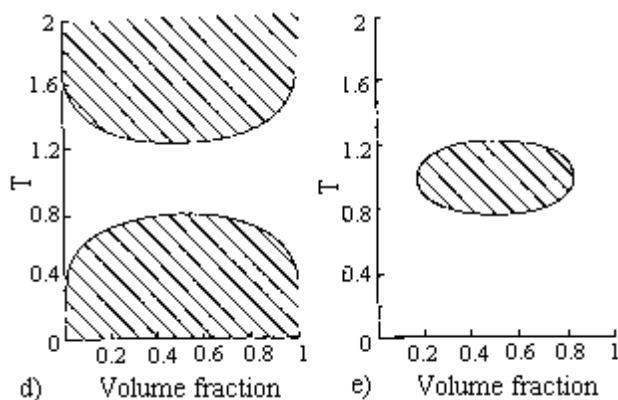


Figure 1.1. Polymer phase diagram type d) UCST/LCST, e) loop

1.3.2.3 Flory-Huggins –Staverman theory

The earliest theories of the thermodynamics of polymer mixtures were given by Flory, Huggins, Staverman and Santen in 1941²³. The thermodynamics of polymer mixture was developed in terms of a lattice model with each monomer repeat unit of the chains occupying a single lattice site.

The main equation is the Flory- Huggins-Staverman (FHS) expression for the free energy of mixing two polymers:

$$\frac{\Delta G_m}{VRT} = \frac{f_1}{n_1 N_1} \ln f_1 + \frac{f_2}{n_2 N_2} \ln f_2 + f_1 f_2 \frac{c}{n} \quad \text{Eq. 1.1}$$

Here V is the total volume of the sample, R is the gas constant, T is the absolute temperature, N_i is the degree of polymerization of component i (= 1 or 2), ϕ_i is the volume fraction of that component, v_i is the molar volume of its mers, and v is an arbitrary volume (often defined as $\sqrt{n_1 n_2}$). The first two terms represent the combinatorial entropy of mixing, and the last term comes from the interaction enthalpy; χ is called the ‘Flory interaction parameter’. This theory has been quite successful in describing many of the qualitative features of polymer blend thermodynamics.

The first of these successes is in terms of an explanation of why most polymer blends show essentially no region of miscibility. Since most polymers of commercial interest have degrees of polymerization of 1000 or more, the first two terms representing the entropy of mixing are generally quite small. This low combinatorial entropy of mixing can be thought of as a direct result of the high configuration entropy that is characteristics of polymer chains^{24, 25}. The entropy of mixing depends on the mole fraction of chains, rather than the volume or weight fraction. This is why the first two terms in **Equation 1.1** are divided by the degrees of polymerization of the two components. The interactions between the two polymers are quite similar to those between their small molecule analogs, since these forces are quite local, extending only over a range of the order of a repeat unit. So the enthalpy of mixing will not depend to any significant amount on the molecular weight of the components. But for most mixtures, the enthalpy of mixing is positive. The entropy of mixing of small molecules can be so large that it overwhelms the positive mixing enthalpy and so causes the components to mix under a wide range temperature and composition. The

reason why polyethylene and polypropylene are immiscible under essentially all conditions whereas, octane and iso-octane are miscible over a large part of their phase diagram, is simply due to the near absence of mixing entropy for the two polymers. Thus the miscibility of polymers is largely determined by the value of χ .

The focus of research on the miscibility of polymers is the determination of the Flory interaction parameter (χ). χ is a technologically very important parameter in polymer blends. The value of χ controls the equilibrium phase diagram for the blend. This can have important implications for processing.

Secondly, a knowledge of χ helps to estimate the interfacial tension, γ , between the two polymers when they are phase separated. The size of the phase domains produced during mixing is controlled in part by γ , as it is the adhesion between the phases. Both factors are crucial determinants of the physical properties of the blend materials. χ can also be used to find the surface tension of a blend which can be related to the adhesion and sealing of the surface. So knowledge of χ can be helpful in understanding the value of current blends and in designing new ones. Two things are very important in the study of polymer blends. These are (i) how incompatible a given blend is, so that a feeling for the need for compatibilizers can be developed and (ii) to know which block or graft copolymers will have sections miscible with the components of the blend and so act as compatibilizers.

In FHS formulation of miscibility, the need is to determine these conditions under which a blend can become miscible. There are basically three general classes of miscible blends based on three separate ways in which miscibility has been achieved: (i) polymer blends consisting quite low molecular weight that the entropy of mixing is large enough to outbalance the enthalpy of mixing. From FHS model, one can derive the following expressions for the critical composition and temperature of the blend:

$$\mathbf{f}_{1,crit} = \frac{1}{1 + \left(\frac{N_2 \mathbf{n}_2}{N_1 \mathbf{n}_1}\right)^{1/2}} \quad \text{Eq. 1.2}$$

$$\mathbf{c}_{crit} = \frac{\mathbf{n}}{2} \left(\frac{1}{N_1 \mathbf{n}_1} + \frac{1}{N_2 \mathbf{n}_2} \right)^2 \quad \text{Eq. 1.3}$$

Blend is symmetric if both components have similar parameters, that is, if $N_1 = N_2 = N$ and $v_1 = v_2 = v$, in that case $\phi_{1,crit} = 0.5$ and $(\chi N)_{crit} = 2$.

In most cases the components of a polymer blend are not very different from one another in molecular weight or density. Therefore, in general these relations for the symmetrical blends are good rules of thumbs for blends. So even if χ is large for a particular blend, if N is small enough, the blend can be miscible. But unfortunately if the molecular weight is so low, then many of the desirable properties of the blends will be lost. The use of low molecular weights is not an effective strategy for achieving a useful miscible blend. Only when the interactions are very weak as in the case of dispersive van der Waals forces (e.g. between polyolefins) then this might be worthwhile²⁶.

(ii) blends which have a negative value of χ and so of the mixing enthalpy, due to the presence of strong attractive interactions between the components. These are called 'specific interactions' as they are not present in either component by itself but only appear when both are present, for example, presence of hydrogen-bonding²⁷ between donating and accepting groups. Other sorts of interactions, such as inomeric^{28, 29} ones or acid-base interactions³⁰ can also induce the mixing of the polymers.

(iii) in this category miscible polymers is also characterized by a negative value of χ , but not because of any special attractive interactions between the components rather one or both of the components are statistical copolymers³¹ and the balance of the forces among the several monomer types that result in miscibility. This has been termed as 'copolymer effect' and it can explain many cases of miscibility that have been discovered.

Although FHS theory explains many of the general observation of immiscibility in blends, it has been certain deficiencies. These are:

- (i) it cannot quantitatively describe blends with a significant degree of miscibility
- (ii) it cannot describe the behavior of blend with an LCST phase diagram
- (iii) FHS theory predicts that χ only depends on temperature and is independent of molecular weight or composition But recent studies have shown that there is a clear compositional dependence of χ , even in blends when only dispersive forces are operating³² and in blends of a polymer with its isotopic twin³³.

1.3.2.4 Kinetics of phase separation

Because of its large size polymer molecules are highly entangled. This results in slow polymer dynamics shown by high viscosity and slow diffusion. Thus, the phase separation of immiscible blends is very slow, and, in most cases the phases do not reach macroscopic size. In most cases of commercial importance, this microscopic phase separation will become locked in at some point by crystallization, vitrification or vulcanization. The scale of this morphology is a critical determinant of the physical properties of blends. One can control this scale through the use of compatibilizers. They are believed to be effective in slowing down or even halting the growth of the phases.

The rate at which phases grow in an immiscible polymer blend can be studied by dissolving the blend in a common solvent, which is good for both of the components. When the solution is dilute enough it will be in a single phase, no matter how repulsive the interactions are between the two polymeric components. The typical ternary phase diagram is shown in **Figure 1.2**, showing that there will generally be a region below 5-10% polymer where a single-phase behavior can be found³⁴. A well-mixed state of the blend can be produced if the solvent can be removed sufficiently quickly so that the polymers do not have time to phase separate. It is difficult to accomplish this simply by heating the solution as it increases the rate of phase separation. The most common way is to place the blend into a non-solvent for both components, so that all solvents rapidly move out of the polymer phase. If one or both of the components either crystallizes or vitrifies at the same time, the blend will freeze in a state where the chains are well mixed with each other³⁵.

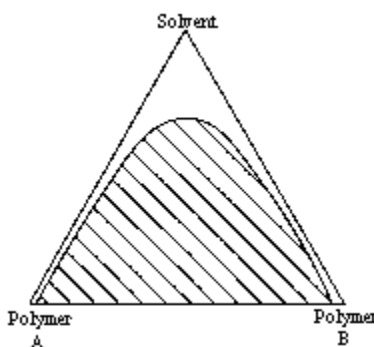


Figure 1.2. Ternary phase diagram for a polymer-polymer-solvent system

Another way to produce a well-mixed state for an immiscible blend is to rapidly flash off the solvent. This has been termed as 'compositional quenching'³⁶. When a super critical fluid is used as solvent which will rapidly flash off when the pressure is lowered below the critical point³⁷. The various regions are illustrated in **Figure 1.3**. Near the phase boundary there is a region of metastability for the phase separation; the free energy of the system is lowered by phase separation in this part but phase separated domains is only stable above a certain size. Domains smaller than the critical size will remix with the matrix while domains, bigger than the critical size will form nuclei for the separated phase which will grow with time until the whole sample is separated into two phases. Thus this region is characterized as 'nucleation and growth'³⁸ and the kinetics are the same as those for the growth of crystals from a liquid by nucleation.

Further from the phase boundary is the region of 'spinodal decomposition'. Here the phase separation is spontaneous because there is no need for a nucleated domain of

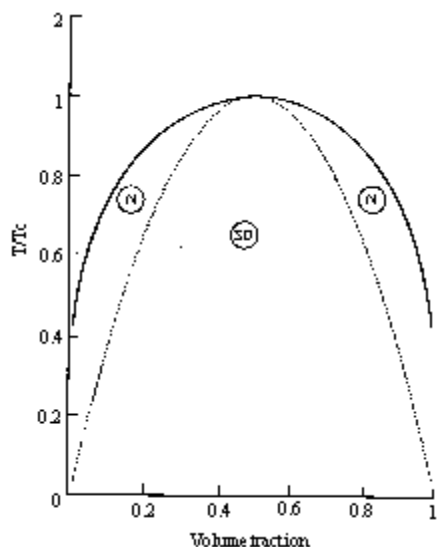


Figure 1.3. Phase diagram showing the regions with various types of phase separation mechanisms: N = nucleation and growth, SD = spinodal decomposition

one phase or the other. The second derivative of the free energy with respect to composition is negative in this region. This results in a cocontinuous structure of the blend of a characteristics size (generally about a micron) with the composition in each phase shifting in time towards these of two equilibrium phases. The phase separation occurs by diffusion of chains from mixed to separated regions. Kotnis and

Muthukumar³⁹ have proposed the existence of a 'transnodal' region in that part of the spinodal region near the metastable region where the phase separation starts due to slow diffusion of one component through a phase with a majority of the other one.

The best experimental study of phase separation in blends has been done by Hashimoto⁴⁰ and by Yoon et al⁴¹. Hashimoto combined both neutron and light scattering methods to look at the phase separation of blends of polystyrene and polybutadiene over a wide range of both time and distance scales. The neutron scattering is useful when the distance scales are small, on the order of 1 to 100 nm. Light scattering becomes useful once the size reach the order of a micron or so. There is gap between 0.1 to 1 μm , which is not covered by both these experiments. The data extrapolate into this range quite well to give a continuous behavior of the phase separation.

Commercially, most blending is done with intensive mixing in the melt. This case is different from the above in two aspects: (i) one starts with totally separate components in the form of pellets which first need to be broken down to small size, (ii) the mixing and phase separation occurs during the shearing and extension of the sample, so that coalescence of the particle is more likely to happen. This brings another possible mechanism for the activity of compatibilizers to reduce domain sizes, which is that of steric stabilization to prevent or slow down the coalescence of dispersed particles. Pictorially this phenomenon can be depicted as in **Figure 1.4**. The theory of particle size dispersion for mixing Newtonian fluids of limited solubility is well described by Grace⁴². The size of the particle during shear is determined by the balance of two forces. The first comes from the repulsive interaction between the two components. This is represented by the interfacial tension, γ , which tends to make the particles grow bigger. The two components interact across the interface, so a reduction in the amount of interfacial area per volume reduces the amount of interaction energy. This is accomplished by increasing the size of the particle. The second force is the shearing itself. This stretches each particle into a long string, which breaks up into a series of spherical particles, which are smaller than the original one. The efficiency of the shear for such break up of the particles depends on the how well the force can be transmitted from the matrix to the disperse particles. This is a function of the viscosities of both the matrix and the particles.

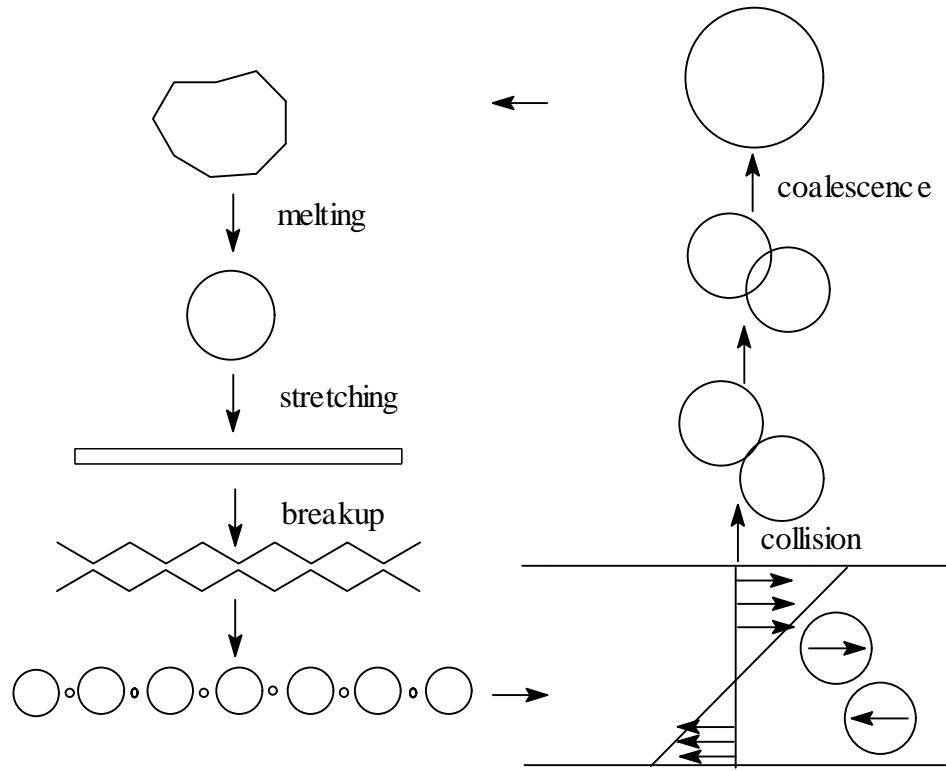


Figure 1.4. Schematic representation of the process occurring during the melt blending of two polymers

The ratio of the viscous force to the surface force is called the capillary or Weber number and is given by:

$$C_a = \frac{\eta_m G a}{\sigma} \quad \text{Eq. 1.4}$$

Where η_m is the matrix viscosity, G is the shear rate, a is the average particle size.

The critical value of C_a at which the particles will break up depends on the ratio of the particle viscosity to that of the matrix, with a minimum at a ratio of 1. At a given shear rate, only 'a' can vary in C_a , so the steady state size of the particles varies with the viscosity ratio.

The treatment of particle break up is done in terms of a single particle and ignores the effects of number of particles present as represented by blend composition. This is important because of particle coalescence, which may be expected to be more common as there is a greater density of particles and so a greater chance for two particles to collide.

Elmendorf and Maalcke⁴³ and Elmendorf and van der Vegt⁴⁴ have considered the probability for two particles to come into close proximity, the process by which all of

the matrix materials between them can be squeezed out and the final merging of the two into a single particle. Cigana et al⁴⁵ show by studies on blends of polystyrene and ethylene-propylene rubber (EPR), how the particle size increases as the concentration of the dispersed phase (EPR) increased. One would expect that the greatest effect of compatibilizers is to reduce the ability of two nearby particles to merge together into a single larger one. Sundararaj and Macosko⁴⁶ have also shown the importance of coalescence in PP/PS mixtures showing that the sizes of the phase domains increased with increasing concentration of the dispersed phase. Recent evidence by Beck et al⁴⁷ suggests that the main action of the compatibilizer is to prevent coalescence of droplets brought into collision by the mixing flow.

1.3.2.5 Measuring miscibility and compatibility

As the heat of mixing is very very small for polymers (entropy of mixing is negligible) it is impossible to measure directly the extent of miscibility by routine calorimetric parameters.

One of the most common ways to determine miscibility is the glass transition temperature (T_g). The T_g of the blend is different from those of the pure components only if the components are mixed on the molecular scale. Generally, if the blend displays two T_g 's at or near the same temperatures of the two components, then it is incompatible. On the other hand, if it shows a single transition at a temperature intermediate between those of the pure components, then the blend is compatible. The advantages of this technique is that it is relatively easy to perform. However, it is limited to blends of materials that have significantly different T_g 's (at least about 30 °C). Furthermore, this measurement provides no quantitative information about the degree of compatibility found in the blend.

There are a number of ways in which Flory interaction parameter, χ , can be measured for a miscible blend. The most useful technique is to directly measure χ by small angle neutron scattering^{48, 49}. This technique requires deuterium labeled polymers and can result in quantitative determination of χ for a wide range of polymer system.

Estimating the degree of compatibility in all immiscible blends needs some measure of the sizes of the phase domains under a given set of conditions. There are two main techniques, light scattering and microscopy. Light scattering is useful because the typical size of polymer blend domains is around a micron, similar to the wavelength

of light. If the difference in refractive index between the two components is sufficiently large, the phase separated blend will scatter light with a maximum in intensity at an angle corresponding to the average size of the phase domains^{50, 51}. The need for a minimum refractive index difference is the limitation of this method, but the advantage is that it can be adapted to a wide variety of conditions. It can be used during shearing in a rheometer⁵² to observe how the size of the phases changes under stress. Small angle X-ray scattering (SAXS)^{53, 54} and wide angle X-ray scattering (WAXS) is very effective in determining polymer blend morphology.

The most widely used and most direct measure of phase size is microscopy. For large phases (several micron or larger) optical microscopy can be used. Phase contrast such as by difference in refractive index or birefringence is needed in this technique. This is the easiest microscopic technique but it is limited to large phases. Since in compatibilization one is trying to make the phase smaller, often less than a micron, this is a significant limitation. Electron microscopy in all its several forms has been very useful to show the size of polymer blend phases and so its degree of compatibility. A number of methods are available⁵⁵ to provide contrast in such blends, and it is possible to measure domain sizes as small as 10 nm.

1.3.2.6 Properties of multiphase polymer blend

- (i) For a miscible blend most physical properties are close to a linear average of those of the two components. Most of the basic characteristics, such as T_g , density, plateau modulus and crystallinity also are intermediate between those of the components.
- (ii) In the case of multiphase blends one can expect to find synergy, that is, a situation in which some property of the blend is significantly greater (or less) than that of either component. The morphology of the immiscible blends adds another factor, which can alter the properties by a large amount from the average of those of the components. The interface between the phases can represent a weakness across which stress can not be transmitted. One of the advantages of using of compatibilizers, is to increase the adhesion between the phases as well as to decrease the interfacial tension, so that the interfacial weaknesses are reduced.
- (iii) The main determinant of the properties is the size and shape of the phase domains. The most important is rubber toughening of plastics. The inclusion of a dispersed rubber phase into a plastic matrix can dramatically enhance its impact strength. The toughness is maximized at some particle size, which varies from a few

tenths of a micron to a few microns. The value depends on toughening mechanism (crazing or shear yielding) and the volume fraction of rubber. The mechanism of compatibilization is thus, a control of rubber phase size which in turn determines the toughness of the blend.

(iv) The domain size can be important for other properties as well (e.g. optical property). If the dispersed particle size is kept small enough then the blend will not scatter light and so it will be clear. Transport properties can also be affected by the size and shape of the domains. Mechanical behavior other than failure properties such as toughness are generally not dependent on particle size. For example Young's modulus of a blend can be shown to be a function of only the matrix and is independent of the size of the dispersed phase⁵⁶.

1.3.3 Polymer blend interfaces

Recently, in multiphase blend much attention has been focused on the interfacial region between the phases. The reasons are (i) the interactions between the phases occur across the interface; hence the driving force for phase separation is located here. This is expressed as an interfacial tension between the phases and one of the main mechanisms of compatibilization is the reduction of the interfacial tension between the phases. (ii) The mechanical behavior of the multiphase system will depend critically on the nature of the interface and its ability to transmit stress from one phase to other.

1.3.3.1 Theory of the interface

The basic physics of blend interfaces involves the balance of two forces. Consider a case where the blend consists of homopolymers of A and B units. The first force arises from the interaction of the A and B units as represented by the parameter χ and leads to the phase separation in the first place, since there is clearly a driving force to reduce the volume over which there is a significant amount of A-B interactions. This can be done by reducing either the interfacial area (by increasing domain size or making the domains more spherical) or the interfacial thickness. The polymeric interfaces are often substantially larger (the interfacial tensions significantly lower) because of the second force, which is related to the configurational entropy of both A and B chains. If interface is as thick as a monomer, this extreme sharpness would impose significant restrictions on the configurations available to those chains near the

interface, resulting in a reduction in the entropy of the polymers. As a result, the interfaces must become somewhat thicker, often of the order of the size of the polymer coils. This increases the number of A-B interactions and hence some sort of balance needs to be achieved between these two forces. The calculation of this balance is the main focus of the various theories.

Helfand's theory: The original work on these calculations was performed by Helfand and Tagami⁵⁷. Let us consider a molten, immiscible, binary blend of polymers A and B, without compatibilizer. Helfand and Tagami⁵⁷, Helfand⁵⁸, Roe⁵⁹ and Helfand and Sapse⁶⁰ have developed quantitative lattice theories of the interphase that still provide a good basis for understanding.

Helfand and Tagami model is based on self-consistent field (SCF) that determines the configurational statistics of the macromolecules in the interfacial region. At the interface, the interactions between statistic segments of polymers A and B are determined by the thermodynamic binary interaction parameter, χ . Since the polymers are immiscible, $\chi > 0$, there is 'repulsive' effect of that must be balanced by the entropic effects that force chains A and B to intermingle. In the mean-field approach: (i) the polymers were assumed to have the same degree of polymerization, (ii) the equations derived for the segmental density profile, ρ , where $i = A$ or B , was solved for infinitely long macromolecules, $M_w \rightarrow \infty$, (iii) the isothermal compressibility was assumed to be negligibly low, (iv) there was no volume change upon blending. The basic scale of the interfacial thickness is provided by Δl which is related to χ and the statistical segment length, b (assuming same for both components):

$$\Delta l_{\infty} = \frac{b}{(6\chi)^{1/2}} \quad \text{Eq. 1.5}$$

and the interfacial tension coefficient

$$\mathbf{g}_{\infty} = b r k T \left(\frac{\chi}{6} \right)^{1/2} \quad \text{Eq. 1.6}$$

where k is the Boltzman constant and T is the absolute temperature.

The Helfand-Tagami lattice theory predicts that (i) the product, $\gamma \Delta l$, is independent of the thermodynamic binary interaction parameter, χ , (ii) the surface free energy is proportional to $\chi^{1/2}$, (iii) the chain-ends of both polymers concentrate at the interface, (iv) any low molecular weight third component is repulsed to the interface and (v) the

interfacial tension coefficient increases with molecular weight to an asymptotic value, γ_∞ :

$$\mathbf{g} = \mathbf{g}_\infty - a_0 M_\psi^{-2/3} \quad \text{Eq. 1.7}$$

The success of this theory is in giving simple expression for the interfacial thickness and tension. There are several ways to extend this model, many of which have been done.

Noolandi's theory: Hong and Noolandi⁶¹ developed a theory, similar to that of Helfand, for interfacial region in systems comprising polymers A and B, as well as either a solvent or a diblock copolymer. Based on the lattice model, the theory uses the mean-field approximations and it is formulated using reduced equation of state variables. Finite molecular weight and conformational entropy effects were considered but the excluded volume was not. The resulting system of equations can be solved numerically for the interfacial composition profile, interfacial tension etc. At low molecular weights of the γ values correctly predicted, but for higher molecular weight the prediction was up to 20 % too high.

The interphase in block copolymer: Theories concerning block copolymer interfaces are complex, involving computation of the domain size, the interphase thickness, the structure and the order-disorder transition. Helfand and Wasserman⁶² using the narrow interphase approximation, showed that **Equation 1.5** is valid in the limit of infinitely immiscible blocks having $M_w \rightarrow \infty$. For large values of χZ_c (Z_c is the degree of polymerization), the narrow interface approximation is valid and the boundary thickness becomes similar to the domain thickness of an A/B mixture. The interfacial thickness Δl was derived as:

$$\Delta l = 2 \left[\frac{(\mathbf{b}_A^2 + \mathbf{b}_B^2)}{2\mathbf{c}} \right]^{1/2} \quad \text{Eq. 1.8}$$

with: $\beta_i^2 = (\rho_{oi} b_i^2)/6$ and $b_i^2 = \langle R_i^2 \rangle / Z_i$, where b_i is the Kuhn's statistical segment length, Z_i is the degree of polymerization, ρ_{oi} is the density and $\langle R_i^2 \rangle$ is radius of gyration of the block i. For identical chains and the lattice size $b^2 = \rho_i b_i^2$, **Equation 1.8** converts to **Equation 1.5**.

Leibler⁶³ showed that for di-block copolymers in the disordered state the critical condition for microphase separation is $\chi Z_c = 10.5$. Later the work was extended to block copolymers with diverse architecture – for diblocks $\chi Z_c = 10.5$ was confirmed,

but for tri-blocks $\chi Z_c = 8.86$ was computed, indicating poor miscibility⁶⁴. Recent theoretical analysis⁶⁵ indicates that for $\chi Z_c \geq 20$, Δl should decrease with Z_c to the limiting value given by **Equation 1.5**:

$$\Delta l = \Delta l_{\infty} \left[1 - \frac{(8 \ln 2)}{(\chi Z_c)} \right]^{1/2} \quad \text{Eq. 1.9}$$

Equation 1.8 and **1.9** are similar, but difference in the range of 40 % have been found in low χZ_c .

1.3.3.2 Measurement of interfacial tension

Knowledge of the interfacial tension is very important for understanding how to improve the performance of a compatibilized blend. The classical methods to determine γ all involve different ways to measure the shapes and the sizes of portions of one component in the presence of the other. This is because the interfacial energy is the product of the interfacial tension and the interfacial area, and so the minimization of the energy involves minimization of the area. Measuring the interfacial tension in the presence of a modifier is an important problem. In a typical blending process, the shear and elongation forces favoring the migration of the compatibilizer to the interface and lowering of the interfacial tension can occur. However, in the methods used to determine the interfacial tension, experiments are carried out under almost 'static' conditions and the migration of the interfacial modifier is more difficult since the modifier must be added to either the matrix or dispersed phase. Interfacial tension measurements have already shown that the addition of a suitable compatibilizing agent can significantly lower the interfacial tension.

Several methods have been developed to measure γ of low-viscosity liquids, for example filament breakup, rotating, pendant or sessile drop, du Nuoy ring light scattering etc. For polymeric melts these methods can be used in decreasing order of reliability. The pendant drop^{66, 67, 68} and spinning drop^{69, 70} techniques being mostly used. These two techniques are equilibrium methods and normally require long times and involve complicated experimental procedures. There are few methods available for measuring the interphase thickness, Δl , such as ellipsometry, microscopy and scattering.

Pendant drop method: A drop of liquid A is introduced into a bath of liquid B. The shape that the drop assumes at equilibrium will depend on a balance of gravitational forces, which tend to pull the drop downwards and elongate it and the interfacial ones, which tend to force it into a sphere in order to minimize the interfacial area. Modern image analysis techniques allow one to determine the shape of the drop quite precisely, so that γ for the mixture can be measured precisely as well. The technique has been used to study a large number of polymer systems, showing the effect of molecular weight⁷¹ and of end groups⁷² on γ . Anastasiadis et al⁷³ have reported for PS/p(S-b-B)/PB system that the interfacial tension was dramatically reduced by the addition of the diblock copolymer. This decrease was seen to be linear in the concentration of the diblock, up to its critical micelle concentration (CMC), in agreement with Noolandi and Hong⁷⁴. However, the need for the drop to come to an equilibrium shape severely limits the usefulness of this technique for high molecular weight polymers. For common molecular weights, the equilibrium time can be of the order of 10^6 sec. and so one might have to wait for weeks to get to the equilibrium shape for such polymers.

Spinning drop method: Here a drop of one liquid is placed inside another immiscible liquid, and the shape of the drop is monitored while it is spun⁷⁵. The deformation of the spinning causes the drop to move from a spherical shape to a more elongated one, which is resisted by the interfacial energy forces, so one can determine the value of γ . The limitations to this method are similar to those of the pendant drop, in that only low viscosity materials will come to an equilibrium shape in reasonable times. This technique has been used to look at the interfacial tension between two polymer solutions⁷⁶, but is not very useful for high polymers.

An extension of this method is the so-called 'spinning rod' technique⁷⁷ where the drop is placed on a thin rod to stabilize it. Higher viscosity liquids can be used in this method, but there are still severe restrictions to its use for polymer blends. The main restrictions is due to the long equilibration time.

Breaking thread method: A simpler and more expeditious technique is the breaking thread method, based on an analysis developed by Tomotika⁷⁸. The interfacial tension can be obtained by studying the break up of a molten polymer fiber embedded in another polymer via a mechanism known as 'capillary instability'. This analysis consists in quantifying the disintegration of an elongated thread, which is subjected to

a sinusoidal distortion. Chapleau et al⁷⁹ evaluated the interfacial tension between polyethylene and a polyamide using this technique. The objective was to study the effect of compatibilizing agent on the interfacial tension between PA and PE and in particular the problems related to migration of the modifier to the interface.

Liang et al⁸⁰ reports the interfacial tension values for LLDPE and PVC system using this technique. They have observed the direct dependence between dispersed phase size and interfacial tension as predicted by Taylor theory.

Another method that depends on the shapes of samples of the polymers in a multiphase situation is to observe the retraction of a fiber of one polymer imbedded in the melt of the other^{81, 82}. This theory relies on the fact that the shape with the lowest interfacial area is the sphere. In the first step a rod of one polymer (with higher T_g or T_m) is embedded in a melt of the other. The temperature is then raised so that the rod melts, and then the relaxation of the embedded polymer from a rod to a sphere is followed with time. The rate at which this takes place can be directly related to the interfacial tension, so that the time to complete the retraction is inversely proportional to γ . In the case of PS/PMMA blend⁸¹ the method has been shown to give a value in agreement with other techniques, with a precision of about 20 %. It has also been used to determine the molecular weight dependence of γ for these blends^{83, 84}. Even though this technique is limited to blends where both polymers melt above room temperature and for which there is sufficient optical contrast to see the particle shape clearly. This method seems to be quite useful for a large class of blends.

Another technique which does not depend on the change in the shape of a particle or drop of one polymer in contact with the other but, rather on a measure of the low frequency rheology of the blend. For a two-phase mixture of a pair of Newtonian fluids, Choi and Schowalter⁸⁵ have shown that the deformation of the droplets of one phase in the other gives rise to an elastic term. This is because the deformation of the drops from spheres to ellipsoidal shapes increases the interfacial area, and so the interfacial energy (at a fixed value of interfacial tension). This is quite apparent for such liquids, as there are no other sources of such an elastic response. For non-Newtonian fluids like polymers, it is more difficult to show that this can occur, but this has been done by several groups^{86, 87}. The basic result is that the same sort of expression holds for non-Newtonian as for Newtonian fluids, which means that it is more difficult to see this effect in polymer mixtures. The reason for this is the

elasticity that polymer melts show due to the entanglements of their chains, so in order for this interfacial tension effect to be measurable one must look at the behavior when the entanglement has relaxed, which is in the terminal region at low frequency. There has been a lot of progress in the last few years in the development of methods to measure γ for polymer blends, and values are becoming available on a large number of systems. The ability of compatibilizers to reduce the interfacial tension is clearly an important part of how they work.

1.3.3.3 Measurement of interfacial structure

The direct determination of the variations in the concentration of each component across the interfacial region is a much more difficult than the measurement of interfacial tension. By the developments in the theory of the compatibilization, there has been a good deal of progress recently which has allowed for the measurement of interfacial profiles.

Nuclear reaction analysis (NRA): One of the most important methods is NRA. It is necessary that one of the components be labeled with deuterium, while the other is not. A thin film of such a blend is produced, onto which is directed a beam of ^3He particles. The basis of this method is the reaction of ^3He nuclei with the deuterons, producing ^4He nuclei and protons, as well as a release of 18.35 MeV of energy. Since the energy spectrum of the incident ^3He particles can be made quite narrow, the spread of energies of out coming ^4He particles is mainly due to the fact that the reactions takes place at different depths, that is, the loss of energy by the ^3He going into the film, and by the ^4He on the way out, that determines the breadth of the energy spectrum of the detected ^4He . There is a direct correlation between the energy of a ^4He particle and the depth at which the nuclear reaction took place. The energy spectrum of the out coming particles can be translated into a depth profile for the deuterons and deuterated component. This technique can look down to depths of as much as a micron, with a resolution of 10-20 nm and so is quite useful for polymer blend interfaces. Zink et al⁸⁸ uses this technique to determine near surface composition profiles in isotopic polymer blends (hPS/dPS). The measured profiles are in good agreement with predictions of the Schmidt-Binder mean field theory. Grinten et al⁸⁹ studied the tracer diffusion of deuterated PS, (dPS), into natural hPS-P α MS (poly α -methyl styrene) as well as the diffusion of dPS-P α MS blends into hPS-P α MS

blends using NRA as a depth profiling technique. The diffusion constant was determined as a function of temperature and composition of blend of the tracer and the matrix. Straub et al⁹⁰ used NRA analysis as a tool for the determination of miscibility and diffusion behavior of deuterated poly(arylether sulphone) (d-PSU) and chemically modified PSUs which are potential compatibilizers for reactive blending.

Forward coil elastic scattering: A similar technique, and one which was applied to polymers prior to advent of NRA, is forward coil elastic scattering⁹¹ (FRES). Here ⁴He particles impinge on the polymer film, causing lighter nuclei (protons and deuterons) to recoil from the film. The energies of these lighter nuclei are detected, and as in NRA these spectra can be directly related to the depth profiles of the deuterated and protonated polymers. While FRES can look at depths on a scale similar to NRA, its resolution is only down to about 70 nm. Xu et al⁹² determines the areal chain density, (Σ), of random copolymers at the phase boundary by FRES technique of random copolymer of deuterated styrene and p-hydroxy styrene to strengthen the weak phase boundary between PS and poly(2-vinylpyridine) (PVP). Dai et al⁹³ measures the fracture toughness of an interface between PS and PVP reinforced with triblock copolymer (PVP-b-dPS-b-PVP) as a function of Σ , of the copolymer at the interface. The failure mechanisms of the interface are studied by FRES.

Neutron reflectivity: This method also involves the use of blends where one component is labeled with deuterium, while the other is not. The method is based on examination of the neutrons that are specularly reflected from a thin polymer film. Since the effective 'refractive index' for polymers with respect to neutrons is slightly less than one, at sufficiently low incidence angles there will be total reflection of the neutrons. The periodicity of the angular dependence of the intensity of these reflected neutrons can be directly related to the shape of the concentration profile of the deuterons (and thus the deuterated component) in the film. This technique is limited to smaller depths than NRA (on the order of 30 nm), but has greater resolution. It has been used for several blends such as PS/PpMS⁹⁴ (poly p-methyl styrene) and PS/PS-b-hPB/PE⁹⁵.

Small angle x-ray scattering: The thickness of the interface between two phases can be measured by small angle x-ray scattering (SAXS), provided there is sufficient contrast between the phases in electron density. This method looks at the deviations

in the scattering from Porod's law, which assumes an infinitely sharp boundary between the phases. From these variations a measure of the interfacial thickness can be derived. Perrin and Prud'homme⁹⁶ have used SAXS in this way to show that the interface of PS/PS-*b*-PMMA blends get thicker as more of the block polymer is added. This technique does not give detailed knowledge of the interfacial profile as do some of the other methods, but it can be used more broadly on a range of polymer blend systems.

Secondary ion mass spectroscopy: The last method is secondary ion mass spectroscopy (SIMS). Again the contrast between the components is provided by deuteration, and looks at the changes in the mass spectrum that come from the sample with time as the ion damage ablates the polymer from the surface down. This technique has a good resolution (~ 10 nm). Surface-induced spinodal decomposition is studied in film of dPS and hPS using dynamic SIMS⁹⁷. The amplitude of this process modified by a PI-*b*-PS diblock copolymer, which segregates predominantly to the surface when admix with isotropic PS blend. Time-of-flight SIMS (ToF SIMS) is used to study the surface morphology of partially miscible blends of ethylene-tetrafluoroethylene copolymer/poly(methyl methacrylate) (ETFF/PMMA)⁹⁸.

1.3.3.4 Measurement of interfacial strength and phase adhesion

The mechanical properties of a multiphase blend will depend to a large extent on the strength of the interfaces between the phase domains⁹⁹. Since these interfaces are often regions of low entanglement density with little interconnection between the phases, so they can be weak points in the blend. One of the benefits of compatibilization is the strengthening of these interfaces by binding the domains with covalent bonds. However, the direct measure of the interfacial strength is difficult.

There are few examples of measurement of the adhesion between two polymer interfaces by measuring the strength of welded joints of the polymer. Willett and Wool¹⁰⁰ reported that for the SAN/PC system the interfacial strength varies inversely with the interaction parameter as suggested by the Helfand-Tagami theory. Schaffer et al¹⁰¹ measured the interfacial strength using 'asymmetric double cantilever' technique. The asymmetric geometry is chosen in order to prevent the crack growth from propagating towards the more compliant material in the case of SAN blends. The asymmetry was achieved by the attachment (gluing) of the SAN side of the laminate to a rigid 2 mm thick aluminium plate. A single edged razor blade was

inserted into the interface between the PC and SAN layers at a constant rate of 100 $\mu\text{m/s}$ using a computer controlled stepping motor. The length of the resulting crack, which, propagate along the interface was measured using an optical microscope with a precision of 0.1 mm. The blade should be inserted sufficiently slowly so that the crack length achieved its equilibrium value.

The effect of reactive reinforced interface on the morphology and tensile properties of amorphous polyamide (a-PA) and SAN copolymer blend have been investigated using styrene maleic anhydride (SMA) as a reactive compatibilizer¹⁰². The anhydride group of SMA copolymer can react with the amine groups of PA and form *in situ* graft copolymers at the a-PA/SAN interfaces during the blend preparation. The interfacial adhesion strength of the reactive reinforced interface was evaluated quantitatively using an 'asymmetric double cantilever beam fracture' test as a function of SMA copolymer content using a model adhesive joint. The interfacial adhesion strength was found to increase with the content of SMA and then levels off. The authors reported that the tensile properties of polymer blend are highly dependent on the interfacial adhesion strength.

1.3.4 Block and graft copolymers

If a polymeric additive is to significantly change the compatibility of a polymer blend, then its molecules need to contain several long sequences, some of which are miscible with one component and some of with the other. This essentially means the compatibilizer need to be a block or graft copolymer (except in the rare case where a compatibilizer C is miscible with both A and B components, even though A and B are not miscible). There is a close analogy to the relation of the efficiency and structure of polymeric compatibilizers to that of low molecular weight surfactants¹⁰³. Both classes of molecules need to be interfacially active.

1.3.4.1 Synthesis

Block copolymer: A polymer which consists of blocks, or long sequences, of significantly different compositions which can covalently linked in a linear fashion. There is sharp change in composition at a bond which links two blocks together. The composition within a block should not vary greatly.

Block copolymer can be synthesized by various methods such as condensation polymerization¹⁰⁴, anionic¹⁰⁵ and cationic polymerization¹⁰⁶, Ziegler-Natta¹⁰⁷, group transfer polymerization¹⁰⁸ (GTP) and living free radical¹⁰⁹ methods.

Living anionic polymerization by sequential addition of monomers is the widely used and well accepted method for the synthesis of block copolymers. This is the most direct method for preparing well-defined block copolymers¹¹⁰. Several important aspects of these systems can be illustrated by considering the preparation of block copolymer, namely, the polystyrene- block- polydiene- block-polystyrene triblock copolymers. The goal of each step in this sequential synthesis is to prepare a block segment with predictable, known molecular weight and narrow molecular weight distribution without incursion of chain termination and transfer. The first step is simple alkyllithium initiated polymerization of styrene¹¹¹. A hydrocarbon solvent is required to obtain polydiene block segments with high 1,4-micro structures and low T_g . For living anionic polymerization at complete monomer conversion, the number average molecular weight is uniquely defined by the simple relationship

$$\bar{M}_n = \text{grams of monomer/ moles of initiator} \quad \text{Eq. 1.10}$$

It is apparent that impurity levels for solvent, monomer and equipment must be reduced to lower than millimolar amount to obtain the desired molecular weights. To obtain a block segment with narrow molecular weight distribution, $M_w/M_n \leq 1.1$ (28) in a living polymerization, it is necessary to use a reactive initiator that effects a rate of initiation competitive with or faster than propagation. Hsieh and McKinney¹¹² have shown that this condition is fulfilled for sec-BuLi but not for n-BuLi with styrene and diene monomers. In a three-stage block copolymer system, at the completion of each step a sample of polymer can be removed and characterized independently with respect to MW, MWD and composition. The second step is the sequential monomer addition which requires the carbanionic chain end of the first block initiates polymerization of the second monomer (diene). The monomer added at this step must be very pure to prevent significant termination of the active polystyryllithium chain ends, otherwise the final product will be contaminated with PS homopolymer and the MW of the second block will be increased because of a decrease in chain end concentration, in accord with **Equation 1.10**. The carbanion formed from addition of the second monomer must be either more stable or of comparable stability relative to the propagating carbanionic chain end corresponding to the first block segment. Thus

styrene and diene can crossover to each other. To obtain a narrow MWD for the second block, the rate of crossover to the second monomer (the initiation reaction for the second block) must be competitive with or faster than the propagation.

Graft copolymer: A polymer which contains blocks of different composition, which are not attached linearly but rather so that one end of one or more blocks is covalently linked to atoms within a block of different composition. The principal difference between graft and block copolymers lies in their structure. The efficiency of graft copolymers depend on the molecular weight, of the backbone as well as the pendant side chains, their molecular weight distributions, distribution of the grafted chain along the polymer chain and on the extent of grafting. In general, there are two different approaches for the synthesis of graft copolymers. In one method, the functional groups on the polymer backbone act as the initiator for the polymerization of another monomer. This method is generally referred to as 'graft from' method. The another one, 'graft onto' method, involves the termination of a growing polymer chain end by the functional group on the polymer backbone or by the coupling between the polymer having an end functional group with the pendant functional group on the polymer backbone. Graft copolymer can be synthesized by condensation polymerization¹¹³, and anionic polymerization¹¹⁴.

It has been demonstrated that anionic synthesis can be used to make star polymers where the arms of star are not chemically identical¹¹⁵. It is possible to make such a 'miktoarm star' or 'heteroarm star' or polymer where two arms are PS and PI and all of the arms are nearly monodisperse. Well-defined 'star-block' copolymer can also be made by living anionic polymerization technique¹¹⁶.

1.3.4.2 Structure and thermodynamics

One of the interesting features in block and graft copolymer is the spontaneous organization of their phases in the scale of 10 to 100 nm, often with a high degree of order. This is result of the covalent linkages between polymeric chain segments, which are chemically distinct. To reduce the enthalpy due to the unfavorable interactions between the unlike monomers, there is a driving force to phase separate, just as in a blend of homopolymers. However, this can only proceed so far, since the covalent bonds between the blocks or graft sections must be maintained, so the scale

of this 'microphase separation' must be similar to the molecules themselves. A great deal of effort has been expended into discovering the origins of these structures¹¹⁷.

The most characteristic feature of a block copolymer is the strong repulsion between unlike sequences even when the repulsion between unlike monomers is relatively weak. However, due to the molecular constraint that A and B chains are covalently bonded in AB block copolymer, the phase separation is restricted to the molecular dimension, giving rise to microdomains whose sizes are controlled by the block molecular weight. This is the phenomenon that is well-known as microphase separation. When the temperature is raised above the thermodynamic transition temperature (T_c) or the concentration of the polymer is lowered below the critical concentration (C_c), the effective repulsive potential or effective Flory-Huggins χ parameter (χ_{eff}) becomes lower than the critical value $\chi_{\text{eff}, c}$ required for maintaining the microphase-separated domain structure, resulting in an order-to-disorder transition (ODT) i.e., the transition involving dissolution microdomains into a disordered mixture.

The phenomena of block copolymer microphase separation are usually divided into two regimes, the weak and strong segregation limits. The former is the region near the transition from a disordered state where the microdomain is dissolved into a homogeneous mixture to one in which there is some ordering (the state where the microdomains exist). The latter region is far from the ODT, where there is little overlap of the distinct blocks and a very sharp interface between the microphases. Most of the polymer pairs are immiscible, therefore most block copolymers are generally found in strong segregation limit region.

A number of different morphologies have been found in microphase separated block copolymers. It was found that spherical domains occurred when there was only a small amount of one block or the other, cylindrical domains at higher volume fractions and lamellar morphology when the amounts of the two blocks were roughly equal¹¹⁸. In latter years another morphology has been discovered which is at the boundary between the lamellar and cylindrical morphologies, a cocontinuous structure called the 'ordered bicontinuous double diamond' (OBDD)^{119, 120}. **Figure 1.5** shows an indication of where each of these structures is found in PS-b-PI polymers with respect to PS volume fraction.

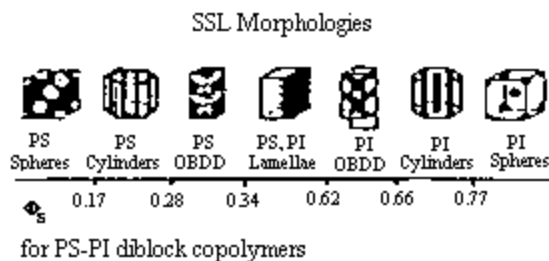


Figure 1.5. Block copolymer morphologies in the strong segregation limit, shown for PS-b-PI as function of styrene volume fraction

Similar structures are also found in graft copolymers¹²¹. The various kinds of morphologies can be found at significantly different volume fractions in the case of the graft copolymers than those established for blocks¹²². The thermodynamics of microphase separation in A-B block copolymers depends on the balance of three forces, one enthalpic and two entropic. The first of these is simply the unfavorable enthalpy due to the A-B interactions. In order to reduce the number of A-B nearest neighbor pairs, there will be a driving force to reduce the interfacial area where the links between the blocks are located. At the extreme, the A-B links will be packed very tightly at the minimum in interfacial area. However, this would force the blocks to stretch into an extended chain conformation, which greatly reduces their entropy. Finally there is also an entropic loss to the chains by the forced localization of the linking bonds in the interfacial volume. Thus a balance is established among these forces of the interface.

Helfand and Wasserman were able to numerically calculate where lamellar, cylindrical and spherical morphologies should be found and analytical solutions to this problem in the strong segregation limit have been performed by a consideration of the stretching energy of the chains¹²³. Milner¹²⁴ reports that OBDD is the most stable morphology in a region between those of cylinders and lamellae and same argument is used to show the dramatic shifts in the mapping of morphology onto volume fraction when graft copolymers are compared to blocks¹²⁴. There is more difficulty with the understanding of the weak segregation limit, that is, the region of phase space near the ODT.

Thus the microphase separation and the ODT in block and graft copolymers are used to help explain the ability of these polymers to modify the morphologies of polymer blends.

1.4 Theory of compatibilization

In the last fifteen years there has been a great amount of work in the theoretical understanding of compatibilization. Much of this has been based on the developments in the study of block copolymers, mainly, as to how diblock copolymers change the phase behavior of a blend and the calculations of the ability of the block copolymers to modify the interfacial tension and profile in a two phase blend. The theoretical studies have been carried out for block copolymer compatibilizer but the work on graft and alternating copolymer is also discussed.

1.4.1 Methods of compatibilization

A number of different approaches have been established for compatibilization: (1) achievement of thermodynamic miscibility, (2) addition of block or graft copolymer, (3) addition of functional/reactive polymers, (4) *in situ* grafting/polymerization (reactive blending)

1.4.1.1 Thermodynamic miscibility

This has been extensively discussed in **Section 1.3.2.2.**

1.4.1.2 Addition of block copolymers

The addition of block copolymers represents the most extensively researched approach for compatibilization of blends. The block and graft copolymers containing segments chemically identical to the blend components are obvious choice as compatibilizer.

1.4.1.2.1 Effect of diblocks on blend phase behavior

Based on the calculations of the microphase transitions in pure block copolymer system, Liebler¹²⁵ shows, how the phase separation of a blend of A and B homopolymers is affected by the addition of A-B diblock copolymers. For a symmetrical blend (i.e., equal degrees of polymerization for both components) without the diblock, the critical value of the interaction parameter is given by $(\chi N)_{\text{crit}} = 2$, where N is the degree of polymerization of either component (**Equation 1.3**). For pure A-B diblock, the critical value for the microphase separation is given by $(\chi N)_{\text{crit}} = 10.5$ where N refers to the total molecular weight of the diblock⁶³. This indicates that there is broad range of conditions (temperature, composition, molecular weight) where a blend will be inhomogeneous and phase separated while the corresponding

diblock is homogeneous and not separated. The basic physical reason for this is that the covalent bond is tying together the two blocks forces a certain level of A-B interactions no matter what the degree of phase separation, so there is less incentive on enthalpic reasons for the separation. Moreover, the diblocks pay an entropic penalty as they stretch away from the interface, which also reduces the advantages of separation. The balance of these two forces controls much of the behavior of diblock interfaces. The existence of this region of homogeneous diblocks but heterogeneous blends leads naturally to the question of whether the addition of diblocks to a blend under such conditions can change the heterogeneity of the system. Using mean field theory, Liebler¹²⁵ was able to show how the addition of the diblock increases the region of miscibility for the blend. But large amount of diblock is necessary to make a significant difference. When diblock is the one third of the total blend (i.e., equal amounts of all three components) the critical value of χN only changes 2 to 3. Thus the low levels of the added diblock of interest in compatibilization should have essentially no effect on the miscibility of the blend. The main conclusion is that one can expect little effect on phase behavior by the addition of one to five percent of a block copolymer.

1.4.1.2.2 Effect of diblocks on interfacial tension and structure

Noolandi and Hong¹²⁶ used a functional integral approach to calculate the interfacial tension and profile for the system containing A and B homopolymers, an A-B diblock and solvent. The interfacial tension, γ , is described as:

$$\mathbf{g} = \int dx (T_1 + T_2 + T_3) \quad \text{Eq. 1.11}$$

T_1 represents the contribution to γ from the A-B interactions in the system. It is assumed that these interactions do not depend on whether the units are on the homopolymer chains or on the diblocks. This term is a driving force for the separation of the A and B units and so increases γ . T_2 comes from the combinatorial entropy of the block copolymer chains. The junctions between the blocks are forced to be in the interfacial region, and this localization of the chains reduces their entropy. T_3 is due to the loss of conformational entropy in the homopolymer and copolymer chains near the interface. This entropy is reduced because the A chains and blocks cannot significantly penetrate the B-rich phase and vice-versa, so a number of their

possible conformations are not allowed. The last term is relatively insensitive to copolymer molecular weight.

From this calculations a number of features of the interfacial tension and profile is determined.

For example **Figure 1.6** shows how γ is reduced by the addition of block copolymers of various molecular weights. From this figure it is clear that only small amounts of diblock can have a dramatic effect on γ , and this effect is greater as the molecular weight of the block increases. This theory allows one to calculate the concentration profiles of the homopolymers and copolymer through the interfacial region. As the molecular weight of the diblock increases, it fills up more of the interfacial region, so the larger diblocks are more efficient at reducing γ . Israels et al¹²⁷ performed simulation and reported that the γ can be reduced to zero only if the blocks in the diblock are larger than the corresponding homopolymer. The one limitation on this is the tendency for the diblocks to form micelles inside one or the other of the two bulk phases, which will occur at a high concentration of the diblock copolymer.

A similar set of calculations were done by Vigils and Noolandi¹²⁸ for the case where the diblock is made from molecules that are different from those of the two homopolymers. This allows for the independent control of the various interactions that occur, so more control over the effectiveness of the compatibilizer.

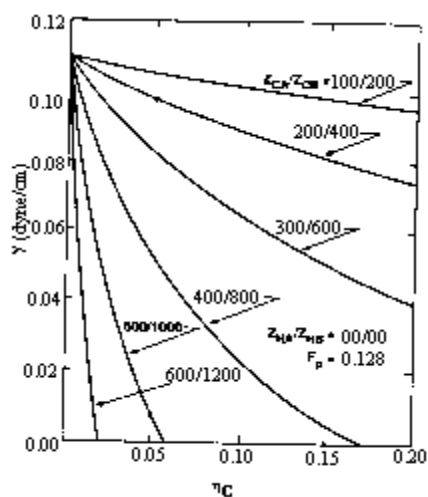


Figure 1.6. Variation on interfacial tension vs. concentration of added block copolymer for a variety of block molecular weight

Leibler¹²⁹ used a mean field approach to determine the interfacial tension and structure of (A/A-b-B/B) blends, which are near the point of miscibility. From this model γ is found as the difference of two terms. The first term, which increases γ , arises from the inhomogeneity of the concentration of the A and B units. The second, which reduces γ , comes from localization of the block copolymer at the interface. The basic results are quite similar to those on Noolandi and Hong as far as the efficiency of the diblock to reduce γ and the shape of the interfacial concentration profile.

The results have been extended to give more detailed descriptions of the features of the interface and their dependence on the characteristics of the diblock compatibilizer^{63, 130}. A different approach was taken by Wang and Safran¹³¹ to understand the effects of diblocks on the structure of blends. The ideas are based on the behavior of surfactants and consider the emulsifying effects of diblocks that are located at the interface of an immiscible blend. In this theory it is assumed that the diblocks would totally cover the interface. The effect of stretching of the blocks on the curvature of the interface is also considered. The larger the block, the greater it has to stretch when there is a high number of chains per unit of interfacial area. Thus, there is a driving force for the interface to curve away from the longer, to reduce the overall entropic loss of the diblock due to stretching. It is calculated that this curvature energy to be so large that, at equilibrium, the shape of the phase domains will be determined by it. For example, if A block is significantly larger than B block, the block copolymer interface will be curved to give disperse B spheres or cylinders, independent of the volume fraction of B homopolymer. Therefore, if there is a great majority of B with respect to A, there will be two macrophases at equilibrium, one with a A matrix and disperse B domains and the other is pure B phase. This is a direct analogy to microemulsions for small molecule surfactant systems. This theory also predicts the formation of lamellar, cylindrical and spherical domains either the A or B component in phase space. Since polymer system are generally far from complete equilibrium in terms of phase separation, this theory may have limited use for the understanding of compatibilization, but it may point to certain limiting cases that influence the growth and shape of phase domains.

Laradji and Desai¹³² studied the elastic properties of homopolymer/homopolymer interface containing diblock copolymer by means of a theory of Gaussian fluctuations. The interfacial tension and the bending rigidity of the interface in the two-phase

coexistence region are calculated from the power spectrum of capillary modes. γ increases monotonically with increasing χN (N is homopolymer molecular weight but bending rigidity does not. In the presence of diblock copolymers, the interfacial tension always decreases with increasing diblock copolymer volume fraction at a given χN . The bending rigidity can show either a decrease or an increase depending on χN and the ratio γ between the molecular weights of a diblock and that of a homopolymer.

1.4.1.3 Graft copolymers

Graft copolymers find wide range of applications as compatibilizer and interfacial agents. This is the most common form of compatibilizers. There is much less understanding of the detailed relation of the structure of these polymers and their utility as compatibilizers. The reason presumably is that it is much more difficult to prepare graft copolymers with well-controlled structures in terms of such variables as the length and number of arms. Moreover, it is difficult to extract the *in situ* prepared graft copolymer from the blend and hence is difficult to characterize its structure.

Olvera de la Cruz and Sanchez⁶⁴ considered the difference between linear diblocks and graft copolymers with a single arm with respect to their tendencies for microphase separation. There are three chains emanating from the junction point for such a graft copolymer, and, therefore a greater degree of overlap of the arms, even for the greatest degree of microphase separation. The critical value of χN is large than of 10.5 for the diblock, depending on the graft structure. This is due to the fact that the arms are more closely tied to the interface than for a diblock of the same molecular weight. This is relevant to the consideration of compatibilization since the greater coverage of the interface may lead to a greater efficiency for the graft on reducing the interfacial tension of the blend. On the other hand the arms of a graft polymer will not extend as far into the two phases and so not be as highly entangled with them as would those of a diblock would be expected to reduce the adhesion between the phases induced by the compatibilizer. This point has been made by Gersappe et al¹³³ who have performed simulation of graft and multiblock polymers at the interface of a blend. Their work has shown how the structure of these chains relates to their ability to cover the interface and to entangle with the blend components.

1.4.1.4 Alternating or multiblock copolymer

Less importance has been given to other forms of copolymers as compatibilizers. Block copolymer made up of many short blocks will not be able to entangle well with the phases. Efficiency is likely to be even less for alternating polymers. Noolandi and Chen¹³⁴ have shown that multiblock copolymer are more effective at reducing the interfacial tension than diblocks provided the blocks are long enough to entangle with the phases, and, thus do not force a large entropic penalty for the block copolymer. Yeung et al¹³⁵ have performed simulations to calculate the interfacial coverage of a series of copolymers, from diblocks to alternating structures. They found that highest efficiencies for both diblocks and alternating copolymers.

1.4.1.5 Addition of functional polymers

The addition of functional polymers as compatibilizers has been described by many workers¹³⁶. A polymer chemically identical to one of the blend components is modified to contain functional (or reactive) units, which have some affinity for the second blend component. This affinity is usually due to the ability to react chemically with the second blend component, but other types of interaction (e.g. ionic) are also possible. The functional modification may be achieved in a reactor or via an extrusion modification process. Thus, on grafting maleic anhydride or similar compounds to poly(olefin)s, the resulting pendant carboxyl acquire the ability to form a chemical linkage with poly(amide)s via a thermal reaction with end amino group of poly(amide)s.

1.4.1.6 Reactive compatibilization

A comparatively new method of producing compatible thermoplastic blends is via reactive blending which relies on the *in situ* formation of copolymers or interacting polymers at the interface of the blends during melt blending¹³⁷. Compared to batch-type melt mixers, continuous processing equipment such as single- or twin-screw extruders are often preferred for reactive blending. Continuous processing equipments have several advantages like excellent temperature control, continuous production as well as the provision for the removal of unwanted reaction products by devolatilization.

A number of reactive blending mechanisms may be exploited, such as

(i) formation of *in situ* graft or block copolymer by chemical bonding reactions between reactive groups on component polymers (also possible by the addition of free radical initiators), (ii) formation of a block copolymer by an interchange reaction in the backbone of the components (this is common in condensation polymers), (iii) mechanical scission and recombination of component polymers to form graft or block copolymers, (iv) Promotion of reaction by catalysis. The area of reactive blending is one in which there is currently a great deal of developmental activity and much proprietary knowledge. A very good review on 'strategies for compatibilization of polymer blends' by Koning et al^{137a} has recently been published.

1.4.2 Effect of molecular architecture of compatibilizer

One of the important question in the area of polymer compatibilization is the role of molecular characteristics of the copolymer, such as molecular weight, chemical composition and architecture, on the efficiency of compatibilization of a given polymer blend. Previous results have shown that in the case of diblock copolymers the more symmetrical the two blocks are and higher their molecular weights, the more effective such copolymers are at reducing the interfacial tension at the blend interface⁴⁵.

Concerning the architecture, the diblock copolymers are more effective compatibilizers than the corresponding triblock, star or graft copolymers¹³⁸. PE/PS blends have been modified by hydrogenated PB-b-PS copolymers of various molecular architectures. This general A/B/A-b-B system has been extensively studied by Fayt et al¹³⁸. On the basis of LDPE/PS blends of two extreme compositions (80/20 and 20/80), it was shown that the efficiency of hydrogenated PB-b-PS is poor, particularly with respect to elongation at break. Triblock copolymers of a radial or linear structure, with a major central HPB block, are either more efficient or less efficient than the grafted copolymer depending on the binary blend composition. When LDPE forms the continuous phase (LDPE/PS 80/20), those copolymers have some beneficial effect on both tensile strength and elongation at break. Diblock copolymers are far more efficient in compatibilizing LDPE and PS over the whole composition range. This superiority is ascribed to the less drastic conformational restraints at the interface and their ability to intimately intermingle with the homopolymer chains. This condition is essential to impart high elongations at break and impact energies, which result from the strong mutual anchoring of the phases.

Finally, the internal structures of diblock copolymers also have an effect on the ultimate properties of blends. Although there is a sharp transition from one block to other one when diblock copolymers are prepared by the sequential addition of the two monomers, this transition may be made more progressive by changing the copolymerization recipe, and the final copolymer is then referred to as a 'tapered' copolymer. Fayt et al¹³⁸ showed the superiority of a tapered variant of HPB-b-PS over the parent pure diblock. Moreover, the lower melt viscosity of the tapered diblock allows the final morphology and the properties to be reached in a much shorter processing time, which is an additional advantage. Cigana and Favis¹³⁹ determined the relative efficacy of diblock and triblock copolymers for a PS/EP rubber interface. Their results show that at 90/10 and 80/20 ratio of PS/EPR blend composition, a diblock copolymer attains a similar critical concentration for interfacial saturation and equilibrium particle size on the emulsion curve. The area, occupied per molecule of diblock modifier is identical at 5.6 nm² despite the fact that the 80/20 system contains twice as much modifier, based on the total blend volume as the 90/10 blend at the critical concentration. This indicates that almost all of the diblock modifier finds its way to the interface. The triblock copolymer is a better emulsifier than the diblock at 90/10 PS/EPR system as shown by the lower C_{crit} and equilibrium particle size (d_{eq}). But when the amount of triblock modifier is doubled in the 80/20 blend, the C_{crit} and d_{eq} values increase considerably with the apparent interfacial area decreasing from 27 to 5.8 nm². This indicates that modifier is not reaching the interface and micelle formation has occurred.

Very recently Lyatskay et al¹⁴⁰, using a self consistent mean field method and analytical theory, have compared a diblock copolymer, a random copolymer, a four-armed star and various combs with fixed molecular weights and composition in terms of their compatibilization efficiency. They conclude diblocks offer the best emulsifying activity. Haubler et al¹⁴¹ used a multiblock copolymer for the compatibilization of immiscible PSU/LCP blends. By using PSU/LCP multiblock copolymers with different molecular weights of the blocks in the appropriate binary, solution-casted blends, it was shown that the interpenetration of the polysulphone phases of the block copolymer and the PSU matrix leads to an improved miscibility of the blend. This effect is retained in ternary blends of PSU, LCP and the multiblock copolymer, assuming a certain critical molecular weight of the multiblock copolymer.

segments. Some mechanical characteristics of PSU/LCP blends such as E-modulus and fracture strength are improved by adding long-segmented multiblock copolymers. Recently, star-shaped block copolymers with a novel architecture named 'heteroarm star copolymer' have been synthesized by anionic polymerization methods^{115, 142}. These polymeric species are star polymers of the general formula A_nB_n bearing two different chemical arms which emanate from a very dense poly(divinyl benzene) core, or other types of junction points^{143, 144}. Recently, the ability of the heteroarm star copolymers act as emulsifying agents in an A/B polymer blend have been studied^{144, 145}. It is reported that heteroarm star copolymers, although exhibiting a complex architecture, migrate easily to the blend interface and reduce the interfacial tension. As a result significant decrease of the microdomain size of the dispersed phase is observed.

1.4.3 Determination of compatibilization

A key component in the development of any compatibilizer is a method of measurement of its efficiency. This involves several aspects such as the location of the compatibilizer (that is, whether it has reached to the interfacial region and if how much it is present), its effect on blend morphology and the growth of phase domains and the resulting physical properties of the blend. There are various characterization techniques that are useful in such a study.

1.4.3.1 Effect on morphology

The main goal of compatibilization is to enhance the compatibility of the blends, as measured by changing the degree of dispersion of the phases in the blend.

1.4.3.1.1 Presence at interface

All of the proposed mechanisms of action of compatibilizers depend on their presence at the interface between the components of the blends. This is true irrespective of whether the compatibilizer is needed to reduce the interfacial tension by separating the two immiscible components or it operates by a mechanism of steric stabilization to prevent the agglomeration of phase domains or it enhances the phase adhesion. Interfacial thickness is very important in determining the efficiency of a compatibilizer, but it is difficult to measure. This is because the layer of compatibilizer is too thin to image microscopically. Furthermore, the parts of the compatibilizer (blocks, arms, backbones) are generally chemically identical to the

components of the blend, which makes it hard to distinguish the compatibilizer from the rest of the sample. For these reasons direct evidence of a compatibilizer at a blend interface has only been obtained rarely. The first publication of such evidence was by Fayt et al¹⁴⁶ for blends of PS/PE modified by poly(hydrogenated butadiene-block-isoprene-block-styrene) (HPB-b-PIP-b-PS) triblock copolymer, the interfacial thickness indicated by the stained PIP block is about 10 nm. Yukioka and Inoue¹⁴⁷ studied the *in situ* reactive compatibilization of amorphous nylon and poly(styrene-co-maleic anhydride) (SMA) blend and single-phase mixture of SMA with poly(styrene-co-acrylonitrile) (SAN). By means of time-resolved ellipsometric analysis they investigated the change of interfacial thickness during annealing at a high temperature. Their results showed that the interface established at late stages was thick ranging from 10-50 nm.

Very recently Zhao and Huang¹⁴⁸ have reported the same observation for PB/PMMA/PB-b-PMMA system that the diblock copolymer chains distribute at the interface and the thickness is around 25 nm as determined by TEM.

Another study by Shull et al^{130, 149} on polystyrene / poly(2-vinyl pyridine) (PS/PVP) blends with added polystyrene-block-poly(2-vinylpyridine) (PS-b-PVP) diblock has shown the ability of a block copolymer to migrate to the interface of a blend. They made thin films (on the order of 200 nm) of the homopolymers and the block copolymer (or a blend of the diblock and one of the homopolymers) and used 'forward recoil spectroscopy' to determine the distributions of each component after different lengths of annealing times. They were able to show that the diblock would migrate over such distance to become located at the interface at time scales of the order of hours. Their results fit well with the ideas of Helfand and Tagami.

1.4.3.1.2 Domain size

From the discussion in **Section 1.3.2.5**, it is clear that the main measure of the degree of compatibility in a blend is the size of the phase domains under a given set of conditions. According to Paul¹⁵⁰ properly chosen compatibilizer should permit finer dispersion of minor phase during mixing and provide a measure of stability against gross segregation.

One of the main goals for compatibilization is not to render the blend homogeneous but rather to control the degree of heterogeneity so to reduce the size of the phase domains found in it. The crucial step in the determination of how well a particular

compatibilizer is working is to characterize its effect on the size of the domains in the multiphase blend. Since the size of interest is in the general range from 10 nm to 10 μm , the main techniques are microscopy (**Section 1.4.3.1.3**), especially, electron microscopy and scattering, especially, light and X-ray (**Section 1.3.2.5**). These techniques have been reviewed by Sawyer and Grubb⁵⁵ and Wignall⁴⁸.

1.4.3.1.3 Microscopy

The microscopic method can be divided into three categories: (i) optical or light microscopy (OM), (ii) scanning electronic microscopy (SEM), and (iii) transmission electron microscopy (TEM). In most cases some mode of sample preparation has to be used: viz. staining, extraction of one phase, etching, phase contrast etc. to increase the contrast between two phases. One of the most important aspect is the resolution needed to see the domains (TEM generally has the highest resolution and optical microscopy the least). It may be necessary to use a combination of techniques if the compatibilization is very effective in greatly reducing the domain sizes. Secondly, the chemical nature of the components will be critical as this will determine the effective means of providing contrast. For example a large difference the degree of unsaturation between the components will allow for the use of OsO_4 staining for electron microscopy. Often the mechanical properties of the blend are important, as they will determine whether the sample can be properly microtomed without deformation. Again, the continuity of the phases can be an important determinant as to which technique will be useful. If the contrast is provided by the extraction of one of the components (commonly used when one component is crystalline and another is amorphous), then clearly this can not be done when the extractable one is the continuous phase as the sample will fall apart.

Scanning electron microscopy (SEM): SEM is the most prevalently used method for the study of polymer blends. It can give information on surface topography of the materials. It can reveal the level of interfacial adhesion of different phases in polymer blends. The shape, size and degree of mixing of dispersed phase can be investigated by SEM. The great advantages of this technique are rapidity, range of readily accessible magnifications and depth of field.

Transmission electron microscopy (TEM): TEM provides information on the fine structure of materials down to the atomic or molecular levels. Preparation of the samples for observation under TEM is more tedious and exacting. The specimens have to be hardened and stained with OsO₄ or RuO₄, microtomed into thin slices ($\geq 20\text{ }\mu\text{m}$), mounted on a grid and polymeric film support and measured. The surface morphology can also be observed under TEM by cryogenic shadow casting and/or replication methods. Here also etching is frequently used to enhance the morphological details.

Optical microscopy (OM): Optical microscopy is carried out on solids and solid-liquid mixtures at magnifications up to about 2000X. A transmitted light beam that 'plane polarized' or is subjected to 'phase contrast' or to 'interference contrast' can be employed.

Light scattering, Neutron scattering, X-ray scattering can give quantitative informations about interaction between the phase (**Section 1.3.2.5**).

1.4.3.2 Mechanical properties

The most common reason for compatibilization is to toughen plastics by controlling the size of a dispersed phase (usually of an elastomer).

Changes in mechanical properties are often used as evidence of compatibilization. However, the relationship between morphology and the physical properties of a blend is not completely understood. In many cases the properties of a blend can be enhanced without affecting phase size due to other mechanisms. On the other hand, depending on factors such as T_g of the phases, in some cases phase size may be reduced without a change in a property such as toughness. Still an improvement in the physical properties of a blend can be considered as evidence of compatibilization.

1.5 Summary

The basic physical principles for compatibilization can be summarized as follows:

- (i) A compatibilizer needs to be a polymer that is made up of chemically distinct sections, some of which are miscible with one component and some with the other.
- (ii) The compatibilizer is most effective when its segments have a higher molecular weight than the corresponding components of the blend.
- (iii) Diblock copolymers are the most efficient form of compatibilizers.

- (iv) Graft copolymers are the most commonly used compatibilizers.
- (v) Compatibilizers improve properties of blends in several ways. They control the sizes of the domains in a multi phase blend by lowering the interfacial tension between the phases or reduce the agglomeration of domains by steric stabilization. An important effect of the use of compatibilizers is the increase in the adhesion between the phases and consequently improving the mechanical strength of the blend. The efficiency of the copolymers is limited by factors such as formation of micelles, diffusion rate to the interface and flow-induced variation of morphology.

1.6 References

1. Bonner, J. M.; Hope, P. S. 'Compatibilization and Reactive Blending', Folkes, M. J.; Hope, P. S. Eds., 'Polymer Blends and Alloys', Chapman and Hall, London, **1993**.
2. Utracki, L. A.; Weiss, R. A. 'Multiphase Polymers: Blends and Ionomers', ACS, Washington DC, **1989**.
3. Giles, H. F. 'Alloys and Blends' Modern Plastic Encyclopedia, **1986**, 105.
4. Manson, J. A.; Sperling, L. H. 'Polymer Blends and Composite', Plenum Press, New York, **1976**.
5. Paul, D. R.; Barlow, J. W. 'Copolymer Compatibility and Incompatibility: Principle and Practice', Solc, K. Eds., MMI Symposium Series, Howard Academic, New York, 3, **1981**.
6. Obalasi, O.; Robeson, L. M.; Shaw, M. T. 'Polymer-Polymer Miscibility', Academic Press, New York, **1976**.
7. Klempner, D.; Frisch, K. L. Eds., 'Polymer Alloy: Blends, Blocks, Grafts and Interpenetrating Network', Plenum, New York, **1977**.
8. Dutta, S.; Lohse, D. J. 'Polymeric Compatibilizers, Uses and Benefits in Polymer Blends', Hanser Pub., **1996**.
9. Prahsarn, C.; Jamieson, A. M. *Polymer*, **1997**, 38, 1273.
10. Cavanaugh, T. J.; Buttle, K.; Turner, J. N.; Nauman, B.; *Polymer*, **1998**, 39, 4191.
11. Mani, R.; Tang, J.; Bhattacharya, M. *Macromol. Rapid Comm.*, **1998**, 19, 283.
12. Majumder, B.; Paul, D. R.; Oshinski, A. J. *Polymer*, **1997**, 38, 1787.
13. Jin, D. W.; Shon, K. H.; Jeong, H. M.; Kim, B. K. *J. Appl. Polym. Sci.*, **1998**, 69, 533.
14. Kim, J. K.; Kim, S.; Park, C. E. *Polymer*, **1997**, 38, 2155.
15. Utracki, L. A. 'Polymer Blends and Alloys' Hanser Press, New York, **1990**.
16. Paul, D. R.; Newman, S. Eds., 'Polymer Blends', Academic Press, New York, **1978**.
17. Walsh, D. J.; Higgins, J. S.; Maconacchie, A. Eds., 'Polymer Blends and Mixtures' NATO ASI Series E, no. 89, Martinus Nijhoff Pulb., Boston,

1985.

18. Coran, A. Y.; Patel, R. *Rubber Chem. Technol.*, **1983**, 56, 1045.
19. Coran, A. Y.; Patel, R. *Rubber Chem. Technol.*, **1983**, 56, 210.
20. Nakatani, A. I.; Kim, H.; Takahashi, Y.; Han, C. C. *Polym. Comm.*, **1989**, 30, 143.
21. Rigby, D.; Lin, L. J.; Roe, R. J. *Macromolecules*, **1985**, 18, 2269.
22. Takagi, Y. T.; Ougizawa, T.; Inoue, T. *Polymer*, **1987**, 28, 103.
23. Flory, P. J. *J. Chem. Phys.*, **1941**, 9, 660.
24. Kuhn, W.; *Kolloid-Zeitschrift*, **1936**, 76, 258.
25. Flory, P. J. 'Statistical Mechanics of Chain Molecules', Wiley-Interscience, New York, **1969**.
26. Lohse, D. J.; Fetters, L. J.; Doyle, M. J.; Wang, H.-C.; Kow, C. *Macromolecules*, **1993**, 26, 3444.
27. Edgecombe, B. D.; Stein, J. A.; Frechet, J. M. J.' Xu, Z.; Kramer, E. J. *Macromolecules*, **1998**, 31, 1292.
28. Bellinger, M. A.; Sauer, J. A.; Hara, M. *Polymer*, **1997**, 38, 309.
29. Pan, Y.; Huang, Y.; Liao, B.; Chen, M.; Cong, G.; Leung, L. M. *J. Appl. Polym. Sci.*, **1997**, 65, 341.
30. Brogly, M.; Nardin, M.; Schultz, J. *Macromol. Symp.*, **1997**, 119, 89.
31. Paul, D. R.; Barlow, J. W. *Polymer*, **1984**, 25, 487.
32. Krishnamoorti, R.; Graessley, W. W.; Balsara, N. P.; Lohse, D. J. *J. Chem. Phys.*, **1994**, 100, 3894.
33. Londono, J. D.; Wignall, G. D.; Narten, A. H.; Honnell, K. G.; Yethiraj, A.; Schweizer, K. S. *Polym. Prep.*, **1993**, 34, 829.
34. Robard, A.; Patterson, D. *Macromolecules*, **1977**, 10, 1021.
35. Lohse, D. J.; *Polym. Eng. Sci.*, **1986**, 26, 1500.
36. Naumann, E. B.; Ariyapadi, M. V.; Balsara, N. P.; Grocela, T. A.; Furno, J. S.; Lui, S. H.; Mallikarajun, R. *Chem. Eng. Comm.*, **1988**, 66, 29.
37. Boen, S. N.; Bruch, M. D.; Lele, A. K.; Shine, A. D. 'Polymer Solutions, Blends and Interfaces; I. Noda and D. N. Rubingh, Eds., Elsevier, Amsterdam, **1992**.
38. Cumming, A.; Wiltzius, P.; Bates, F. S. *Phys. Rev. Lett.*, **1990**, 65, 863.
39. Kotnis, M. A.; Muthukumar, M. *Macromolecules*, **1992**, 25, 1716.

40. Hashimoto, T. 'Materials Science and Technology: A Comprehensive Treatment: Structures and Properties of Polymers' Cahn, R. W.; Hassen, P.; Kramer, E. J. Eds., John Wiley and Sons., New York, Chap. 6, **1994**, 12, 251.
41. Yoon, T.; Kim, B. S.; Lee, D. S. *J. Appl. Polym. Sci.*, **1997**, 66, 2233.
42. Grace, H. P. *Chem. Eng. Comm.*, **1982**, 14, 225.
43. Elmendrop, J. J.; Maalcke, R. J. *Polym. Eng. Sci.*, **1985**, 25, 1041.
44. Elmendrop, J. J.; van der Vert A. K. *Polym. Eng. Sci.*, **1986**, 26, 1332.
45. Cigana, P; Favis, B. D.; Jerome, R. *J. Polym. Sci., Polym. Phys.* **1996**, 34, 1691.
46. Sundararaj, U.; Macosko, C. W. *Macromolecules*, **1995**, 28, 2647.
47. Beck, N. G.; Tai, S. K.; Briber, R. M. *Polymer*, **1996**, 37, 3509
48. Wignall, G. D. 'Encyclopedia of Polymer Science and Engineering' John Wiley and Sons., New York, **1987**, 10, 112.
49. Reichart, G. C.; Graessley, W. W. Register, R. A.; Krishnamoorti, R.; Lohse, D. J. *Macromolecules*, **1997**, 30, 3363.
50. Chu, F.; Graillat, C.; Guillot, J.; Guyot, A. *Colloid. Polym. Sci.*, **1997**, 275, 986.
51. Charoensirisomboon, P.; Saito, H.; Inoue, T.; Weber, M.; Koch, E. *Macromolecules*, **1998**, 31, 4963
52. Wu, R.; Shaw, M. T.; Weiss, R. A. ACS Div. Polym. Mat. Sci. and Eng., Preprints, **1993**, 68, 264.
53. D'orazio, L.; Guarino, R.; Mancarella, C.; Martuscelli, E.; Cecchin, G. *J. Appl. Polym. Sci.*, **1997**, 65, 1539.
54. Lescance, R. L.; Fetters, L. J.; Thomas, E. L. *Macromolecules*, **1998**, 31, 1680.
55. Sawyer, L. C.; Grubb, D. T. 'Polymer microscopy" 2nd Ed. Chapman and Hall, New York, **1995**.
56. Datta, S.; Lohse, D. J. *Macromolecules*, **1993**, 26, 2064.
57. Helfand, E.; Tagami, Y. *J. Chem. Phys.*, **1972**, 56, 3592.
58. Helfand, E, *Macromolecules*, **1975**, 8, 552, *J. Chem. Phys.*, **1975**, 62, 999, *J. Chem. Phys.*, **1975**, 63, 2192.
59. Roe, R. J. *J. Chem. Phys.*, **1975**, 62, 490.

60. Helfand, E.; Sapse, A. *J. Chem. Phys.*, **1975**, 62, 1327.
61. Hong, K. M.; Noolandi, J. *Macromolecules*, **1980**, 13, 964, *ibid.*, **1981**, 14, 727, *ibid.*, **1981**, 14, 736.
62. Helfand, E.; Wasserman, Z. R. *Macromolecules*, **1976**, 9, 879, *ibid.*, **1978**, 11, 960, *ibid.*, **1980**, 13, 994.
63. Leibler, L. *Macromolecules*, **1980**, 13, 1602, *Makromol. Chem., Macromol. Symp.*, **1988**, 16, 1.
64. Olvera de la Cruz, M.; Sanchez, I. *Macromolecules*, **1986**, 19, 2501.
65. Spontak, R. J.; Zielinski, J. M. *Macromolecules*, **1993**, 26, 396.
66. Kamal, M. R.; Lai-Fook, R.; Demarquette, N. R. *Polym. Eng. Sci.*, **1994**, 34, 1834.
67. Hu, W.; Koberstein, J. T.; Lingelser, J. P.; Gallot, Y. *Macromolecules*, **1995**, 28, 5209.
68. Jo, W. H.; Nam, K. H.; Cho, J. C. *J. Polym. Sci., Polym. Phys.*, **1996**, 34, 2169.
69. Patterson, H. T.; Hu, K. H.; Grimstaff, T. H. *J. Polym. Sci., Part C*, **1971**, 34, 31.
70. Elmendrop, J. J.; De Vos, G. *Polym. Eng. Sci.*, **1986**, 26, 415.
71. Jalbert, C.; Koberstein, J. T.; Yilgor, I.; Gallagher, P.; Krukoni, V. *Macromolecules*, **1993**, 26, 3069.
72. Fleischer, C. A.; Koberstein, J. T.; Krukoni, V.; Wetmore, P. A. *Macromolecules*, **1993**, 26, 4172.
73. Anastasiadas, S. H.; Gancarz, I.; Koberstein, J. T. *Macromolecules*, **1989**, 22, 1449.
74. Noolandi, J.; Hong, K. M. *Macromolecules*, **1984**, 17, 1531.
75. Princen, H. M.; Zia, I. Y.; Mason, S. G. *J. Colloid Interfaces Science*, **1967**, 23, 99.
76. Heinrich, M.; Wolf, B. A. *Polymer*, **1992**, 33, 1926.
77. Than, P.; Preziosi, L.; Joseph, D. D.; Arney, M. *J. Colloid Interfaces Science*, **1988**, 124, 552.
78. Tomotika, S. *Proc. Roy. Soc. London (A)*, **1935**, 150, 322.
79. Chapleau, N.; Favis, B. D.; Carreau, P. J. *J. Polym. Sci., Polym. Phys.*, **1998**, 36, 1947.

80. Liang, H.; Favis, B. D.; Yu, Y. S.; Eisenberg, A. *Macromolecules*, **1999**, *32*, 1637.
81. Carriere, C. J.; Cohen, A.; Arends, C. B.; *J. Rheol.*, **1989**, *33*, 681.
82. Carriere, C. J.; Cohen, A. 'Controlled Interphases in Composite Materials', Eds., H. Ishida, Elsevier Sci. Pub., Amsterdam, **1990**, 781.
83. Ellingson, P. C.; Strand, D. A.; Cohen, A.; Sammler, R. L.; Carriere, C. J. ACS Preprints of Div. of Polym. Mat. Sci. and Eng., **1993**, *69*, 183.
84. Ellingson, P. C.; Strand, D. A.; Cohen, A.; Sammler, R. L.; Carriere, C. J. *Macromolecules*, **1994**, *27*, 1643.
85. Choi, S. J.; Schowalter, W. R. *Phys. Fluids*, **1975**, *18*, 420.
86. Palierne, J. -F. *Rheol. Acta*, **1990**, *29*, 204.
87. Graebing, D.; Muller, R. *Colloids and Surfaces*, **1991**, *55*, 89.
88. Zink, F.; Kerle, T.; Klein, J. *Macromolecules*, **1998**, *31*, 417.
89. van der Grinten, M. G. D.; Clough, A. S.; Shearmur, T. E.; Geoghegan, M.; Jones, R. A. L. *Polymer*, **1998**, *39*, 3623.
90. Straub, W.; Ermer, H.; Coen, M. C.; Mader, D.; Kressler, J.; Brenn, R.; Weber, M. *J. Polym. Sci., Polym. Phys.*, **1997**, *35*, 2083.
91. Genzer, J.; Composto, R. J. *Macromolecules*, **1998**, *31*, 870.
92. Xu, Z.; Kramer, E. J.; Edgecombe, B. D.; Frechet, J. M. J.; *Macromolecules*, **1997**, *30*, 7958.
93. Dai, C. -A.; Jandt, K. D.; Iyengar, D. R.; Slack, N. L.; Dai, K. H.; Davidson, W. B.; Kramer, E. J. *Macromolecules*, **1997**, *30*, 549.
94. Schnell, R.; Stamm, M. *Macromolecules*, **1998**, *31*, 2284.
95. Hermes, H. E.; Bucknall, D. G.; Higgins, J. S.; Scherrenberg, R. L. *Polymer*, **1998**, *39*, 3099.
96. Perrin, P.; Prud'homme, R. E. *Macromolecules*, **1994**, *27*, 1852.
97. Rysz, J.; Bernasik, A.; Emer, H.; Budkowski, A.; Brenn, R.; Hashimoto, T.; Jedlinski, J. *Euro. Phys. Lett.*, **1997**, *40*, 503.
98. Weng, L. -T.; Smith, T. L.; Feng, J.; Chan, C. -M. *Macromolecules*, **1998**, *31*, 928.
99. Inoue, T.; Suzuki, T. *J Appl. Polym. Sci.*, **1996**, *59*, 1443.
100. Willett, J. L.; Wool, R. P. *Macromolecules*, **1993**, *26*, 5336.
101. Schaffer, M.; Janarthanan, V.; Deng, Y.; Seala, J. L.; Guo, L.; Rafailovich,

- M.; Sokolov, J.; Stein, R. S.; Strzhemechny, Y.; Schwarz, S. A. *Macromolecules*, **1997**, *30*, 1225.
102. Cho, K.; Seo, K. H.; Ahn, T. O. *J Appl. Polym. Sci.*, **1998**, *68*, 1925.
 103. Eastmond, G. C. 'Polymer Surfaces and Interfaces', Eds., Feast, W. J.; Munro, H. S.; J. Wiley, New York, **1987**, ch. 6, 119.
 104. Adamas, R. K.; Hoeschele, G. K. 'Thermoplastic Elastomer: A Comprehensive Review' Eds., Legge, N. R.; Holden, G.; Schroeder, H. E.; Hanser, Munich, **1987**, ch. 8, 163.
 105. Hild, G.; Lamps, J. -P.; *Polymer*, **1998**, *39*, 2637.
 106. Mah, S.; You, D.; Cho, H.; Chai, S.; Shin, J. -H. *J Appl. Polym. Sci.*, **1998**, *69*, 611.
 107. Mulhaupt, R.; Duschek, T.; Rieger, B. *Macromol. Chem., Macromol. Symp.*, **1991**, *48/49*, 317.
 108. Sogah, D. Y.; Hertler, W. R.; Webster, O. W.; Cohen, G. M. *Macromolecules*, **1987**, *20*, 1473.
 109. Baethge, H.; Butz, S.; Schmidt-Naake, G. *Macromol. Rapid Comm.*, **1997**, *18*, 911.
 110. Morton, M.; Fetters, L. J. *Rubber Chem. Technol.*, **1975**, *48*, 359.
 111. Fetters, L. J.; Morton, M. 'Macromolecular Synthesis' Coll. Vol. *1*, Moore, J. A., Eds., Wiley, New York, **1977**, 463.
 112. Hsieh, H. L.; McKinney, O. F. *J Appl. Polym. Lett.*, **1966**, *4*, 843.
 113. Steurer, A.; Hellmann, G. P. *Polym. Adv. Technol.*, **1998**, *9*, 297.
 114. Feng, H.; Ye, C.; Tian, J.; Feng, Z.; Huang, B. *Polymer*, **1998**, *39*, 1787.
 115. Tsitsilianis, C.; Papanagopoulos, D.; Lutz, P. *Polymer*, **1995**, *36*, 3745.
 116. Bi, L.-K.; Fetters, L. J. *Macromolecules*, **1976**, *9*, 732.
 117. Bates, F. S.; Fredrickson, G. H.; *Annu. Rev. Phys. Chem.* **1990**, *41*, 525.
 118. Molau, G. E. 'Block copolymers' Eds., Aggarwal, S. L., Plenum Press, New York, **1970**.
 119. Hashimoto, T.; Ijichi, Y.; Fetters, L. J. *J. Chem. Phys.*, **1988**, *89*, 2463.
 120. Hajduk, D. A.; Harper, P. E.; Gruner, S. M.; Honeker, C. C.; Kim, G.; Thomas, E. L.; Fetters, L. J. *Macromolecules*, **1994**, *27*, 4063, (b) Sakurai, S.; Irie, H.; Umeda, H.; Nomura, S.; Lee, H. H.; Kim, J. K. *Macromolecules*, **1998**, *31*, 336.

121. Rabeony, M.; Peiffer, D. G.; Dozier, W. D.; Lin, Y. M. *Macromolecules*, **1993**, 26, 3676.
122. Hadjichristidis, N.; Iatrou, H.; Behal, S. K.; Cludzinski, J. J.; Disko, M. M.; Graner, R. T.; Liang, K. S.; Lohse, D. J.; Milner, S. T. *Macromolecules*, **1993**, 26, 5812.
123. Milner, S. T.; Witten, T. A.; Cates, M. E.; *Macromolecules*, **1988**, 21, 2610.
124. Milner, S. T. *Macromolecules*, **1994**, 27, 2333.
125. Liebler, L. *Makromol. Chemie., Rapid Comm.*, **1981**, 2, 393.
126. Noolandi, J.; Hong, K. M. *Macromolecules*, **1984**, 17, 1531.
127. Israels, R.; Jasnow, D.; Balazs, A.C.; Krausch, G.; Sokolov, J.; Rafilovich, M. *J. Chem. Phys.*, **1995**, 102, 8149.
128. Vigils, T. A.; Noolandi, J. *Macromolecules*, **1990**, 23, 2941.
129. Leibler, L. *Macromolecules*, **1982**, 15, 1283.
130. Shull, K. R.; Kramer, E. J. *Macromolecules*, **1990**, 23, 4769.
131. Wang, Z. -G.; Safran, S. A. *Journal de Physique*, **1990**, 51, 185.
132. Laradji, M.; Desai, R. C. *J. Chem. Phys.*, **1998**, 108, 4662.
133. Gersappe, D.; Harm, P. K.; Irvine, D.; Balazs, A. C. *Macromolecules*, **1994**, 27, 720.
134. Noolandi, J.; Chen, Z. Y. *Die Makromolekulare Chemie, Theory and Simulation*, **1992**, 1, 387.
135. Yeung, C.; Balazs, A.C.; Jasnow, D. *Macromolecules*, **1992**, 25, 1357.
136. (a) Aycock, D. F.; Ting, S. P. *US Patent no. 4600741*, **1986**, (b) *ibid.*, 4642358, **1987**.
137. Jeon, H. K.; Kim, J. K. *Polymer*, **1998**, 39, 6227.
- 137a Koning, C.; Duin, M. V.; Pagnoulle, C.; Jerome, R. *Prog. Polym. Sci.*, **1998**, 23, 707.
138. Fayt, R.; Jerome, R.; Teyssie, Ph. *J. Polym. Sci., Polym. Phys.* **1989**, 27, 775.
139. Cigana, P; Favis, B. D. *Polymer*, **1998**, 39, 3373.
140. Lyatskay, A.C.; Gersappe, D.;Gross, N.A. and Balazs, A.C. *J. Phys. Chem.*, **1996**, 100,1449.
141. Haubler, L.; Pospiech, D.; Eckstein, K.; Janke, A.; Vogel, R. *J. Appl.*

- Polym. Sci.*, **1997**, 66, 2293.
142. Pitsikalis, M.; Pipas, S.; Mays, J. W.; Hadjichristidis, N. *Advance in Polym Sci.*, **1998**, 1, 135.
 143. Avgeropoulos, C.; Poulos, Y.; Hadjichristidis, N.; Roovers, J. *Macromolecules*, **1996**, 29, 6076.
 144. Migata, K.; Watanabe, Y.; Itaya, T.; Tanigaki, T.; Inoue, K.; *Macromolecules*, **1996**, 29, 3694.
 145. Tsitsilianis, C.; Voulgaris, D.; Kosmas, M. *Polymer*, **1998**, 39, 3571.
 146. Fayt, R.; Jerome, R.; Teyssie, Ph. *J. Polym. Sci., Lett.*, **1986**, 24, 25.
 147. Yukioka, S.; Inoue, T. *Polymer*, **1994**, 35, 1182.
 148. Zhao, H.; Huang, B. *J. Polym. Sci., Polym. Phys.*, **1998**, 36, 85.
 149. Shull, K. R.; Kramer, E. J.; Hadziioannou, G.; Tang, W. *Macromolecules*, **1990**, 23, 4780.
 150. Paul, D. R., "Polymer Blends" Eds. D. R. Paul and S. Newman, Academic Press, New York, **1978**, Ch.12.

CHAPTER -II

OBJECTIVES OF THE PRESENT INVESTIGATION

2.1 Introduction

Polymer blends have received significant attention in recent years. Though blending is an elegant method to create new properties in polymers, it is complicated by the fact that most of the constituent polymers are immiscible and incompatible. Very often, the resulting materials exhibit poor mechanical properties due to incompatibility resulting from the lower entropy of mixing of high molecular weight polymers and the unfavorable enthalpic interaction between the constituent components. Enhancement in the degree of compatibility between the constituent components can be achieved by use of a compatibilizer. A block copolymer is very effective in reducing the interfacial tension and in improving the interfacial adhesion by entanglement or bridging different polymer chains near the interface. For the effective compatibilizing process, the interpenetration of segments of copolymers and blend components is necessary to achieve a strong mechanical adhesion caused by the reduction of the interfacial tension due to the presence of copolymers. This indicates that molecular architecture is an important parameter for achieving efficient compatibilities. Moreover, as each block of the copolymer is mixing with the corresponding homopolymers the adhesion between the A and B phases is strengthened, and therefore the mechanical properties of the blend are significantly improved.

Determination of compatibility in polymer blends is of considerable importance because manifestation of their superior properties depends on compatibility or miscibility of homopolymers at a molecular level. Many experimental and theoretical methods have been used to investigate polymer compatibility¹. There is a need to find simpler and quicker methods for determining compatibility². Homogeneous mixing on a molecular scale is a prerequisite for polymer compatibility. Though several blending procedures are available such as, melt,

dry and solution blending, the choice of solution blending for this study stems from the following: (1) equilibrium is established between the different polymer components in solution; and (2) viscosity is measured effectively. In this study the use of viscometric method and phase separation techniques is highlighted. A large number of investigations have been carried out on polymer blend miscibility by viscosity measurements of the corresponding ternary (polymer-polymer-solvent) systems³. The basis of this method, dilute solution viscometry (DSV), relies on the assumption that repulsive interaction may cause shrinkage of the macromolecular coils giving rise to a negative deviation of viscosity from additivity.

2.2 Objective of the present work

There are a number of reports in the literature on compatibilizing effect of block copolymer on heterogeneous blends⁴. The objective of the present work is to explore the compatibility of diblock copolymer of poly(styrene) and cis-poly(isoprene) (PS-*b*-PI) as a emulsifying agent for improving the compatibility of PS/NR blend. Previous work by Asaletha *et al.*⁵ used a NR-*g*-PS as a compatibilizer for NR/PS blends. The present study is aimed at the synthesis of linear PS-*b*-PI having different block length, and wide range of compositions using living anionic polymerization technique and examine the influence of block copolymer concentration, molecular weight of homo and copolymers, composition of block copolymers, its mode of addition and nature of the casting solvent on the morphology and properties of the blends. Attempts have been made to deduce the block copolymer conformation at the interface. Finally, the experimental results are explained based on the theories of Noolandi and Hong^{6,7}.

One of the important questions that has remained unresolved in polymer blends research relates to the role of molecular architecture on the performance of copolymer compatibilizer. There have been few experimental⁸⁻¹⁰ and theoretical¹¹ studies which examine compatibilizers with fixed molecular weights but possessing different architecture.

Recently 'heteroarm star polymers' have been synthesized by living anionic polymerization method⁸. These polymeric species are star polymers of the general formula A_nB_n bearing two different chemical arms diverge from a very dense poly(divinylbenzene) (DVB) core, or other types of junction points^{9, 12}.

Therefore, heteroarm star and star block copolymer, A_nB_n , of styrene and isoprene with varying number of arms and chemical compositions were synthesized by living anionic polymerization using *sec*-BuLi as initiator and DVB as coupling agent. The ability of heteroarm star polymer as an emulsifying agent on compatibilizing efficiency in A/B polymer blends was studied. The effect of molecular architecture on emulsifying ability was explored. A comparison of the interfacial activity of a linear diblock, heteroarm star and star block copolymer possessing similar arm molecular weight and composition has been made.

Dilute solution viscosity (DSV) measurement has been used as a tool to predict polymer-polymer compatibility. Chee's method was applied to determine ΔB and μ of polymer blend solution, where ΔB and $\mu \geq 0$ signifies miscibility and < 0 indicates phase separation. The influence of the nature of the solvent on the miscibility of polymer blend was also studied.

Compatibilizing effect of PS-*b*-PI in heterogeneous SAN/NR blend was studied. Blend morphology was observed by optical and scanning electron microscopy.

Comparison of particle size and impact strength of commercial HIPS and compatibilized blend of PS/NR/PS-*b*-PI having similar composition of HIPS was studied. Similarly, comparison of particle size and impact strength of commercial ABS and compatibilized blend of SAN/NR/PS-*b*-PI having similar composition of ABS was studied.

2.3 Approaches

- 2.3.1 Compatibilization study of PS-*b*-PI as emulsifying agent for PS/NR blends
 - 2.3.1.1 Synthesis of linear PS-*b*-PI of having different block length and chemical compositions
 - 2.3.1.2 Copolymers were characterized by SEC-RI and SEC-MALLS
 - 2.3.1.3 The effect of block copolymer concentration, molecular weight of homo- and copolymers, composition of block

copolymers, its mode of addition and nature of the casting solvent on the morphology and properties of the blends.

2.3.2 Evaluation of heteroarm star polymer (A_nB_n) as emulsifying agent for PS/NR blends

2.3.2.1 Heteroarm star polymer (A_nB_n) and star block $(AB)_n$ copolymers of styrene and isoprene with varying number of arms and chemical composition were synthesized by living anionic polymerization using sec-BuLi as initiator and DVB as coupling agent. The number of arms of star polymer was varied by changing the ratio of $[DVB]/[Li]$.

2.3.2.2 The influence of concentration of star polymer on morphology and mechanical property was studied. The effect of number of arms of star on emulsifying ability was also studied.

2.3.3 Molecular architectural effect of compatibilizers was studied using star- block, heteroarm star and linear diblock copolymer of PS and PI having similar arm molecular weight and composition.

2.3.4 DSV and phase separation techniques were used to predict polymer-polymer compatibility.

2.3.5 Compatibilizing effect of PS-b-PI in heterogeneous SAN/NR blend was studied. Blend morphology was studied by optical microscopy and SEM. Mechanical properties of compatibilized and uncompatibilized blends were studied.

2.3.6 Comparison with commercial polymer and compatibilized blends

2.3.6.1 Comparison of particle size and impact strength of commercial HIPS and compatibilized blend of PS/NR/PS-b-PI having similar composition of HIPS.

2.3.6.2 Comparison of particle size and impact strength of commercial ABS and compatibilized blend of SAN/NR/PS-b-PI having similar composition of ABS.

2.4 References

1. Krause, S. Polymer-Polymer Compatibility in Polymer Blends (Edited by D.R. Paul and S. Newman), Academic Press, New York, Vol. 1, **1978**.
2. Williamson, G. R.; Wright, B. J. *J. Polym. Sci.*, **1968**, 1, 260.
3. Mathew, M.; Ninan, K. N.; Thomas, S. *Polymer*, **1998**, 39, 6235.
4. Kim, J. R.; Jamieson, A. M.; Hudson, S. D.; Manas, Z. I.; Ishida, H. *Macromolecules*, **1998**, 31, 5383.
5. Asaletha, R., Thomas, S. and Kumaran, M. G. *Rubber Chem. and Tech.*, **1995**, 68, 671.
6. Noolandi, J. *Polym. Eng. Sci.*, **1984**, 24, 70.
7. Noolandi, J. and Hong, K. M. *Macromolecules*, **1984**, 17, 1531.
8. Tsitsilianis, C.; Voulraris, D.; Kosmas, M. *Polymer* **1998**, 39, 3571.
9. Miyata, K.; Watanabe, Y.; Itaya, T.; Tanigaki, T.; Inoue, K. *Macromolecules* **1996**, 29, 3694.
10. Edgecombe, B. D.; Stein, J. A.; Frechet, J. M. J.; Xu, Z.; Kramer, E. J. *Macromolecules* **1998**, 31, 1292.
11. Israels, R.; Foster, D. P.; Balazs, A. C. *Macromolecules*, **1995**, 28, 218.
12. Avrerpoulos, C.; Poulos, Y.; Hadjichristidis, N.; Roovers, J. *Macromolecules*, **1996**, 29, 6076.

CHAPTER-III

SYNTHESIS AND CHARACTERIZATION OF LINEAR AND BRANCHED POLYMERS VIA LIVING ANIONIC POLYMERIZATION TECHNIQUE

3.1 Introduction

Macromolecules possess a wide variety of applications, and their suitability for a given application is often determined by their specific structural and molecular parameters, such as molecular weight, molecular weight distribution and the nature and number of functional groups as well as its spatial location. The synthesis of macromolecules with well-defined structures has, therefore, received significant attention from the polymer chemist because of their potential applications.

Living anionic polymerization is an attractive technique which enables one to tailor-make macromolecules of well-defined structures, such as graft, block, star and ω -functional polymers. Such polymers find useful applications as compatibilizers for polymer blends, additives for lubricating oil, general purpose resins, adhesives, impact modifiers, processing aids etc.

A living polymerization is a chain polymerization that proceeds in the absence of chain transfer and termination reactions. The polymerization proceeds until all the monomer has been consumed and further addition of monomer results in continued polymerization. These characteristics of living polymerization provide the best means to control the primary structure of polymer chains and has, thus, emerged as the most preferred method for the synthesis of polymers with precise molecular architecture. Polymers with predictable molecular weights and nearly uniform chain lengths are obtained by this method. Well-defined block and graft copolymers, macromolecules with novel topologies, such as star, comb and macrocyclic polymers as well as end-functionalized polymers, are accessible by method of living polymerization. The potential importance, both academic and industrial, of such polymers has been well reviewed in the literature^{1, 2}.

Although the concept of living polymerization was anticipated by Flory, the first homogeneous anionic polymerization of styrene, free of termination and chain-transfer was reported by Szwarc³ in 1956. Based on innumerable scientific studies, a good understanding of anionic polymerization of hydrocarbon non-polar monomers such as styrene and dienes in apolar and polar solvent has been achieved⁴. The kinetics of the alkyllithium initiation reactions for styrene and diene polymerization in hydrocarbon solvent has been investigated extensively⁵⁻⁷. Other alkali metal derivatives are not soluble in hydrocarbon media. Although initiation rates are faster in polar solvents such as ether, decomposition reaction often occur in polar media and diene microstructure is quite dependent on solvent. The rates of alkyllithium initiation reactions with monomers are faster in aromatic than aliphatic solvents. Roovers and Bywater⁸ have reported that the rate of sec-BuLi initiated polymerization of isoprene is 2000 times faster in benzene than hexane at a concentration 10^{-3} (M). The kinetic order dependence is prevalingly first order in alkyllithium in aliphatic solvents, but fractional order dependence is observed in aromatic solvents. One of the most important observations is that lithium is unique among the alkali metals in providing polydienes with high 1,4-microstructure. For isoprene, this corresponds to >90 % cis-1,4-microstructure; for butadiene, it is a mixture of 39 % cis and 52 % trans content. High 1,4-microstructures for polydienes results in polymers which exhibit low T_g (e.g -64 to -70 °C for PI⁹ and -94 °C for PB¹⁰ [11% 1,2]); these polydienes with high 1,4-microstructure exhibit good elastomeric properties at room temperature and above. Very careful NMR studies of the active polydiene chain end have demonstrated that in hydrocarbon solvents the species may be identified as a 4,1-covalent polydienyllithium. The model proposed by Morton and co-workers¹¹ is shown in **Figure 3.1**. They suggested that the concerted reaction between the chain ends and the monomer could also account for the strong preference of the chain ends for dienes in copolymerization with styrene.

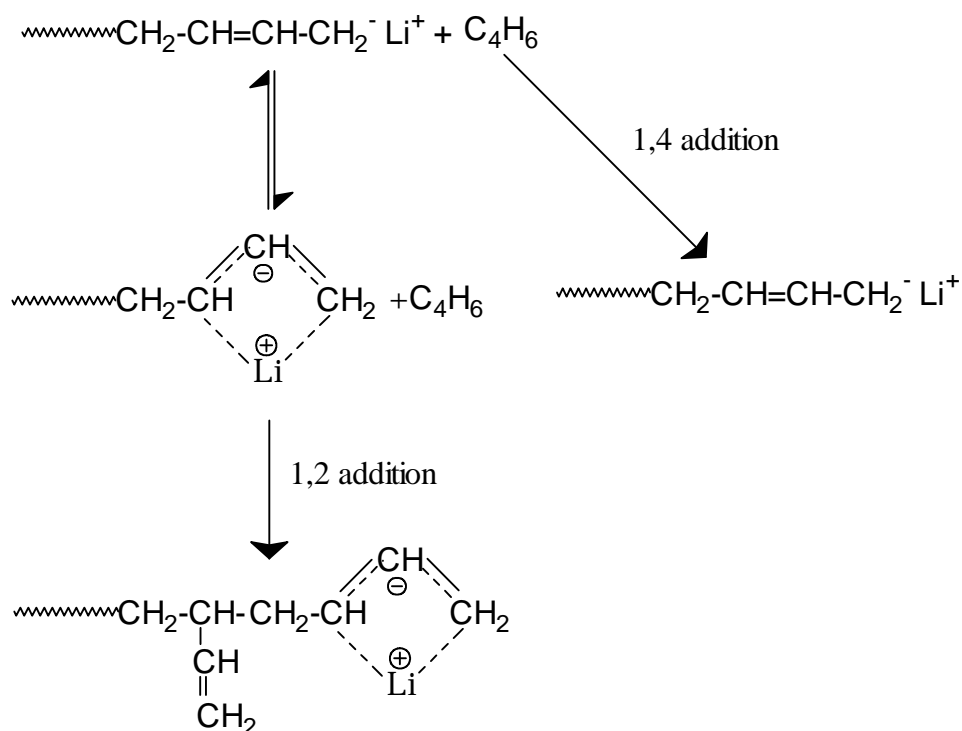


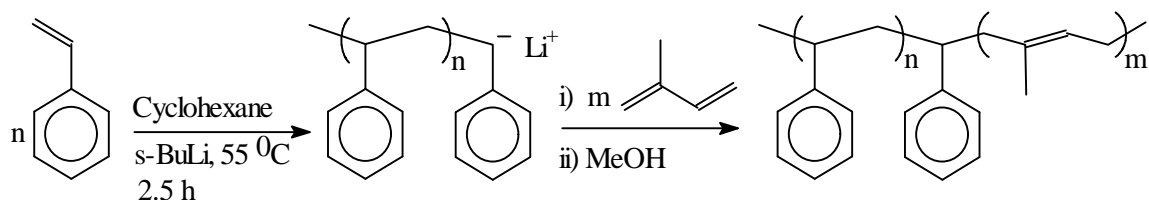
Figure 3.1. Localized-delocalized equilibrium of chain ends

Block Copolymers

Block copolymer structures are produced when extended sequences of one monomer are linked to extended sequence of another chemically dissimilar monomer. The sequential arrangement of these chemically dissimilar sequence for varying repeating structures are to be synthesized: AB diblock ABA triblock, $(AB)_n$ multiblock.

The sequential addition of monomers via living polymerization is one of the most useful techniques. In the absence of termination reaction, the sequential addition method inherently allows for the synthesis of well-defined block copolymers of predictable molecular weight and block architecture. Regardless of the method employed, namely sequential addition of monomers, use of difunctional initiators or coupling of living polymers, living polymerization technique for the preparation of block copolymers are limited by two factors¹²:

- ★ The monomer involved must be polymerized to a high degree of conversion by the selected polymerization technique
- ★ The propagating species generated by the first monomer must be capable of rapidly initiating the polymerization of the succeeding monomer.



Scheme 3.1 Synthesis of PS-b-PI by anionic polymerization

Branched Polymers

Multiarm star-branched polymers contain a central core with linear polymer chains (arms) radiating outward. These polymers are of great practical and theoretical interest due to their characteristic architecture when compared to the linear macromolecules of equal molecular weight¹³. Several routes can be used to synthesize star polymers.

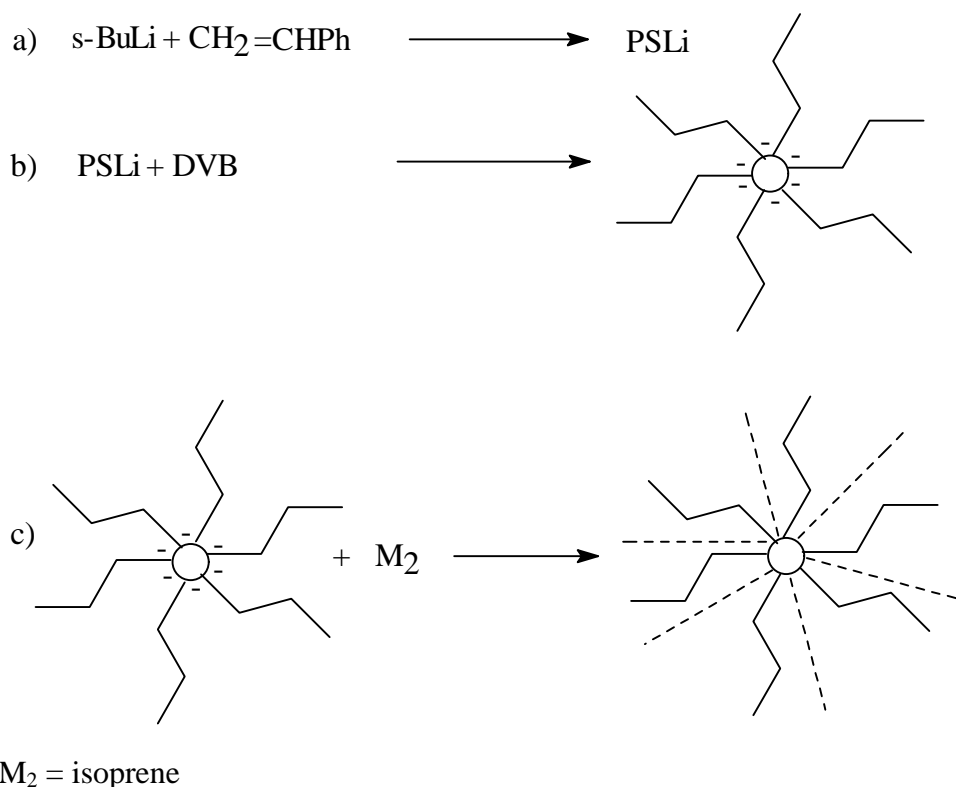
Arm-first method: A linear polymer is initially synthesized and, in a subsequent step, it is linked to a central core by deactivation to a plurifunctional electrophilic agent, in exact stoichiometric proportion or in slightly excess, to form star-branched polymers. This method is termed as “linking” method. The advantage of this method is that the number of arms per molecule within a given sample is invariant and precisely controlled by the functionality of the linking agent. The first example of the preparation of star-branched polymers by this method, using living anionic polymerization, was the work of Morton et al¹⁴ in 1962.

Secondly, star-branched polymers have been synthesized by sequential addition of a di- or polyfunctional vinyl compound, such as DVB, to living monofunctional polymeric anions. Crossover to the polyfunctional vinyl compounds creates pendant vinyl groups at the end of the polymer chains, leading to intermolecular addition reactions and microgel core formation. This general method, described as “arm-first, core-last” was first explored by Milkovich¹⁵ in 1965 and latter successfully exploited for the synthesis of star-branched PS by Rempp and co-workers^{16, 17}. An extension of this procedure led to the synthesis of multiarm star-branched polyisoprene (PI) homopolymers and polystyrene-polydiene block copolymers¹⁸⁻²⁰. Using this method, star-branched polymers possessing many arms can be synthesized. The disadvantage of the arm-first method is that the end-functionalization of the polymer chain is not possible.

Core-first method: The second general method for producing star-branched polymers, termed the “core-first, arm-last” method, involves the use of a multi-functional initiators that is either prepared externally to the polymerization reaction or in situ, just prior to the polymerization of the arm-forming monomer. The advantage of this method is that end-functionalization of the branched polymer is possible and the disadvantage is that the produced polymer has varying number of arms and exhibit broad molecular weight distribution as a result of an uncontrolled distribution of number of anions per core.

Strategy for star-branched polymer synthesis:

A. Heteroarm star polymers (A_nB_n): The synthesis of heteroarm star polymers involves a three step procedure (**Scheme 3.2**). In the first step a living polymer precursor is formed, yielding the first generation of arms.



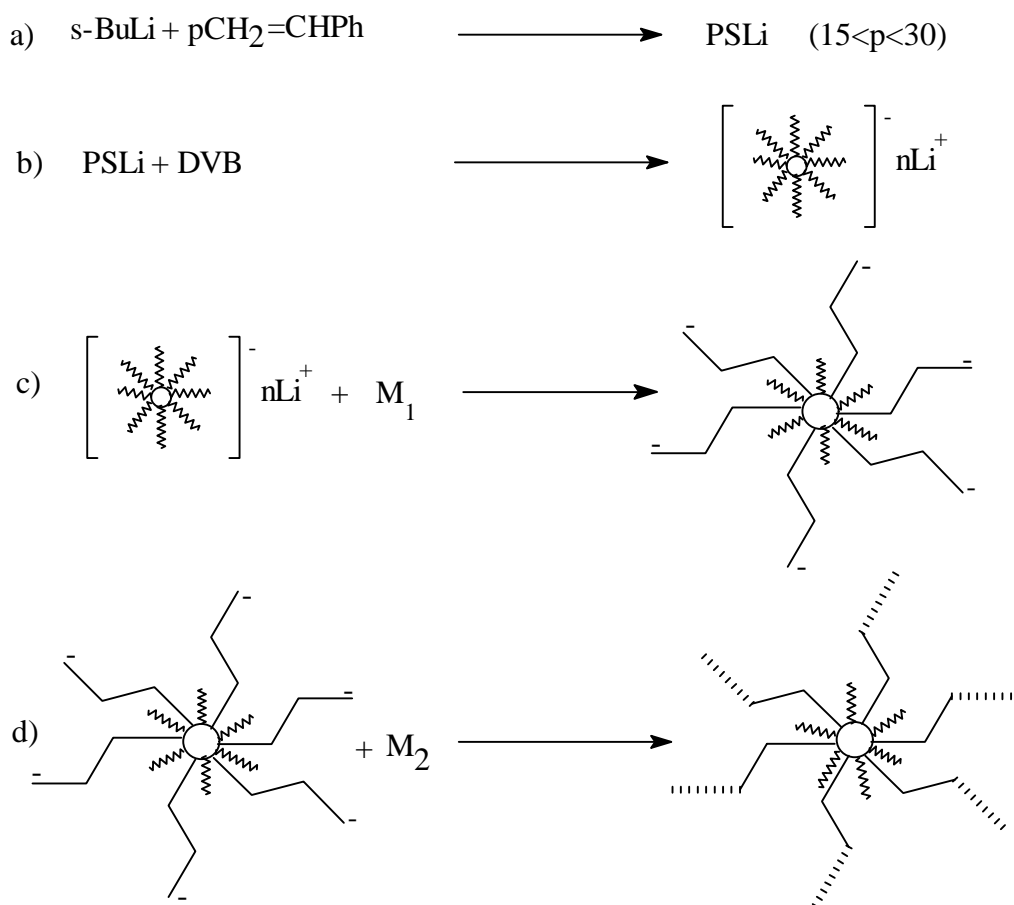
Scheme 3.2 Synthesis of heteroarm star by a combination of arm-first and core-first method

In the second step, a densely cross-linked core is built by reacting the living precursor polymer with a small amount of divinylbenzene (DVB). A living star polymer thus is formed bearing with its core a number of active sites which is equal to the

functionality (numbers of arms) of the star polymer. Finally in the third step, the living sites within the core are used to initiate the polymerization of another monomer of suitable electroaffinity. This possibility was recognized first by Eschwey and Burchard²¹ whereby they prepared styrene-styrene or styrene-isoprene “mixed stars”, with very high functionality. During the polymerization of this monomer new generation of arms springs out from the core provided that no accidental deactivation occurs. The resulting polymeric species are star copolymers bearing two kinds of arms of equal numbers.

B. Star block copolymers $(AB)_n$: Star-block copolymer can be synthesized by two methods.

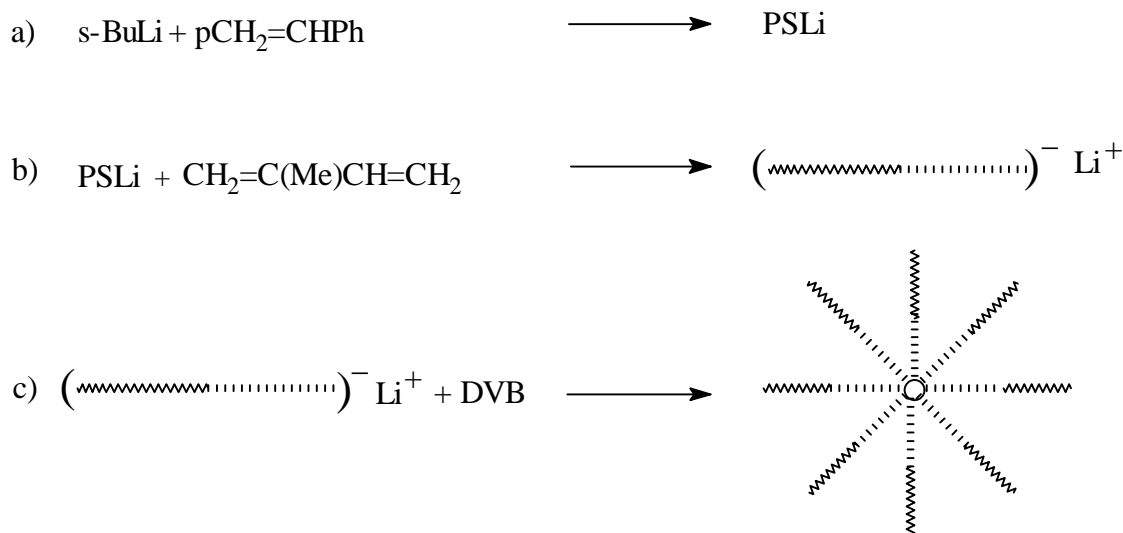
i) Core-first method - In this method a "seed star" is prepared by using a very short, living polystyrene chain to generate the living grafted poly(DVB) core (**Scheme 3.3.1**)²².



Scheme 3.3.1 Synthesis of star-block copolymer by core-first method

These living "seed star" molecules can be used to initiate the polymerization of another monomer yielding a set of branches of long length. Thus by addition of suitable second monomer star-block copolymer of the type $(AB)_n$ can be prepared. But plurifunctional initiators are not easily synthesized and they tend to associate and to precipitate out of the reaction medium. Burchard²³ was the first to succeed in making plurifunctional lithium organic cores by reacting BuLi with DVB at very low concentration in a non-polar solvent. The resulting cores were subsequently used to initiate the polymerization of various monomers such as styrene or dienes.

ii) Arm-first method - This method was applied to star-block copolymer synthesis. A linear monocarbanionic diblock copolymer was reacted with a small amount of a bisunsaturated monomer such as DVB. The polymerization of the latter leads to the formation of the cores. Star-block copolymers containing branches of PS-b-PI were made by this method²⁰. Alternatively star-block copolymer can be synthesized by deactivation of an anionic living polymer by means of a plurifunctional electrophile. Star-block copolymer of styrene and isoprene were also prepared following this method²⁴ (**Scheme 3.3.2**).



Scheme 3.3.2 Synthesis of star-block copolymer by arm-first method

3.2 Materials

Sodium metal (S. D. Fine Chemicals, India), potassium metal (Ranbaxy, India), benzophenone (Loba Chemie, India), lithium metal, calcium hydride were procured from Aldrich, USA and used as received.

Styrene was obtained from Thermax Ltd., India. Isoprene and divinylbenzene (DVB) were procured from Aldrich, USA. 1- and 2-chlorobutane (Aldrich, USA) were dried under vacuum (0.001mm Hg) over CaH_2 for 6 h prior to use. Solvents, such as tetrahydrofuran (THF), toluene and cyclohexane were supplied by S. D. Fine Chemicals.

3.3 Purification of solvents and other reagents

3.3.1 Purification of nitrogen gas

Commercial nitrogen gas (NG-300, Nitrogen Generator, Anamed, Bombay, India) contained traces of moisture, H_2 and O_2 . In order to remove these impurities, N_2 gas was first passed through a stainless steel column (1 m) containing active A4 molecular sieves, two columns (1 m) containing active Cu deposited on Kieselguhr kept at 250 °C and again through another two columns (1 m) containing activated A5 molecular sieves. The molecular sieves and Cu columns were regularly activated. The copper column was activated by passing H_2 at 170 °C for 10-14 h. Water formed from the reaction of H_2 and CuO was removed under vacuum. The activation of copper column was completed when the Cu turns into maroon color. Molecular sieves column was activated under vacuum at 200 °C for several hours and cooled under N_2 flow. The purified N_2 was further bubbled through a solution of toluene containing living styryllithium anion. The red color of the oligo styryllithium anion in toluene serves as a indicator for the purity of N_2 . The pure N_2 was connected to a manifold through a rubber tube from where the N_2 was taken into reaction flask or distillation unit through rota-flow/glass stop-cocks.

3.1.2 Solvents

THF was purified by refluxing over deep purple colored sodium-benzophenone complex. The required amount of THF was distilled over sodium-benzophenone complex and collected into bulb "A" of a distillation unit (**Figure 3.2 i**) under pure N_2 pressure using stainless steel capillary tube through a rubber septum (S). The traces of protic impurities present in THF was titrated using a solution of toluene containing

living-oligostyryllithium anion. The orange solution of oligostyryllithium in toluene was added drop by drop under stirring into THF until the orange color of anion persisted. This ensures the removal of traces of moisture or other impurities present in THF. Just before polymerization, the pure THF was condensed under vacuum into the cylinder "B" of the distillation unit and transferred into a polymerization flask under pure N₂ pressure through capillary tubes via septum (S).

Toluene was distilled in a similar way.

Cyclohexane was refluxed over CaH₂ for 8-9 h and stored over Na-K alloy in vacuum line and subsequent distillation just prior to use.

3.1.3 Monomers

Styrene: Inhibitors was removed by treating with 10 % aqueous NaOH solution and the inhibitor free styrene was then washed with distilled water repeatedly until the wash water was neutral to pH paper. Initial drying was done by keeping the monomer over fused anhydrous CaCl₂ overnight. It was filtered and stirred over CaH₂ overnight at 0 °C under nitrogen, distilled under vacuum (using distillation-unit, **Figure 3.2 i**) (10⁻³ mm of Hg) and stored at -10 °C under nitrogen. It was finally distilled over fluorenyllithium solution in toluene under reduced pressure (10⁻³ mm of Hg) just prior to use.

Isoprene: Isoprene was stirred over CaH₂ over night at 0 °C. It was then distilled under reduced pressure and stored under nitrogen at -10 °C. Isoprene was then transferred into a nitrogen filled monomer purification apparatus (**Figure 3.2 i**) via cannula. n-Butyl lithium (n-BuLi) in cyclohexane solution was added drop by drop to the monomer under N₂ until a persistent straw-yellow color formed. The persistence of straw-yellow color indicates the monomer is free of protic impurities. Then the pure monomer was condensed using liquid nitrogen bath into cylinder "B" of the distillation unit. The monomer was then transferred into the polymerization flask containing initiator solution using a syringe or cannula.

Divinyl benzene: It was stirred over CaH₂ for overnight at 0 °C under nitrogen, distilled under vacuum and stored under nitrogen at -10 °C.

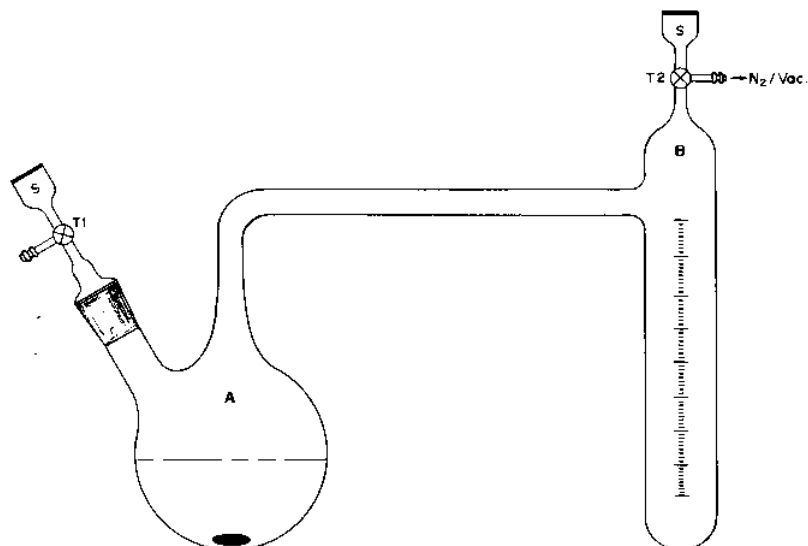


Figure 3.2i. Distillation apparatus, (S) rubber septum, (T) three-way stop-cock, vacuum or nitrogen line is connected through is way

3.4 Synthesis of alkyl lithium initiator

Butyl lithium (BuLi) was prepared from the reaction of butyl chloride and activated lithium sand under argon atmosphere. The reaction is highly exothermic. Butyl chloride was dried over fused CaCl_2 for 12 h and fractionally distilled at 76°C . To make activated Li powder, required quantity of Li wire (2.5 mole compared to butyl chloride) was taken in a separating funnel with paraffin oil and heated up to 200°C with vigorous shaking. Then it is thoroughly washed with dried cyclohexane. The dried activated Li powder was transferred into a round bottom flask with magnetic stirring bar and 500 mL dry cyclohexane was added to it. The previously dried butyl chloride was added through the syringe-pump at the rate of 10 mL/h. The whole flask was kept in an ice bath. After the addition, the solution was refluxed at 60°C for 6-7 h in case of n-BuLi in order to complete the reaction. However, in case of sec-BuLi refluxing was not necessary.

3.4.1 Estimation of initiator concentration

The concentration of initiators such as n-BuLi and sec-BuLi was estimated using Gilman's double titration method²⁵. Definite amount of (1-2 mL) of the initiator solution was added to excess dry 1,4-dibromobutane (Aldrich, distilled over CaH_2) solution in 5 mL THF at 0°C . The solution was stirred for few minutes, during which all the lithium in the initiator as RLi was completely converted into LiBr. Thereafter,

a small amount of water (1 mL) and methanol (5 mL) was added to the solution in order to convert other lithium species (such as alkoxides etc.) into LiOH. The concentration of LiOH was determined by titration against standard solution of potassium hydrogenphthalate (KHP). This gives the concentration of lithium present as other-than-RLi form in the known amount of initiator solution. The same amount of the initiator solution was hydrolyzed in dry THF directly by slow addition of water. To this solution, 5 mL of methanol was added for dilution and the solution was titrated against standard acid (0.1 N KHP) which gave the total amount of lithium in the known amount of initiator solution. The difference of the above two titration values give the actual amount of RLi present in the initiator solution. The titrations were repeated twice and in case of slight deviation in the titration result ($> 5\%$), the average value was used as the initiator concentration.

3.5 Methods of polymerization and copolymerization

General remark: All glass-ware were predried at 120 °C for at least 24 h, assembled hot and cooled under a stream of purified nitrogen. All manipulations were conducted under a nitrogen atmosphere by using standard benchtop inert atmosphere techniques.

3.5.1 Synthesis of linear diblock copolymer of styrene and isoprene (PS-b-PI)

The synthesis of PS-b-PI was carried out in a specially designed glass apparatus (**Figure 3.2 ii**). The flask containing a magnetic stirring bar, in main bulb “A”, was assembled under N₂ while hot. To this flame dried bulb “A” fitted with a septum adopter with N₂/vacuum inlet, required amount of dry solvent (cyclohexane or toluene) was transferred by stainless steel capillary tube under N₂. The sec-BuLi solution was added drop by drop until a persistent faint-yellow color of the initiator remained. Usually 1 mL to 2 mL of 0.04(M) initiator solution was required for 300 mL of cyclohexane to completely quench all the impurities. Subsequently, the calculated amount of initiator was added through syringe. The required amount of purified styrene (first monomer) was added to the initiator solution within few seconds through stainless steel capillary tube. Immediate formation of orange-yellow color solution after addition of few drops styrene indicates that the initiation of styrene monomer by sec-BuLi initiator was taken place. The reaction mixture was allowed to stir for 5 min at room temperature. The temperature was slowly increased

to 55 °C by using an oil bath and then stirred for another 2.5 h. Thereafter, the living polystyryllithium solution was cooled to room temperature and the first pick out was taken for linear PS (first block) by opening the corresponding rota-flow (R_1), placed between bulb “A” and “C” and by applying little vacuum through the septum adopter of bulb “C”. The known amount of reaction mixture can be sampled out as bulb “C” was a graduated one. Now the required amount of purified isoprene (second monomer) was transferred to bulb “B” under N_2 through capillary and by opening the rota-flow (R_2), placed between bulbs “B” and “A”, rapid transfer of isoprene to the reaction mixture in bulb “A” occurred. An immediate sharp color change from orange-yellow (characteristic of polystyryl anion) to straw-yellow (characteristic color of isoprenyl anion) was observed which indicates the cross-over reaction had taken place. The solution was heated to 55 °C and stirred for another 2.5 h. Reaction was terminated with degassed methanol at room temperature.

The polymer solution was concentrated and the polymer was precipitated by adding drop by drop into excess methanol (4 times of polymer solution). The polymer was dried under vacuum for 10 h at 50 °C. In some cases the polymer was recovered by removing solvent and the residue was dissolved in benzene and freeze dried.

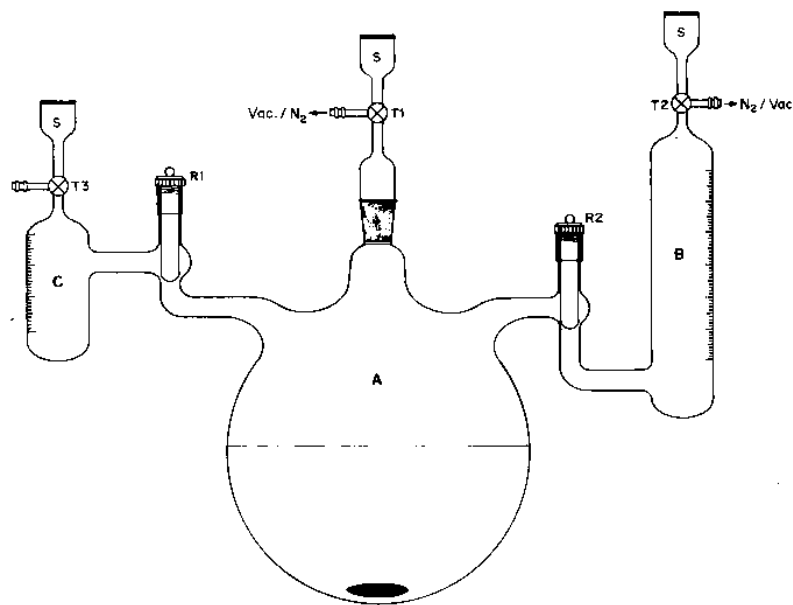


Figure 3.2 ii. Reactor for synthesizing block copolymer in bulk

3.5.1.1 Extraction of dead homopolymer from diblock copolymer by selective solvent treatment

In order to obtain pure diblock copolymer, the homopolymer contaminated copolymer was dissolved in THF (common solvent for both PS and PS-*b*-PI). Then acetone, a good solvent for PS but a non-solvent for PS-*b*-PI, was added drop by drop with stirring. The block copolymer precipitated from the solution. The precipitate was thoroughly washed with acetone for several times and dried under vacuum at 50 °C for 10 h. The SEC result revealed complete removal of homopolymer.

3.5.2 Synthesis of star-branched copolymer

The synthesis of star-branched copolymer was carried out in a specially designed apparatus (**Figure 3.2 iii**) with provision of taking pick out under positive pressure of N₂. It has two parts (A and B) and both the parts are attached through B19M/B19F joints. All the glass-wares were flame dried under reduced pressure and cooled by replacing vacuum by N₂. Heteroarm star and star-block copolymer of styrene and isoprene were synthesized using DVB as a coupling agent. Heteroarm star polymer was prepared by first polymerizing styrene in bulb “A” using *s*-BuLi at 55 °C for 2.5 h, cooling to room temperature followed by first pick out taken into the graduated portion of the bulb “B” by opening the rota-flow (R₁) for linear PS. By opening the rota-flow, R₁, solution comes thorough tube T₁ under N₂ pressure and after collecting the required quantity of solution this valve was closed. The solution remained in tube T₁ and 'Y' portion of the reactor. To push back the solution from these parts, rota-flow, R₂, was opened upon which N₂ will come through tube T₂ and push the whole solution into the bulb "A". The required quantity of DVB was added and the reaction temperature was increased to 55 °C for 2 h. A sharp color change from orange yellow to red was noticed as an indication of cross-over reaction. Then, a second pick out was taken in order to characterize the resulting polystyrene star molecule. This star molecule contains a DVB-core, which still has some active anionic sites which was utilized for the polymerization of isoprene. The required amount of isoprene was added at room temperature and again heated to 55 °C for 2 h. The reaction was terminated with degassed methanol. For star block copolymer linear diblock copolymer was synthesized first and then DVB was added at room temperature and

heated for 5 h at 55 °C in presence of polar solvent like THF in order to get efficient coupling between DVB and living PS-b-PI chains.

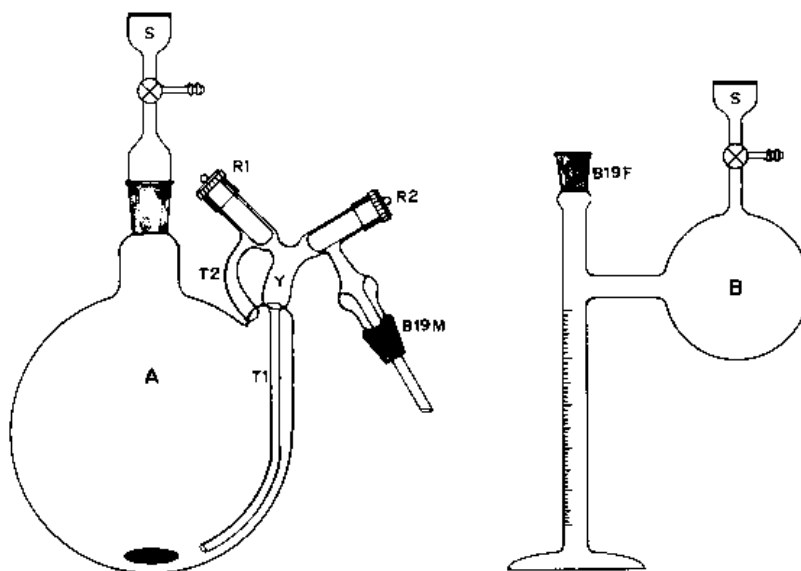


Figure 3.2 iii. Reactor for synthesizing branched copolymer

3.6 Characterization of polymers

3.6.1 Determination of molecular weight using SEC-RI

The number average molecular weight (\bar{M}_n) and polydispersity of PS were determined using Waters Gel Permeation Chromatography model GPC/ALC 150C equipped with refractive index detector using μ -styragel columns (10^5 , 10^4 , 10^3 , 500, 100 Å) at 30 °C and THF as eluant (0.5% weight solution in THF, flow rate 1 mL/min). Monodisperse PS was used for calibration.

3.6.2 Determination of absolute molecular weight using SEC-MALLS

Size exclusion chromatography (SEC) measurements were done using a Waters GPC 150C equipped with a R401 refractive index detector (Waters) and a multiangle laser light scattering (MALLS) detector, Dawn F from Wyatt Technology Corporation, USA. The column set comprised of five columns packed with a crosslinked μ -polystyrene gel with nominal porosities of 10^6 , 10^5 , 10^4 , 10^3 , 500 Å (300 X 7.8 mm) and the mobile phase used was THF. The columns were housed in 150C oven maintained at 30 °C. The eluants from the column were directed through the Dawn F

flow through cell and then through R401 RI detector to avoid subjecting fragile refractometer cell to high back pressure. The outputs of the Dawn F and the R401 were sent to an IBM PC through HPIB intelligent interface. Astra software from Wyatt Technology was used to perform calculations.

3.7 Results and discussion

A schematic representation of star-branched copolymers is shown in **Figure 3.3**.

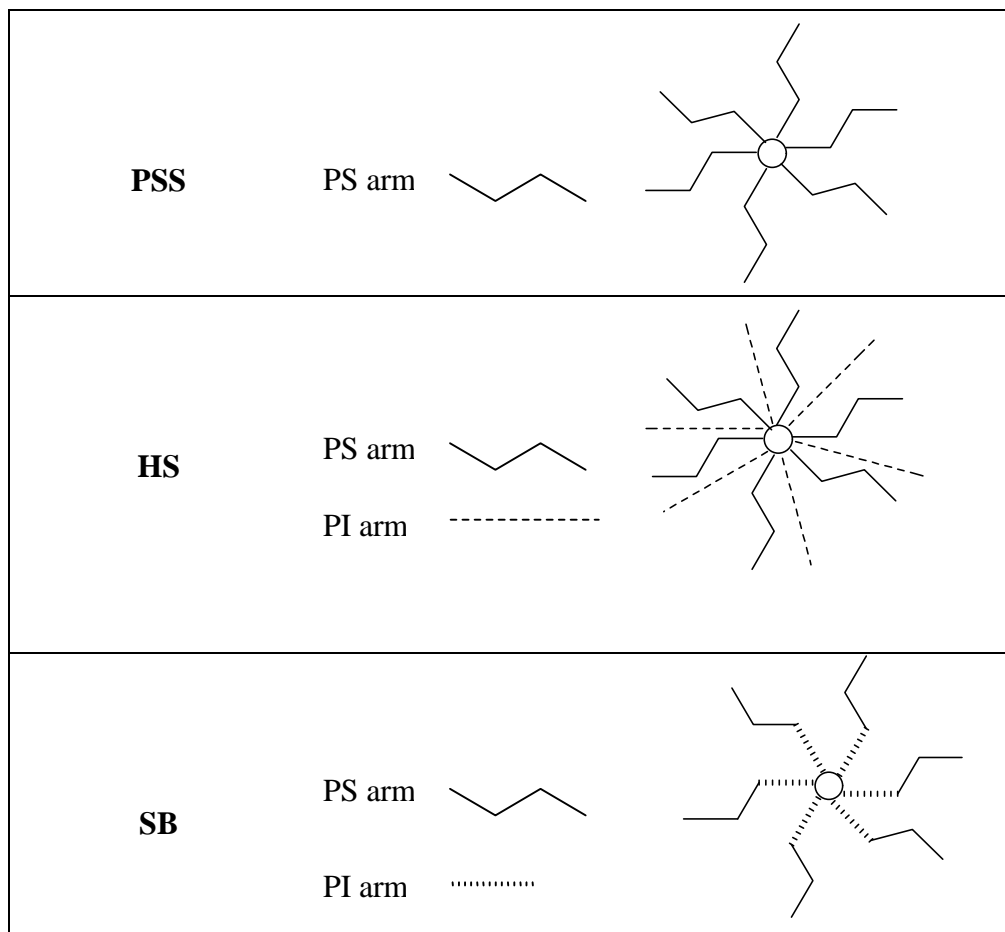


Figure 3.3. Schematic representation of star-branched copolymers

3.7.1 Determination of dn/dc values

A Brice-Phoenix, Model BP-2000V, differential refractometer was used for the precise measurement of the differential refractive index increment (dn/dc) for each

polymer at 25 °C in THF. The values measured were between 0.140 to 0.189 (**Table 3.1**).

Table 3.1: dn/dc values of Linear-Diblock and Star-Branched Copolymers

Code. No.	Copolymer type	PS:PI (wt%)	dn/dc
B ₁ to B ₅	Diblock	50:50	0.160
B ₆	Diblock	30:70	0.140
B ₇	Diblock	70:30	0.149
B ₈	Diblock	85:15	0.183
PSS ₁	Star poly(styrene)	-	0.189
PSS ₂	Star poly(styrene)	-	0.180
HS ₁	Heteroarm star	50:50	0.147
HS ₂	Heteroarm star	50:50	0.153
SB	Star Block	50:50	0.165

3.7.2 Characterization of linear PS-b-PI

The characteristics of the block copolymers synthesized are given in **Table 3.2**.

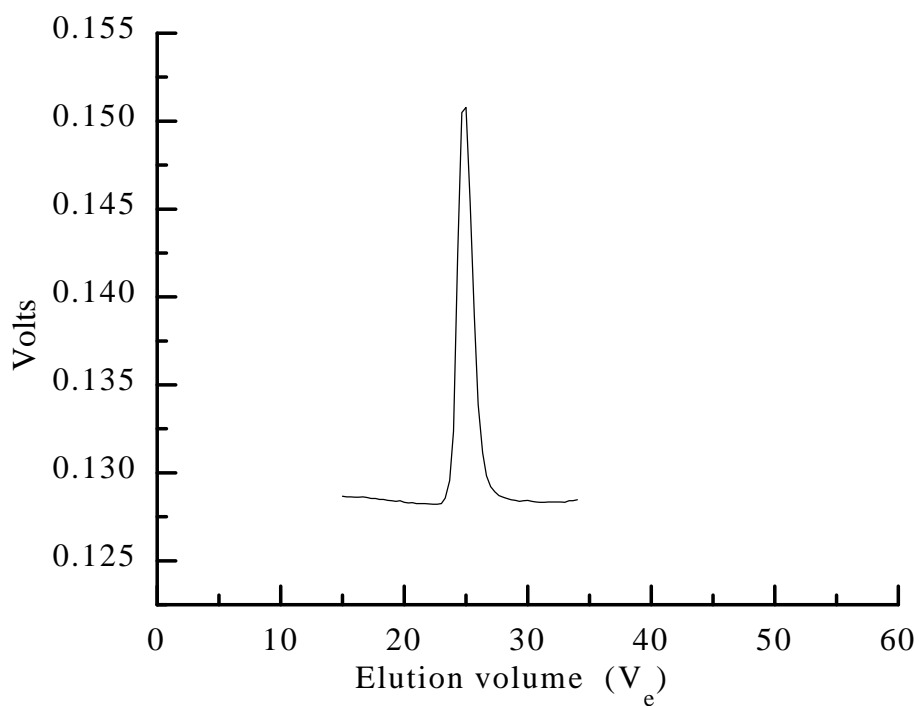
Table 3.2: Characteristics of block copolymers synthesized

Diblock copolymer (B)	$\overline{M}_n^a \times 10^{-5}$	MWD ^b of PS-b-PI	Wt % composition (S:I) ^c
B ₁	0.96	1.20	50:50
B ₂	1.54	1.17	50:50
B ₃	2.29	1.20	50:50
B ₄	2.58	1.09	50:50
B ₅	2.00	1.12	50:50
B ₆	2.00	1.20	30:70
B ₇	2.00	1.20	70:30
B ₈	2.00	1.20	85:15

a) and b) determined by SEC in THF at 30 °C

c) determined by ¹H NMR

The typical SEC chromatogram for diblock copolymer (**B₃**, **Entry no. 3** in **Table 3.2**) is shown in **Figure 3.4**.

**Figure 3.4. SEC chromatogram of linear diblock copolymer (B₃)**

3.7.3 Characterization of star-branched copolymers

The properties of the star-branched copolymers synthesized are given in **Table 3.3**.

Table 3.3: Characteristics of the copolymers synthesized

Sample	SEC - MALLS Results ^{b)}								
	PS _{arm}		PI _{arm}	Star PS		Star-branched copolymer			
	$\bar{M}_n \times 10^{-3}$	D	$\bar{M}_n \times 10^{-3}$	$\bar{M}_n \times 10^{-3}$	D	$\bar{M}_n \times 10^{-3}$	D	S:I ^{c)}	n ^{d)}
HS ₁	20	1.10	37	114	1.30	323	1.22	50:50	6
HS ₂	15	1.03	39	256	1.08	920	1.40	46:54	17
	Linear PS			Linear diblock		Star-branched copolymer			
	$M_n \times 10^{-3}$	D		$M_n \times 10^{-3}$	D	\bar{M}_n	D	S:I ^{c)}	n ^{d)}
SB	16	1.03		35	1.04	432	1.09	54:46	12
B ₅	100	1.12		228	1.03	-	-	50:50	1

a) DVB/Li ratio has been corrected for 35% ethylvinylbenzene present in commercial DVB.

b) μ -styragel columns were used of 500, 10³, 10⁴, 10⁵, 10⁶ Å in THF at 30 °C

c) determined by ¹HNMR (wt%)

d) average number of each kind of arms, calculated by the formula $n = \bar{M}_n(\text{PS}_n) / \{ \bar{M}_n(\text{PS}_{\text{arm}}) + m_0[\text{DVB}]/[\text{LE}] \}$ and for star block, n (total no. of arms) = $\bar{M}_n(\text{star}) / \{ \bar{M}_n(\text{linear block}) + m_0[\text{DVB}]/[\text{LE}] \}$

e) B - Linear diblock, HS - Heteroarm star, SB - Star block copolymer

3.7.4 Determination of copolymer compositions by ¹H NMR

The compositions of the copolymers were determined by ¹H NMR using a 200 MHz Bruker NMR spectrometer at 30 °C in CDCl₃ (conc. 4 mg/mL) using a 5 mm diameter NMR tube: 6.5, 7.0 (m. m. aromatic CH), 4.7, 5.1 (d. s. =CH olefinic). (**Figure 3.5**).

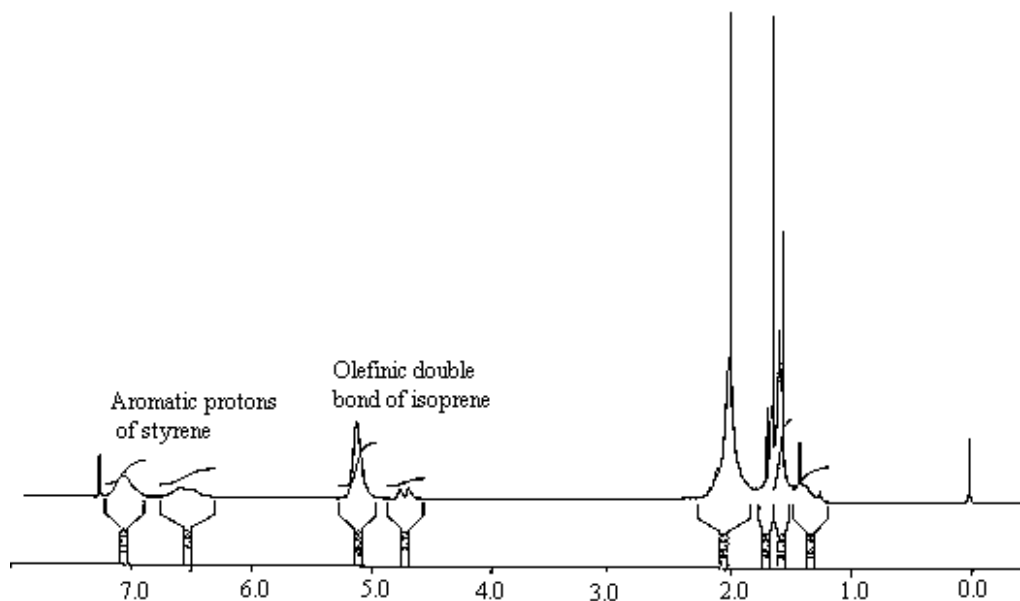


Figure 3.5. ^1H NMR spectrum of PS-b-PI

3.7.5 Confirmation of structure of copolymer by FT-IR

The IR spectra of the copolymers were recorded on a Perkin-Elmer 16 PC FT-IR spectrometer. IR (KBr pellet, cm^{-1}) 3026 ($=\text{CH}$ stretching), 3000-2900 (C-H stretching), 1492, 1600 (aromatic C=C stretching), 1375 (C-H stretching of PI), 837, 1244 (C=C and C-C stretching of PI) (**Figure 3.6**).

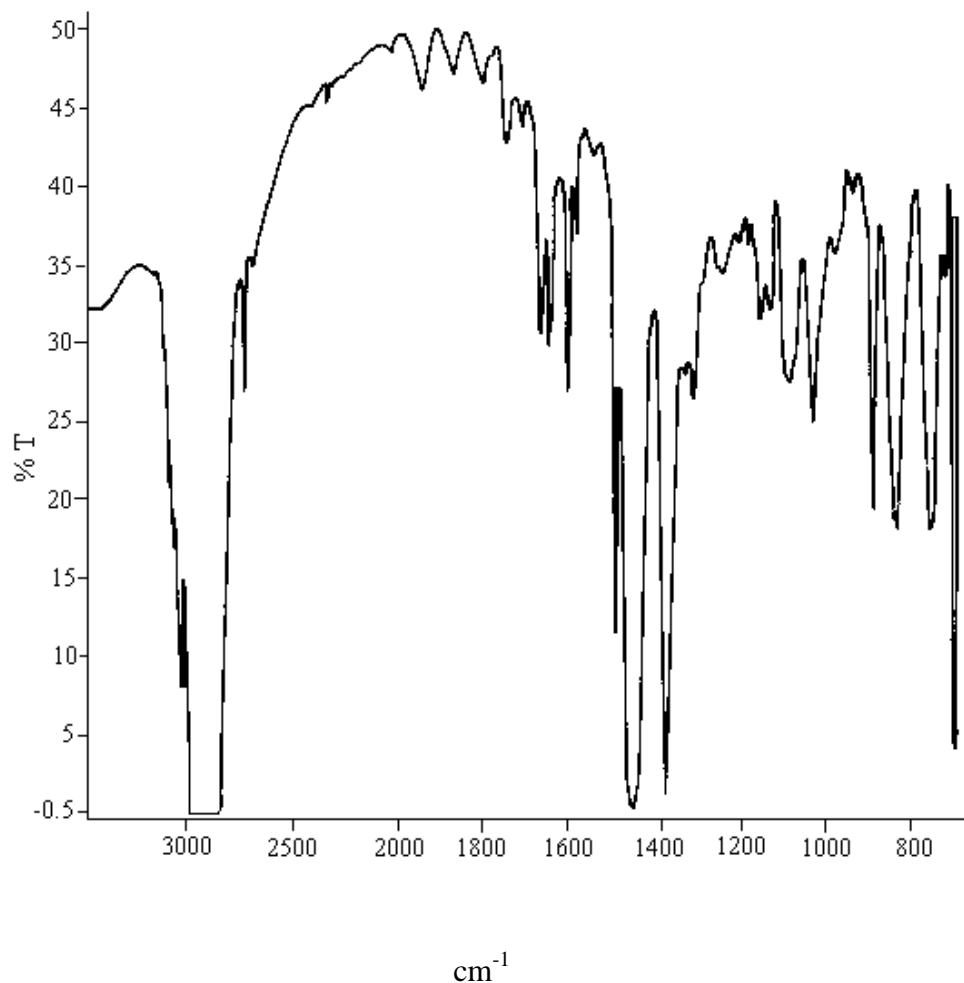


Figure 3.6. IR spectrum of PS-b-PI

3.8 Conclusions

Linear diblock copolymers of styrene and isoprene with \overline{M}_n in the range of 50,000 to 2.6×10^5 and with narrow polydispersities (<1.20) were synthesized over a wide composition range. Star-branched copolymers of styrene and isoprene having different molecular architectures as well as heteroarm stars having different number of arms were synthesized. ^1H NMR spectra of the copolymers were used to determine the chemical compositions. The structure of copolymers was confirmed by FT-IR.

3.9 References

1. Morton, M. 'Anionic Polymerization: Principles and Practice', Academic press, **1983**.
2. Mark, H. F.; Bikales, N. M.; Overberger, L. G.; and Menges, G. Eds., 'Encyclopedia of Polymer Science and Engineering', (2nd. Edn.) Suppl. Vol. 380, Wiley-Interscience, **1989**.
3. Szwarc, M.; Levy, M.; Milcovich, R. *J. Am. Chem. Soc.* **1956**, 78, 2656.
4. Szwarc, M. *Adv. Polym. Sci.* **1983**, 49, 108.
5. Cubbon, R. C. P.; Margerison, D. 'Progress in Reaction Kinetics', Porter, G. Eds., Pergamon Press, New York, **1965**, 3, 405.
6. Bywater, S. 'Comprehensive Chemical Kinetics', 15, 'Non-radical Polymerization', Bamford, C. H.; Tipper, C. F. H. Eds., Elsevier, New York, **1976**, 1.
7. Hsieh, H. L.; Glaze, W. H. *Rubber Chem. Tech.*, **1970**, 43, 22.
8. Roovers, J. E. L.; Bywater, S. *Macromolecules*, **1968**, 1, 328.
9. Meyer, G. C.; Widmaier, J. M. *Macromolecules*, **1981**, 14, 823.
10. Oberster, A. E.; Bouton, T. C.; Valaitis, J. K. *Angew. Makromol. Chem.*, **1973**, 29/30, 291.
11. Morton, M.; Sanderson, R. D.; Sakata, R. *Polym. Lett.*, **1971**, 61, 9.
12. Odian, G. "Principles of Polymerization" 2nd Ed.; John-Wiley and Sons., New York, **1981**.
13. Bauer, B. J.; Fetters, L. J. *Rubber Chem. Tech.* **1978**, 51, 406.
14. Morton, M.; Helminiak, T. E.; Gadkary, S. D.; Bueche, F. *J. Polym. Sci.* **1962**, 57, 471.
15. Milkovich, R. *Canadian Pat.* 716,645.
16. Worsfold, D. J.; Zilliox, J. G.; Rempp, P. *Can. J. Chem.* **1969**, 47, 3379.
17. Kohler, A.; Polacek, J.; Koessler, T.; Zilliox, J. G.; Rempp, P. *Eur. Polym. J.* **1972**, 8, 627.
18. Quack, G.; Fetters, L. J. *ACS Div. Polym. Chem. Polym. Prepr.* **1977**, 18, 558.
19. Bi, L. -K.; Fetters, L. J. *Macromolecules* **1975**, 8, 90.
20. Bi, L. -K.; Fetters, L. J. *Macromolecules* **1976**, 9, 732.

21. Eschwey, H.; Burchard, W. *Polymer* **1975**, *16*, 180.
22. Tsitsilisnis, C.; Boulgaris, D. *Macromolecular Reports* **1995**, *A32 (SUPPLS. 5 & 6)*, 569.
23. Eschwey, H.; Burchard, W. *Polymer* **1980**, *16*, 180.
24. Alward, D. B.; Kinning, D. J.; Thomas, E. L.; Fetters, L. J. *Macromolecules* **1986**, *19*, 215.
25. Gilman, H.; Haubein, A. H. *J. Am. Chem. Soc.*, **1944**, *66*, 1515.

CHAPTER -IV

COMPATIBILIZING EFFECT OF POLY(STYRENE)-b- POLY(ISOPRENE) COPOLYMERS IN HETEROGENEOUS POLYSTYRENE / NATURAL RUBBER BLENDS

4.1 Introduction

Although blending of polymers is an elegant method to create new properties in polymers, it is complicated by the fact that most polymer pairs are immiscible and incompatible. Very often, the resulting materials exhibit poor mechanical properties due to incompatibility resulting from the lower entropy of mixing of high molecular weight polymers and the unfavorable enthalpic interaction between the constituent components^{1, 2}. Enhancement in the degree of compatibility between the constituent components can be achieved by use of a compatibilizer. A block or a graft copolymer is known to be very effective in reducing the interfacial tension and in improving the interfacial adhesion by entanglement or bridging different polymer chains near the interface³⁻⁸. Block copolymers are, generally, more efficient than graft polymers as compatibilizer^{9, 10}. Usually the block segments of the compatibilizer are identical, either in structure or in properties, to the blend components. Such block copolymers are expected to be present at the interface of blend because one segment of the compatibilizer is miscible with one component and the other segment with the second component of the blend¹¹. The compatibilizer is designed to reduce the interfacial energy, improve the interfacial adhesion and permit a finer dispersion during mixing of the blend components.

Poly(styrene) (PS) and natural rubber (NR) form incompatible blends and require the addition of a compatibilizing agent to achieve satisfactory interfacial adhesion in order to develop an efficient stress transfer between the two phases. Methods to synthesize compatibilizing agent and to improve phase adhesion between two immiscible components are the subjects of many research studies¹²⁻¹⁶.

Compatibilizing action of poly(styrene)-block-poly(isoprene) (PS-b-PI) in poly(styrene)/poly(isoprene) blend has been reported by Inoue and coworkers^{17, 18}. It

was found that addition of 75 wt % of the block copolymer resulted in a fine morphology. The effect of the molecular structure of the styrene-isoprene block copolymer on the interfacial tension, the morphology and the interfacial adhesion of PS/PI blends has been reported¹⁹. It was found that interfacial strength was significantly increased when the isoprene-rich diblock copolymer was used as a compatibilizer. A symmetric diblock copolymer was generally more efficient as a compatibilizer than the asymmetric diblock copolymer of the same molecular weight²⁰⁻²².

Asaletha et al.²³ used a NR-g-PS as a compatibilizer for NR/PS blends. It was found that with increasing percentage of the graft polymer, the particle domain size decreased and leveled off at critical micelle concentration (CMC).

This chapter describes the influence of PS-b-PI block copolymer concentration, the molecular weight of homo and copolymers, the composition of block copolymers, its mode of addition and the nature of the casting solvent on the morphology and properties of the blends of PS and NR. Attempts have been made to deduce the block copolymer conformation at the interface. Finally, the experimental results are explained in terms of the theories of Noolandi and Hong²⁴⁻²⁶.

4.2 Experimental

4.2.1 Materials

Commercial polystyrene (SC-206E) was supplied by Supreme Plastics, Bombay. Natural rubber (ISNR-5) was supplied by Rubber Research Institute of India, Kottayam, Kerala. The characteristics of the materials used are given in **Table 4.1**.

Table 4.1: Characteristics of materials used

Material	$[\eta]^a$ dl/g	Solubility parameter(cal/cc) ^{1/2}	$\bar{M}_v \times 10^{-5}$
NR ₀	5.38	7.75	11.0
NR ₅	4.02	7.75	7.20
NR ₁₀	3.06	7.75	4.73
NR ₁₅	2.94	7.75	4.45
NR ₂₀	2.23	7.75	2.94
PS	0.68	8.56	1.89

a) determined in toluene at 25 °C, $a = 0.75$ and $k = 7.5 \times 10^{-3}$ mL/g

b) NR suffix indicates time of mastication in minutes. Mastication was performed in a mixing mill in presence of peptizing agent

4.2.2 Synthesis of PS-b-PI

The diblock copolymer of styrene and isoprene (PS-b-PI) with different molecular weights and compositions were prepared by sequential living anionic polymerization using *s*-butyl lithium as an initiator in cyclohexane at 55 °C using the method of Hsieh²⁷. The experimental methods have been described in the preceding chapter (Chap. III, Sec. 3.5.1).

4.2.3 Characterization of PS-b-PI

The PS-b-PI was characterized by GPC, ¹H NMR, IR spectroscopy and gravimetric methods. The characteristics of the block copolymers synthesized are given in the proceeding chapter (Chap. III, Sec. 3.7.2).

4.2.4 Preparation of blends

PS and NR were solution blended in chloroform (2 wt % solution) in different proportions. Blends having wt % compositions of PS/NR 50/50, 40/60 and 30/70 were made with and without the addition of the block copolymer (PS-b-PI). After mixing PS, NR and block copolymer in chloroform, the mixture was kept overnight and then stirred for 12 h using a magnetic stirrer. The blend films were cast on a glass plate and were dried in air at room temperature. To study the effect of the casting solvent, blends were also made from carbon tetrachloride. The influence of the mode of addition of block copolymer was studied in three ways. In the first case the minor

phase (PS) and the block copolymer were premixed, kept overnight and then stirred for 12 h. Therefore NR was added to the mixed solution, kept overnight again and stirred for a further period of 12 h. In the second case, the same procedure was repeated by premixing the major phase (NR) and block copolymer. In the third case, the block copolymer was added to the PS/NR blend directly. The morphologies of all the system were examined by optical microscopy and SEM. The effect of homopolymer and block copolymer molecular weight on compatibilization was studied by using NR and PS-b-PI of different molecular weight.

4.2.5 Analysis

4.2.5.1 Morphological observation

In order to determine the particle size and distribution of the dispersed phase in blends, the morphology of the samples was examined using an optical microscope (Leitz Laborlux 12 Pol S). For SEM study osmium tetroxide (OsO_4) stained samples were vacuum coated with gold and examined in a scanning electron microscope (Stereoscan 440, Leica Cambridge). In order to gain a better understanding of the morphology, the samples were etched with acetone for 2 to 7 days. OsO_4 fixation technique was also adopted to increase the contrast between the two phases.

4.2.5.2 DSC study

Differential scanning calorimetry (DSC) analysis was carried out on a Mettler-20 thermal analyzer. For DSC analysis about 20 mg sample was first cooled to $-100\text{ }^\circ\text{C}$ and then it was heated under nitrogen at the heating rate of $10\text{ }^\circ\text{C}/\text{min}$. Al_2O_3 was used as the reference sample

4.2.5.3 Measurement of mechanical properties

A 5 % solution of blends in chloroform was made for casting. Sheets were casted on a teflon mould and were dried in air at room temperature and then dried in a vacuum oven at $80\text{ }^\circ\text{C}$ for 48 h. Mechanical properties were determined according to ASTM standards using Instron testing machine (model 4204, pneumatic grip model 2712-002) using a cross head speed of $25\text{ mm}/\text{min}$.

Specimens for tensile impact were injection molded at $180\text{ }^\circ\text{C}$. The diameter of the tab of the bar was 4.5 mm and of the neck 1.5 mm. The tensile impact strength was

determined by impact tester model CS-183 T1-085 (CSI, Cedar Knolls, New Jersey, USA) using the ASTM D-1822 method ²⁸.

4.3 Results and discussion

4.3.1 Effect of block copolymer concentration on morphology

Compatibility of PS and NR is poor and can be improved by the addition of a block copolymer of polystyrene and polyisoprene which decreases the phase separation and reduces the particle size. Morphology of the dispersed phase in the blend was followed by increasing the concentration of the block copolymer in the blend. It was observed that the domain size decreases with increasing concentration of the block copolymer. A quantitative assessment of the compatibilizing effect was made by measuring the diameter of about 100 domains. In a 50/50 wt % blend, a 58 % domain size reduction was observed by the addition of 0.5 wt % of block copolymer. Addition of another 3 wt % block copolymer causes a size reduction of about 64 % followed by a leveling off at higher copolymer concentrations (**Figure 4.1**).

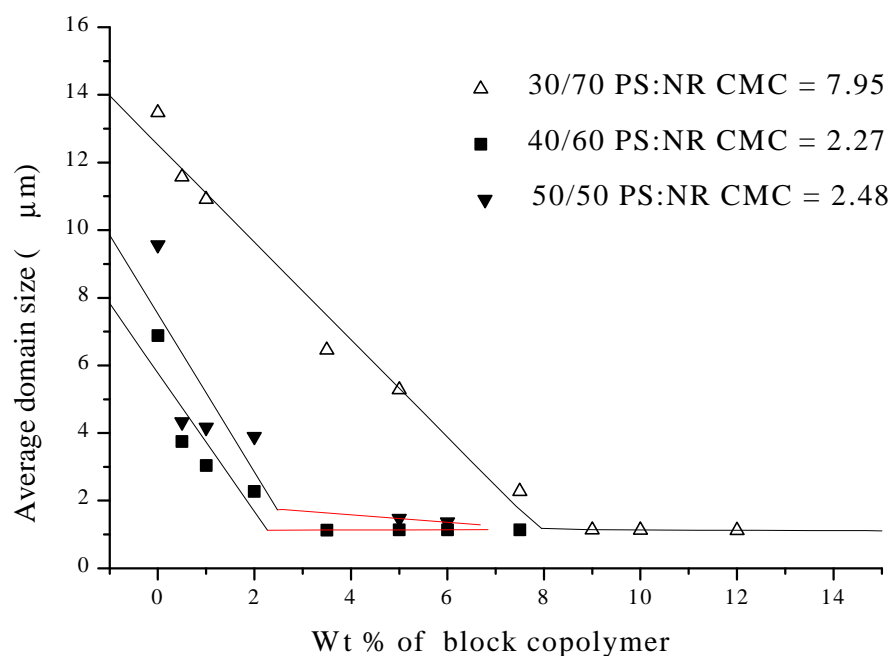


Figure 4.1. Effect of block copolymer concentration on the domain size of the dispersed phase of different PS/NR blends

The leveling point can be taken as the CMC i.e., the lowest concentration at which micelles are formed. CMC values were estimated from the intersection of the straight lines (Figure 4.1) obtained at low concentration and leveling off line at higher concentration. The inter particle distance also decreases with increasing concentration of the block copolymers and attains a constant value at higher concentration (Figure 4.2). For 30/70 PS/NR CMC is about 7.95 %. The corresponding values for 50/50 wt % and 40/60 wt % PS/NR were 2.48 and 2.27 % respectively.

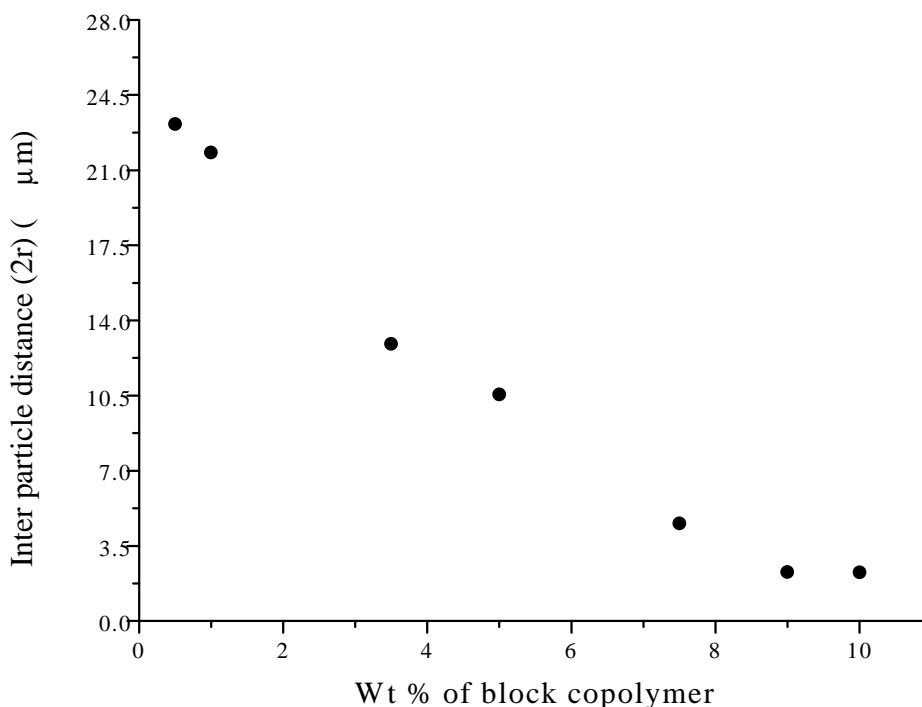
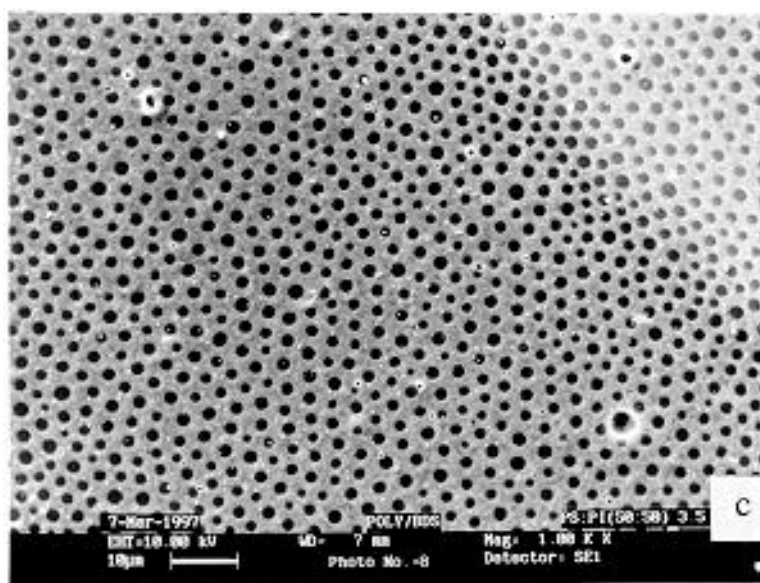
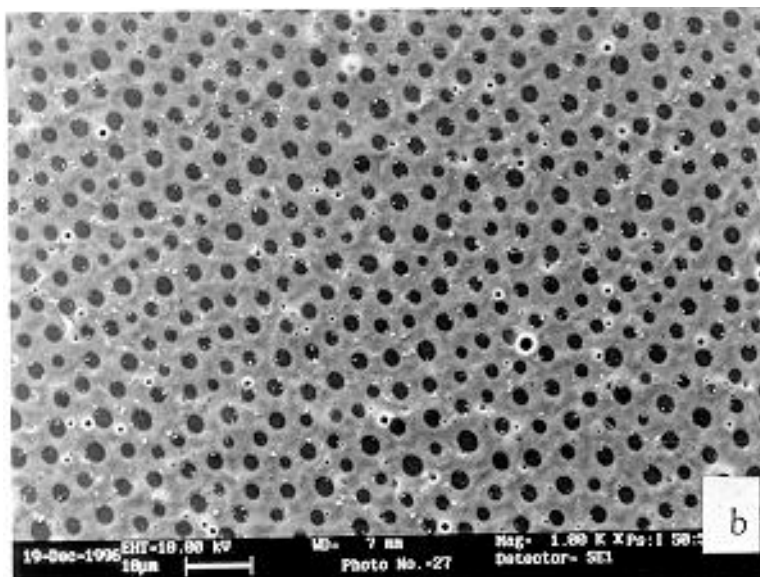
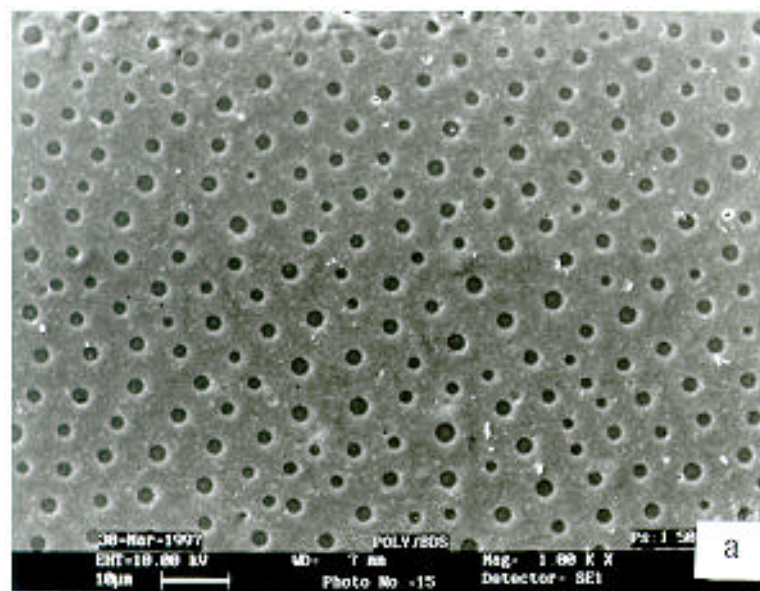


Figure 4.2. Effect of block copolymer concentration on inter particle distance of the dispersed phase in 30/70 PS/NR blends

Figure 4.3 shows SEM micrographs of binary blends of PS/NR and ternary blends of PS/NR/PS-b-PI. The beneficial effect of the compatibilizer on the morphology of the ternary blend can be demonstrated in these micrographs. The continuous phase is PS and the dark spots are NR stained by OsO₄. In uncompatibilized blend (Figure 4.3a), the particle sizes are not uniform with various domain sizes. For the compatibilized blends, the NR domains are dispersed in the PS matrix as uniform particles. The presence of 1.5 phr PS-b-PI clearly (Figure 4.3b) results in uniform and smaller domain size, with an even larger reduction in the dimensions of the dispersed phase



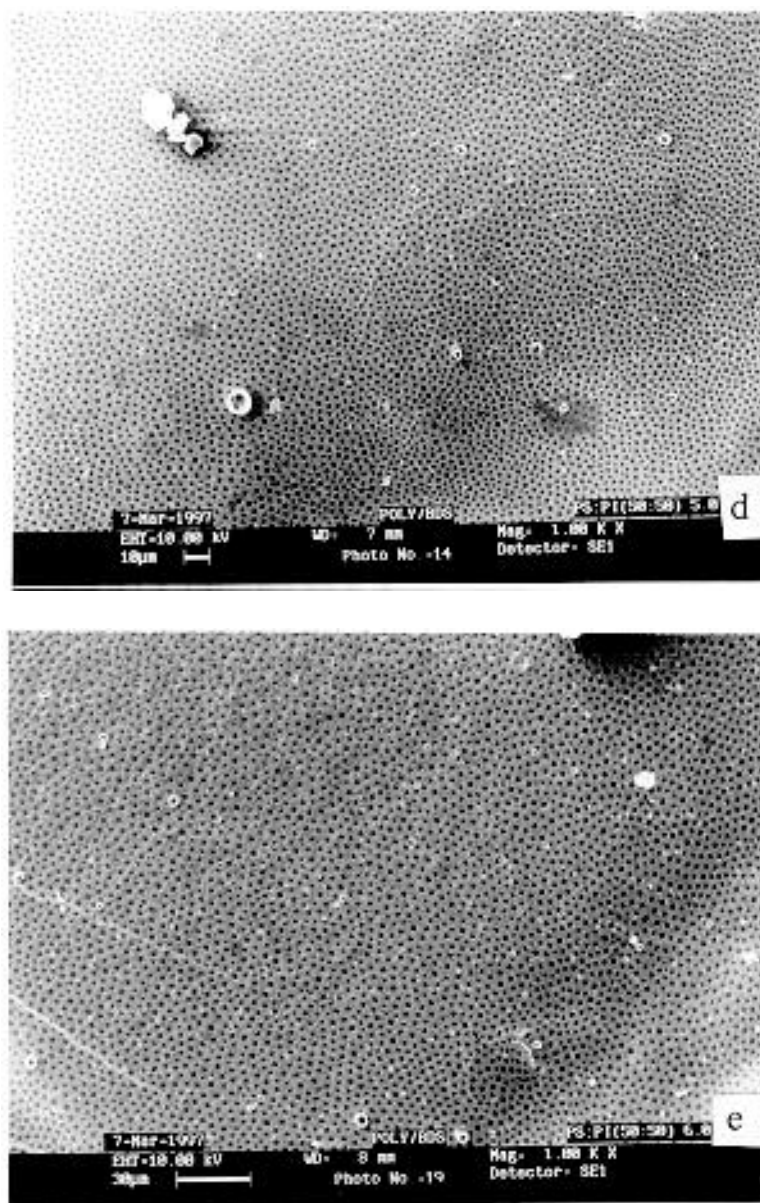
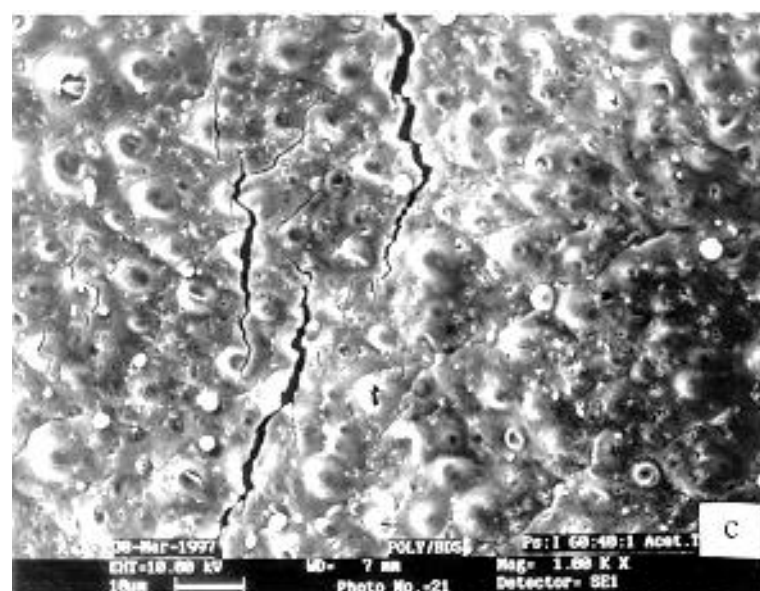
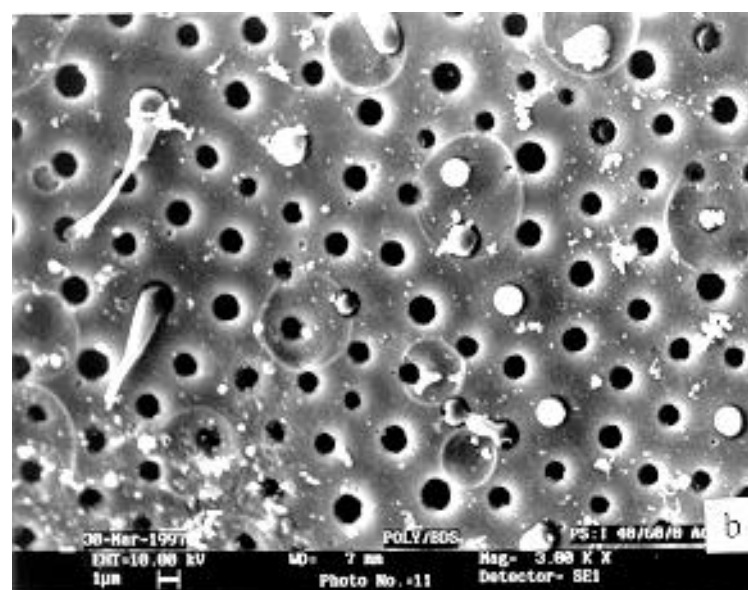
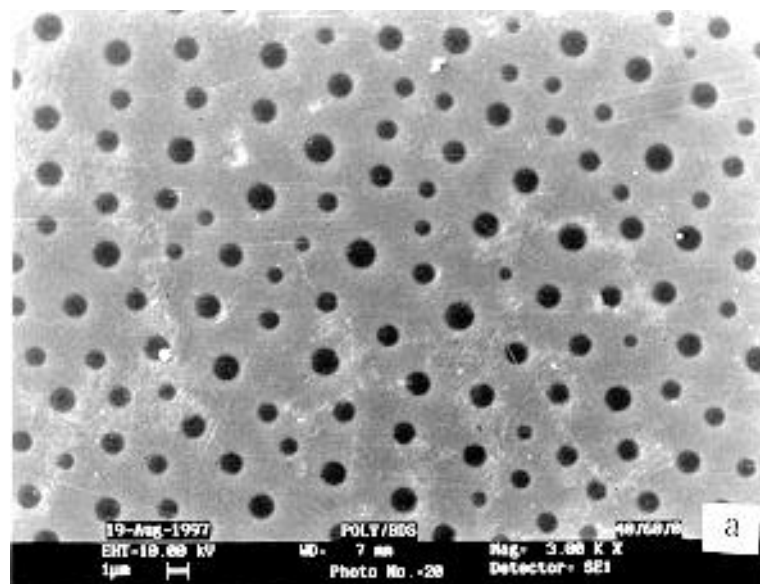


Figure 4.3. SEM photographs of 50/50 PS/NR blends with block copolymer loading (a) 0%, (b) 1.5 %, (c) 3.5 %, (d) 5 % and (e) 6 %

being observed at higher concentration of compatibilizer (**Figure 4.3d** and **Figure 4.3e**). Better dispersion and improved interfacial adhesion are observed at higher compatibilizer loading. To gain a better understanding regarding blend morphology and to increase the contrast between the two phases, the PS phase was extracted with acetone for 2 to 7 days. **Figure 4.4a** is the micrograph of uncompatibilized blends of PS/NR. After 2 days acetone treatment (**Figure 4.4b**), the PS phase is almost completely removed and dark holes are left. Acetone is a selective solvent for PS and nonsolvent for NR. From the SEM micrographs it is clear that the PS domains are extracted out from the matrix by selective solvent treatment. But for a compatibilized blend (**Figure 4.4c**), (1 wt % compatibilizer), after 2 days acetone treatment, the PS matrix appears swollen and is non-extractable. This clearly indicates that extended period of solvent treatment is required to extract out completely the PS from the blend. The situation is clear in **Figure 4.4d** which shows that after 7 days solvent treatment the PS has been completely extracted out. The size of the dark hole formed, for compatibilized bend is much more smaller than that of uncompatibilized blend and is indicative of particle size reduction with higher % loading of compatibilizer. The situation is more interesting with higher % loading of PS-b-PI (1.5 wt %, **Figure 4.4e**), where even 7 days acetone treatment is not sufficient to fully remove the PS from the blend. Thus, by increasing the amount of the compatibilizer, the interfacial adhesion between two phases increases and removal of one phase becomes more and more difficult.



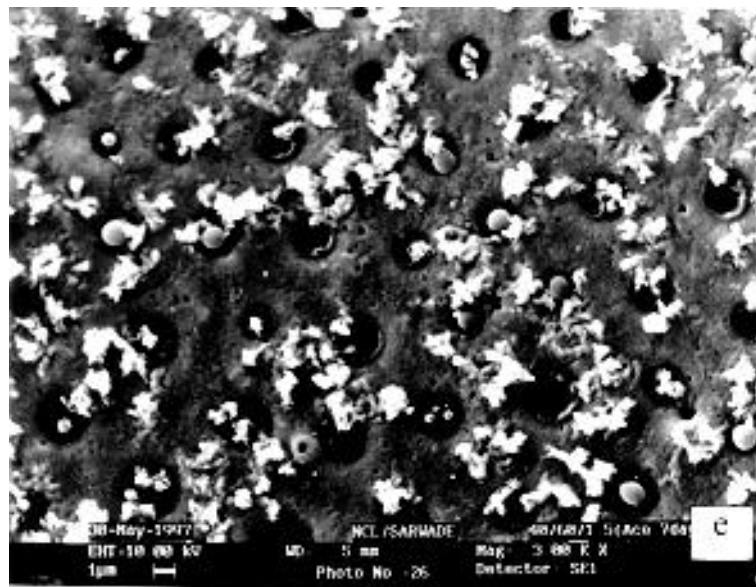
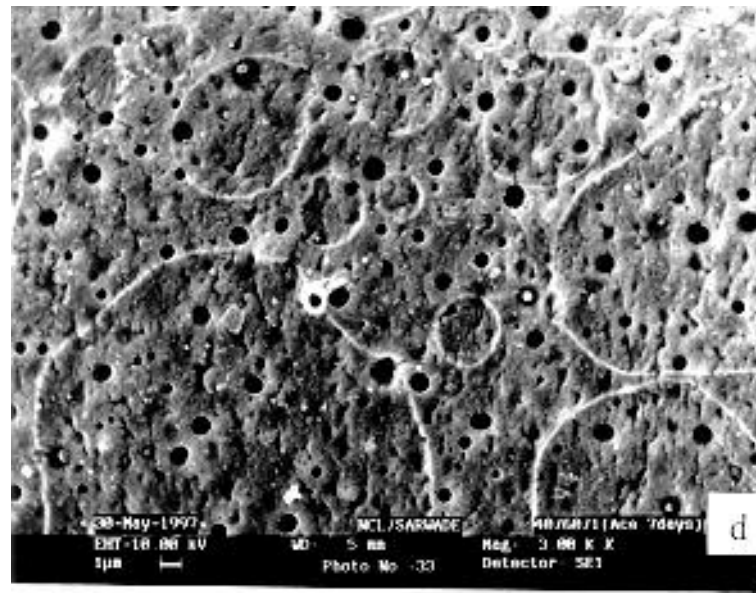


Figure 4.4. SEM photographs of (a) 40/60/0 (b) 40/60/0, 2 days acetone etching, (c) 40/60/1, 2 days acetone etching (d) 40/60/ 1, 7 days acetone etching (e) 40/60/1.5, 7days acetone etching

4.3.2 Effect of molecular weight of NR on morphology

The effect of addition of block copolymer on the domain size of the dispersed phase was studied as a function of NR molecular weight (**Figure 4.5**). The amount of block copolymer required for compatibilization is proportional to the viscosity average molecular weight (M_v) of the constituent of the blend. The optimum amount of block copolymer required to saturate unit volume of the interface (CMC) is found to decrease linearly with the decrease of molecular weight (**Figure 4.6**).

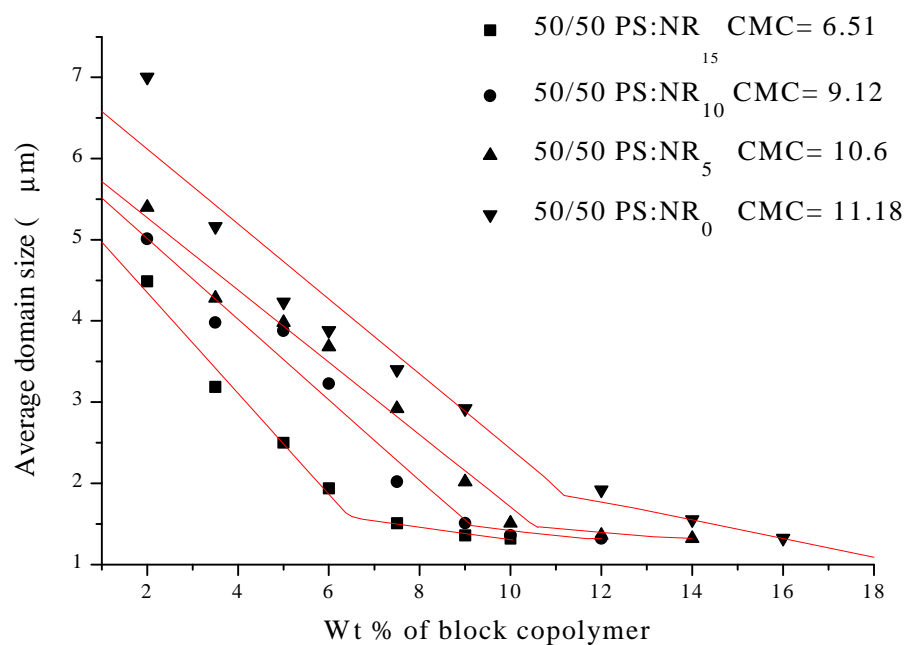


Figure 4.5. Influence of molecular weight of NR on morphology

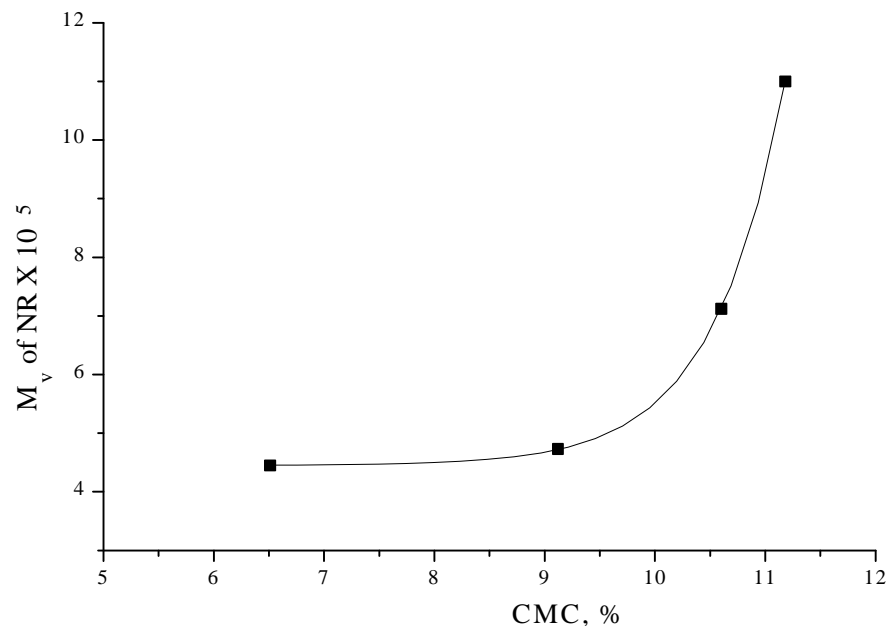


Figure 4.6. Effect of molecular weight of NR on CMC

4.3.3 Effect of block copolymer concentration on particle size distribution

To assess quantitatively the block copolymer concentration on particle size distribution, the domain size distribution of the 30/70 wt % PS/NR blend was examined with and without the addition of block copolymer (**Figure 4.7**). A reduction in the domain size by the addition of block copolymers is evident from the decrease in the width of the distribution curve. The blend contains larger number of bigger particles in the absence of copolymer and therefore the polydispersity is high. The distribution curve of 50/50 and 40/60 PS/NR blend also follows same pattern. Similar results have been reported by Willis and Favis²⁹ and Zhao et al.³⁰ for poly(butadiene)/poly(methylmethacrylate) blends using poly(butadiene-*b*-methyl methacrylate) as compatibilizer.

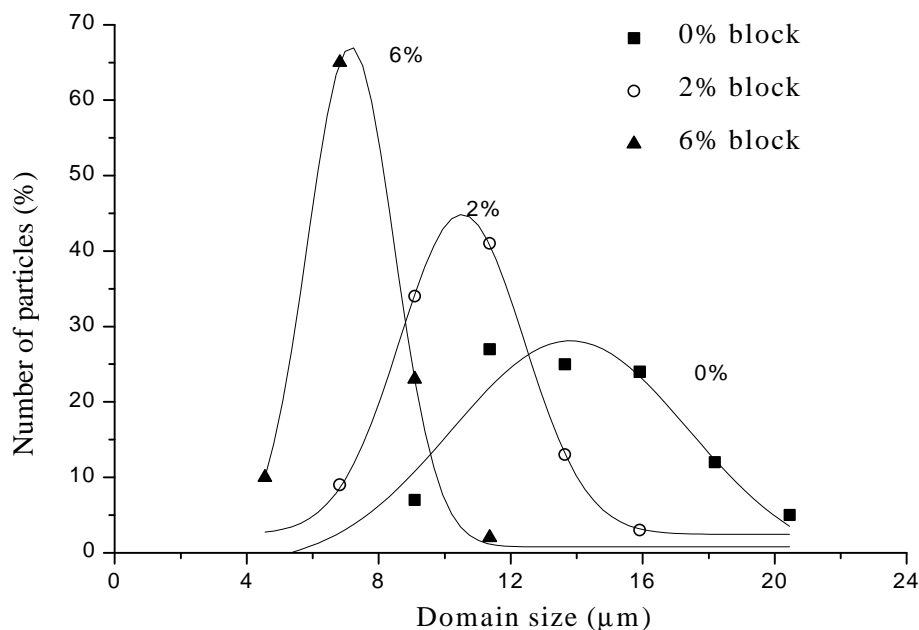


Figure 4.7. Effect of PS-b-PI concentration on domain size distribution of 30/70 PS/NR blends

4.3.4 Effect of block copolymer molecular weight on particle size distribution

An increase in the molecular weight of block copolymer at constant PS/PI wt % composition of 50/50 results in progressive particle size reduction. The effect is more pronounced in case of B₃ and B₄. This observation can be understood based on the theory of Riess and Jolivet³¹. According to them the emulsifying efficiency of copolymers can be compared by defining the ratio of the molecular weight of the homopolymer and the graft copolymer. The same theory is also true for block copolymer. If α is the ratio of molecular weight of PS in the homopolymer to that in the copolymer and β is the ratio of the molecular weight of NR homopolymer to that in the copolymer (PI), then the copolymer is less efficient as an emulsifier if $\alpha > 1$ and $\beta > 1$. The emulsifying properties of the copolymer is optimum when $\alpha < 1$ and $\beta < 1$. In the most ideal case, when $\alpha = \beta < 1$, the copolymer has no preferential solubility. It can be seen that the α and β values decreases as the weight % of block copolymer in blend increases. Data presented in **Table 4.2** support the theory of Riess and Jolivet.

Table 4.2: Effect of block copolymer molecular weight on particle size distribution

Wt. % of block ^a copolymer	No. average domain size (μm)			
	B ₁ (\bar{M}_n = 96,000)	B ₂ (\bar{M}_n = 1,54,00)	B ₃ (\bar{M}_n = 2,29,00)	B ₄ (\bar{M}_n =2,58,000)
0	9.56	9.56	9.56	9.56
2.0	6.25	6.58	4.64	4.00
3.5	4.87	4.93	3.31	3.72
5.0	4.46	3.42	2.79	3.45
6.0	3.26	2.86	1.67	2.72
7.5	2.25	2.42	1.64	1.88
9.0	2.25	2.25	1.57	1.60

a) All block copolymers have 50/50 PS / PI wt % composition

The emulsification curves obtained with interfacial agents B₁, B₂, B₃, and B₄ are shown in **Figure 4.8**. These copolymers have identical structures and similar compositions, but have very different molecular weights. From **Figure 4.8**, at low interfacial agent concentrations (below C_{crit}), the emulsifying effect is stronger for the high-molecular weight copolymers: the number-average diameters obtained in the range of interfacial agent concentrations (2-6 wt %) decreases with increasing molecular weight of the copolymer. Finally, the critical concentration for emulsification also decreases with increasing molecular weight: from 4.5-5 wt % for B₃ (\bar{M}_n = 229,000) to 6-7 wt % for B₁ and B₂ (\bar{M}_n = 96,000 and 154,000, respectively). If the equilibrium particle size can be associated with a state of interfacial saturation, one must conclude, in the light of the results obtained using these diblocks, that once the critical concentration has been attained, the state of the interface is similar, regardless of the block molecular weight of the interfacial agent, since the minor phase particle size is approximately equal. However, the critical concentration is reached more rapidly with a higher molecular weight modifier. This can be explained by the fact that longer copolymer chains occupy a larger area at the interface. It is therefore possible, and necessary, to pack more molecules at the interface. This results in the higher critical concentrations for the low-molecular

weight interfacial agents (B_1 and B_2) versus the high-molecular weight copolymer (B_3 and B_4).

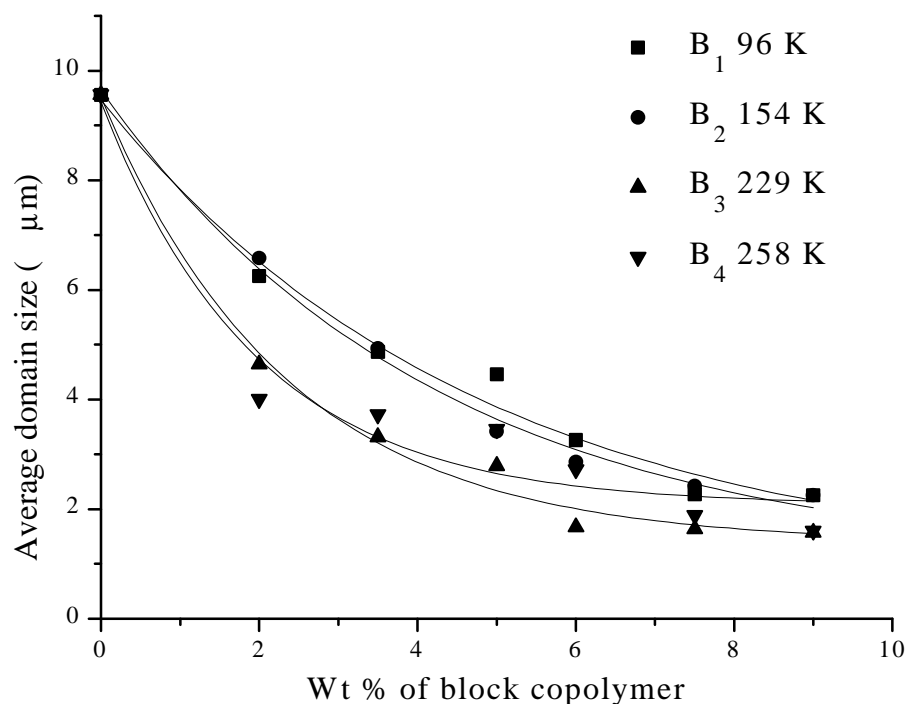


Figure 4.8. Effect of the molecular weight of the interfacial agent on the emulsification

From thermodynamic arguments, Noolandi and Hong^{25, 26} had predicted that the efficacy of a diblock copolymer to compatibilize a blend of immiscible homopolymers would increase with increasing molecular weight. Longer chains would increase the thickness of the interface, which would decrease the enthalpy of the system. The experimental results shown here support these hypotheses, at least in the low range of interfacial agent concentrations.

Vilgis and Noolandi³² have reported that the most efficient compatibilization of a binary polymer system would be obtained by adding the lowest possible concentration of an interfacial agent having the highest possible molecular weight which would not form micelles. Obviously, one wonders whether the interfacial agents used in this study tend to form a large quantity of micelles, or essentially migrate to the interface. Clearly, if micelle formation were an important factor in the system, it would more

readily occur with the high-molecular weight copolymer, B₄, than with the low-molecular weight copolymer. If a high fraction of B₄ is 'lost' as micelles in one of the two phases, one would expect a higher critical concentration for emulsification with interfacial agent B₄ and in fact this trend is observed: the critical concentration is similar for B₄ with other low-molecular weight modifiers. This is a strong indication that in to some extent micelle formation is occurring in this particular case.

4.3.5 Effect of block copolymer composition on morphology

Block copolymer with equal segment length show superior compatibilizing action (**Table 4.3**) as this copolymer is more or less located at the interface. This behaviour leads to a large reduction in interfacial tension and domain size and an increase in interfacial thickness. In contrast, other block copolymers (B₆, B₇, B₈) of unequal segment length is not able to improve the interfacial properties even at higher copolymer concentration (7.5 wt %). Diblocks with unequal segmental mass are not effective in promoting miscibility²⁰⁻²². Leibler³³ has suggested that diblock copolymers with a balanced composition (symmetrical) would be more effective interfacial agents than asymmetrical copolymers. This would be due to the fact that a symmetrical diblock copolymer would be less severely constrained at a plane interface than in a spherical micelle (the interface of a spherical particle with a diameter of a few tenths of a micron is essentially plane on a molecular scale); the asymmetrical diblock, on the other hand, would 'prefer' the spherical micelle formation.

Table 4.3: Effect of block copolymer composition on morphology

Polymer blend composition	Number average domain size(μm)			
	B ₅ (50/50)	B ₆ (30/70)	B ₇ (70/30)	B ₈ (85/15)
50/50/2	3.89	3.77	3.53	3.60
50/50/3.5	3.53	3.27	3.20	3.78
50/50/5	1.47	2.70	3.24	3.88
50/50/6	1.36	2.60	3.25	3.87
50/50/7.5	1.35	2.80	2.10	2.28

All block copolymers having molecular weight $\cong 2 \times 10^5$

Thus, according to Leibler, the more symmetrical a diblock copolymer, the more efficient it would be in emulsifying a polymer blend. The experimental results reported here point in that direction as well.

4.3.6 Effect of mode of addition of block copolymer

The morphology of the blend depends on the mode of preparation of the blends³⁴. Variation in the conditions of the blend preparation can change the morphology. The two step of mixing can be done in two ways. Blending the solution of the dispersed phase (PS) with the compatibilizer first and then blending with the matrix polymer (NR). In the second case, the matrix polymer was blended with the compatibilizer first and then blending with the dispersed polymer. Preblending the compatibilizer with the dispersed phase (PS) is found to improve the interaction between the copolymer and the dispersed phase³⁵.

The particle size of PS/NR₂₀ blends prepared by two step mixing are compared with that of the blend prepared by one step mixing. In the case of 40/60 wt % PS/NR blends (one step mixing) the CMC was attained at 2.27 wt % (**Figure 4.1**) of the block copolymer. When the copolymer phase was preblended with the dispersed phase the CMC was attained at 0.486 wt % of the block copolymer loading (**Figure 4.9**). In this case a much greater reduction in the domain size of the dispersed phase was observed. In one step mixing the particle size of the domains at 0.5 wt % block copolymer loading was found to be 3.75 μm whereas in two step mixing the corresponding value is 1.59 μm . At 1 % block loading, the values were 3.04 μm and 1.36 μm respectively. When the matrix polymer was preblended with the copolymer, the CMC was the same as in the case of one step mixing.

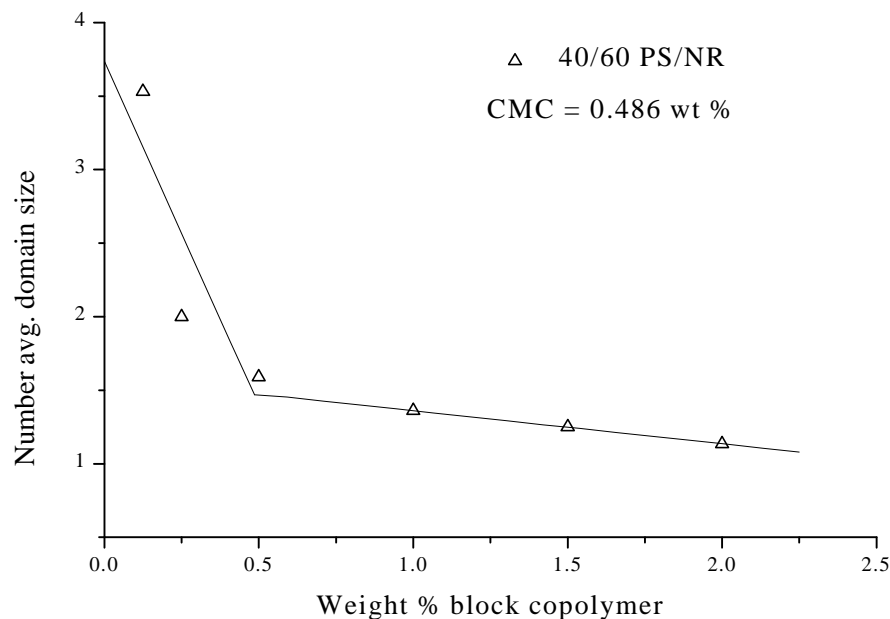


Figure. 4.9. Effect of mode of addition of block copolymer on blend morphology

The above findings reveal that the mode of addition of the compatibilizer has an important role in determining the morphology of the blends. Compared to one step mixing, the two step mixing i.e., by preblending the compatibilizer with the dispersed phase, results in the increased amount of the compatibilizer available at the interface and the distance traveled by the compatibilizer to reach the blend interface can be minimized. This leads to better interfacial interaction of the compatibilizer and results in a finer morphology.

4.3.7 Effect of copolymer concentration on blend miscibility

DSC studies of the compatibilized and uncompatibilized blends indicate the existence of two transitions corresponding to PS and NR phases. The compatibilized blends do not show any appreciable shift (**Table 4.4**) in the T_g values. This indicates that, addition of the compatibilizer does not alter the level of miscibility. In other words, incorporation of the compatibilizer does not promote molecular level miscibility. This is in agreement with the conclusion made by Paul⁴¹, who suggested that if two polymers are far from being miscible, then no copolymer is likely to make it a one-phase system. In a completely immiscible system, the main role of the copolymer is to

act as an interfacial agent. The typical DSC chromatogram for 50/50 PS/NR blend (Entry no. 4 in **Table 4.4**) is shown in **Figure 4.10**.

Table 4.4: DSC study of 50/50 PS/NR blend

Wt % of block copolymer ^a	T _g (°C)
0	-63 , 106
0.5	-58, 105
1.0	-62, 103
2.0	-60, 100
3.5	-53, 99

Diblock copolymer B₃, having PS:PI composition 50:50, is used for compatibilization study

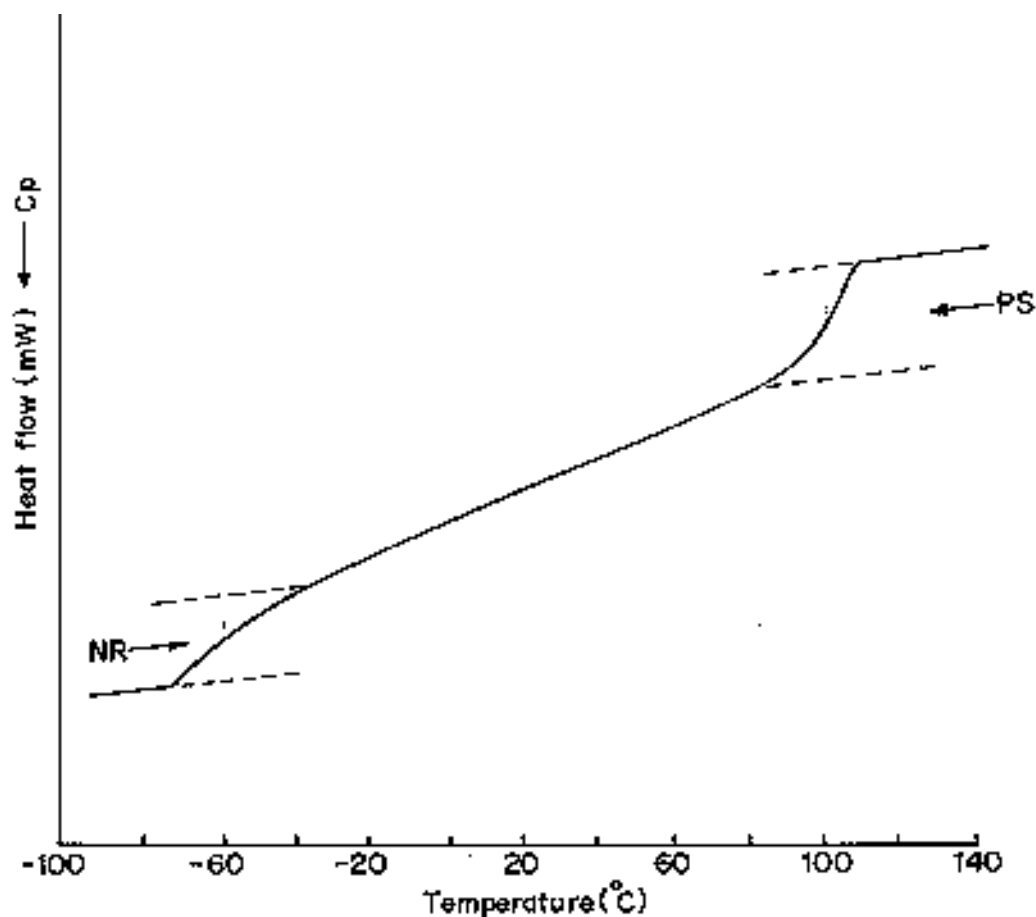


Figure 4.10. DSC of 50/50 PS/NR blend

4.3.8 Effect of block copolymer on mechanical properties

Blend morphology has a significant effect on the mechanical properties of the blends. Many studies have been reported on the morphology-mechanical property relationship of polymer blends. Addition of copolymer is reported to improve the interfacial adhesion and the mechanical properties. We have examined the mechanical properties such as modulus, tensile strength and elongation at break of the compatibilized blends. **Table 4.5** shows that the tensile strength and modulus increases with the addition of the copolymer and finally levels off at higher concentration. Although the mechanical properties are improved, the elongation at the break of the samples were adversely affected by the addition of the block copolymer. In case of modulus, the change is more pronounced. The impact strength of blend is greatly dependent upon the capacity for dissipating the impact energy through the matrix and the delivery of the internal stress of the continuous phase to the dispersed phase. Therefore, the interfacial condition between the phases is important. It seems that the enhanced adhesion of interface resulting from the compatibilization of block copolymer reduces the extent of diminution of impact strength (**Figure 4.11**). The improvement in the mechanical properties due to enhanced interfacial bonding between PS and NR is also evident from the SEM study.

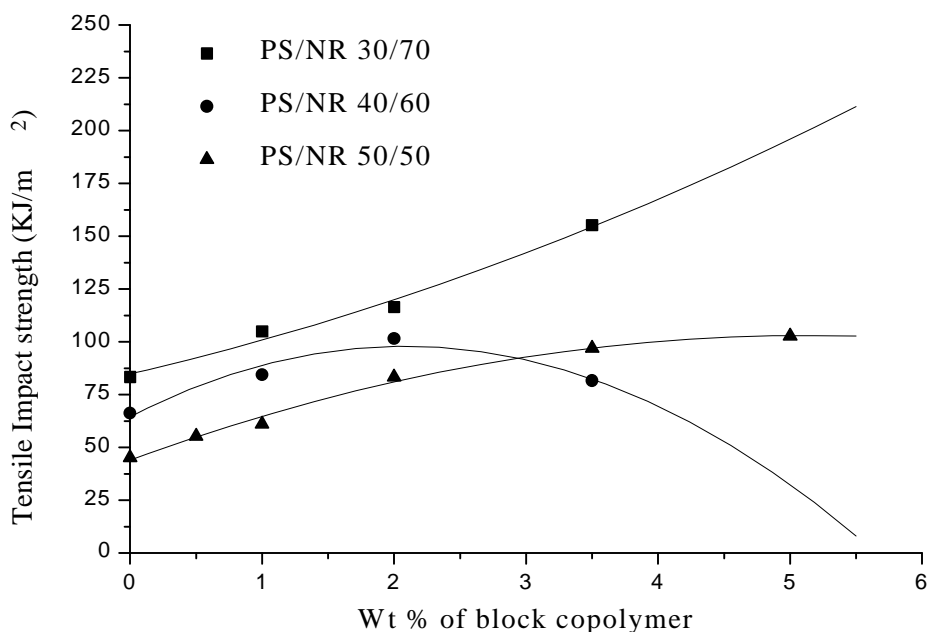


Figure 4.11 Tensile Impact strength of PS/NR blends with different blend composition

Several studies have been carried out to understand the compatibilizing action of block copolymer in immiscible polymer blends. The high interfacial tension existing between the phases which is responsible for macrophase separation can be reduced by the addition of compatibilizer. There are different parameters, which govern the interfacial saturation. These are molecular weight of the copolymers, polymer(s) structures, mode of addition of compatibilizer, processing conditions, affinity of the copolymer for the dispersed phase, orientation of the polymer at the interface etc.

Table 4.5: Mechanical Properties of 50/50 PS/NR blend

Wt % of block copolymer	Tensile strength (MPa)	Elongation at break (%)	Young's modulus (MPa)	Tensile Impact strength (KJ/M ²)
0	0.26	481	5.9	45.1
1.0	0.64	271	14.9	61.0
2.0	0.76	344	25.5	83.3
3.5	0.78	217	28.3	97.1
5.0	1.20	225	29.3	102.7
7.5	1.40	235	31.6	-

4.3.9 Interfacial area occupied per molecule and Physical model of conformation of the block copolymer at the blend interface

Almost all the experimental and theoretical studies related to the compatibilization of heterogeneous blends, including the present work, suggest that a critical concentration of the compatibilizer is required to saturate the blend interface (CMC) beyond which addition of the compatibilizer leads to undesirable micelle formation which very often reduces the total performance of blend system. One can also explain the interfacial saturation point using Taylor's Equation²⁹

$$W_e = \frac{\eta_m dn \gamma}{2g_{12}} \quad \text{Eq. 4.1}$$

Where W_e is the critical Weber number, η_m is the viscosity of the matrix, γ is the shear rate, γ_{12} is the interfacial tension, dn is the number average diameter of the dispersed phase. On the addition of the compatibilizer, the interfacial tension decreases and there is a consequent particle break down (deformation). From the equation there is a critical value of W_e , at which there is a balance of interfacial tension and particle deformation. Below the critical value no particle deformation occurs and a result a critical particle size. Therefore, there must be a maximum quantity of compatibilizer which can saturate the interface. An expression for interfacial tension reduction was developed by Noolandi and Hong based on thermodynamics to explain the

emulsifying effect of the A-b-B in immiscible A/B blends (A/A-b-B/B). The expression for interfacial tension reduction ($\Delta\gamma$) in a binary blend upon the addition of the copolymer is given by the following expression^{25, 26}

$$\Delta g \cong d f_c \left[\left(\frac{1}{2} \phi_c + \frac{1}{Z_c} \right) - \frac{1}{Z_c} \exp\left(Z_c \frac{\phi_c}{2}\right) \right] \quad \text{Eq. 4.2}$$

where d is the width at half height of the copolymer profile reduced by Kuhn statistical segment length, ϕ_c is the bulk volume fraction of the copolymer in the system, χ is the Flory-Huggins interaction parameter between A and B segment of the copolymer and Z_c is the degree of polymerization of the copolymer. According to this theory, at concentration smaller than CMC, the interfacial tension is expected to decrease linearly with copolymer concentration, whereas, at concentration higher than CMC a leveling off is expected. Since the interfacial tension reduction is directly proportional to the particle size reduction as suggested by Wu⁴², one can replace the interfacial tension reduction ($\Delta\gamma$) term as by Thomas et al⁴³. Therefore,

$$\Delta d \cong k d f_c \left[\left(\frac{1}{2} \phi_c + \frac{1}{Z_c} \right) - \frac{1}{Z_c} \exp\left(Z_c \frac{\phi_c}{2}\right) \right] \quad \text{Eq. 4.3}$$

where k is the proportionality constant

The particle size reduction was plotted as a function of the volume per cent of block copolymer concentration. It is noticed in **Figure 4.12** that at low concentration of the copolymer particle size reduction (Δd) decreases linearly with copolymer content and at high concentration Δd levels off as indicated by Noolandi and Hong. Reduction in domain size is due to the decrease in the interaction energy between homopolymers by the localization of the block copolymer in the interfacial area. The interfacial activity of the copolymer decreases the interaction energy and hence the domain size.

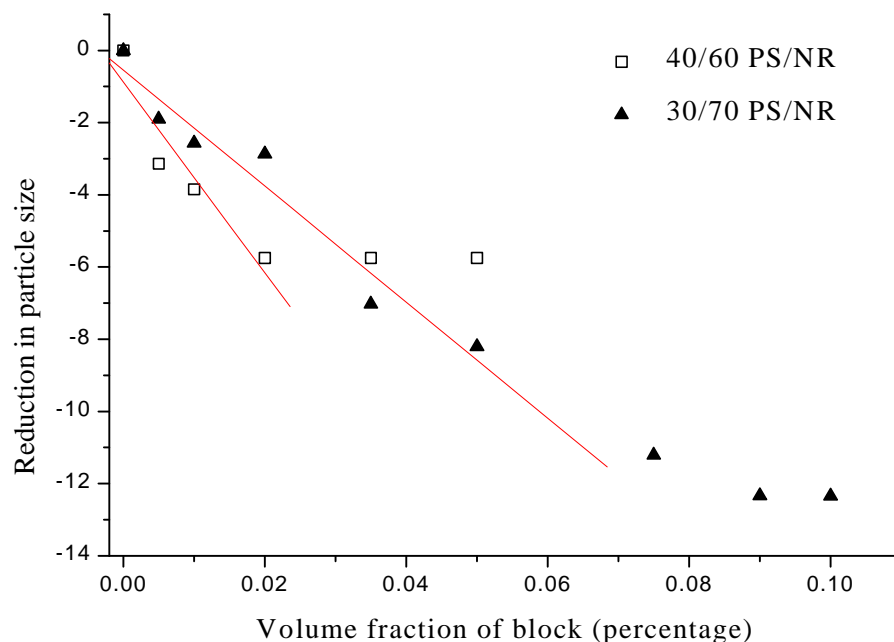


Figure 4.12. Effect of block copolymer volume fraction on particle size distribution

Another interesting feature of the experimental result is that the CMC values decreases as the molecular weight of the NR decreases (**Figure 4.6**). CMC values reported in this figure are obtained by keeping the copolymer and PS molecular weight constant and varying the molecular weight of NR homopolymer. The molecular weight dependence of CMC indicates that one can have two choices to compatibilize an immiscible blend: either to select a relatively high concentration of a medium molecular weight (compared to the molecular weight of homopolymer) copolymer or conversely a small amount of very high molecular weight (as compared to the molecular weight of homopolymer) block copolymer. If the molecular weight becomes extremely high, the larger molecules of copolymer will form micelles. However, at high viscosity the dispersion can cause problems, resulting in poor compatibilizing effect. Similar findings were observed by Noolandi and Hong. They derived the mean field equations for a ternary system consisting of two immiscible homopolymers and diblock copolymer and found a reduction in interfacial tension with increasing copolymer concentration and molecular weight.

The area occupied by the block copolymer at the interface of PS/NR blends can be estimated using the following equation of Paul⁴¹

$$\Sigma = \frac{3f_a M}{mRN} \quad \text{Eq. 4.4}$$

where, a is the area occupied by the block copolymer at the interface, ϕ_a is the volume fraction of the dispersed PS phase, M is the molecular weight of copolymer, m is mass of the copolymer required to saturate unit volume of interface, R is the radius of the dispersed PS spherical domain, N is Avogadro's number. The CMC values (m values) and the radius R of the dispersed phase at CMC measured by microscopy, and ' Σ ' values calculated from the above equation are in given **Table 4.6**. The CMC values are estimated by the interaction of the straight line drawn at the low concentration and the leveling off line at high concentration. While doing so, one important assumption must be made. It must be assumed that at the critical concentration, all the interfacial agents added to the system is located at the interface. This is probably not the case, however, the results obtained in the study of the effect of interfacial agent molecular weight suggest that the assumption is still reasonable, at least, in the case of symmetrical diblock copolymers (B_1 , B_2 , B_3). As stated earlier, the dynamic effects, which would potentially hinder the migration of the copolymer to the interface would be more significant for the higher molecular weight copolymers. Since the lowest critical concentration is obtained using the highest molecular weight diblock copolymer (**Entry no. 13, Table 4.6**), the assumption is reasonable. So there is a direct relationship between the molecular weight of the interfacial agents and the area occupied per molecule. Matos et al⁴⁴ have reported for PS/EPR system that higher values of interfacial area: 13, 18, and 45 nm²/ molecule for triblock copolymers as emulsifying agent, with molecular weights of 50,000, 70,000 and 174,000, respectively. The interfacial area occupied by a triblock is higher than that occupied by a diblock copolymer of same molecular weight.

Table 4.6: Dispersed phase radius (r) at CMC and ' Σ ' values of the system

Entry no.	Polymer blends	Solvent	CMC (m %)	Radius 'r' at CMC (μm)	' Σ ' (nm^2)
1.	50/50 (PS/NR ₂₀)	CHCl ₃	2.48	0.87	23.23
2.	40/60 (PS/NR ₂₀) ^a	CHCl ₃	2.27	0.56	31.35
3.	30/70 (PS/NR ₂₀)	CHCl ₃	7.95	0.59	6.34
4.	40/60 (PS/NR ₂₀) ^b	CHCl ₃	0.486	0.74	111.55
5.	40/60(PS/NR ₂₀) ^c	CHCl ₃	2.26	0.54	32.65
6.	40/60 (PS/NR ₂₀)	CCl ₄	2.31	2.18	7.91
7.	50/50 (PS/NR ₁₅)	CHCl ₃	6.51	0.80	9.62
8.	50/50 (PS/NR ₁₀)	CHCl ₃	9.15	0.74	7.36
9.	50/50 (PS/NR ₅)	CHCl ₃	10.60	0.73	6.43
10.	50/50 (PS/NR ₀)	CHCl ₃	11.18	0.93	4.82
11.	50/50 (PS/NR ₂₀ /B ₁)	CHCl ₃	6.00	1.63	2.44
12.	50/50 (PS/NR ₂₀ /B ₂)	CHCl ₃	6.00	1.43	4.47
13.	50/50 (PS/NR ₂₀ /B ₃)	CHCl ₃	5.00	1.37	8.36
14.	50/50 (PS/NR ₂₀ /B ₄)	CHCl ₃	6.00	1.36	7.87

a) one step mixing, b) two step mixing NR to PS + B, c) two step mixing PS to NR + B

It is noticed that as the molecular weight of the homopolymer (NR) decreases, the area occupied by the compatibilizer molecule at the interface (Σ) increases (**Figure 4.13**). The ' Σ ' value also dependent on the mode of addition of the compatibilizer to the blend system. In two-step process where the copolymer is preblended with the dispersed phase, the Σ value is 111.55 nm^2 . This indicates that the interaction of the copolymer and homopolymer is higher in two-step process, compared to the one-step process where $\Sigma = 31.35 \text{ nm}^2$. Greater interaction would increase interfacial area and reduce interfacial tension. One can also comment on the conformation of the block copolymer based on the Σ values.

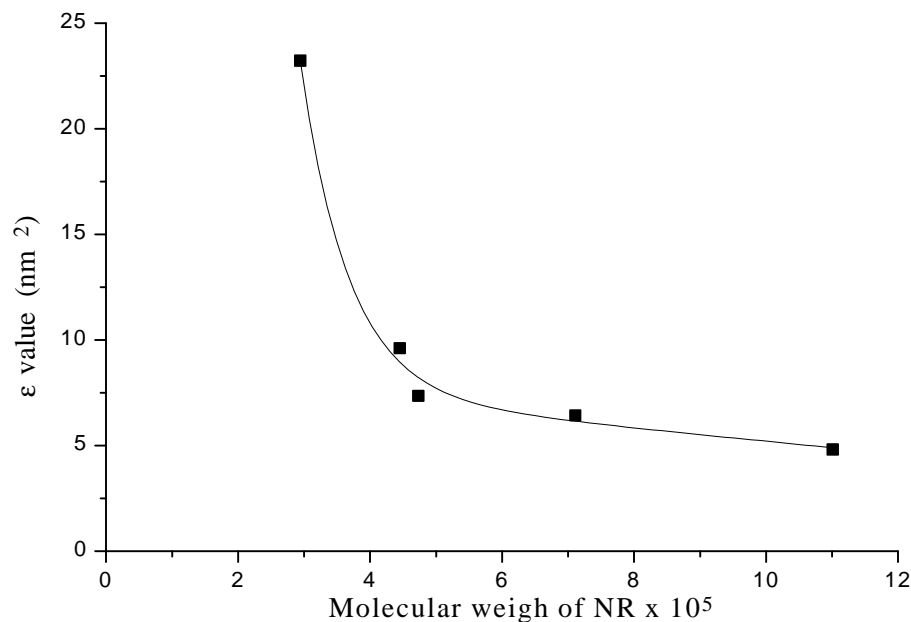


Figure 4.13. Effect of homopolymer molecular weight on the calculated area occupied by the copolymer molecule at the blend interface, Σ

Two physical models illustrating the conformation of the compatibilizer at the interface are given in the literature^{41, 45}. One model visualizes the blocks as extending into the corresponding homopolymer phases as shown in **Figure 4.14a**. In such a case, the occupied area at the interface is the cross-sectional area of the extended copolymer molecule. This is approximately equal to 0.6 nm^2 . In the second model (**Figure 4.14b**), the copolymer lies flat at the interface and here the occupied area is the lateral surface area of the entire copolymer molecules⁴⁵. By considering each block as a spherical random coil, we have calculated the lateral surface area of the copolymer using the experimental values of root mean square radius of gyration of the PS block, reported in literature⁴⁶, which is 8.73 nm . The lateral surface area is approximately equal to 274 nm^2 . The experimental ' Σ ' values lie between 4.8 to 111.6 nm^2 , which is intermediate between those of extended and the flat model given in the literature. This suggests that neither of these models represent the actual situation. The behaviour of the copolymer can thus be represented by a third model (**Figure 4.14c**). In this model, the copolymer cannot completely penetrate into the corresponding homopolymer phases. A substantial part of the copolymer molecules stay at the interface between the PS and NR phases.

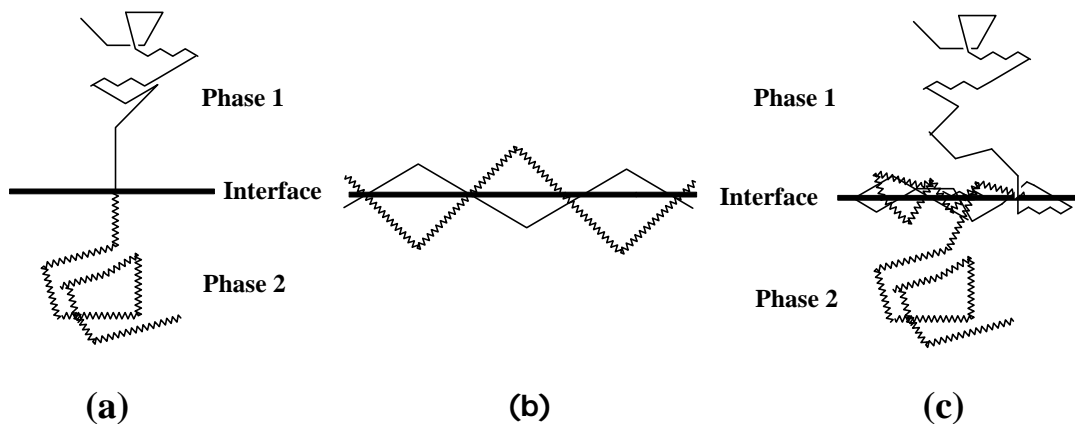


Figure 4.14. Physical models illustrating the conformation of the copolymer at the interface

4.4 Conclusions

The effect of addition of a small amount of block copolymer of polystyrene and polyisoprene (PS-*b*-PI) on the interfacial properties of PS and NR blends has been studied. Both the morphology and mechanical properties of PS/NR blend have been investigated. Concentration, composition, and molecular weight of the copolymer, composition of the blend, mode of addition of the compatibilizer, homopolymer molecular weight and processing conditions were the controlling parameters on blend morphology. The domain size of the dispersed phase decreases upon addition of a small amount of copolymer, followed by leveling off at higher concentration, which is an indication of the interfacial saturation by the copolymer. For concentration less than CMC, the theories of Noolandi and Hong predict a linear decrease of interfacial tension with copolymer volume fraction. Considering that interfacial tension is directly proportional to the domain size, it is demonstrated that the experimental data are in agreement with these theories.

The area occupied by the compatibilizer molecule at the interface (Σ) has been estimated. The (Σ) values were influenced by the molecular weight of homopolymer, blend composition, mode of addition and the nature of the casting solvent. The mechanical properties are in agreement with the morphological changes. It was found that the tensile strength, modulus and tensile impact increases upon the addition of diblock copolymer.

Attempts were made to establish the conformation of the compatibilizer at the blend interface. Different models are discussed. The actual conformation is neither fully

extended nor flat. A portion of the copolymer penetrates into the corresponding homopolymer and the rest remains at the interface.

4.5 References

1. Folkes, M. J.; Hope, P. S. 'Polymer Blends and Alloys', Blackie, London, **1993**.
2. Utracki, L. A. 'Polymer Alloys and Blends', Carl Hanser Verlag, New York, **1989**.
3. Chapleau, N.; Favis, B. D.; Carreau, P. J. *J. Polym. Sci., Polym. Phys.*, **1998**, 36, 1947.
4. Dedecker, K.; Groeninckx, G.; Inoue, T. *Polymer*, **1998**, 39, 5001.
5. Yu, Z. -Z.; Ou, Y. -C.; Hu, G. -H., *J. Appl. Polym. Sci.*, **1998**, 69, 1711.
6. Eklind, H.; Schantz, S.; Maurer, F. H. J.; Jannasch, P.; Wesslen, B., *Macromolecules*, **1996**, 29, 984.
7. Gersappe, D.; Irvine, D.; Balazs, A. C.; Liu, Y.; Sokolov, J.; Rafailovich, M.; Schwarz, S.; Peiffer, D. G. *Science*, **1994**, 265, 1072.
8. Creton, C.; Kramer, E. J.; Hadziioannou, G. *Macromolecules*, **1991**, 24, 1846.
9. Riess, G.; Kohler, J.; Tournut, C.; Banderet, A. *Makromol. Chem.*, **1967**, 101, 58.
10. Reiss, G.; Jolivet, Y. 'Copolymers, Polyblends and Composites' (N.A.J. Platzer, ed.), Am. Chem. Soc., *Advan. Chem. Ser.*, **1975**, 142, 76.
11. Brown, H. R.; Daline V. R.; Green, P.F. *Nature*, **1989**, 341, 221.
12. Dutta, S.; Lohse, D. J. *Macromolecules*, **1993**, 26, 2064.
13. Pu, H.; Tang, X.; Xu, X. *Polym. Int.*, **1998**, 45, 169.
14. Feng, H.; Ye, C.; Tian, J.; Feng, Z.; Huang, B. *Polymer*, **1998**, 39, 1787.
15. Guo, H. F.; Packirisamy, S.; Mani, R. S.; Avonson, C. L.; Gvozdic, N. V.; Meier, D. J., *Polymer*, **1998**, 39, 2495.
16. Yu, J. M.; Dubois, P.; Jerome, R. *J. Polym. Sci., Polym. Chem.*, **1997**, 35, 3507.
17. Inoue, T.; Soen, T.; Hosimoto, T.; Kawai, H. *Macromolecules*, **1970**, 3, 87.
18. Moritani, M.; Inoue, T.; Motegi, M.; Kawai, H. *Macromolecules*, **1970**, 3, 433.
19. Jo, W. H.; Nam, K. H.; Cho, J. C. *J. Polym. Sci., Polym. Phys.*, **1996**, 34, 2169.

20. Cigana, P.; Favis, B. D.; Jerome, R. *J. Polym. Sci., Polym. Phys.*, **1996**, *34*, 1691.
21. Israels, R.; Jasnow, D.; Balazs, A. C.; Guo, L.; Krausch, G.; Sokolov, J.; Rafailovich, M. *J. Chem. Phys.*, **1995**, *102*, 8149.
22. Cigana, P.; Favis, B. D. *Polymer*, **1998**, *39*, 3373.
23. Asaletha, R.; Thomas, S.; Kumaran, M. G. *Rubber Chemistry and Technology*, **1995**, *68*, 671.
24. Noolandi, J. *Polym. Eng. Sci.*, **1984**, *24*, 70.
25. Noolandi, J.; Hong, K. M. *Macromolecules*, **1982**, *15*, 482.
26. Noolandi, J.; Hong, K. M. *Macromolecules*, **1984**, *17*, 1531.
27. Hsieh, H. L. *J. Polym. Sci. Part A*, **1965**, *3*, 153.
28. Annual Book of ASTM standard, American Society for Testing and Materials, Philadelphia, **1981**, 1979, part 35.
29. Willis, J. M.; Favis, B. D. *Polym. Eng. Sci.*, **1988**, *28*, 1416.
30. Zhao, H.; Huang, B. *J. Polym. Sci., Polym. Phys.*, **1998**, *36*, 85.
31. Reiss, G.; Jolivet, Y. *Am. Chem. Soc., Advan. Chem. Ser.*, **1975**, *142*, 243.
32. Vilgis, T. A.; Noolandi, J. *Macromolecules*, **1990**, *23*, 2941.
33. Leibler, L. *Makromol. Chem. Macromol. Symp.*, **1988**, *16*, 1.
34. Ohlsson, B.; Hassander, H.; Tornell, B. *Polymer*, **1998**, *39*, 4715.
35. Oommen, Z.; Thomas, S. *J. Mat. Sci.*, **1997**, *32*, 6085.
36. Bank, M.; Leffingwell, J.; Thies, C. *Macromolecules*, **1971**, *4*, 43.
37. Barlow, J. W.; Paul, D. R. *J. Polym. Sci., Polym. Phys. Edu.*, **1987**, *25*, 1459.
38. Caravatti, P.; Neuenschwander, P.; Ernst, R. R. *Macromolecules*, **1985**, *18*, 119.
39. Robard, A.; Patterson, D. A. *Macromolecules*, **1977**, *10*, 1021.
40. Chen, C. T.; Morawetz, H. *Macromolecules*, **1989**, *22*, 159.
41. Paul, D. R. "Polymer Blends" (Eds D. R. Paul and S. Newman), Academic Press, New York, **1978**, Ch12.
42. Wu, S. *Polym. Eng. Sci.*, **1987**, *27*, 335.
43. Thomas, S.; Prud'homme, R. E. *Polymer*, **1992**, *33*, 4260.
44. Matos, M.; Favis, B. D.; Lomellini, P. *Polymer*, **1995**, *36*, 3899.
45. Plochochi, A. P.; Dagli, S. S.; Andrews, R. D. *Polym. Eng. Sci.*, **1990**, *30*,

741.

46. Kirste, R. G.; Kruse, W. A.; Ibel, K. *Polymer*, **1975**, *16*, 120.

CHAPTER -V

HETEROARM STAR POLYMERS AS EMULSIFYING AGENTS AND INFLUENCE OF MOLECULAR ARCHITECTURE OF COMPATIBILIZER IN POLYMER BLENDS

5.1 Introduction

Polymer blends constitute one of the important topics of research in polymer science. The main goal of this research is to combine different properties and/or to produce new ones by mixing at least two polymeric materials. The problem arises from the fact that mixing of polymers is a thermodynamically unfavorable process. In most of the cases, the entropy of mixing is very small and cannot compensate the entropically unfavorable interactions between the unlike polymer segments. This leads to immiscible polymer blends with macroscopically phase separated structures with poor mechanical properties. In order to overcome the incompatibility between two immiscible homopolymers A and B, a small amount of a block or graft copolymer is added to the system as a compatibilizing agent. The copolymer migrates to the interface of the A and B polymer blend and reduces significantly the interfacial tension, imparting an efficient phase dispersion. For the effective compatibilizing process, the interpenetration of segments of copolymers and blend components is necessary to achieve a strong mechanical adhesion caused by the reduction of the interfacial tension due to the presence of copolymers. This indicates that molecular architecture is an important parameter for achieving efficient compatibilities. Moreover, as each block of the copolymer is mixing with the corresponding homopolymers the adhesion between the A and B phases is strengthened. Thus, the mechanical properties of the blend are significantly improved.

In recent years the compatibilizing efficiency of the copolymers have received much attention from both experimental and theoretical points of view¹⁻¹¹. There are several reports on the role of molecular structure, molecular weight, chemical composition and molecular architecture of the compatibilizing agent on the ultimate properties of polymer blends. Literature evidence do suggest that the most desirable compatibilizer from the stand point of the reduction of interfacial tension in a system of polymer A

and B is a symmetric diblock copolymer A-B. Since the interfacial activity increases with increasing chain length, the block chain length must be relatively long, but an upper limit exists due to micelle formation^{12, 13}. As long as molecular architecture of the compatibilizer is concerned diblocks are more effective than graft, triblock or star-shaped polymers¹⁴. Similar observation is reported by Koklas et al¹⁵. Balazs et al¹⁶ examined this effect by using self-consistent mean field theory and analytical methods and concluded that at fixed molecular weight, the diblock copolymers are the most efficient emulsifying agent compared to a random copolymer, a four-armed star and various comb polymers.

Nevertheless, several aspects of the effect of molecular architecture on the performance of copolymer compatibilizer still remain unresolved. There have been only few experimental¹⁶⁻²⁰ or theoretical^{21, 22} reports on the study of compatibilizers possessing different molecular architecture.

Recently, "heteroarm star polymers" have been synthesized by anionic polymerization method^{17, 23}. These polymeric species are star polymers of the general formula A_nB_n bearing two different chemical arms diverge from a very dense poly(divinylbenzene) core, or other types of junction points^{18, 24}.

The current work deals with a study of the role of heteroarm star polymers as emulsifying agents. The effect of number of arms of the star polymer on compatibilizing efficiency in A/B polymer blends has been examined. The effect of molecular architecture on emulsifying ability is reported. The interfacial activity of a linear diblock, heteroarm star and star block copolymer having similar arm molecular weight and composition have been compared. The first work in this field is a report by Inoue et al¹⁸ that heteroarm star shaped block copolymer with cyclotriphosphazine core with polystyrene and nylon 6 arms can be used as an efficient compatibilizer for poly(2,6-dimethylphenylene oxide)/nylon 6 blends. While the present work was in progress, Tsitsilianis et al¹⁷ reported the emulsifying ability of heteroarm star polymer of polystyrene/polyethylmethacrylate (PS_nPEMA_n) in PS/PEMA blend system. A comparative study on linear diblock of PS-b-PEMA and varying number of arms of PS_nPEMA_n (where $n = 6$ and 9) was reported in this work. Heteroarm star bearing 6 number of arms of each kind was the most efficient emulsifying agent.

5.2 Experimental

5.2.1 Materials

Commercial polystyrene (SC-206E) was supplied by Supreme Plastics, Bombay. Natural rubber (ISNR-5) was supplied by Rubber Research Institute of India, Kottayam, Kerala. The characteristics of these materials are given in **Table 5.1**.

5.2.2 Synthesis of copolymers

All the copolymers, linear and star-branched involved in this study were synthesized by anionic polymerization under an inert atmosphere. PS-b-PI linear diblock anions were prepared by the usual sequential anionic polymerization using sec-BuLi as an initiator and cyclohexane as solvent. In the next step, isoprene monomer was added into this solution containing living polystyryl anion (**Chap III, Sec. 3.5.1**).

Heteroarm star polymer and star block copolymer of styrene and isoprene was synthesized using DVB as a coupling agent²⁶. By varying the DVB/Li ratio, number of arms were varied. Sec-BuLi was used as initiator and polymerization was carried out in cyclohexane at 55 °C. Polymerization was carried out in a specially designed apparatus with provision of taking pick-out under positive pressure of nitrogen. In all steps a small part of the reaction solution was sampled out and the polymeric species were isolated for the purpose of characterization. For heteroarm star polymer (A_nB_n), a combination of arm first and core first method was used, whereas for star block copolymer $(AB)_n$, arm first method was used²⁷ (**Chap. III, Sec. 3.5.2**).

5.2.3 Characterization of star branched polymers

The star-branched polymers were characterized by GPC-MALLS, ¹H NMR, IR spectroscopy and gravimetric method (**Chap. III, Sec. 3.6**). The characteristics of the copolymers synthesized are given in an earlier chapter (**Chap. III, Sec. 3.7.3**).

5.2.4 Preparation of blends

PS and NR were solution blended in chloroform (2 wt % solution) in different proportions. Blends having wt % compositions of PS/NR 50/50, 40/60 and 30/70 were made with and without the addition of the star-branched copolymer. After mixing PS, NR and star-branched copolymer in chloroform, the mixture was kept overnight and then stirred for 12 h using a magnetic stirrer. The blend films were cast on a glass plate and were dried in air at room temperature. The morphologies of all the system were examined by optical microscopy and SEM. The effect of number of

arms of star-branched copolymer on compatibilization was studied by using heteroarm star having different number of arms. The effect of molecular architecture of copolymers on compatibilization ability was also studied by using different star-branched copolymers and linear diblock copolymers of similar arm molecular weight and chemical composition.

5.2.5 Analysis

5.2.5.1 Morphological observation

In order to determine the particle size and distribution of the dispersed phase in blends, the morphology of the samples was examined using an optical microscope (Leitz Laborlux 12 Pol S). For SEM study osmium tetroxide (OsO_4) stained samples were vacuum coated with gold and examined in a scanning electron microscope (Stereoscan 440, Leica Cambridge). In order to gain better understanding of morphology, after prolonged drying under vacuum the specimens were etched with acetone for 2 to 7 days which is a selective solvent for PS. OsO_4 fixation technique was also adopted to increase the contrast between the two phases. The etched and stained specimens were dried adequately before the microscopic observation.

5.2.5.2 DSC study

Differential scanning calorimetry (DSC) analysis was carried out on Mettler-20 thermal analyzer. For DSC analysis about 20 mg sample was first cooled to $-100\text{ }^\circ\text{C}$ and then it was heated under nitrogen at the heating rate of $10\text{ }^\circ\text{C}/\text{min}$. Al_2O_3 was used as the reference sample.

5.2.5.3 Measurement of mechanical properties

A 5 % solution of blends in chloroform was made for casting. Sheets were cast on a Teflon mould and were dried in air at room temperature and then dried in a vacuum oven at $80\text{ }^\circ\text{C}$ for 48 h. Mechanical properties were determined according to ASTM standards using Instron testing machine (model 4204, pneumatic grip model 2712-002) using a cross head speed of $25\text{ mm}/\text{min}$.

Specimens for tensile impact were injection molded at $180\text{ }^\circ\text{C}$. The diameter of the tab of the bar was 4.5 mm and of the neck 1.5 mm. The tensile impact strength was determined by an impact tester model CS-183 T1-085 (CSI, Cedar Knolls, New Jersey, USA) using the ASTM D-1822 method²⁸.

5.3 Results and discussion

Table 5.1: Characteristics of materials used

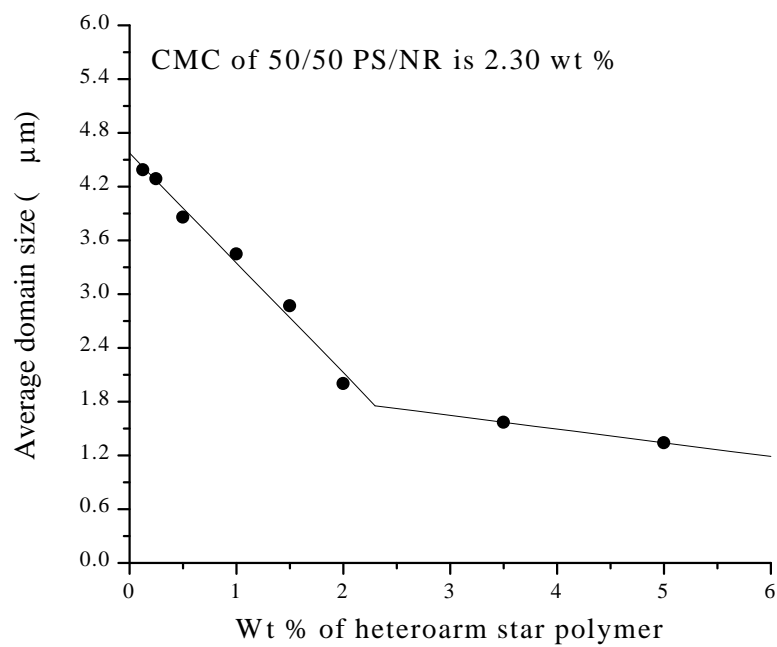
Material	$[\eta]^a$ dl/g	Solubility parameter(cal/cc) ^{1/2}	$\bar{M}_v \times 10^{-5}$
NR ₂₀	2.23	7.75	2.94
PS	0.68	8.56	1.89

a) determined in toluene at 25 °C, b) NR suffix indicates time of mastication in minutes

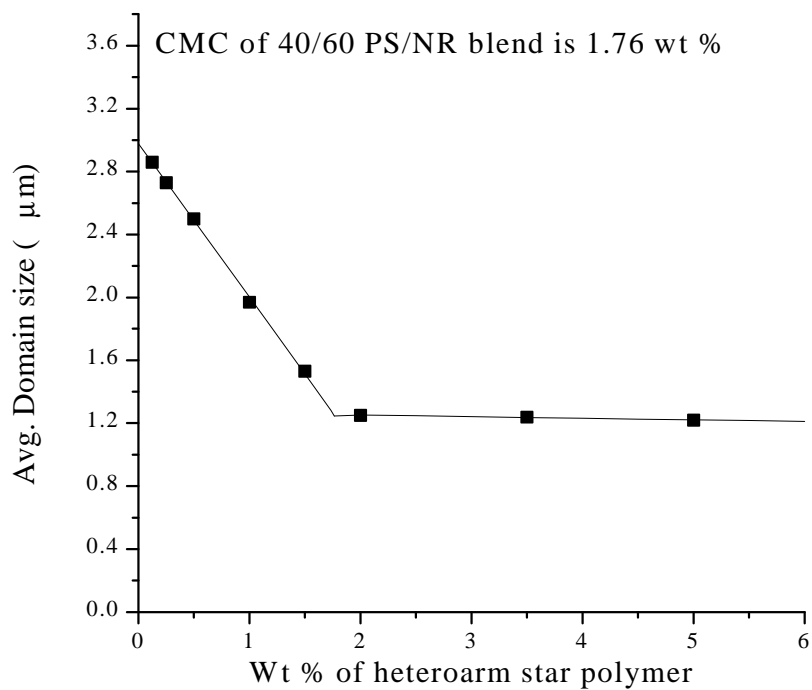
5.3.1 Effect of heteroarm star polymer (HS₁) concentration on morphology

Compatibility of PS and NR is poor and can be improved by the addition of a heteroarm star polymer of polystyrene and polyisoprene which, decreases the phase separation and reduces the particle size. Morphology of the dispersed phase in the blend was followed by increasing the concentration of the star polymer in the blend. The system shows typical emulsifying behavior, with a rapid drop in particle size at low concentrations of interfacial agent, followed by a leveling off at a certain critical concentration. It was observed that the domain size decreases with increasing concentration of the star polymer. A quantitative assessment of the compatibilizing effect was made by measuring the diameter of about 100 domains. In a 50/50 wt % blend, a 54 % domain size reduction was observed by the addition of 0.125 wt % of block copolymer. Addition of another 0.75 wt % block copolymer causes a size reduction of about 64 % followed by a leveling off at higher copolymer concentrations (**Figure 5.1a**).

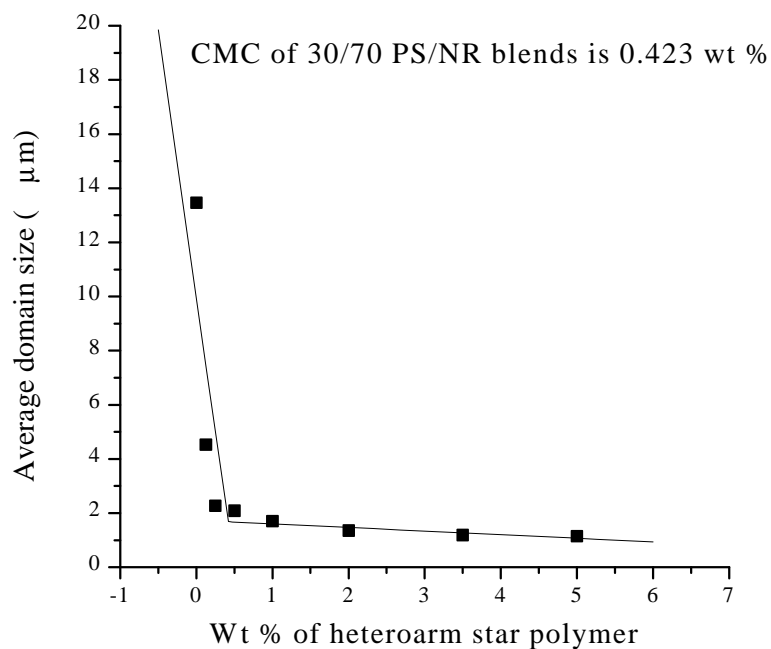
The leveling point can be taken as the CMC i.e., the lowest concentration at which micelles are formed. CMC values are estimated from the intersection of the straight lines (**Figure 5.1**) obtained at low concentration and leveling off line at higher concentration. The inter particle distance also decreases with increasing concentration of the star polymers and attains a constant value at higher concentration (**Figure 5.2**). For 30/70 PS/NR CMC is about 0.423 %. The corresponding values for 50/50 wt % and 40/60 wt % PS/NR are 2.30 and 1.78 % respectively.



(a)



(b)



(c)

Figure 5.1. Effect of heteroarm star polymer (HS₁) concentration on the domain size of the dispersed phase of different PS/NR blends

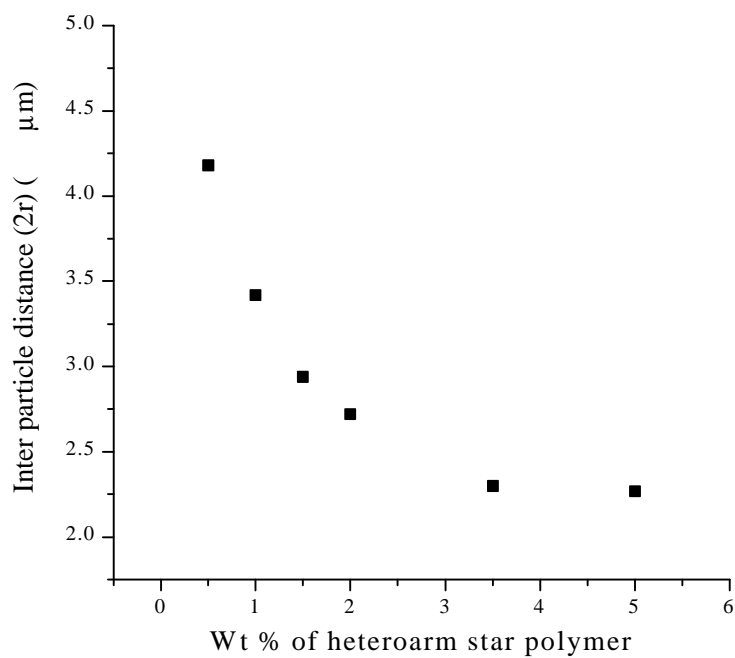
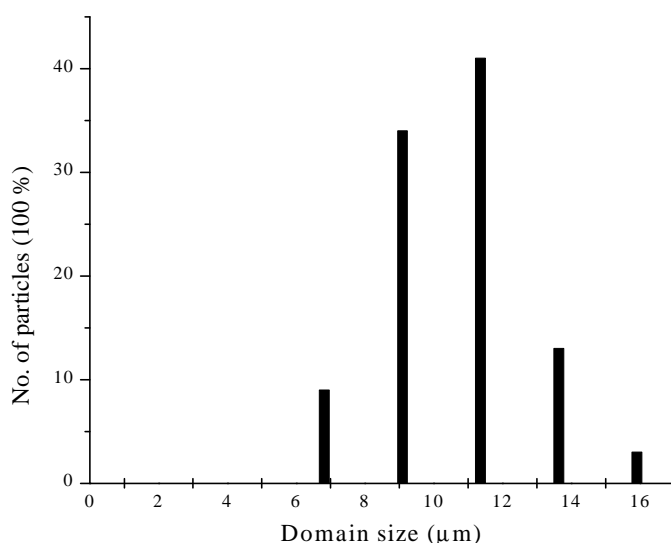


Figure 5.2. Effect of heteroarm star polymer (HS₁) concentration on interparticle distance of the dispersed phase in 30/70 PS/NR blends

5.3.2 Effect of heteroarm star polymer (HS₁) concentration on particle size distribution

Addition of interfacial agent to the system affects not only the particle size but the particle size distribution as well. To assess quantitatively the effect of heteroarm star polymer concentration on particle size distribution, the domain size distribution of the 30/70 wt % PS/NR blend was examined with and without the addition of star polymer (**Figure 5.3**). It is observed that with addition of the star polymer the distribution of the size of the dispersed particle changes. The results shows that in absence of star polymer, the radius of the dispersed particles range from 6.8 to 15.9 μm . When star polymer is added, the particle size of the dispersed phase decreases. When the star polymer content reaches 0.5 wt % and 1.0 wt %, the radius of dispersed particles range from 2.3 to 4.6 μm and 2.3 to 3.4 μm , respectively. The blend contains larger number of bigger particles in the absence of copolymer and therefore the polydispersity is high. The distribution curve of 50/50 and 40/60 PS/NR blend also follows the same pattern. Similar results have been reported by Zhao and Huang²⁹ for polybutadiene/polymethylmethacrylate blends using poly(butadiene-b-methylmethacrylate) as compatibilizer and by Kim et al³⁰ for poly(ethylene-ran-acrylic acid)/PS blends using poly(styrene-ran-glycidylmethacrylate) as compatibilizer.



(a)

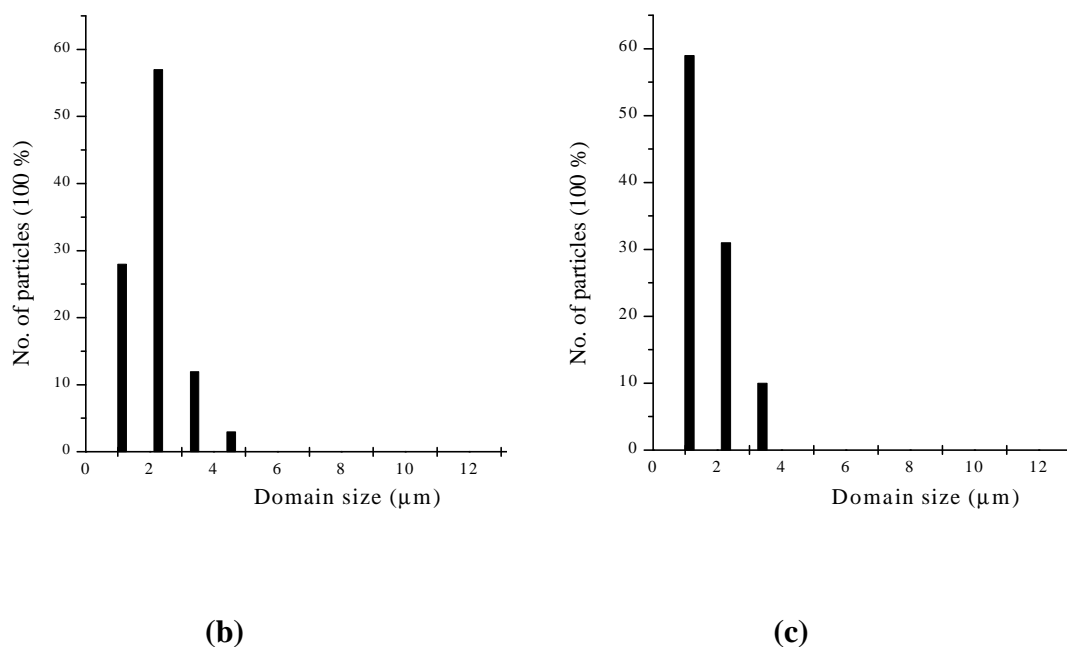


Figure 5.3. Particles distribution of dispersed NR in PS/NR blends (30/70 w/w) compatibilized by different amounts of HS₁. (5.3a) Blends containing 0 wt % copolymer; (5.3b) blends containing 0.5 wt % copolymer and (5.3c) blends containing 1.0 wt % copolymer

5.3.3 Effect of heteroarm star polymer (HS₁) concentration on blend miscibility

DSC studies of the compatibilized and uncompatibilized blends indicate the existence of two transitions corresponding to PS and NR phases. The compatibilized blends do not show any appreciable shift (**Table 5.2**) in the T_g values. This indicates that, addition of the compatibilizer does not alter the level of miscibility. In other words, incorporation of the compatibilizer does not promote molecular level miscibility. This is in agreement with the conclusion made by Paul³¹, who suggested that if two polymers are far from being miscible, then no compatibilizer is likely to make it a one-phase system. In a completely immiscible system, the main role of the compatibilizer is to act as an interfacial agent.

Table 5.2: DSC study of 50/50 PS/NR blend

Wt % of heteroarm star polymer ^a	T _g (°C)
0	-63 , 106
0.25	-63, 104
0.5	-63, 103
1.0	-62, 103
3.5	-62, 100

heteroarm star polymer, having PS:PI composition 50:50, is used for compatibilization study

5.3.4 Effect of heteroarm star polymer (HS₁) on mechanical properties

Blend morphology has a significant effect on the mechanical properties of the blends. Many studies have been reported on the morphology-mechanical property relationship of polymer blends. Addition of star polymer is expected to improve the interfacial adhesion and the mechanical properties. We have examined the mechanical properties such as modulus, tensile strength and elongation at break of the compatibilized blends. **Table 5.3** shows that the tensile strength, elongation at break and modulus increases with the addition of the heteroarm star polymer. In case of modulus, the change is more pronounced. The impact strength of a blend is determined by the capacity for dissipating the impact energy through the matrix and the delivery of the internal stress of the continuous phase to the dispersed phase; thus, the interfacial adhesion between the phases is important. It seems that the enhanced adhesion of interface resulting from the compatibilization of heteroarm star polymers reduces the extent of diminution of impact strength. As shown is **Figure 5.4**, the addition of heteroarm star polymer gives higher impact strength and increases with wt % loading of compatibilizer. The improvement in the mechanical properties due to enhanced interfacial bonding between PS and NR is evident from the SEM. That is, the star polymer, presumably, locates at the interface, and effective penetration of the arms into the corresponding blend components is indicated. But at higher loading of compatibilizer say 5 wt %, the adverse effect on mechanical property is observed. The reason may be due to micelle formation of star polymer at higher concentration.

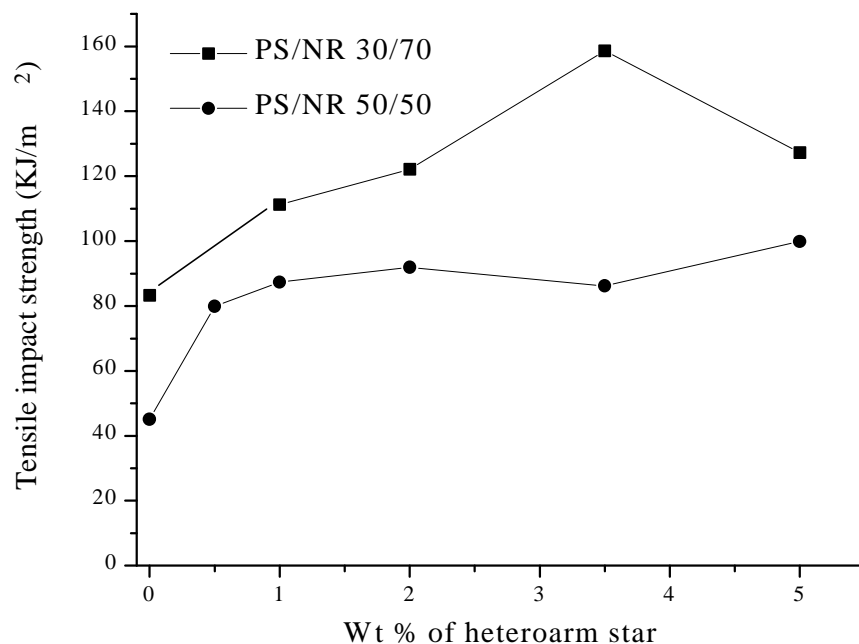


Figure 5.4. Tensile impact strength of PS/NR blends using heteroarm star polymer (HS₁) as compatibilizer

Table 5.3: Mechanical Property measurement of 30/70 PS/NR blend using heteroarm star polymer (HS₁) as compatibilizer

Blend Composition (wt%)	Tensile strength (MPa)	% Elongation	Young's modulus (MPa)
30/70/0	0.76	528	14.80
30/70/0.5	1.03	553	17.45
30/70/1.0	1.09	539	20.53
30/70/2.0	1.38	512	21.60
30/70/3.5	1.75	581	28.30
30/70/5.0	1.29	533	22.08

5.3.5 Effect of number of arms of heteroarm star polymer on morphology

The compatibilizing effect of the AB block copolymers in A/B blends is strongly dependent on the molecular weights of the individual blocks of the copolymers. It has been demonstrated, the most efficient compatibilizer should have equal or higher

block molecular weights than those of the corresponding homopolymers of the blend³².

Another aspect that should be considered is the phase behavior of the A_nB_n star-shaped copolymers as described by the theoretical predictions of Olvera de la Cruz and Sanchez³³. Assuming that the A_nB_n star copolymers can be considered as n identical diblock copolymers joined together at their A-B junction points, the critical value χN remains 10.5 as in the case of diblock copolymers independent of the number of arms n . Herein, χ is the Flory-Huggins interaction parameter and $N = N_A + N_B$ which is the sum of the degree of polymerization of the A and B arms. This implies that the microphase separation of nearly symmetrical heteroarm star copolymers depends solely on the molecular weight of the arms and not that of the whole star polymer. Taking into account of the above, the heteroarm stars prepared for this work were designed so as to have nearly the same chemical compositions (50 wt % styrene) but differing in the number of arms.

The phase behavior of the block copolymers used as compatibilizers were first investigated by means of DSC, and their T_g s are listed in **Table 5.4**

Table 5.4: DSC study of copolymers

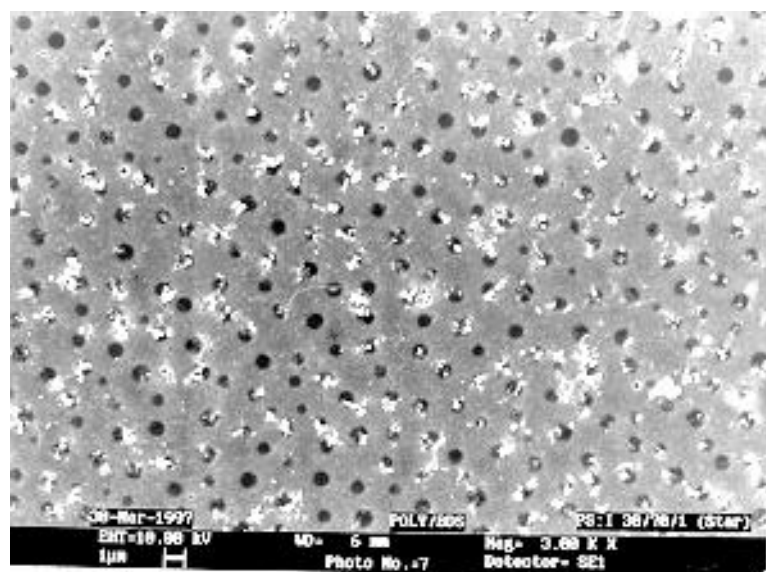
Samples	T_g (°C)
B ₅	-60 , 103
HS ₁	-59 , 99
HS ₂	-70 , 98
SB	-70 , 86

For all four samples two distinct glass transition temperatures (T_g s) are observed, revealing a microphase separation in accordance with the theoretical prediction³³ and experimental findings³⁴⁻³⁶. The higher T_g s are attributed to the PS-rich phase and the lower ones to the PI-rich phase.

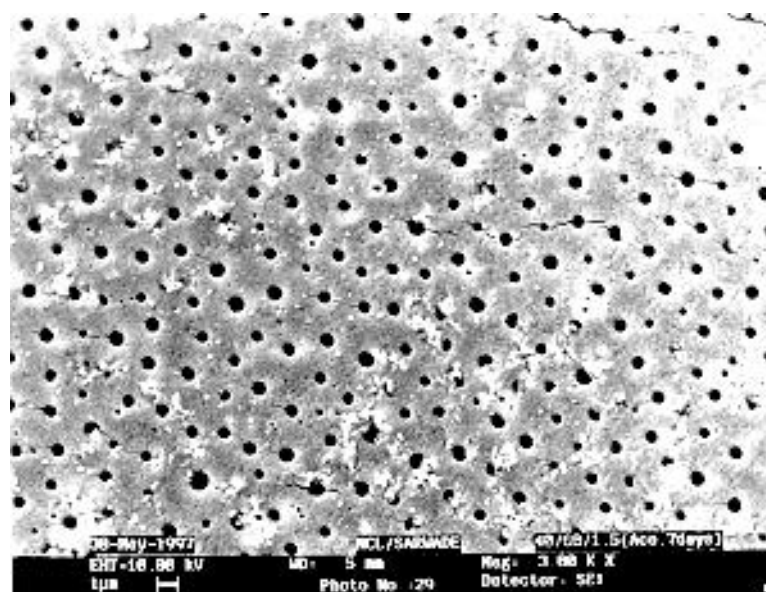
Although the position of T_g s for B₅ and HS₁ are the same, the T_g of the PI-rich phase for HS₂ and SB is about 10 °C lower than those of the two other samples. This could be attributed to the different microstructures (1,2 or 1,4) of the PI chains. The T_g of PS-rich phase in SB is extremely low compare to other three.

The efficacy of the heteroarm star polymer as interfacial agent can be appreciated qualitatively by a visual observation of micrographs. **Figure 5.5** shows SEM micrographs of ternary blends of PS/NR/star polymer (30/70/1). The effect of the compatibilizer (heteroarm star having different number of arms) (**Chap. III, Table 3.3**) on the morphology of the ternary blend can be demonstrated in these micrographs. The continuous phase is PS and the dark spots are NR stained by OsO₄. In **Figure 5.5a** and **5.5c**, in both cases 1 wt % compatibilizer is present. But in case of **Figure 5.5c** uniform smaller domain size, with an even larger reduction in the dimensions of the dispersed phase compare to **Figure 5.5a** being observed. To gain a better understanding regarding blend morphology and to increase the contrast between the two phases, PS phase was extracted with acetone for 7 days. Acetone is a selective solvent for PS and nonsolvent for NR. From the SEM micrographs (**Figure 5.5b**) it is clear that the PS domains are extracted out completely from the matrix and dark holes corresponds to the PS dispersed phase, are left by selective solvent treatment. But in case of **Figure 5.5d** after 7 days acetone treatment, the PS matrix appears swelled that indicates this period of solvent treatment is not sufficient to fully remove the PS from the blend. Thus, by increasing the number of arms of star polymer, the interfacial adhesion between two phases increases and removal of one phase becomes more and more difficult.

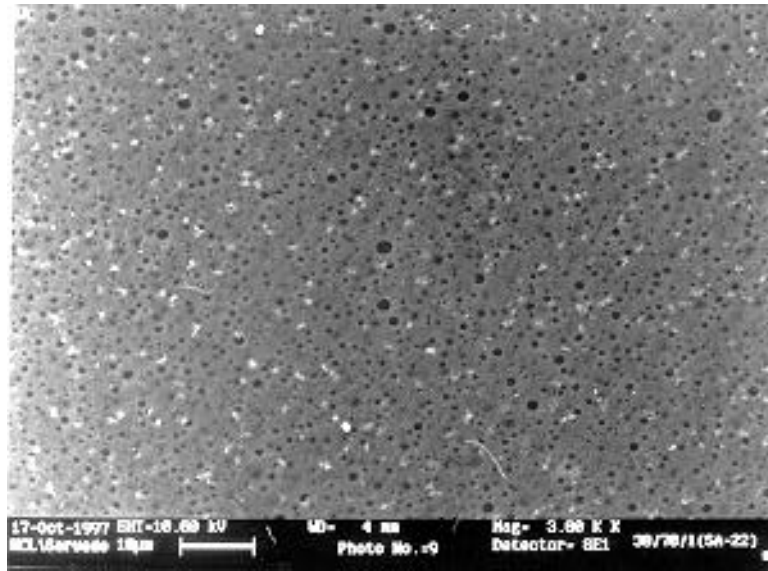
A similar trend is observed by changing the blend composition from 30/70, (PS/NR), to 50/50 (**Figure 5.5e – 5.5h**) keeping the amount of interfacial modifier (1 wt %) constant. From **Figure 5.5f** and **5.5h**, the corresponding photographs of etched samples, it is again verified that particle sizes are smaller and uniform in case of heteroarm star having higher number of arms (**Figure 5.5h**) compared to **Figure 5.5f** where heteroarm star having lesser number of arms (HS₁) is used as a compatibilizer.



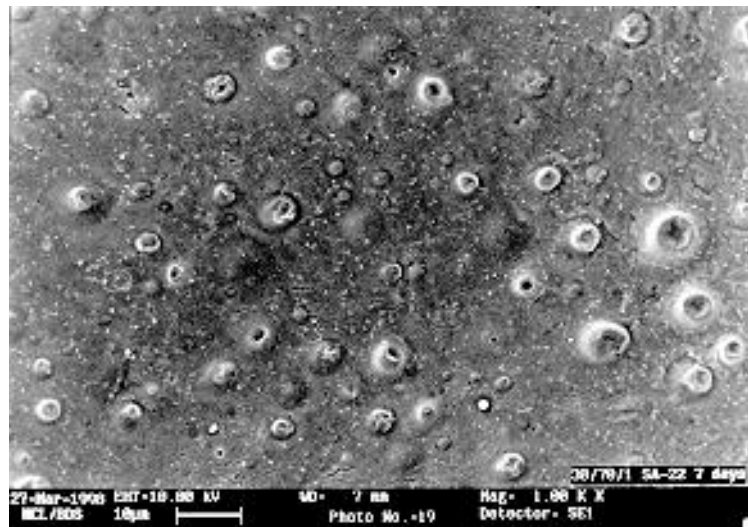
(a)



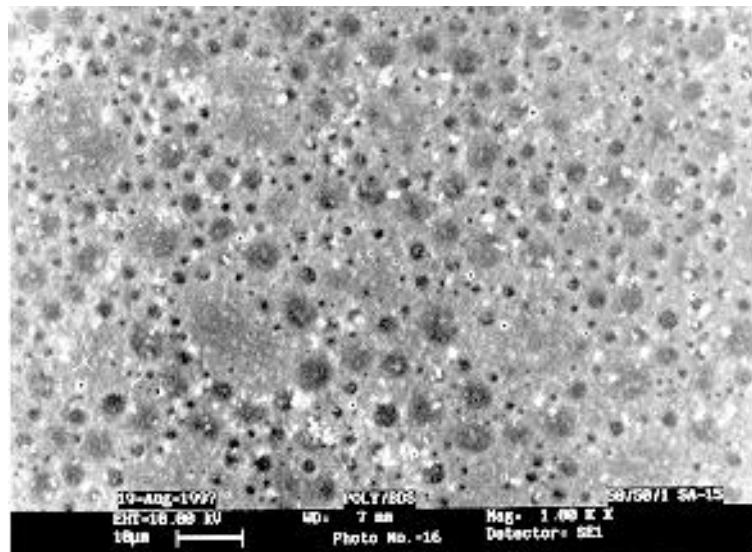
(b)



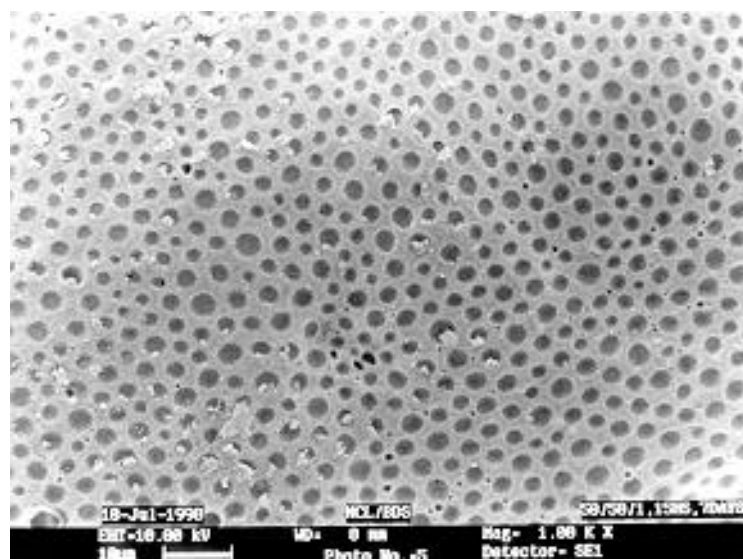
(c)



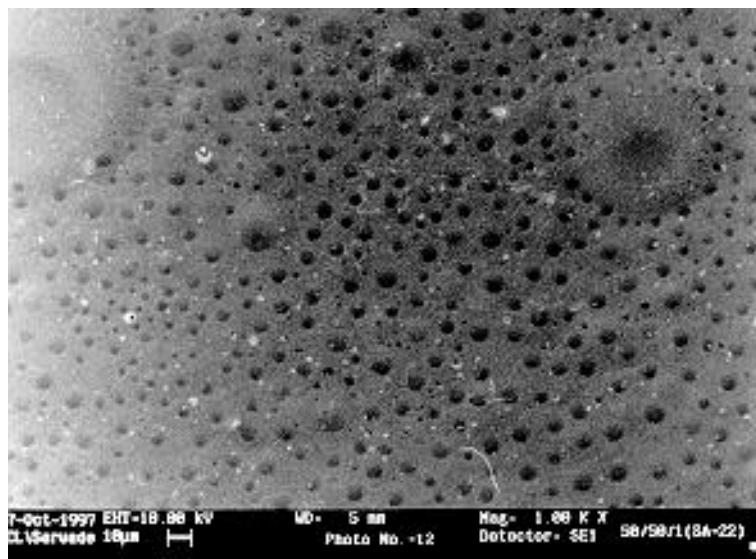
(d)



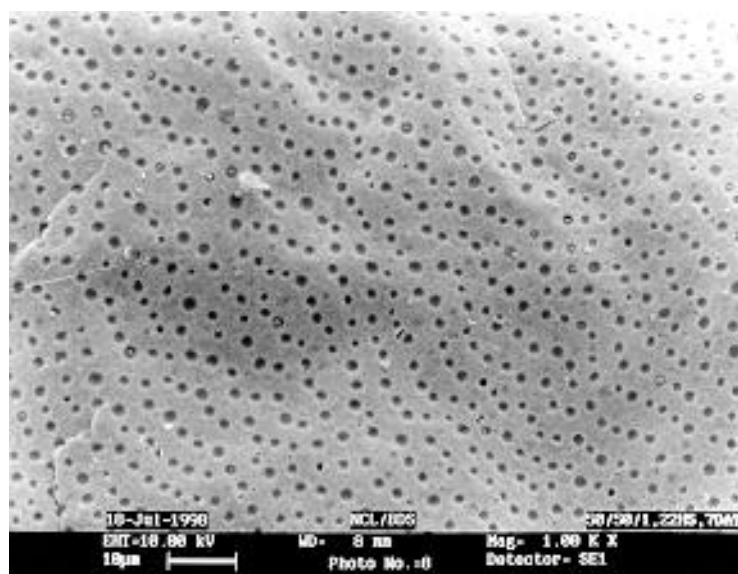
(e)



(f)



(g)



(h)

Figure 5.5. SEM photographs of PS/NR blends (a) 30/70/1, HS₁ as compatibilizer, (b) 30/70/1, HS₁ as compatibilizer-7days acetone etching, (c) 30/70/1, HS₂ as compatibilizer, (d) 30/70/1, HS₂ as compatibilizer-7days acetone etching, (e) 50/50/1, HS₁ as compatibilizer, (f) 50/50/1, HS₁ as compatibilizer-7 days acetone etching, (g) 50/50/1, HS₂ as compatibilizer and (h) 50/50/1, HS₂ as compatibilizer-7 days acetone etching

5.3.6 Effect of number of arms of heteroarm star polymer on mechanical properties

From **Table 5.5a** and **5.5b**, it is clear that with increase in the number of arms of star polymer, modulus, strength and elongation at break are improved. Tensile impact strength gradually increases with increase in the concentration of compatibilizer. These improvements are due to the increase of adhesion at the PS/NR interface by the star polymer. The interfacial adhesion is in greater extent in case of star polymer with higher number of arms. PS and PI chains diverge from the DVB core, penetrate and spread into the corresponding domains. As the number of arms of the star is increased, they are able to penetrate to a greater extent provoking a much better dispersion of the minor phase, so star polymer with higher number of arms act more efficiently as a compatibilizer.

Table 5.5a: Comparison of mechanical properties of PS/NR blend using different heteroarm star polymers as a compatibilizer

Compatibilizer	Tensile strength (MPa)	% Elongation	Young's modulus (MPa)	Total no. of arms (2n)
30/70/0 (without compatibilizer)	0.76	529	15	-
HS ₁	1.40	512	22	12
HS ₂	1.80	549	24	34

in all cases PS/NR/compatibilizer = 30/70/2 blend composition is used.

Table 5.5b: Comparison of tensile impact properties of PS/NR blends using different heteroarm star polymers as a compatibilizer

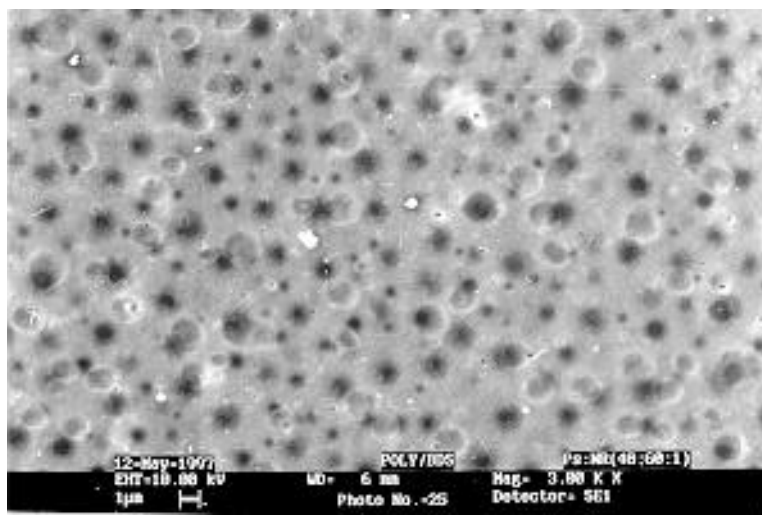
Weight % of copolymer	Tensile impact strength (KJ/m ²)	
	HS ₁ (2n = 12)	HS ₂ (2n = 34)
0	83	83
1.0	112	115
2.0	122	133
3.5	159	166
5.0	127	-

PS/NR composition used 30/70. 2n = total no. of arms of star polymer (PS arm + PI arm)

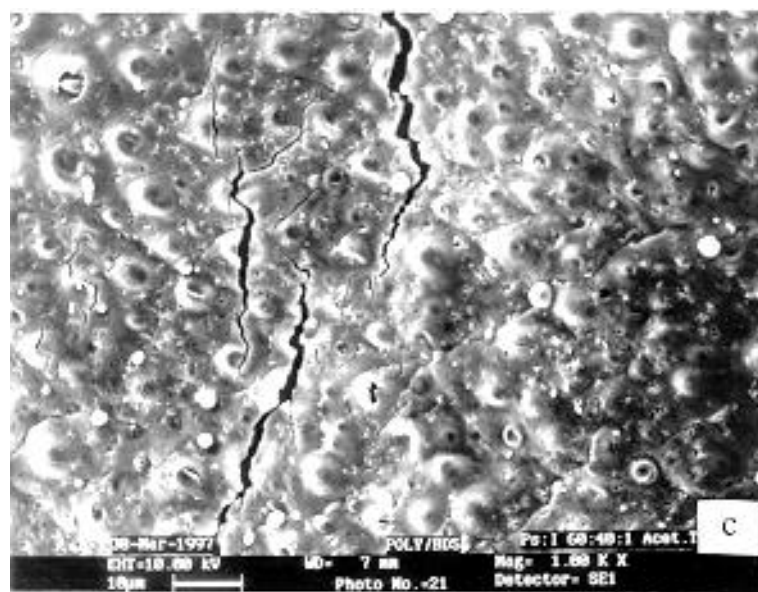
5.4 Comparative study of compatibilizing efficiency of linear diblock, heteroarm star and starblock copolymer having similar arm molecular weight and chemical composition

5.4.1 Effect of molecular architecture on morphology

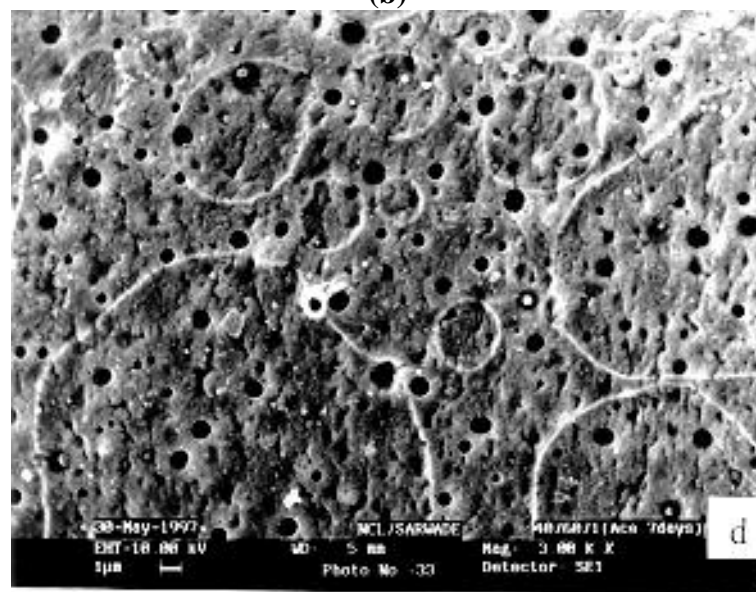
In order to investigate the effect of molecular architecture of compatibilizer on compatibilizing activity, blends of 40/60 PS/NR were modified by adding 1 wt % of the compatibilizing agent. In **Figure 5.6** scanning electron micrographs (SEM) of the modified blends are illustrated. In all cases samples were etched for 2 days and 7 days with acetone in order to etch the PS phase selectively to get better contrast between two phases. As acetone is the selective solvent for PS, the rubber phase remained intact even after long time etching. For all cases it was shown that 2 days etching cannot remove the PS phase completely. The particle size became larger after 2 days acetone etching due to swelling of the PS phase. Therefore, the etching period was increased to 7 days. From the SEM it is clear that after 7 days acetone treatment, the PS phase is removed completely leaving the holes corresponding to the PS dispersed phase. All the micrographs of modified blends show emulsion behavior, since a significant decrease of the microdomain size of the dispersed phase is evident. It seems that the heteroarm star polymer, although exhibiting a complex architecture, migrates easily to the PS/NR interface (**Figure 5.7**).



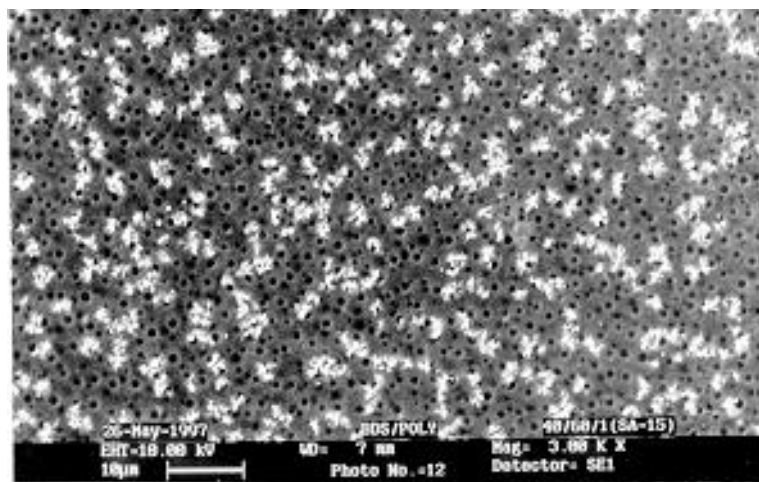
(a)



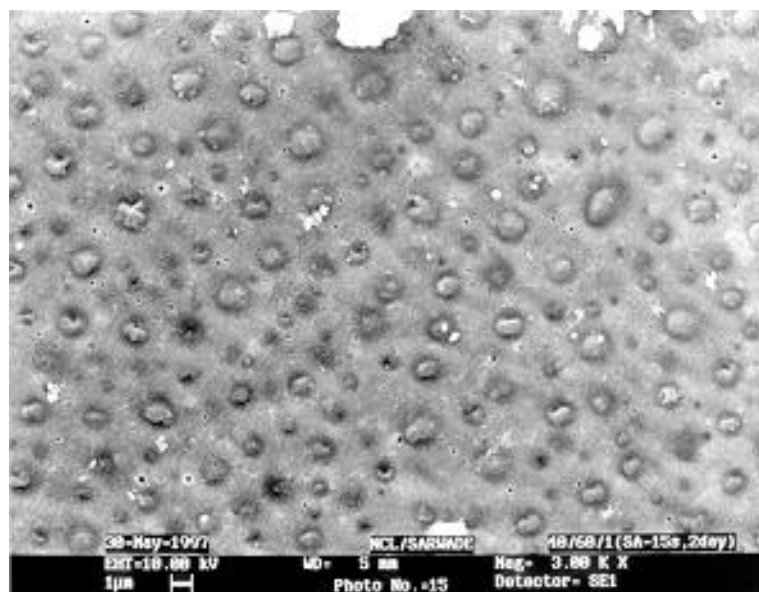
(b)



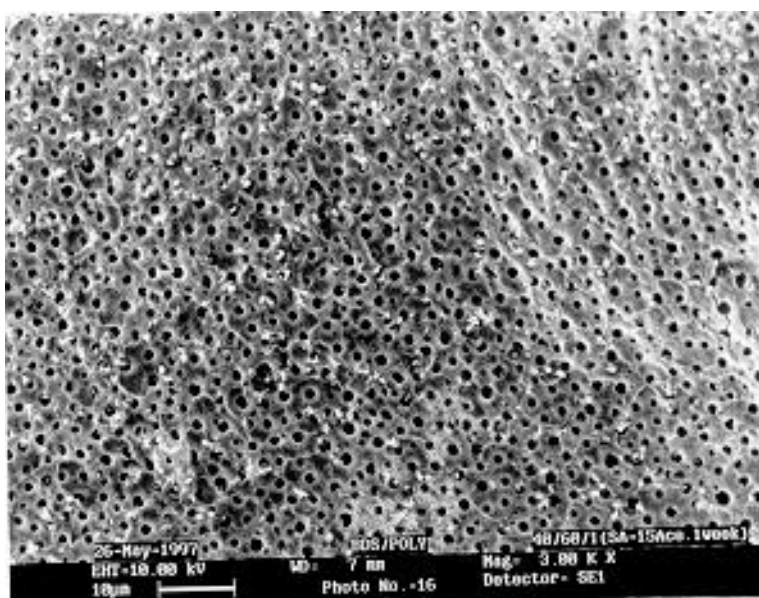
(c)



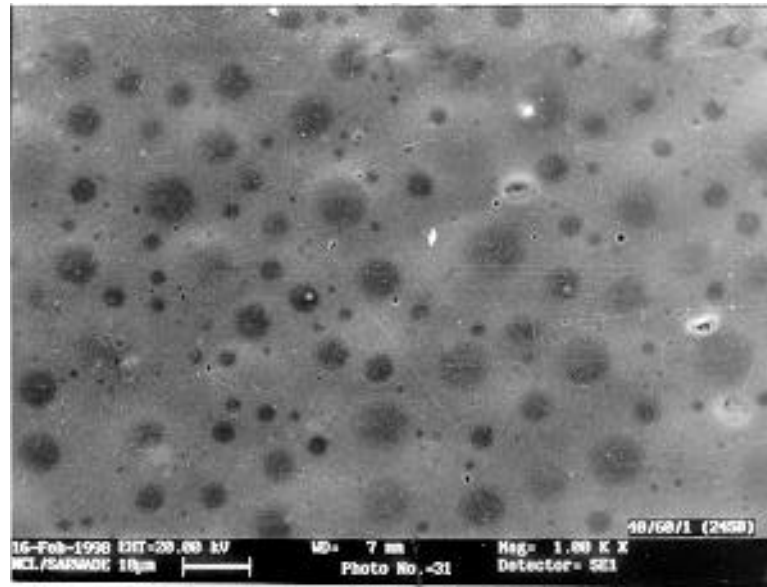
(d)



(e)



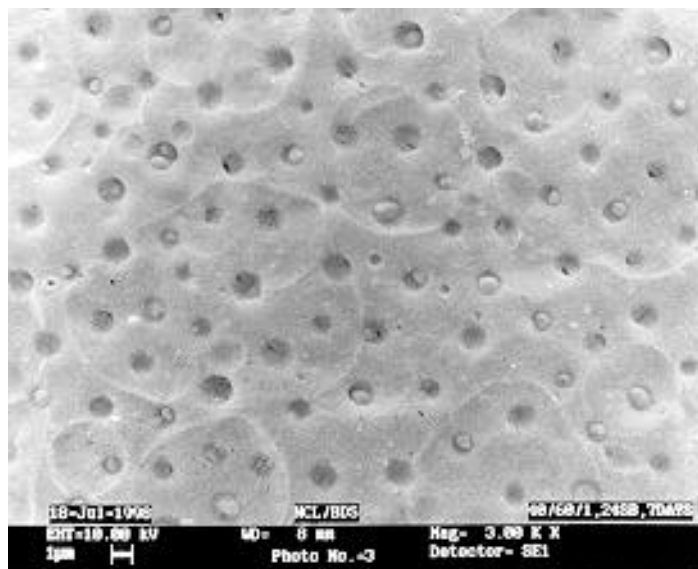
(f)



(g)



(h)



(i)

Figure 5.6. SEM photographs of 40/60/1 PS/NR blend (a) B_5 as compatibilizer, (b) B_5 as compatibilizer-etched for 2 days, (c) B_5 as compatibilizer-etched for 7 days, (d) HS_1 as compatibilizer, (e) HS_1 as compatibilizer- etched for 2 days, (f) HS_1 as compatibilizer- etched for 7 days, (g) SB as compatibilizer, (h) SB as compatibilizer- etched for 2 days and (i) SB as compatibilizer- etched for 7 days

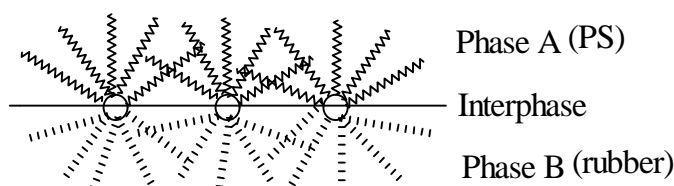


Figure 5.7. Schematic representation of HS polymer at blend interface

Though all the three copolymers investigated can act a compatibilizer, their emulsification activity is different. It appears that the heteroarm star copolymer promotes a finer dispersion of the PS phase (**Figure 5.6d-5.6f**) and exhibits better emulsifying properties when compared to the diblock copolymer (**Figure 5.6a-5.6c**).

5.4.2 Effect of molecular architecture on CMC

Table 5.6 contains the critical micelle concentration (CMC) values for all three different copolymers used as compatibilizers. The CMC values are obtained from the emulsification curve. All systems shows typical emulsion behavior, with a rapid drop in particle size at low concentrations of interfacial agent followed by a leveling off to a certain critical concentration. From the **Table 5.6** it is clear that the CMC for emulsification is lowest when heteroarm star polymer is used as compatibilizer. This is also true for all blend compositions. This indicates that very small amount of heteroarm star is sufficient to saturate the interfacial area. Therefore, it exhibits the best properties amongst the various modifiers investigated.

Table 5.6: Comparison of CMC values

Compatibilizer	n ^{a)}	CMC (Wt. %)		
		Blend composition (PS/NR)		
		30/70	40/60	50/50
B ₅	1	7.95	2.27	2.47
HS ₁	6	0.42	1.76	2.3
HS ₂	17	0.23	1.58	1.50
SB	12	4.02	2.66	6.32

a) average number of each kind of arms and for star block, n = total no. of arms

5.4.3 Effect of molecular architecture on mechanical properties

The main interest in compatibilization and its potential to control the phase domain sizes and shapes is due to the effect this has on properties, particularly, those in the area of mechanical properties. Though block copolymers are efficient dispersing agents for polymer blends, it is observed that the mechanical properties are only slightly improved, probably due to the lack of sufficient interpenetration of segments of the block of the copolymers and blend components (**Table 5.7a and 5.7b**). Comparative experiments on mechanical properties were carried out between a simple binary and ternary blends containing 1, 2, 3.5 and 5 wt % of different compatibilizer (**Table 5.7a**). As shown in **Table 5.7b**, the addition of 2 wt % heteroarm star polymer gives highest modulus and strength. These improvements are due to the increase of adhesion at the PS/NR interface by the copolymer. That is, the heteroarm star polymer properly locates at the interface and the effective penetration of each block sequence of the copolymer into the blend components is operative; in other words polystyrene and polyisoprene chains diverged from the DVB core penetrate and spread into the corresponding domains of the blend components.

Table 5.7a: Comparison of Tensile Impact strength

Wt. % of Compatibilizer	Tensile impact strength (KJ/M ²)			
	B ₅ n ^a = 1	HS ₁ n = 6	HS ₂ n = 17	SB n = 12
0	83	83	83	83
1.0	105	112	115	97
2.0	116	122	133	96
3.5	155	159	166	120
5.0	-	127	-	139

blend composition used 30/70 PS/NR, a) average number of each kind of arms and for star block, n = total no. of arms

Table 5.7b: Comparison of Mechanical properties

Compatibilizer	n ^{a)}	Tensile strength (MPa)	% Elongation at break	Young's modulus (MPa)
In absence of compatibilizer	-	0.76	529	15
B ₅	1	1.10	487	16
HS ₁	6	1.40	512	22
HS ₂	17	1.80	549	24
SB	12	1.20	418	19

blend composition used: 30/70/2 PS/NR/compatibilizer, a) average number of each kind of arms and for star block, n = total no. of arms

5.5 Conclusions

Heteroarm star polymers act as a compatibilizer of immiscible PS/NR blends. Star polymer with higher number of arms are particularly efficient. Consequently, the modulus, tensile strength and elongation at the break improve substantially. These results indicate that each arm penetrates efficiently into the corresponding blend components resulting in increase of adhesion at the PS/NR interphase.

Amongst linear diblock, heteroarm star and star block copolymer having similar molecular weight and chemical composition, it is observed that the heteroarm star polymer is the most efficient emulsifying agent, presumably because it can migrate easily to the blend interface. Therefore, the molecular architecture of compatibilizer is an important parameter for achieving efficient compatibilization.

5.6 References

1. Israels, R.; Jasnow, D.; Balazs, A. C.; Guo, L.; Krausch, G.; Sokolov, J.; Rafailovich, M. *J. Chem. Phys.*, **1995**, *102*, 8149.
2. Cigana, P.; Favis, B. D. *Polymer*, **1998**, *39*, 3373.
3. Cigana, P.; Favis, B. D.; Albert, C.; Vu-khanh, T. *Macromolecules* **1997**, *30*, 4163.
4. Horak, Z.; Fort, V.; Hlavata, D.; Lednický, F.; Vecerka, F. *Polymer*, **1996**, *37*, 65.
5. Laurer, J. H.; Smith, S. D.; Samseth, J.; Mortensen, K.; Spontak, R. J. *Macromolecules* **1998**, *31*, 4975.
6. Rangarajan; P. Haisch, C. F.; Register, R. A.; Adamson, D. H.; Fetters, L.Z. *Macromolecules* **1997**, *30*, 494.
7. Laradji, M.; Desai, R. C. *J. Chem. Phys.* **1994**, *35*, 1991.
8. Zhu, S.-H.; Chan, C.-M. *Macromolecules* **1998**, *31*, 1690.
9. Janert, P. K.; Schick, M. *Macromolecules* **1998**, *31*, 1109.
10. Feng, H.; Ye, C.; Tian, J.; Feng, Z.; Huang, B. *Polymer* **1998**, *39*, 1787.
11. Dutta, S.; Lohse, D. J. *Macromolecules*, **1993**, *26*, 2064.
12. Guo, H.F.; Packirisamy, S.; Mani, R.S.; Aronson, C.L.; Gvozdic, N.V.; Meier, D.J. *Polymer*, **1998**, *39*, 2495
13. Cigana, P.; Favis, B.D.; Jerome, R. *J. Polym. Sci., Polym. Phys.* **1996**, *34*, 1691.
14. Fayt, R.; Jerome, R.; Teyssie, Ph. *J. Polym. Sci., Polym. Phys.* **1989**, *27*, 775.
15. Koklas, S. N.; Gravalos, K. G.; Kalfoglou, N. K. *Polymer* **1994**, *35*, 1425.
16. Lyatskaya, Y.; Gersappe, D.; Gross, N. A.; Balazs, A. C. *J. Phys. Chem*, **1996**, *100*, 1449.
17. Tsitsilianis, C.; Voulgaris, D.; Kosmas, M. *Polymer* **1998**, *39*, 3571.
18. Miyata, K.; Watanabe, Y.; Itaya, T.; Tanigaki, T.; Inoue, K. *Macromolecules* **1996**, *29*, 3694.
19. Gia, H.B.; Jerome, R.; Teyssie, Ph. *J. Polym. Sci., Polym. Phys.* **1980**, *18*, 2391.
20. Edgecombe, B. D.; Stein, J. A.; Frechet, J. M. J.; Xu, Z.; Kramer, E. J. *Macromolecules* **1998**, *31*, 1292.

21. Gersappe, D.; Harm, P.; Irvine, D.; Balazs, A. C. *Macromolecules*, **1994**, 27, 720.
22. Israels, R.; Foster, D. P.; Balazs, A. C. *Macromolecules*, **1995**, 28, 218.
23. Tsitsilianis, C.; Papanagopoulos, D.; Lutz, P. *Polymer* **1995**, 36, 3745.
24. Avrerpoulos, C.; Poulos, Y.; Hadjichristidis, N.; Roovers, J. *Macromolecules*, **1996**, 29, 6076.
25. Gilman, H.; Haubein, A. H. *J. Am. Chem. Soc.*, **1944**, 66, 1515.
26. Eschwey, H.; Burchard, W. *Polymer* **1975**, 16, 180.
27. Bi, L.-K.; Fetters, L. J. *Macromolecules*, **1976**, 9, 732.
28. *Annual Book of ASTM standard, American Society for Testing and Materials, Philadelphia*, **1981**, 1979, part 35.
29. Zhao, H.; Huang, B. *J. Polym. Sci., Polym. Phys.* **1998**, 36, 85.
30. Kim, J. K.; Kim, S.; Park, C. E. *Polymer* **1997**, 38, 2155.
31. Paul, D.R. in “*Polymer Blends*” (Eds D.R. Paul and S. Newman), *Academic Press, New York*, **1978**, Ch12.
32. Tucker, P.S.; Barlow, J.W.; Paul, D.R. *Macromolecules*, **1988**, 21, 2794.
33. Olvera De la Cruz, M.; Sanchez, J.C. *Macromolecules*, **1986**, 19, 2501.
34. Tsitsilianis, C. *Macromolecules*, **1993**, 26, 2977.
35. Ishizu, K.; Kuwahara, K. *Polymer* **1994**, 22, 4907.
36. Beyer, F. L.; Gido, S. P.; Poulos, Y.; Avgeropoulos, A.; Hadjichristidis, N. *Macromolecules*, **1997**, 30, 2373.

CHAPTER – VI

COMPATIBILITY STUDIES ON SOLUTION OF POLYMER BLENDS (POLYSTYRENE/NATURAL RUBBER) BY VISCOMETRIC AND PHASE SEPARATION TECHNIQUE

6.1 Introduction

Determination of extent of compatibility in polymer blends is of considerable importance. Superior properties of blends are determined by compatibility or miscibility of the constituent homopolymers at a molecular level. Many experimental and theoretical methods have been used to investigate polymer compatibility¹. The determination of heat of mixing, glass transition temperature, morphology by electron microscopy and dynamic mechanical response are some of the methods extensively reported in the literature¹. But there is still a need to find simpler and quicker methods for determining compatibility². Homogeneous mixing at a molecular scale is a prerequisite for polymer compatibility. Several blending methods are available such as melt, dry and solution blending. Blending the polymer in solution ensures effective attainment of equilibrium between the different polymer components in solution. Furthermore, viscosity can be measured effectively. A large number of investigations have been carried out on polymer blend miscibility using viscosity measurements of the corresponding ternary (polymer-polymer-solvent) systems³⁻¹¹. This method based on, dilute solution viscometry (DSV) relies on the assumption that repulsive interaction may cause shrinkage of the macromolecular coils giving a negative deviation of viscosity from additivity.

In this chapter, we report our results of investigation of compatibility of a blend of polystyrene and natural rubber using viscometric and phase separation techniques.

6.1.1 Theory

Chee¹⁰ proposed a simple method to predict miscibility in PVC/PMMA, PVC/PiBMA, PMMA/PiBMA blends using DSV. The results were confirmed by DSC studies of these blends. Basically dilute solution viscometry is based on the

classical Huggins equation¹², which express the specific viscosity, η_{sp} , of a single-solute solution as a function of the concentration C , i.e.

$$\eta_{sp} = [\eta] C + bC^2 \quad \text{Eq. 6.1}$$

where $[\eta]$ is the intrinsic viscosity and b is related to the Huggins coefficient k_H by

$$b = k_H [\eta]^2 \quad \text{Eq. 6.2}$$

For non-electrolyte dilute solutions, a plot of η_{sp}/C vs C should yield a straight line with intercept and gradient respectively equal to $[\eta]$ and b . Theoretically, the parameter $[\eta]$ measures the effective hydrodynamic specific volume of an isolated polymer and b reflects the binary interactions between polymer segments. For a ternary system containing a solvent (component 1) and two polymers (component 2 and 3), we have

$$C = C_2 + C_3 \quad \text{Eq. 6.3}$$

$$w_2 = C_2/C \quad \text{and} \quad w_3 = C_3/C$$

where w_2 and w_3 are the weight fraction of the two polymers.

For a ternary system, $[\eta]$ and b in the Huggins equation will be

$$[\eta] = w_2 [\eta]_2 + w_3 [\eta]_3 \quad \text{Eq. 6.4}$$

$$\text{and} \quad b = w_2^2 b_{22} + w_3^2 b_{33} + 2 w_2 w_3 b_{23} \quad \text{Eq. 6.5}$$

$$b_{23} = \frac{(b - w_2^2 b_{22} - w_3^2 b_{33})}{2w_2 w_3} \quad \text{Eq. 6.6}$$

Chee proposed a differential parameter, ΔB , as a simple measure of intermolecular interactions. ΔB is given as

$$\Delta B = b_{23} - \frac{(b_{22} + b_{33})}{2} \quad \text{Eq. 6.7}$$

$$\text{Substituting for } b_{23} \text{ from Equation 6.6, we get } \Delta B = \frac{b - \bar{b}}{2w_2 w_3} \quad \text{Eq. 6.8}$$

$$\text{Where } \bar{b} = w_2 b_{22} + w_3 b_{33} \quad \text{Eq. 6.9}$$

Equation 6.8 has been used to predict the polymer-polymer miscibilities, in general. Here, b_{22} and b_{33} are the specific interaction coefficients of polymers 2 and 3 in single polymer solutions, b is the specific interaction coefficient between the two polymers and w_2 and w_3 are the weight fractions of the two polymers in the blend.

Accordingly, $\Delta B \geq 0$ signifies miscibility and $\Delta B < 0$ indicates phase separation. However, if $[\eta]_2$ and $[\eta]_3$, i.e. intrinsic viscosities of polymer 2 and 3 in pure solvent,

are sufficiently far apart, a more effective parameter, μ , has been suggested. μ is given as

$$\mu = \frac{\Delta B}{([\mathbf{h}]_3 - [\mathbf{h}]_2)^2} \quad \text{Eq. 6.10}$$

and can be written as
$$\mu = \frac{\frac{b - b_{22}}{([\mathbf{h}] - [\mathbf{h}]_2)} - \frac{b_{33} - b_{22}}{([\mathbf{h}]_3 - [\mathbf{h}]_2)}}{2([\mathbf{h}]_3 - [\mathbf{h}])} \quad \text{Eq. 6.11}$$

Equation 6.11 is valid when $[\eta]_2 \neq [\eta]_3$

The dimensionless μ can be conventionally computed using the data of DSV measurements. However, Chee considered ΔB and μ to be equal to zero for the pure components of the blend. But, when either w_2 or $w_3 = 0$, ΔB will be equal to infinity from **Equation 6.8**.

Hugelin and Dondos¹³ studied the influence of the nature of the solvent on the miscibility of polymer, PS/PMMA and poly(2-vinylpyridine)/PMMA. They observed that the intrinsic viscosity of polymer A, measured in a solution of polymer B in solvent S was lower than that of the same polymer A, measured in the pure solvent. Danait and Despande^{4, 5} have proposed a simple method which is a slight modification of that proposed by Hugelin and Dondos. In their approach, the intrinsic viscosity of a polymer is measured when transferred from a pure solvent to a "mixed solvent", i.e. the intrinsic viscosity of polymer 2 is determined separately in a pure solvent ($[\eta]^\circ$) and also in a solvent containing a constant concentration (C^*) of polymer 3, ($[\eta]^*$). In the latter case, the "solvent" is now a solution of concentration C^* of polymer 3 in solvent S and the flow time of this "mixed solvent" is found out and taken as the reference. Then a plot of reduced viscosity (η_{sp}/C_2) vs the concentration of polymer 2 (C_2) is made. On extrapolating to zero concentration one can get $[\eta]^\circ$, intrinsic viscosity of polymer 2 in solvent S and $[\eta]^*$, intrinsic viscosity of polymer 2 in mixed solvent (3 + S). Thus, the difference, $([\eta]^* - [\eta]^\circ) = \Delta[\eta]$, gives a measure of the interaction between the polymer 2 and 3 in a solvent S. $\Delta[\eta]$ is called intrinsic viscosity of transfer. Depending on the strength of the interaction, the magnitude of $\Delta[\eta]$ varies. $\Delta[\eta] < 0.1$ dL/g suggests very little or no interaction, and hence immiscible blends. A high positive value of $\Delta[\eta]$, i.e. ≥ 0.1 dL/g, indicates an

increase in the hydrodynamic volume due to strong associative interactions and hence miscible blends.

Another method for detecting polymer blend compatibility is phase separation technique in a dilute solution. Molau et al^{14, 15} presented the mechanism of action of graft and block copolymer at the interface of the two components in the solution. A solution of immiscible polymer pair A and B in a mutual solvent separates into two phases and demixes to form two layers. When a small amount of graft or block copolymer is added as an emulsifier, a stable polymeric oil in oil emulsion results and the emulsifier locates at the interface. A suitable graft or block copolymer molecule locates at the interface between polymer A solution and polymer B solution. In the interface copolymer molecule can be so arranged that the polymer A backbones are located in the polymer A solution with which they are compatible while the polymer B side chains are located in the polymer B solution with which they are also compatible. Thus, the reason for the accumulation of the graft copolymer in the interface appears to be due to repulsion between two different homopolymer chains. It is suggested that graft copolymer can be only thermodynamically stable at the interface. The molecular weight, length of backbone, number of side chains per backbone etc. influence the stability action of these materials in polymeric oil in oil emulsions. Molau^{14, 15} also indicated the fact that the graft or block copolymer must be oriented in a definite manner for the stabilization mechanism. Molau analyzed the emulsification with radiation graft copolymer. The demixing time was found to be a function of the radiation dose which, the emulsifier has already received.

In this paper we present two simple methods to predict the compatibility between PS/NR blends. In the first technique viscosity measurements have been carried out and the polymer-polymer interaction parameter is calculated. In the second method compatibility of PS/NR by the addition of block copolymer is followed as the function of the phase separated NR and the time for phase separation. The influence of the molecular weight of the block and homopolymer, composition of the blends, concentration of the block copolymer, effects of solvents and mode of addition of the block copolymer on the properties have been studied.

Hughes and Brown¹⁶ have studied the influence of styrene grafted poly(ethyl acrylate) on the phase separation of poly(ethyl acrylate) and polystyrene in a common solvent. The immiscibility is shown by the separation of the mixture into two distinct

layers. But the addition of graft copolymer of poly(ethyl acrylate) and styrene did not give two liquid layers.

6.2 Experimental

6.2.1 Materials

Commercial polystyrene (SC-206E) was supplied by Supreme Plastics, Bombay. Natural rubber (ISNR-5) was supplied by Rubber Research Institute of India, Kottayam, Kerala. The characteristics of the materials used are given in **Table 6.1a**.

6.2.2 Synthesis of PS-b-PI

The diblock copolymer of styrene and isoprene (PS-b-PI) with different molecular weights and compositions were prepared by sequential living anionic polymerization using s-butyl lithium as an initiator in cyclohexane at 55 °C. Reactions were carried out in specially designed glass reactor using standard bench top inert atmosphere technique under positive pressure of ultra high pure nitrogen (**Chap. III, Sec. 3.5.1**).

6.2.3 Characterization of the materials

The PS-b-PI was characterized by SEC, ¹HNMR, IR spectroscopy and gravimetric method (**Chap. III, Sec. 3.6**).

The characteristics of the block copolymers synthesized are given in **Table 6.1b**.

Table 6.1a: Characteristics of the materials used

Materials	$[\eta]^a$ (dl/g)	Solubility parameter (cal./cc) ^{1/2}	$M_v \times 10^{-5}$
NR ₀	5.38	7.75	11.0
NR ₂₀	2.20	7.75	2.94
PS	0.79	8.56	2.30

a) Determined in toluene at 25 °C, b) NR suffix indicates time of mastication in min.

Table 6.1b Characteristics of the block copolymers synthesized

Diblock copolymer (B)	$\bar{M}_n^a \times 10^{-5}$	MWD ^b of PS-b-PI	Wt % composition (PS:NR) ^c
B ₄	2.58	1.09	50:50
B ₁	0.96	1.26	50:50

a) and b) Determined by GPC, in THF at 30 °C, c) Determined by ¹H NMR

6.2.4 Analysis

6.2.4.1 Dilute solution viscometry (DSV) measurements

0.2% (w/v) solutions of each polymer in toluene were prepared. Various blends of PS and NR were made by mixing solutions of the polymer in toluene in the required proportions. The total concentration of the blend was kept constant for all the blend systems. Similarly 'mixed solvents' containing a constant concentration of 0.2 g/dL of polymer B in toluene were prepared.

A suspended-level Ubbelohde viscometer was fabricated. All viscosity measurements were made using a Schott Gerate AVS 440 automatic viscosity measuring system. The temperature was maintained constant at 25 °C. Flow times of pure and “mixed solvents” and polymer solutions were determined by a serial dilution technique. Five dilutions were made for each polymer and blend. Knowing the flow times, relative, specific and reduced viscosities were calculated at the different concentrations. Finally, reduced viscosity was plotted against concentration and intrinsic viscosity ($[\eta]$) and slopes were determined from the plots. Intrinsic viscosities of polymers in pure and “mixed solvent”, $[\eta]^\circ$ and $[\eta]^*$ respectively, and the difference, $\Delta[\eta]$, were estimated. Chee's parameters ΔB and μ , were also calculated.

Densities of the experimental solutions were determined using a specific gravity bottle and correlated with the theoretically calculated values, assuming additivity of volumes of the constituent polymers. The densities are accurate to four decimal places.

Phase separation experiments were carried out by preparing the solution of 50/50 wt % PS/NR blends in chloroform with and without the addition of block copolymer. The blend solution was stirred for 24 h and kept standing. The sample was examined for phase separation as a function of time and block copolymer concentration. The volume fraction of the phase separated NR layer was observed at different time interval and block copolymer concentration. The experiment was repeated with toluene solvent, with block and homopolymer of various molecular weights and also by changing the mode of addition of the block copolymer.

6.3 Results and discussion

6.3.1 Chee's method

Plots of ΔB and μ vs weight fraction of one of the blend components (NR) are shown in **Figure 6.1** and **Figure 6.2** respectively. Over the entire composition range, ΔB and μ have negative values indicating that this blend exhibit phase separation and hence immiscible.

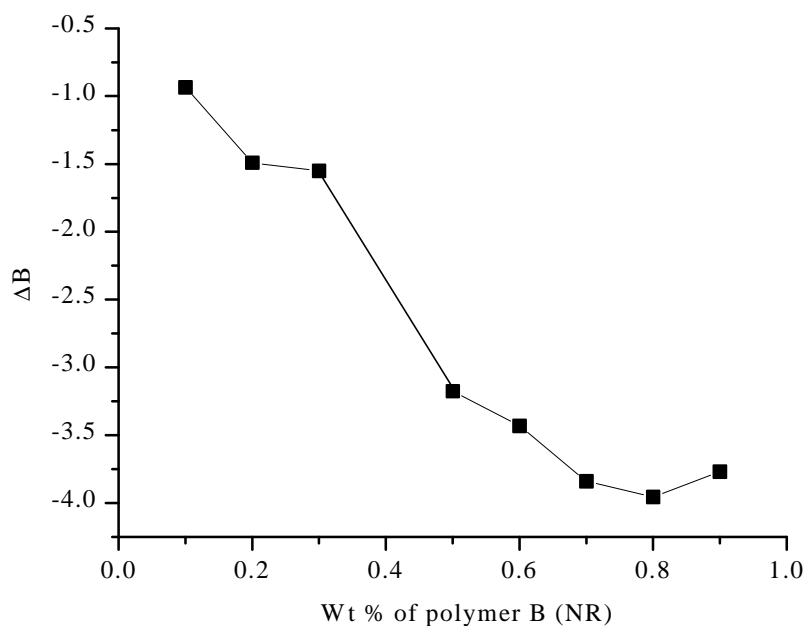


Figure 6.1. Plot of Chee's factor ΔB vs. wt. fraction of polymer B (NR) for PS/NR (polymer A /polymer B) blends in toluene at 25 °C

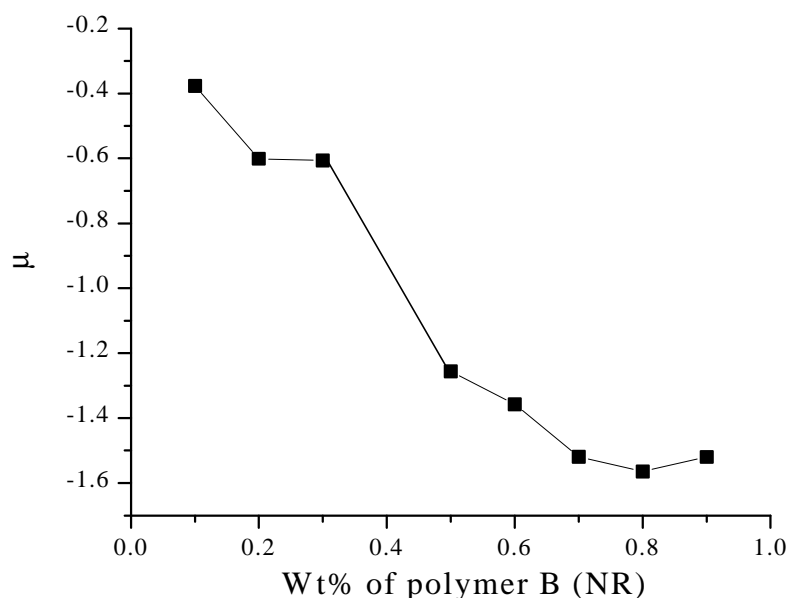


Figure 6.2. Plot of Chee's factor μ vs. wt. fraction of polymer NR (polymer B) for PS/NR (polymer A /polymer B) blends in toluene at 25 °C

6.3.2 Intrinsic viscosity of transfer

The plots of reduced viscosities of polymers in pure solvent are linear with respect to concentration. The plots of change in the viscosity in 'mixed solvent' show interesting results. The values of $[\eta]^\circ$, $[\eta]^*$ and $\Delta[\eta]$ for the blend system are given in **Table 6.2**. In pure solvent the reduced viscosities increase linearly with concentration as expected (**Figure 6.3**). The change in reduced viscosity of PS in 'mixed solvent' for PS/NR is shown in **Figure 6.4**. Similarly the change in reduced viscosity of NR in 'mixed solvent' for PS/NR is shown in **Figure 6.5**. In (NR + toluene) solvent, the reduced viscosity of PS increases slowly with increase in the PS concentration. Also, as the concentration reaches a certain limit, above 0.11g/dL, viscosity decreases very sharply. But over the concentration range of PS, the viscosity of the solution is lower as compared to that of pure solvent (**Figure 6.4**). It can be concluded that at higher the concentration of PS in blend, PS/NR blend become more and more immiscible. The behavior of NR in 'mixed solvent' (PS + toluene) is different compared to PS in NR + toluene. In both cases $\Delta[\eta]$ is found to be negative. At low concentration of NR, there is an initial decrease in the viscosity of the solution as compared with that in the pure solvent. This indicates a tendency towards miscibility at intermediate

concentration. As the concentration reaches a certain limit, say to 0.1g/dL, viscosity remains constant and further increase in concentration does not show any change in viscosity. Based on the negative $\Delta[\eta]$ value, the PS/NR blend can be considered as an immiscible blend system.

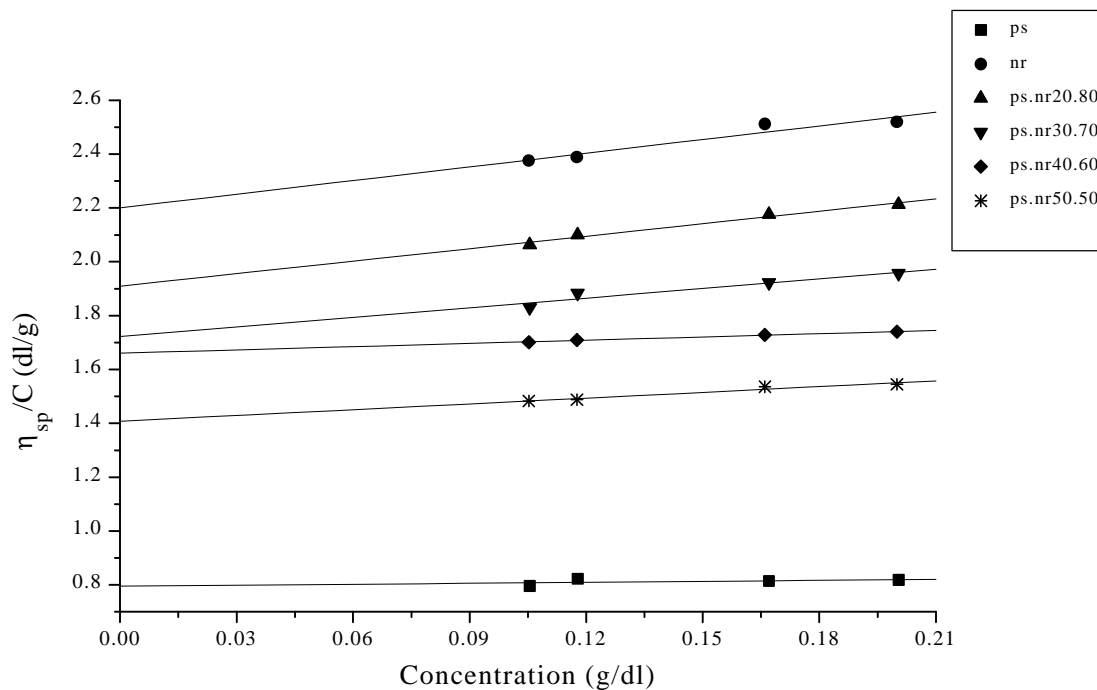


Figure 6.3. η_{sp}/C vs C for PS/NR blend solution of different composition in toluene at 25 °C

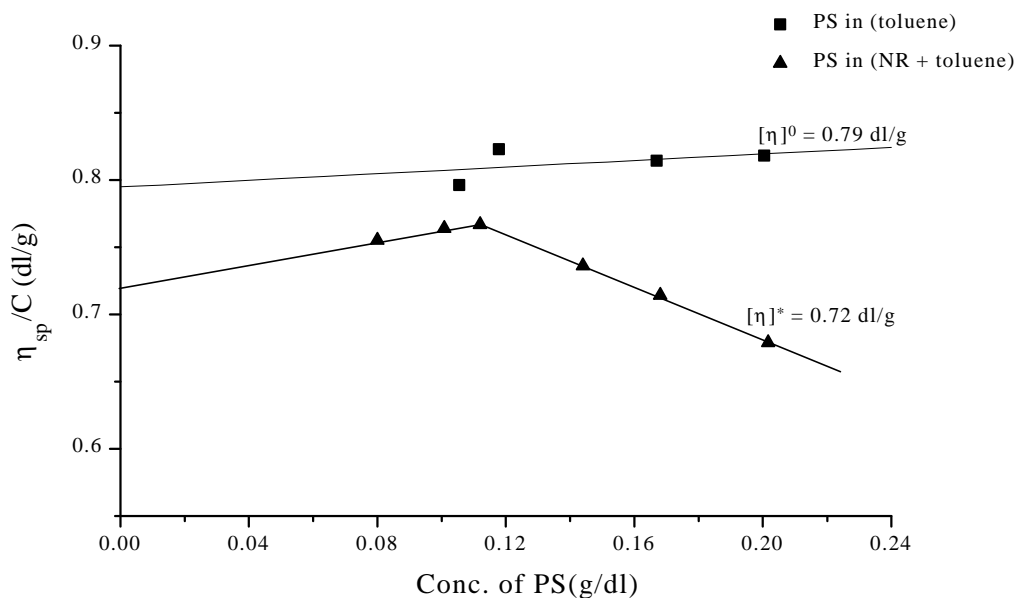


Figure 6.4. Plots of η_{sp}/C vs C of PS for PS/NR blends in pure and 'mixed' solvents at 25 °C

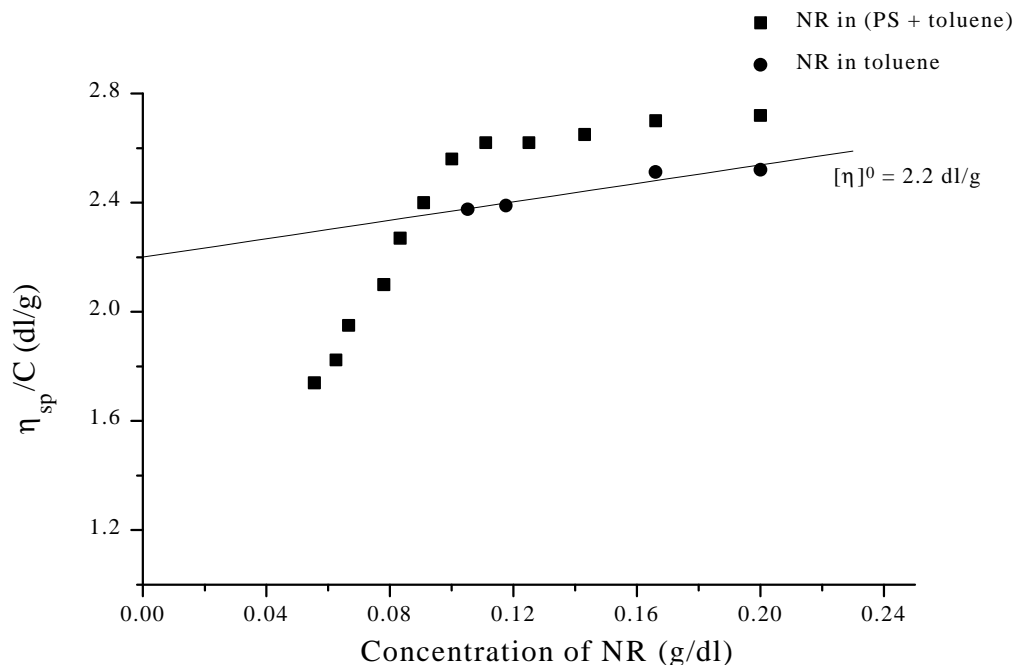


Figure 6.5. Plots of η_{sp}/C vs C of NR for PS/NR blends in pure and 'mixed' solvents at 25 °C

Table 6.2: Intrinsic viscosity of transfer for different blend systems

Blend system	$[\eta]^{\circ}$ (dl/g)	$[\eta]^*$ (dl/g)	$\Delta[\eta]$ (dl/g)
PS in (NR + toluene)	0.79	0.72	-0.07
NR in (PS + toluene)	2.20	1.40	-0.80

6.3.3 Heat of mixing and compatibility

Schneier¹⁷ has calculated the heat of mixing for a number of compatible and incompatible polymer blends. The heat of mixing is an approximate measure of free energy of mixing^{18, 19} and thus may indicate the degree of compatibility. Schneier suggested that the following equation may be deduced for the heat of mixing for two component polymer blends from the formulation of Gee²⁰.

$$\Delta H_m = [x_1 M_1 \mathbf{r}_1 (\mathbf{d}_1 - \mathbf{d}_2)^2 \left\{ \frac{x_2}{(1-x_2)M_2 \mathbf{r}_2 + (1-x_1)M_1 \mathbf{r}_1} \right\}^2]^{\frac{1}{2}} \quad \text{Eq. 6.12}$$

where x = weight fraction of polymer, ρ = polymer density, M = molecular weight of the monomer unit, δ_1 and δ_2 are the solubility parameters of the polymer A and B respectively.

The above method is used for predicting miscibility of blends of PMMA/PVA, PVC/PVA, PMMA/PS by Singh et al⁷ and for NR/PMMA blend by Oommen et al³.

Figure 6.6 shows the variation of calculated heat of mixing with composition. The calculated values of PS/NR blends are found to be above the compatibility limit (10×10^{-3} cal/mol) for all compositions confirming the fact that PS/NR blends are incompatible in all compositions.

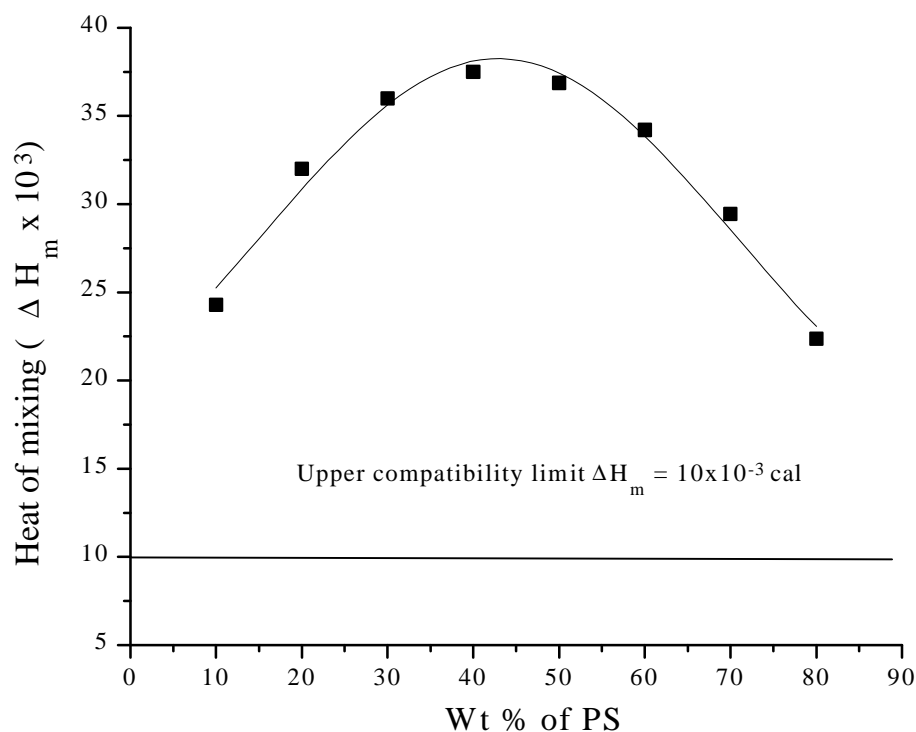


Figure 6.6. Heat of mixing (ΔH) vs. wt % of PS (polymer A) in PS/NR blends

6.3.4 Density and compatibility

A comparison between the experimental and calculated densities for the blend shows that, experimental values are lower than those of calculated ones assuming volume additivity of the constituents (**Table 6.3**).

Table 6.3: Observed and calculated densities of solution of PS/NR blend in toluene at 25 °C

Polymer blend composition (PS:NR)	Observed density (g/cc)	Calculated density (g/cc)
90:10	0.8641	0.8669
80:20	0.8659	0.8669
70:30	0.8659	0.8669
60:40	0.8649	0.8670
50:50	0.8664	0.8670
40:60	0.8649	0.8670
30:70	0.8665	0.8670
20:80	0.8661	0.8670
10:90	0.8642	0.8670

This difference, even though not so pronounced in this case in toluene, can be assumed to be appreciable. This density decrease is attributed^{6, 8, 21} to lower chain packing resulting from decreased molecular interaction and incompatibility.

6.3.5 Polymer blend-solvent interaction

The solubility of a polymer in any solvent is mainly determined by the solubility parameters of the constituents. The solubility of a polymer in a given solvent is favored if the solubility parameters of polymer and solvent are equal. The measure of interaction in a polymer solution is the interaction parameter χ_i , is given by the following relation²²

$$\mathbf{c}_i = \frac{V_i}{RT} (\mathbf{d}_2 - \mathbf{d}_1)^2 \quad \text{Eq. 6.13}$$

Where δ_2 and δ_1 are the solubility parameters of polymer and solvent respectively and V_i , R and T are molar volume of solvent, gas constant and absolute temperature respectively. The same expression has also been used for calculating the interaction parameters between the polymers in polymer blends²³.

The blend-solvent interaction parameters have been calculated according the method adopted by Singh et al⁷. The solubility parameter of the blends are given by the following expression :

$$\delta = x_1 \delta_1 + x_2 \delta_2 \quad \text{Eq. 6.14}$$

where x_1 and x_2 are the weight fractions of the component polymer of the blends and δ_1 and δ_2 are their solubility parameters. **Table 6.4** gives the interaction parameters of the blend studied. The interaction parameters for the blend-solvent system are given in **Table 6.5**. The incompatibility between polymer pair in solution is evident from the fact that the interaction parameter between PS and NR exceeds that of PS/NR blend and cyclohexane. It is also important to mention that all interaction parameter values are positive indicating immiscibility.

Table 6.4: Interaction parameter for the polymer-polymer system

System	Polymer as component 1	Molar volume of component 1	Interaction parameter
PS-NR	PS	100.14	12.13×10^{-2}
	NR	75.68	9.17×10^{-2}

Table 6.5: Interaction parameter for polymer blend-solvent system

System (PS/NR)	Solubility parameter of blend (cal./cc) ^{1/2}	Interaction parameter of the blend-solvent (10 ⁻²)
100/0	8.60	2.90
90/10	8.52	1.79
80/20	8.43	0.96
70/30	8.34	0.38
60/40	8.26	0.065
50/50	8.17	0.013
40/60	8.09	0.22
30/70	8.00	0.69
20/80	7.92	1.40
10/90	7.83	2.40
0/100	7.75	3.70

6.3.6 Phase separation behavior

6.3.6.1 Effect of block copolymer concentration

The PS/NR forms a heterogeneous system and a solution of these two in chloroform separates into two phases with a sharp interface after an interval of 12 h. This clearly shows that PS and NR have no chemical interaction and they are incompatible even after stirring the solution for 24 h in a common solvent like chloroform. But the presence of 1 wt % linear diblock copolymer (PS-*b*-PI), the phase separation took place after a period of 55 h compare to 12 h in the system without block copolymer. Again the extent of volume fraction of NR separated at equilibrium is found to be smaller than the system with no compatibilizer. The influence of copolymer concentration on the phase separation process is visible to the naked eye and is shown in **Figure 6.7**.

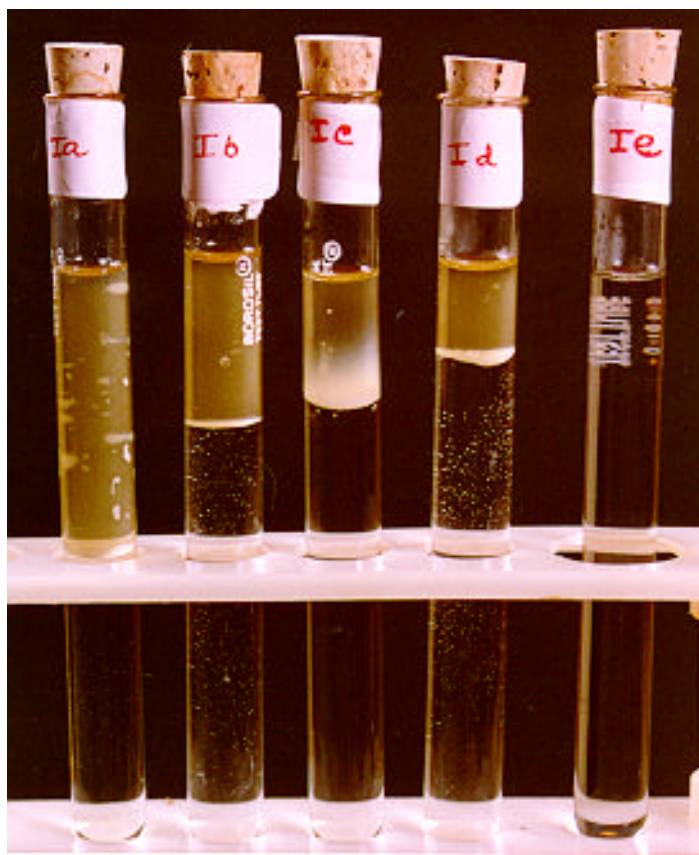


Figure 6.7. The influence of block copolymer on phase separation of 50/50 PS/NR blends

The volume of NR phase separated layer decreases from left to right as the amount of copolymer increases from 0 to 5 wt %. When the copolymer content reaches 5 %, no

phase separation can be observed. As the amount of block copolymer increases, the time required for phase separation increases sharply. The results are shown in **Table 6.6** and **Table 6.7** where the time required for phase separation and the volume fraction of the phase separated NR layer are given for PS/NR blend containing up to 7.5 wt % of block copolymer.

Table 6.6: Phase separation times for various PS/NR blends (time in hours)

% of PS-b-PI (compatibilizer)	^a System-I PS/NR ₂₀ /B ₄	^b System-II PS/NR ₀ /B ₄	^b System-III PS/NR ₂₀ /B ₄	^b System-IV PS/NR ₂₀ /B ₁	^c System-V PS/NR ₂₀ /B ₄
0	12	7	12	12	14
1.0	64	40	55	53	58
2.0	118	73	108	82	114
3.5	294	146	252	240	278
5.0	* *	230	290	272	* *
7,5	* *	* *	* *	* *	* *

* * : No phase separation

a) Chloroform as solvent and two step mixing

b) Chloroform as solvent and one step mixing

c) Toluene as solvent and one step mixing

d) The suffix of NR indicates the time of mastication in min.

e) The \bar{M}_n of B₄ (PS-b-PI) = 2.58×10^5 and \bar{M}_n of B₁ = 0.96×10^5

The time required for phase separation is 108 h, 252 h and 290 h for 2, 3.5 and 5 wt % block copolymer concentration respectively using chloroform as solvent. On further addition of block copolymer (7.5 wt %), no phase separation could be observed for several weeks (6 weeks). This happens when the copolymer content reaches above the equilibrium concentration which can be considered as ‘critical micelle concentration’ (CMC). The same trend can be obtained by observing the volume fraction of the phase separated NR layer with block copolymer concentration. In chloroform the volume fraction of phase separated NR layer decreases with block copolymer concentration and no phase separation occurs after 5 wt % of block copolymer which indicates interfacial saturation.

Table 6.7: Volume fraction of the phase separated NR layer

% of PS-b-PI (compatibilizer)	^a System-I PS/NR ₂₀ /B ₄	^b System-II PS/NR ₀ /B ₄	^b System-III PS/NR ₂₀ /B ₄	^b System-IV PS/NR ₂₀ /B ₁	^c System-V PS/NR ₂₀ /B ₄
0	0.5273	0.5502	0.5273	0.5273	0.5805
1.0	0.3182	0.4262	0.3206	0.3612	0.3086
2.0	0.2072	0.3463	0.2208	0.2362	0.2174
3.5	0.1636	0.2180	0.1697	0.1780	0.1647
5.0	* *	0.1960	0.1040	0.1280	* *
7.5	* *	* *	* *	* *	* *

* * : No phase separation

a) Chloroform as solvent and two step mixing

b) Chloroform as solvent and one step mixing

c) Toluene as solvent and one step mixing

d) The suffix of NR indicates the time of mastication in min.

e) The \bar{M}_n of B₄ (PS-b-PI) = 2.58×10^5 and \bar{M}_n of B₁ = 0.96×10^5

Literature²⁴⁻³¹ and the present study suggest that there is an optimum amount of compatibilizer which can saturate the interface. Further addition of compatibilizer above the optimum amount will not modify the interface any more but create micelle formation which is highly undesirable.

These results are in agreement with the theoretical prediction of Noolandi and Hong³²⁻³⁴ which states that there is a maximum quantity of compatibilizer which can saturate the interface of the binary blend. As the copolymer content increases the time for phase separation increases, the volume fraction of the phase separated NR layer decreases and finally the system reaches the interfacial saturation. At this point no phase separation could be seen. The long time required for phase separation is due to the decrease in the interfacial tension between the homopolymers by the localization of the block copolymer in the interfacial area. The interfacial activity of the copolymer decreases the interaction energy and hence the polymer-polymer solution does not undergo any phase separation.

6.3.6.2 Effect of nature of solvent on phase separation

Phase separation has been studied by changing the solvent system from chloroform to toluene. In both cases the behavior is similar. However, the saturation point is

attained at a copolymer content 3.5 wt % in case of toluene which is lower compared to 5 wt % for chloroform solvent (**Table 6.6**). The time required for demixing in toluene is also higher. The volume fraction of the NR layer separated in toluene is smaller compared to chloroform (**Table 6.7**). Toluene solvates the polymer species more effectively than chloroform. Consequently, the interaction between toluene and PS/NR blend is higher. The difference in behavior between the solvents is due to the difference in solubility parameter. The solubility parameter difference between PS and toluene ($\Delta\delta$ 0.34) is less than that between PS and chloroform ($\Delta\delta$ 0.74). The difference in solubility parameter between NR and toluene is 1.15 ($\Delta\delta$) and that between NR and chloroform is 1.55 ($\Delta\delta$). So in both the cases toluene is a better solvent compared to chloroform. Therefore, polymer blend solution made in toluene takes longer time for demixing.

6.3.6.3 Effect of mode of addition on phase separation

In the morphological study of nylon/rubber blends Cimmino et al³⁵ observed additional size reduction when blends were prepared in two step in comparison to one step mixing. Same conclusion was drawn by Asaletha et al³⁶ for NR/PS blend system using NR-g-PS as compatibilizer.

Two step mixing was carried out by blending the dispersed phase with the compatibilizer first and then blending it with the matrix polymer. By preblending the modifier with the dispersed phase, it was possible to increase the interaction between the copolymer and the dispersed phase. Preblending with the dispersed phase helps to locate the copolymer at the interface^{37, 38}. A similar observation was made by Oommen et al³.

The effect of mode of addition of the block copolymer on phase separation of the blends was studied. It was found that in two step mixing, the time required for phase separation is relatively higher and the amount of block copolymer required for interfacial saturation is less compared to one step mixing (**Table 6.6**). It is also seen in two step mixing that the volume fraction of the phase separated layer is less than that of one step mixing (**Table 6.7**). By preblending block copolymer with the minor phase the amount of copolymer that can diffuse into the interface can be increased and the distance traveled by the copolymer to reach the interface can be minimized. This

will help in the preferential location of the block copolymer at the PS/NR interface during mixing leading to better interfacial interaction.

6.3.6.4 Effect of block copolymer/homopolymer molecular weight on phase separation

The influence of block copolymer molecular weight and homopolymer molecular weight on the phase separation behavior of the blends has been studied by using block copolymers of molecular weight 2.58×10^5 and 0.96×10^5 and NR of molecular weight 11×10^5 and 2.94×10^5 . As the molecular weight of block copolymer decreases the time taken for phase separation decreases and the volume fraction of phase separated NR layer increases (**Table 6.6 and 6.7**). The effect of molecular weight of copolymers on demixing process can be explained by theories of Riess and Jolivet³⁹. According to them emulsification efficiency of the copolymer can be compared by defining the ratio of the molecular weight of the homopolymer and the block copolymer. If

$$\alpha = \frac{\text{Molecular weight of PS homopolymer}}{\text{Molecular weight of PS component in the block copolymer}}$$

$$\beta = \frac{\text{Molecular weight of NR homopolymer}}{\text{Molecular weight of NR component in the block copolymer}}$$

then, the copolymer is less efficient as an emulsifier if $\alpha > 1$ and $\beta > 1$. The emulsifying properties of the copolymer is optimum when $\alpha < 1$ and $\beta < 1$. In an ideal case, when $\alpha = \beta < 1$, the copolymer has no preferential solubility.

As the molecular weight of the block copolymer increases, α and β values of block and homopolymers decreases. For system III, α and β values are less compared to system IV, as block copolymer molecular weight decreases from 2.58×10^5 to 0.96×10^5 (from system III to IV) keeping homopolymer (PS and NR) molecular weights constant. Therefore, the tendency of block copolymer (with higher molecular weight) to stay at the interface increases and strengthen the compatibilization. This is reflected on demixing time as well (**Table 6.6 and 6.7**). One can notice that the extent of compatibilization is much higher in system III compared to system IV. In other words the time for demixing increases as the molecular weight of block copolymer increases.

Comparing the system II and III, where, homopolymer NR molecular weight decreases from 11×10^5 to 2.94×10^5 one notices that β values are higher for system II compared to system III. So demixing time is less and volume fraction of phase separated layer is more in case of system II than that of system III (**Table 6.6 and 6.7**). Noolandi and Hong³²⁻³⁴ pointed out that molecular weight of the copolymer is important in reducing the interfacial tension of immiscible polymer blends. The localization of the copolymer at the interface and the separation of the blocks into corresponding homopolymer phases lead to various phenomenon, such as, lowering of the interaction energy between two immiscible polymers, the broadening of the interface between the homopolymers and reduction in entropy of the system. It is observed that as the molecular weight of block copolymer increases or homopolymer molecular weight decreases, α and β values become less and there is a greater reduction in interfacial tension. The reduction in interfacial tension is clear from the higher time for phase separation and lower amount of phase separated NR layer (**Table 6.6 and 6.7**).

6.4 Conclusions

The interactions in blends was studied by the simple measurements of viscosity, heat of mixing, interaction parameters, density and phase separation techniques. PS/NR blends are found to be incompatible from the results obtained for Chee's parameters ΔB and μ . The negative value of ΔB and μ is an indication of incompatibility of PS/NR blends in all compositions. The heat of mixing values (ΔH_m) and the interaction parameters (χ) of PS/NR blends further support this conclusion. The 'intrinsic viscosities of transfer' approach gives a very good qualitative picture of the interaction among the polymers and, hence, the miscibility. Depending on the strength of the interaction, the magnitude of $\Delta[\eta]$ varies. The effect of block copolymer on the compatibility between polymer-polymer solution and the amount of copolymer required for compatibilization were evaluated. The incompatibility causes the phenomenon of phase separation of the polymer blend solutions. The block copolymer acts as an emulsifier which locates at the interface and extends into the homopolymer phases with which it is compatible.

The time required for the phase separation was taken as an indication of the extent of compatibilization. The phase separation took place quickly (7-14 h) for blends with

no block copolymer. Presence of small amounts of block copolymer substantially increases the phase separation time. No phase separation is observed once the critical micelle concentration was attained. The experimental results are qualitatively in agreement with the theoretical predictions of Noolandi and Hong³²⁻³⁴. Toluene was found to be a better solvent because its solubility parameter is closer to that of homopolymers. Two step mixing helps in the preferential location of the block copolymer at the interface during mixing and promotes better interfacial interactions. The extent of localization of the block copolymer at the interface and, hence, the efficiency of the compatibilizer can be enhanced by the selection of block copolymers of suitable molecular weights.

6.5 References

1. Krause, S. Polymer-Polymer Compatibility in Polymer Blends (Edited by D. R. Paul and S. Newman), Vol. 1, Academic Press, New York, **1978**.
2. Williamson, G. R.; Wright, J. *J. Polym. Sci.*, **1968**, 1, 260.
3. Oommen, Z.; Thomas, S. *J. Mat Sci.*, **1997**, 32, 6085.
4. Danait, A.; Deshpande, D. D. *Eur. Polym. J.*, **1995**, 31, 1221.
5. Danait, A.; Deshpande, D. D. *Polym. Int.* **1997**, 42, 257.
6. Mamza, P. P. A. P.; Folaranmi, F. M. *Eur. Polym. J.*, **1996**, 32, 909.
7. Singh, Y. P.; Singh, R. P. *Eur. Polym. J.*, **1983**, 19, 535.
8. Lizymol, P. P.; Thomas, S. *Eur. Polym. J.* **1994**, 30, 1135.
9. Lizymol, P. P.; Thomas, S. *J. Appl. Polym. Sci.*, **1994**, 51, 635.
10. Chee, K. K. *Eur. Polym. J.*, **1990**, 26, 423.
11. Thomas, G. V.; Nair, M. R. G. *J. Appl. Polym. Sci.*, **1996**, 62, 2229.
12. Huggins, M. L. *J. Am. Chem. Soc.*, **1942**, 64, 2716.
13. Hugelin, C.; Dondos, A. *Makromol. Chem.* **1969**, 126, 206.
14. Molau, G. E. *J. Polym. Sci.*, **1965**, A 3, 1267.
15. Molau, G. E. *J. Polym. Sci.*, **1965**, A 3, 4235.
16. Hughes, L. J.; Brown, G. L. *J. Appl. Polym. Sci.*, **1963**, 7, 59.
17. Schneier, B. O. *J. Appl. Polym. Sci.* **1973**, 17, 3175.
18. Krause, S. *J. Macromol. Sci.*, **1972**, C7, 251.
19. Flory, P. J. *Principles of Polymer Chemistry*, Cornell University Press, New York, **1953**.
20. Gee, G. *Trans. Faraday Soc.*, **1942**, 38, 418.
21. Shur, Y. J.; Randby, B. *Pure Appl. Chem.*, **1981**, 53, 421.
22. Vinogradov, G. V.; Malkin, A. Y. *Rheology of Polymers*, p. 192. Mir Publishers, Moscow (**1980**).
23. Kern, R. J. *J. Polym. Sci.*, **1956**, 21, 19.
24. Datta, S.; Lohse, D. J. *Macromolecules*, **1993**, 26, 2064.
25. Cigana, P.; Favis, B. D.; Jerome, R. *J. Polym. Sci., Polym. Phys.*, **1996**, 34, 1691.
26. Zhao, H.; Haung, B. *J. Polym. Sci., Polym. Phys.*, **1998** 36, 85.
27. Guo, H. F.; Packirisamy, S.; Mani, R. S.; Aronson, C. L.; Gvozdic, N. V.;

- Meier, D. J. *Polymer*, **1998**, 39, 2495.
28. Fayt, R.; Jerome, R.; Teyssie, Ph. *J. Polym. Sci. Polym. Lett. Edn.*, **1986**, 24, 25.
29. Wagner, M.; Wolf, B. A. *Polymer*, **1993**, 34, 1460.
30. Jo, W. H.; Nam, K. H.; Cho, J. C. *J. Polym. Sci., Polym. Phys.*, **1996**, 34, 2169.
31. Inoue, T.; Soen, T.; Hashimoto, T.; Kawai, H. *Macromolecules*, **1970**, 3, 87.
32. Noolandi, J. *Polym. Eng. Sci.*, **1984**, 24, 70.
33. Noolandi, J.; Hong, K. M. *Macromolecules*, **1982**, 15, 482.
34. Noolandi, J.; Hong, K. M. *Macromolecules*, **1984**, 17, 1531.
35. Cimmino, S.; Coppola, F.; D'orazio, L.; Greco, R.; Maglio, G.; Malinconico, M.; Mancarella, C.; Martusceli, E.; Ragosta, G. *Polymer*, **1986**, 27, 1874.
36. Asaletha, R.; Thomas, S.; Kumaran, M. G. *Rubber Chem. Technology*, **1995**, 68, 671.
37. Willis, J. M.; Favis, B. D. *Polym. Eng. Sci.*, **1975**, 142, 243.
38. Favis, B. D.; Chalifoux, J. P. *Polymer*, **1988**, 29, 1761.
39. Riess, G.; Jolivet, Y. *ACS, Adv. Chem. Ser.*, **1975**, 142, 243.

CHAPTER -VII

COMPATIBILIZING EFFECT OF PS-b-PI IN HETEROGENEOUS SAN/NR BLENDS

7.1 Introduction

The use of polymer blends is becoming an important factor in satisfying the needs of specific sectors of the polymer industry owing to economic incentives¹⁻³. Though not always the most efficient, blending is the least expensive but most versatile technique that can produce new polymeric materials from existing commodity polymers. The immiscibility between polymeric pairs is responsible for the poor phase structure and mechanical properties of polymer blends. Therefore, enhancing the compatibility of immiscible polymer pairs is a key technology to obtain polymer blends with desirable properties.

Various methods have been used for compatibilizing polymer blends, namely, the introduction of strong specific interaction (e.g hydrogen bonding⁴, ion-dipole interaction⁵, ion-ion interaction⁶, intramolecular repulsive interaction⁷ etc.), the formation of an interpenetrating network and crosslinking⁸ and the addition of block or graft copolymer in blend which is very similar in the sense of the emulsifying effect of a surfactant in oil/water mixtures⁹. Generally, when an A-b-B diblock copolymer is added to an A/B binary blend, a compatibilizing effect of the copolymer is observed. On the other hand, the approaches using an A-b-C diblock copolymer to bridge the incompatibility gap between two polymers A and B have also proven to be successful^{10, 11}.

In this present work the compatibilizing effect of linear diblock copolymer of styrene and isoprene (PS-b-PI) in heterogeneous SAN/NR blend was studied. It was found that with increasing percentage of the block copolymer, the particle domain size decreased and leveled off at critical micelle concentration (CMC). The influence of block copolymer concentration on impact strength of the blends was also examined. Many of the commodity thermoplastics lack toughness to a degree that excludes them from many applications. However, it has been found that this deficiency can be

eliminated by properly blending glassy polymers with small amounts of suitable rubbery polymers^{1, 12}. It is well known that rubber-matrix adhesion and rubber particle size are two important factors that determine the toughness of polymer-rubber blends. If adhesion between the glassy polymer and elastomer is not good, voids can form at the interfaces and can into a crack. In general, a critical particle size exists for toughening different plastics. The impact strength of the blend decreases markedly if the average particle size is reduced below this critical size. The decrease in impact strength is not as drastic when the particle size increased beyond the optimum value, but larger particles produce poor surfaces on molded and extruded articles and are of no practical use¹². For several matrices, it has been established that the rubber particles must be above a certain critical size which is about 1-2 μm while for poly(styrene-co-acrylonitrile) (SAN), it is about 0.1 - 1 μm ^{12, 13}. There is evidence that the distribution of particle sizes is an important factor along with the mean size. It has been reported that bimodal distributions are superior to unimodal size distribution in toughening rigid plastics^{14, 15}.

Among many rubber toughened plastics, rubber toughened PS, often termed high-impact PS (HIPS), and rubber toughened SAN (acrylonitrile-butadiene-styrene, ABS) have become very successful commercial resins^{16, 17}. In most cases the rubber type is polybutadiene. ABS is made by the copolymerization of styrene and acrylonitrile in the presence of polybutadiene rubber resulting in grafting with subsequent blending with SAN copolymer. It consists of a continuous rigid SAN matrix phase in which the elastomeric polybutadiene phase is finely dispersed in the form of spherical particles. The elastic rubber particles in the brittle matrix act as stress concentrators so that they can initiate and terminate crazes when their size is appropriate¹². Although rubber addition is a useful method for toughening plastics, increasing the concentration of the rubber phase generally leads to a decrease in the tensile modulus and strength of brittle or pseudo ductile matrix polymer¹⁸.

The objective of the present work is to compare the properties, such as particle size and impact strength, of commercial ABS and HIPS with compatibilized SAN/NR and PS/NR blends respectively, having similar chemical compositions.

7.2 Experimental

7.2.1 Materials

Commercial SAN was supplied by Polychem., India. Natural rubber (ISNR-5) was supplied by Rubber Research Institute of India, Kottayam, Kerala. Commercial polystyrene (SC-206E) and high impact polystyrene (HIPS) (SH-760) was supplied by Supreme Plastics, Bombay. ABS (Polylac) was supplied by Polychem., India. The characteristics of the materials used are given in **Table 7.1**.

Table 7.1: Characteristics of materials used

Material	$[\eta]$ dl/g	$\bar{M}_v \times 10^{-5}$	Composition ^d
NR ₂₀	2.23 ^a	2.94	-
PS	0.68 ^a	1.89	-
SAN	0.75 ^b	1.62	-
ABS	-	-	SAN: rubber (95:5)
HIPS	-	-	PS: rubber (94:6)

a) determined in toluene at 25 °C, b) determined in THF at 25 °C, c) NR suffix indicates time of mastication in minutes, (d) chemical composition determined by ¹H NMR.

7.2.2 Synthesis of PS-b-PI

The diblock copolymer of styrene and isoprene (PS-b-PI) with different molecular weights and compositions were prepared by sequential living anionic polymerization using sec-butyl lithium as the initiator in cyclohexane at 55 °C. Reactions were carried out in a specially designed glass reactor using standard bench top inert atmosphere technique under a positive pressure of ultra high pure nitrogen (**Chap. III, Sec. 3.5.1**).

7.2.3 Characterization of PS-b-PI

The PS-b-PI was characterized by GPC, ¹H NMR, IR spectroscopy and gravimetric method (**Chap. III, Sec. 3.6**). The characteristics of the block copolymers synthesized are given in **Table 7.2**.

Table 7.2: Characteristics of block copolymers synthesized

Diblock copolymer (B)	$\bar{M}_n^a \times 10^{-5}$	MWD ^b of PS-b-PI	Wt % composition (S:I) ^c
-----------------------	------------------------------	--------------------------------	---

B ₄	2.58	1.09	50:50
B ₅	2.00	1.12	50:50

a) and b) determined by GPC, in THF at 30 °C, c) determined by ¹H NMR

7.2.4 Preparation of blends

SAN and NR were solution blended in chloroform (2 wt % solution) in different proportions. Blends having wt % compositions of SAN/NR 40/60 and 95/5 were made with and without the addition of the block copolymer (PS-*b*-PI). Similarly PS and NR were mixed in 94/6 wt % proportion. After mixing PS or SAN, NR and block copolymer in chloroform, the mixture was kept overnight and then stirred for 12 h using a magnetic stirrer. The blend films were cast on a glass plate and were dried in air at room temperature.

7.2.5 Analysis

7.2.5.1 Morphological observation

In order to determine the particle size and distribution of the dispersed phase in blends, the morphology of the samples was examined using an optical microscope (Olympus, B201).

7.2.5.2 Measurement of mechanical property

Specimens for tensile impact were injection molded at 180 °C. The diameter of the tab of the bar was 4.5 mm and that of the neck 1.5 mm. The tensile impact strength was determined using an impact tester model CS-183 T1-085 (CSI, Cedar Knolls, New Jersey, USA) using the ASTM D-1822 method¹⁹.

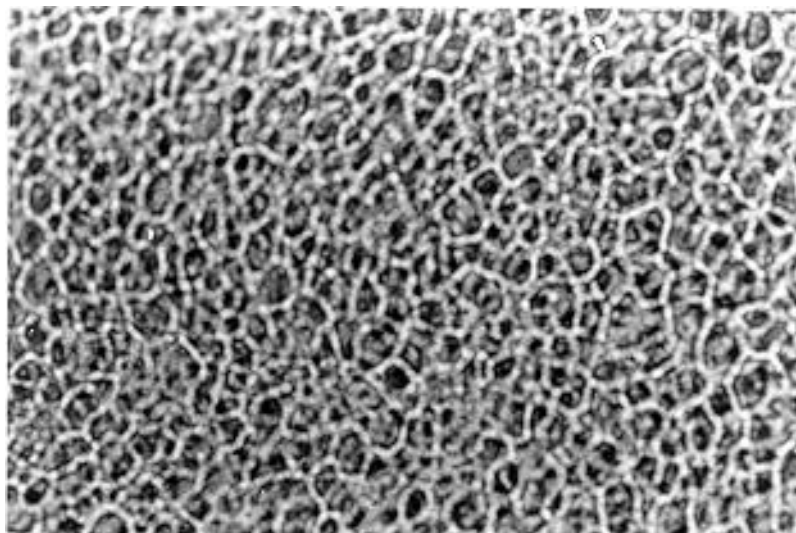
7.3 Results and discussion

7.3.1 Compatibilization study of PS-*b*-PI in SAN/NR blends

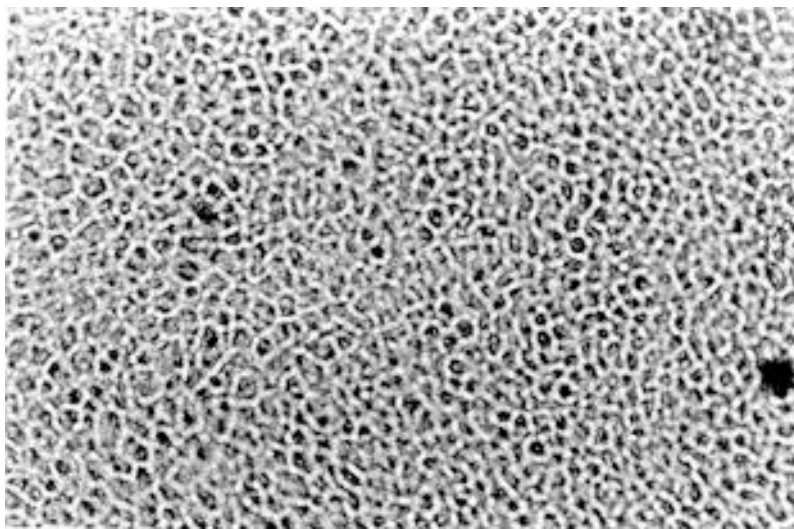
7.3.1.1 Effect of block copolymer concentration on morphology

Interfacial tension and adhesion between two phases are the key parameters governing the degree of dispersion and stability against coalescence or stratification²⁰. Morphology changes in 40/60 (wt/wt) SAN/NR blends on addition of PS-*b*-PI are shown in **Figure 7.1**, where the dispersed phase is SAN. The large domain size and non-uniform size distribution of the blend, **Figure 7.1a**, which are generally determined by, large interfacial tension, poor interface adhesion indicate the

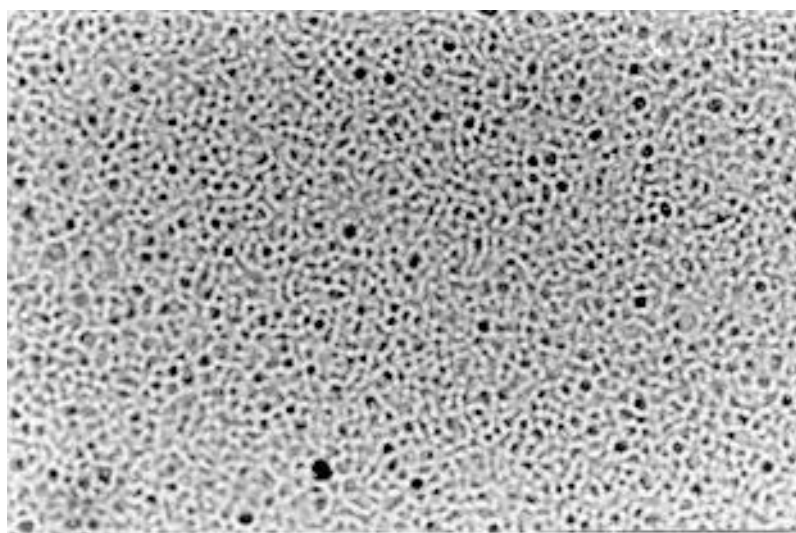
immiscibility of SAN and NR. When a small amount of PS-*b*-PI is added, **Figure 7.1 (a- e)**, more regular and finer dispersion is observed. This results from the decrease in the interfacial tension between the two immiscible polymers and/or the enhancement of interfacial adhesion. When the amount of PS-*b*-PI is further increased up to 7.5 wt % (**Figure 7.1e**), the morphology of the blend does not change much as compared to that of the compatibilized blend with 6 wt % of PS-*b*-PI. In the uncompatibilized blend **Figure 7.1a**, the particles of the dispersed phase are coarse and their average radius is 3.94 μm . However, in the blend compatibilized by 6 wt % PS-*b*-PI (**Figure 7.1d**), the average radius of particles of the dispersed phase is reduced to 0.88 μm . It is evident from these morphological observations that PS-*b*-PI diblock copolymer plays an effective compatibilizer for SAN/NR blends. The leveling point can be taken as the CMC i.e., the lowest concentration at which micelles are formed. CMC values were estimated from the intersection of the straight lines (**Figure 7.2**) obtained at low concentration and leveling off line at higher concentration. For 40/60 SAN/NR blend CMC is about 5.40 wt %.



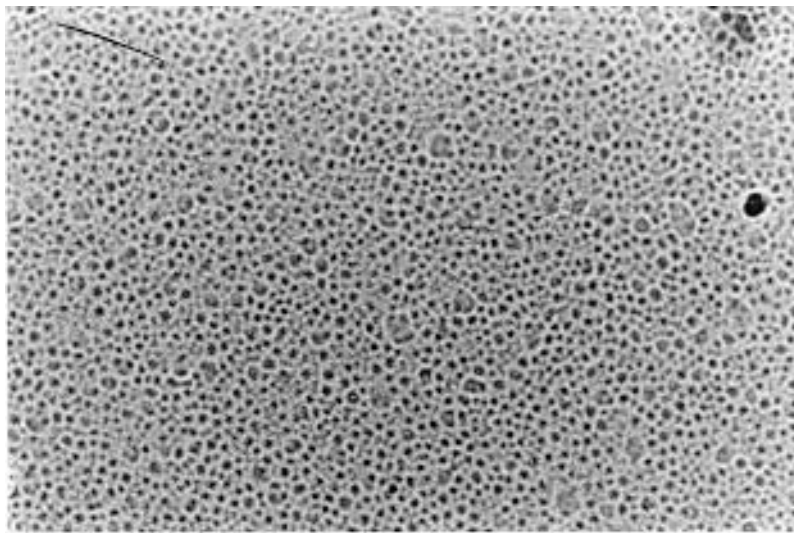
(a)



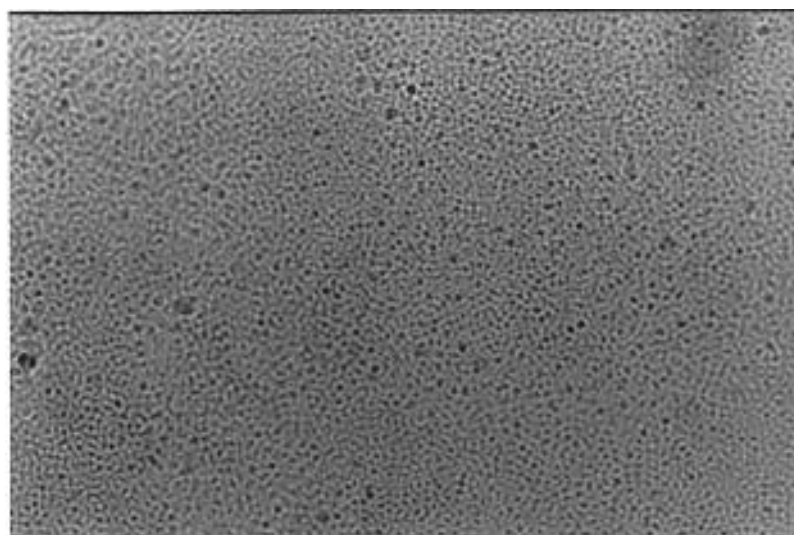
(b)



(c)



(d)



(e)

Figure 7.1. Optical photographs of SAN/NR (40/60) blends with block copolymer loading (a) 0 %, (b) 2%, (c) 3.5%, (d) 6 % and (e) 7.5 %
Scale used : 1 mm = 2 μ m

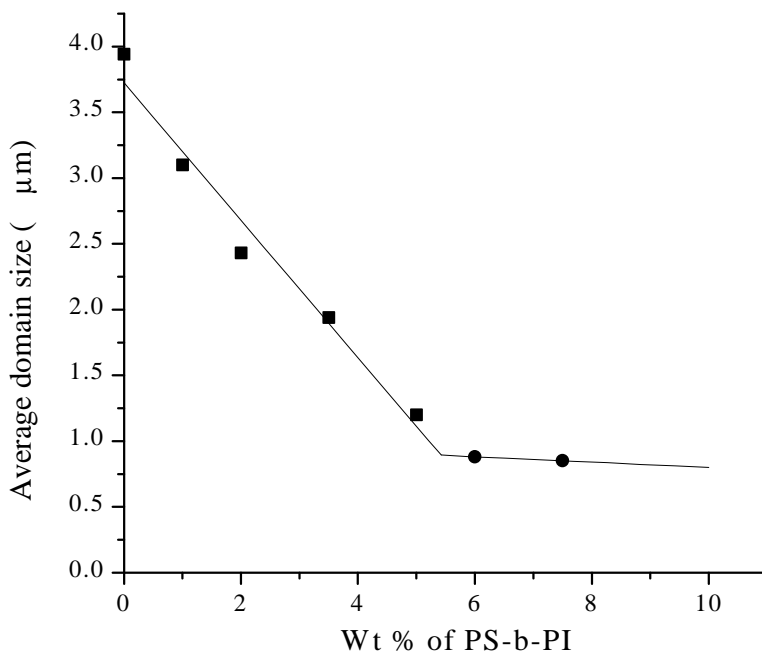


Figure 7.2. Effect of PS-b-PI concentration on particle size of SAN/NR blends

7.3.1.2 Effect of block copolymer concentration on particle size distribution of SAN/NR blends

Quantitative analysis of the optical micrographs is shown in **Figure 7.3**, where the changes in the number of domains and average domain sizes upon the addition of diblock copolymer are obtained (from randomly chosen 100 number of particles and the average diameter was taken).

Decrease in domain size and increase in the number of domains with block copolymer concentration was observed. It can be seen that with increasing concentration of compatibilizer the particle size decreases due to the prevention of SAN coalescence. For a given blend composition (SAN/NR = 40/60) the average particle size decreases and the size distribution narrowed with increasing the concentration of PS-b-PI (**Figure 7.3**). This trend was also evident for the other blend composition (e.g. 95/5) examined.

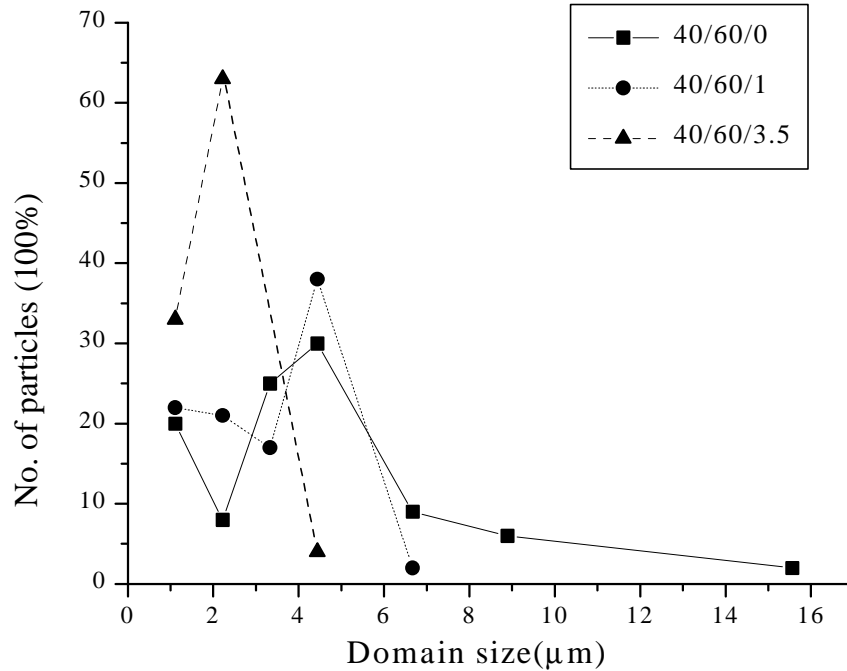


Figure 7.3. Effect of PS-b-PI concentration on domain size distribution of 40/60 SAN/NR blends

7.3.1.3 Effect of block copolymer on mechanical property of SAN/NR blends

The values of the impact strength measured for the neat system (uncompatibilized) and modified system (compatibilized using different amount of PS-b-PI), are given in **Figure 7.4**. The use of copolymer containing an elastomer block improves the impact strength of brittle thermoplastic/rubber blends. These positive effects always result from the same causes: decrease of the particle size and thus of the interparticle distance. Factors that may be responsible for this mechanical reinforcement are creation of smaller scale microstructure and increase in the interfacial adhesion. However, it is difficult to isolate the individual effects of these factors.

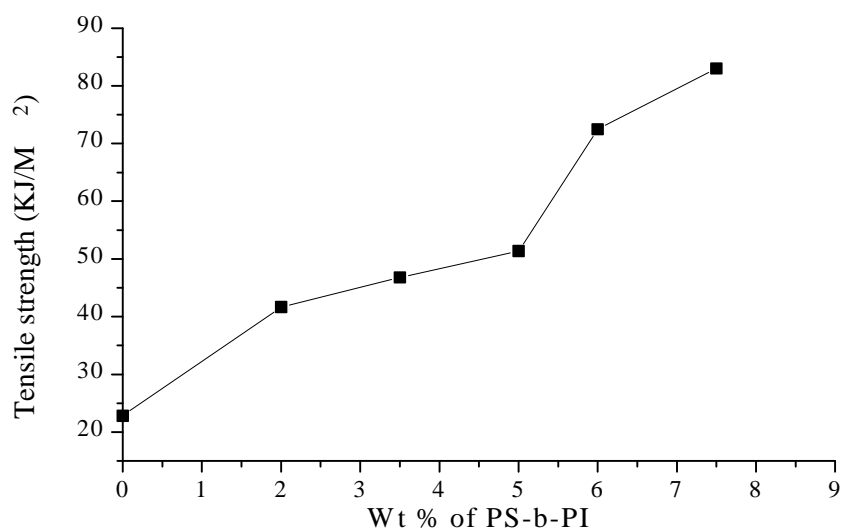
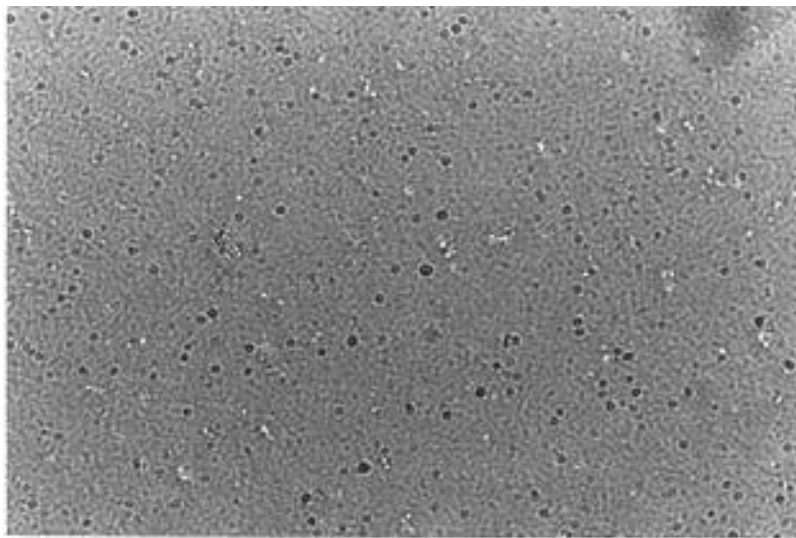


Figure 7.4. Tensile impact strength of SAN/NR (40/60 wt/wt) using PS-b-PI as compatibilizer

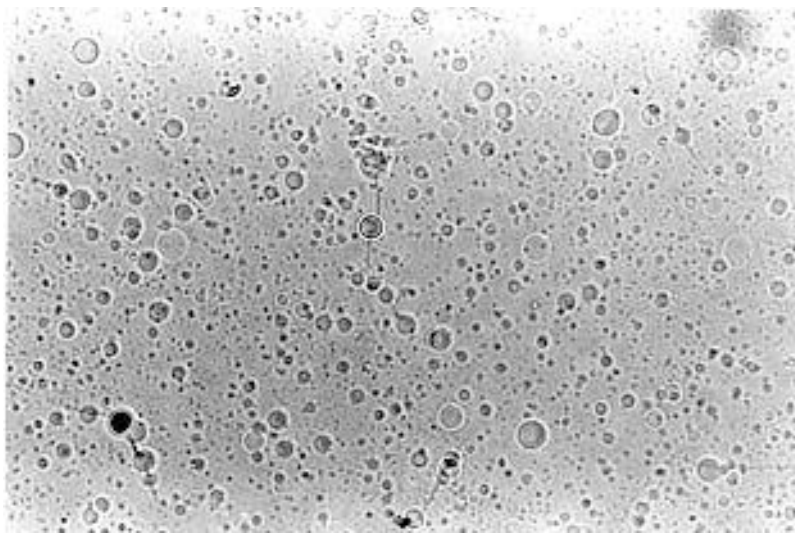
7.3.2 Comparative study of properties of commercial ABS and compatibilized blend of SAN/NR/PS-b-PI having similar chemical composition of ABS

7.3.2.1 Morphological observation

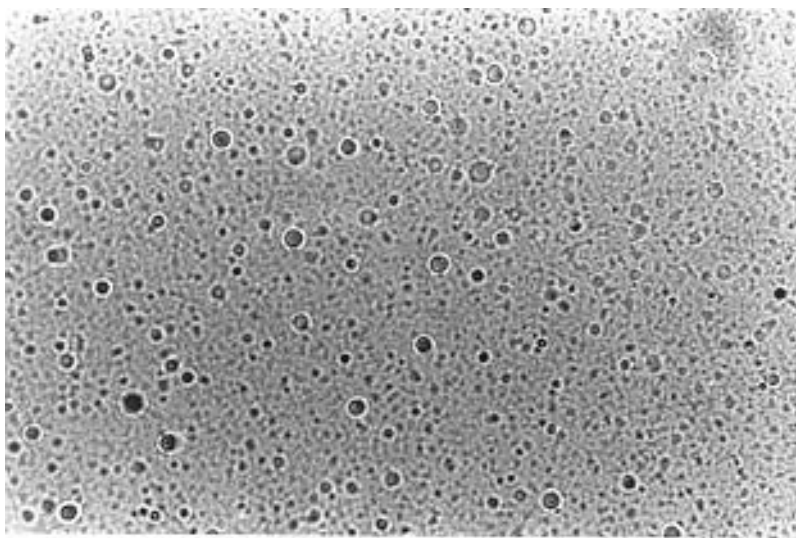
Based on the results discussed above, it is clear that PS-b-PI can act as an efficient compatibilizer for SAN/NR system. The amount of SAN present in ABS is 95 % by wt and the balance being rubber. In order to compare the morphology of commercial ABS and compatibilized SAN/NR blend, SAN and NR were mixed in the same proportion as they are present in ABS, in presence of different amounts of PS-b-PI. Particle size of all the samples were measured by optical microscope. **Figure 7.5** shows the optical photographs of blended system as well as commercial ABS. It is found that particle size of ABS is 2.7 μm (**Figure 7.5a**) whereas particle size of uncompatibilized blend is 3.9 μm . With increasing concentration of PS-b-PI, the particle size gradually decreases (**Figure 7.5 b-e**) and then levels off at higher concentrations (**Figure 7.5 f**). In presence of 3.5 wt% PS-b-PI, the particle size distribution is quite broad but the average particle size is 2.98 μm . When PS-b-PI concentration is increased upto 5 wt %, the particles become smaller (2 μm) and more uniform in size. The particle sizes become even smaller (1.25 μm) and uniform at 6



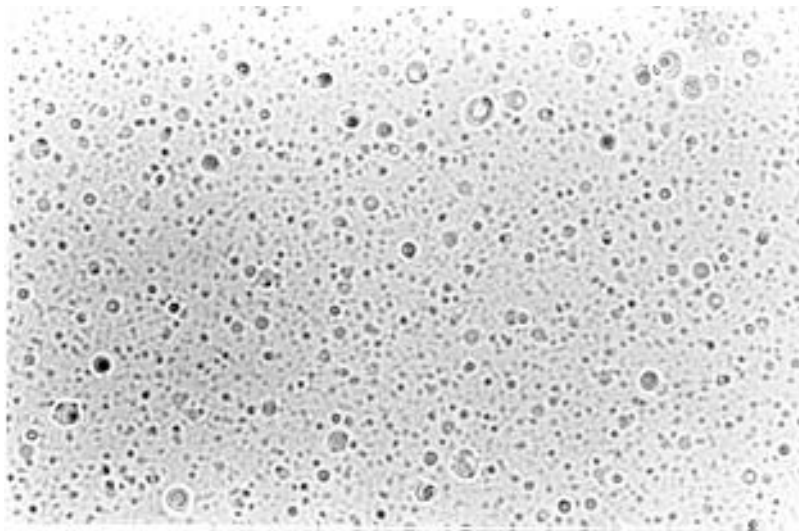
(a)



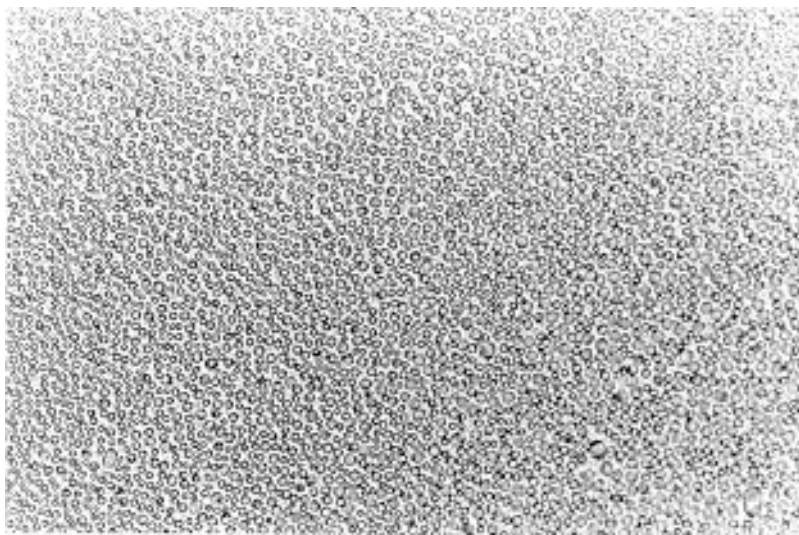
(b)



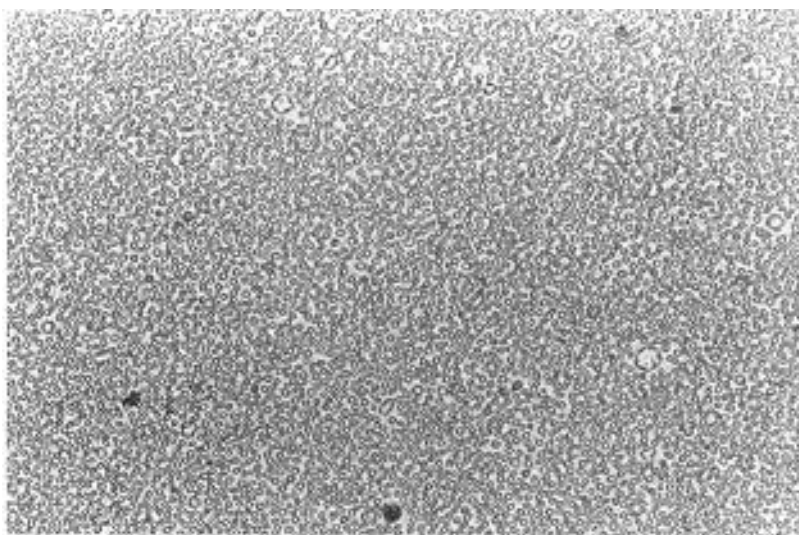
(c)



(d)



(e)



(f)

**Figure 7.5. Optical photographs of (a) ABS. SAN/NR (95/5) blends with block copolymer loading (b) 0 %, (c) 2%, (d) 3.5%, (e) 5 % and (f) 6 %
Scale used : 1 mm = 2 μ m**

wt % of PS-b-PI. So it can be expected that compatibilized blends of SAN/NR using 5 wt % PS-b-PI, may show properties comparable to commercial ABS. The same conclusion can be drawn from the results of impact strength measurement (Sec. 7.3.2.2).

7.3.2.2 Determination of impact strength

The effect of linear diblock copolymer (PS-b-PI) on the impact strength of the SAN/NR blend is shown in **Figure 7.7**.

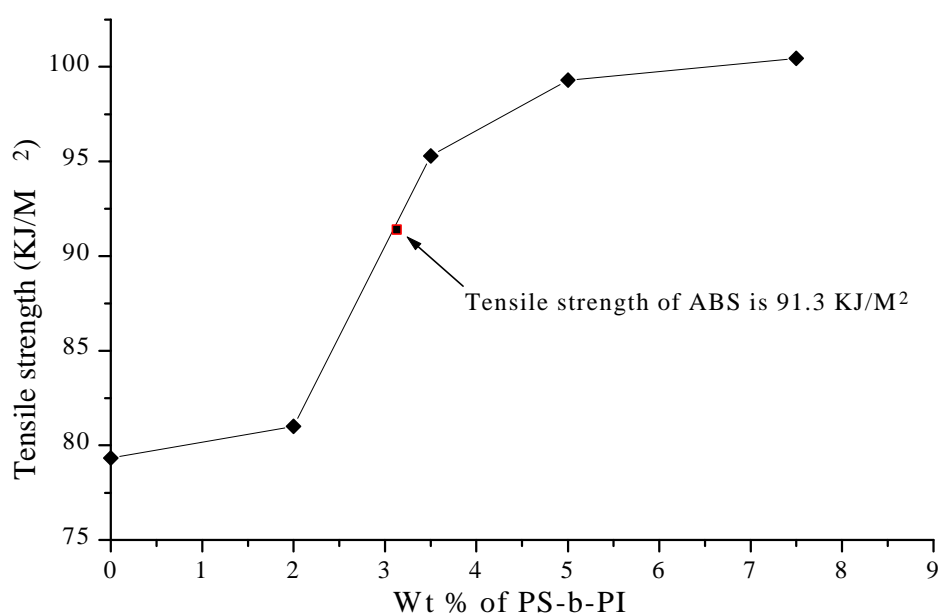


Figure 7.7. Impact strength of compatibilized SAN/NR (95/5 wt/wt) blend compared with commercial ABS

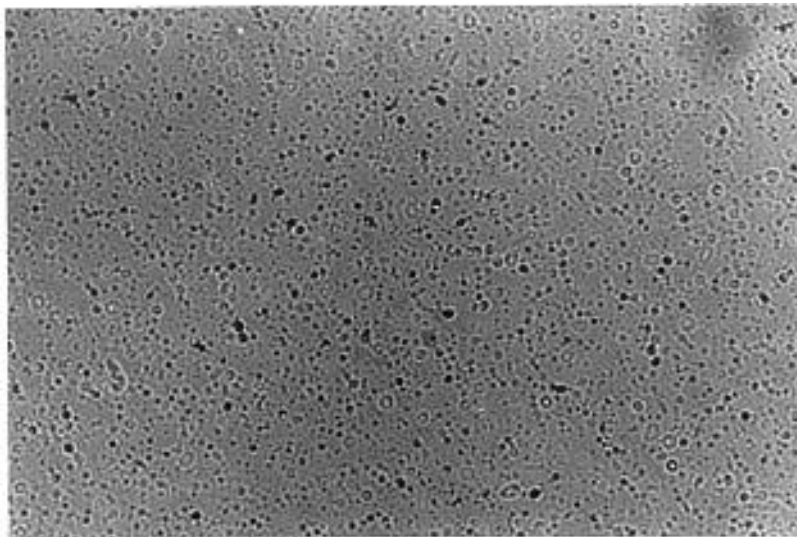
The type of stress-strain curve depends on the blend ratio. The compatibilizing effect of a block copolymer also depends on the blend ratio. The block copolymer properly locates at the interface and improves the adhesion between the two phases which helps in stress transfer through the interface. The impact strength of ABS is 91.3 KJ/M², which was determined by using same method (impact tester model CS-183 T1-085, CSI, Cedar Knolls, New Jersey, USA, using the ASTM D-1822). From ¹H NMR study the chemical composition of ABS was found to be SAN : rubber ratio 95:5. So for compatibilized blends of SAN and NR, a similar ratio was maintained.

With increasing the block copolymer concentration, the impact strength of the SAN/NR blend increases gradually. At 3.5 wt % and higher loading of compatibilizer, the impact strength of SAN/NR blends are higher than commercial ABS (91.3 KJ/M²). Thus, when suitably compatibilized, SAN/NR blend possesses physical properties similar to reactor synthesized ABS.

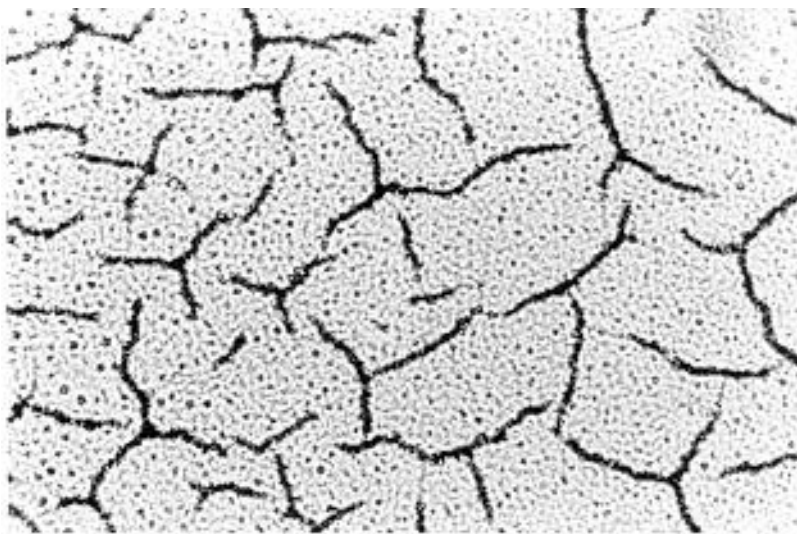
7.3.3 Comparative study of properties of commercial HIPS and compatibilized blend of PS/NR/PS-b-PI having similar chemical composition of HIPS

7.3.3.1 Morphological observation

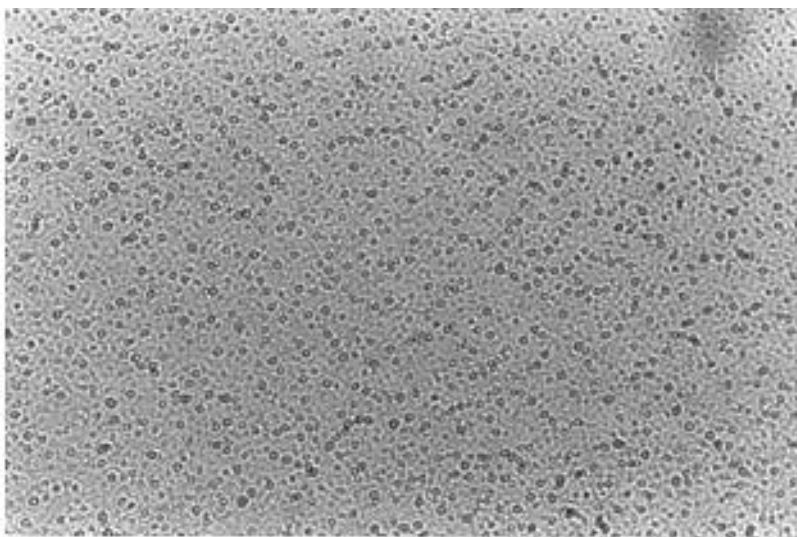
From our previous study (**Chap. IV**) it was found that PS-b-PI can act as an efficient compatibilizer for PS/NR blend. Commercial HIPS contains 94 % (by weight) PS and 6 % rubber. Therefore, blends of PS and NR were prepared having similar composition to that of commercial HIPS. **Figure 7.8** shows the optical photographs of commercial HIPS as well as blended system. For uncompatibilized blend (**Figure 7.8 b**) the particles have coalesced and formed sheet like morphology. But with increasing concentration of PS-b-PI, the extent of coalescence decreased and formation of spherical particles was evident. At a concentration of 7.5 wt % (**Figure 7.8e**), particles are near spherical and almost uniform in size i.e. finely dispersed.



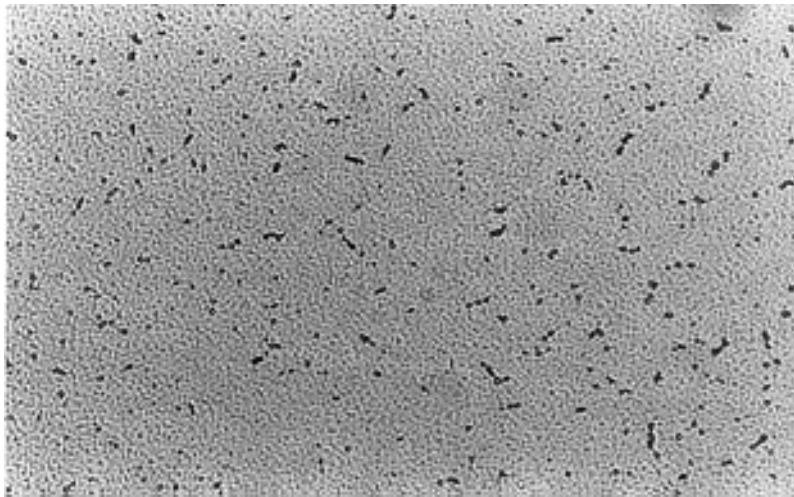
(a)



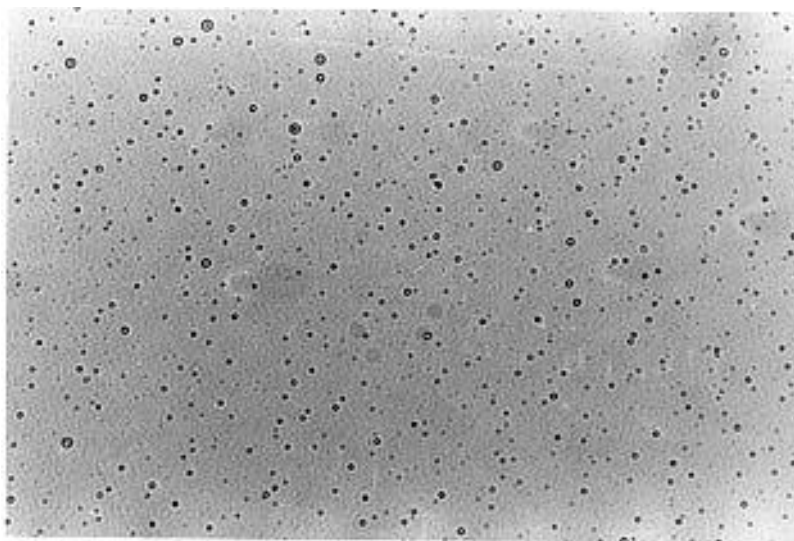
(b)



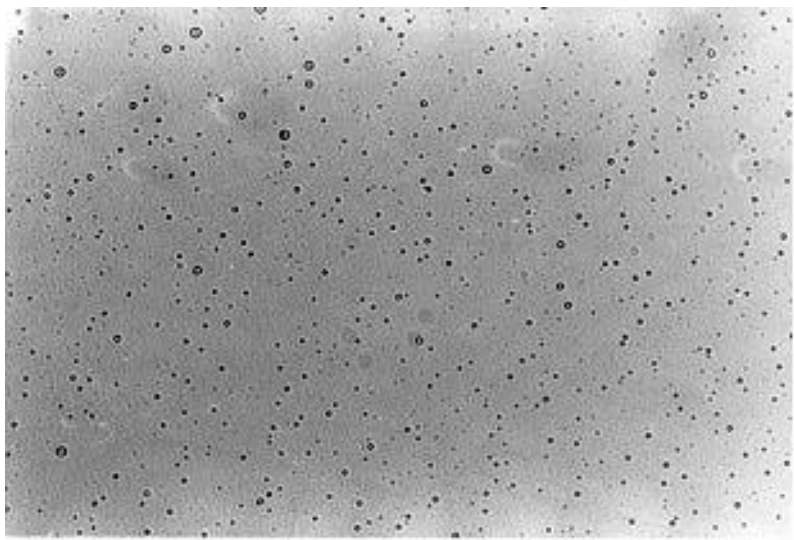
(c)



(d)



(e)



(f)

Figure 7.8. Optical photographs of (a) HIPS. PS/NR (94/6) blends with block copolymer loading (b) 0 %, (c) 2%, (d) 5%, (e) 7.5 % and (f) 9 %.

Scale used : 1 mm = 2 μ m

7.3.3.2 Determination of impact strength

The effect of linear diblock copolymer (PS-b-PI) on the impact strength of the PS/NR blend is shown in **Figure 7.9**. The impact strength of commercial HIPS is 79.9 KJ/M² (was determined using an impact tester model CS-183 T1-085 ,CSI, Cedar Knolls, New Jersey, USA, using the ASTM D-1822 method). With increasing block copolymer concentration, the impact strength of the compatibilized blend having similar chemical composition as commercial HIPS, increased gradually and attained a constant value. At 5 wt % loading of PS-b-PI, the impact strength of compatibilized blend is higher (82.5 KJ/M²) than commercial HIPS. Therefore, compatibilized blends of PS/NR (amount of PS-b-PI 5 wt % and above) have attractive properties as toughened poly(styrene).

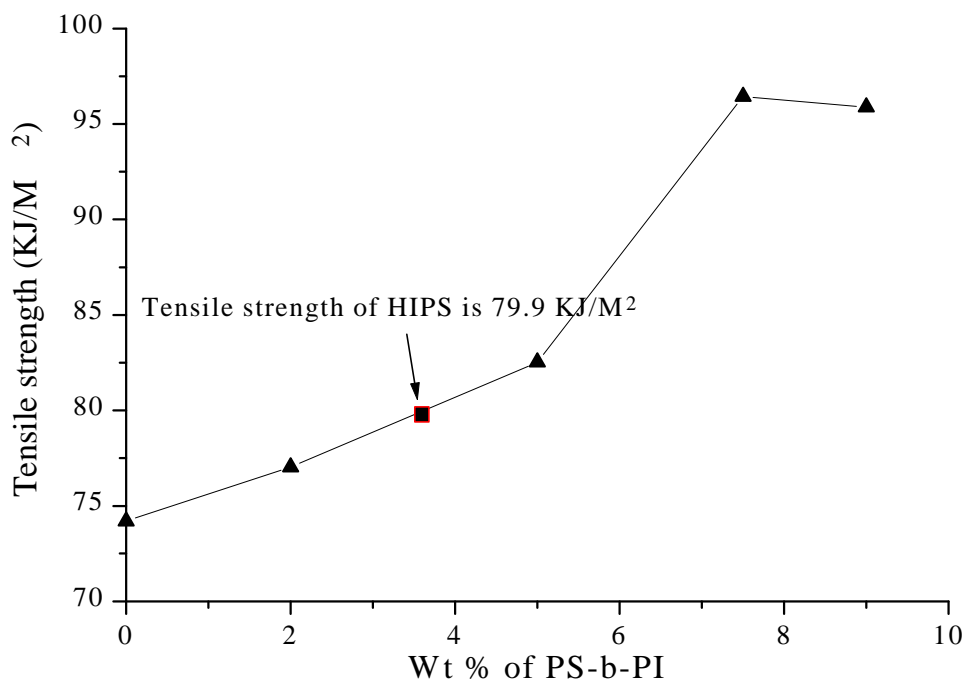


Figure 7.9. Impact strength of compatibilized PS/NR (94/6 wt/wt) blend compared with commercial HIPS

7.4 Conclusions

The compatibilization efficiency of PS-b-PI on solution blended immiscible SAN/NR blends were examined in terms of morphology and improvement in impact strength. Addition of small amount of PS-b-PI results in a finer dispersion of the minor phase. The compatibilizing effect of PS-b-PI on the mechanical properties of the blends depends on the blend ratio. PS-b-PI substantially contributes to the improvement of impact strength of both poly (styrene) and poly (styrene-co-acrylonitrile).

7.5 References

1. Paul, D. R. *Polymer Blends*, Eds. Paul, D. R. and Newman S., Academic Press, New York, **1978**, 2, Ch 12.
2. Olabisi, O.; Roberson, L. M.; Shaw, M. T. *Polymer-Polymer Miscibility*, Academic Press, NY, **1979**.
3. Paul, D. R.; Sperling, L. H. *Multicomponent Polymer Materials*, Washington, DC, ACS, **1986**.
4. Meaurio, E.; Cesteros, L. C.; Katime, I. *Macromolecules*, **1997**, 30, 4567.
5. Varguhese, K. T.; Nando, G. B.; De, P. P.; De, S. K. *J. Mater. Sci.*, **1988**, 23, 3894.
6. Michaels, A. S. *Ind. Eng. Chem.* **1965**, 57(10), 32.
7. Chiu, S.-C.; Smith, T. G. *J. Appl. Polym. Sci.*, **1984**, 29, 1797.
8. Fang, Z.; Xu, C.; Bao, S.; Zhao, Y. *Polymer*, **1997**, 38, 131.
9. Molau, G. E. *J. Polym. Sci.*, **1965**, A3, 1267.
10. Schwarcz, M. C.; Keskkula, H.; Barlow, J. W.; Paul, D. R. *J. Appl. Polym. Sci.*, **1988**, 35, 653.
11. Prahsarn, C.; Jamieson, A. M. *Polymer*, **1997**, 38, 1273.
12. Bucknall, C. B. *Toughened Plastics*, Applied Science Pub. London, **1977**.
13. Folkes, M. J.; Hope, P. S. *Polymer Blends and Alloys*, Chapman and Hall, **1993**.
14. Rudin, A. *J. Macromol. Sci.-Rev. Macromol. Chem.* **1980**, 19, C2, 267.
15. Grancio, M. R. *Polym. Eng. Sci.*, **1972**, 12, 213.
16. Fowler, M. E.; Keskkula, H.; Paul, D. R. *Polymer*, **1987**, 28, 1703.
17. Svec, P.; Rosik, L.; Horak, Z.; Vecerka, F. *Styrene-Based Plastics and Their Modification*, Ellis Horwood, **1987**.
18. Collyer, A. A. *Rubber Toughened Engineering Plastics*, Chapman and Hall, London, **1994**.
19. Annual Book of ASTM standard, American Society for Testing and Materials, Philadelphia, **1981**, 1979, part 35.
20. Plochocki, A. P.; Dagli, S. S.; Andrews, R. D. *Polym. Eng. Sci.*, **1990**, 30, 741.